



Universidad de Valladolid



PROGRAMA DE DOCTORADO EN CIENCIAS DE LA VISIÓN

TESIS DOCTORAL:

DEVELOPMENT OF NEW CARRIERS
TO IMPROVE THE BIOAVAILABILITY OF
NATURAL COMPOUNDS TO TREAT
OCULAR SURFACE DISORDERS

Presentada por **Luna Krstić** para optar al grado de
Doctora por la Universidad de Valladolid

Dirigida por:
Dra. Yolanda Diebold Luque
Dra. María J. González-García

*This one goes up to
everybody who believes that
maybe, just maybe, we were
all born with the moral
obligation to leave this
world a better place than the
world we found.*

Радите свој посао не гледајући ни лево ни десно,
ни иза себе ни преда се,
али свој циљ постављајте високо. . .
Будите неверљиви и стварни,
строги према себи при извођењу сваке појединости,
скромни при њиховој оцени.
-И. Андрић

Contents

I Preface

Table of Abbreviations	I
Financial Support	III
Short <i>Curriculum Vitae</i>	V
Scientific Dissemination	VII
Abstract	XI

II Introduction 1

1. Introduction	3
1.1. The Ocular Surface and the Lacrimal Functional Unit	3
1.1.1. Tear Film	3
1.1.2. Cornea	6
1.1.3. Conjunctiva	7
1.2. Ocular Surface Diseases	8
1.2.1. Dry Eye Disease	8
1.2.2. Pathophysiological Mechanism of Dry Eye Disease	9
1.2.3. Epidemiology and Risk Factors	11
1.2.4. Current Treatments and Their Limitations	12
1.3. Polyphenols	14
1.3.1. Synthetic Pathways of Polyphenols	14
1.3.2. Classification of Polyphenols	15
1.3.3. Sources of Polyphenols	17
1.3.4. Resveratrol	18
1.3.5. Quercetin	19
1.3.6. Limitations of QUE and RSV to their Therapeutic Applications	19
1.4. Drug Delivery Systems	20

1.4.1.	Drug Delivery to the Anterior Segment of the Eye: Barriers and Routes of Administration	21
1.4.2.	Drug Delivery Systems for Ophthalmic Applications	23
	References of Chapter 1	27
2.	Motivation	43
3.	Hypothesis	45
4.	Objectives	47
III	Development	49
5.	Liposomes	51
5.1.	Materials and Methods	52
5.1.1.	Materials	52
5.1.2.	Methods	53
5.2.	Results and Discussion	54
5.2.1.	Characterization of Liposomal Formulations	54
5.3.	Conclusions	56
	References of Chapter 5	57
6.	Inclusion Complexes with Cyclodextrins	61
6.1.	Materials and Methods	63
6.1.1.	Materials	63
6.1.2.	Physicochemical Characterization of the Formulations	64
6.1.3.	Biological Assays	67
6.2.	Results and Discussion	69
6.2.1.	Chemical Stability of Complexed QUE and RSV	69
6.2.2.	Solubility of QUE and RSV in the Formulations	71
6.2.3.	Fourier Transformed Infrared Spectroscopy	73
6.2.4.	Particle Size Characterization	75
6.2.5.	Atomic Force Microscopy	75
6.2.6.	<i>In Vitro</i> Biocompatibility of Inclusion Complexes	76
6.2.7.	Intracellular Antioxidant Activity of Formulations	77
6.2.8.	<i>In Vitro</i> Evaluation of the Anti-Inflammatory Activity	80
6.3.	Conclusions	81
	References of Chapter 6	83

CONTENTS

7. ELR-based Nanoparticles	87
7.1. Synthesis of the Outcomes Obtained in Collaboration	88
7.2. Materials and Methods	89
7.2.1. Materials	89
7.2.2. Methods	90
7.3. Results and Discussion	93
7.3.1. ELR-NPs Morphology and Size	93
7.3.2. Release Studies	95
7.3.3. <i>In Vitro</i> Biocompatibility of ELR-NPs	97
7.3.4. Intracellular Antioxidant Activity of ELR-NPs	98
7.3.5. Cellular Uptake of ELR-NPs	100
7.3.6. Penetration of ELR-NPs in <i>Ex Vivo</i> Porcine Corneas	103
7.4. Conclusions	107
References of Chapter 7	109
8. Contact Lenses Embedded with Micelles	115
8.1. Materials and Methods	117
8.1.1. Materials	117
8.1.2. Methods	117
8.2. Results and Discussion	121
8.2.1. Hydrogel Synthesis	121
8.2.2. Micelles Characterization	122
8.2.3. Hydrogel Characterization	123
8.2.4. Loading and Release of Pluronic® F127 Micelles and Free Drugs from Hydrogels	125
8.3. Conclusions	126
References of chapter 8	129
IV Concluding Remarks	133
9. Limitations and Future Work	135
10. Conclusions	137
V Resumen	139
11. Resumen	141
11.1. Motivación del estudio	141

11.2. Organización de la tesis doctoral	142
11.3. Hipótesis	144
11.4. Objetivos	144
11.5. Los Liposomas como Plataforma de Administración de Polifenoles Naturales	144
11.5.1. Objetivo	144
11.5.2. Metodología	145
11.5.3. Resultados	146
11.5.4. Conclusiones	147
11.6. Complejos de inclusión con ciclodextrinas: comparación entre complejos binarios y ternarios	147
11.6.1. Objetivo	147
11.6.2. Metodología	148
11.6.3. Resultados	151
11.6.4. Conclusiones	156
11.7. Nanopartículas basadas en ELR: potencial sistema de administración de fármacos para el tratamiento de la EOS	156
11.7.1. Objetivo	156
11.7.2. Metodología	157
11.7.3. Resultados	159
11.7.4. Conclusiones	166
11.8. Lentes de contacto embebidas en micelas: Un enfoque innovador para la administración oftálmica	166
11.8.1. Objetivo	166
11.8.2. Metodología	167
11.8.3. Resultados	168
11.8.4. Conclusiones	169
11.9. Limitaciones y trabajo futuro	170
11.10. Conclusiones de la tesis	171
Referencias del Capítulo 11	173

VI	Appendices	177
A. Review Article		179
B. Original Research Paper I		181
C. Original Research Paper II		183

CONTENTS

D. Original Research Paper III	185
E. Original Research Paper IV	187

CONTENTS

I

Preface

Table of Abbreviations

AFM	Atomic Force Microscopy	Microscopia de Fuerza Atómica
ANOVA	One-way Analysis of Variances	Análisis de varianza
API	Active Pharmaceutical Ingredient	Ingrediente Activo Farmacéutico
Bad	Bcl-2 Associated agonist of cell death	Bcl-2 Agonista Asociado a Muerte Celular
BAK	Benzalkonium chloride	Cloruro de Benzalconio
Bax	Bcl-2 Associated X-protein	Regulador de Apoptosis BAX
BCA	Bicinchoninic Acid	Ácido Bicinconínico
Bcl-2	B-cell lymphoma 2	Célula-B Linfoma 2
BSA	Bovine Serum Albumin	Albúmina de Suero Bovino
CALT	Conjunctiva-associated lymphoid tissue	Tejido Linfoide Asociado a Conjuntiva
CD	Cyclodextrin	Ciclodextrina
CE	Complexation Efficiency	Eficacia de la Complejación
CLs	Contact Lenses	Lentes a Contacto
CMC	Critical Micellar Concentration	Concentración Micelar Crítica
CN V	Cranial Nerve V	Nervio Cranial V
CN VII	Cranial Nerve VII	Nervio Cranial VII
CsA	Cyclosporine	Ciclosporina
Da	Dalton	Dalton
DDS	Drug delivery System	Sistema de Administración de Medicamento
DED	Dry Eye Disease	Síndrome de Ojo Seco
DLS	Dynamic Light Scattering	Dispersión Dinámica de la Luz
DMEM	Dulbecco's modified Eagle's medium	Medio de Eagle Modificado por Dulbecco
DMSO	Dimethylsulfoxide	Dimetilsulfóxido
DPBS	Dulbecco's phosphate buffered saline	Solución Salina Tamponada con Fosfato de Dulbecco
DSPC	1,2-Dioctadecanoyl-sn-glycero-3-phosphocholine	Distearoilfosfatidilcolina
EDTA	Ethylenediaminetetraacetic Acid	Ácido Etilendiaminetetraacético
EE	Encapsulation Efficiency	Eficiencia de Encapsulación
ELR	Elastin-like Recombinamer	Recombinámeros Basados en Elastina
EtOH	Ethanol	Etanol
FBS	Fetal Bovine Serum	Suero Fetal Bovino
FT-IR	Fourier-Transformed Infra-Red Spectroscopy	Espectrómetro de Infrarrojos por Transformada de Fourier
HA	Hyaluronic Acid	Ácido Hialurónico
HCE	Human Corneal Epithelial cells	Células Epiteliales Corneales Humanas
hEGF	Human Epithelial Growth Factor	Factor de Crecimiento Epitelial Humano
HEMA	Hydroxyethylmethacrylate	Hidroxietil Metacrilato
HPLC	High Pressure Liquid Chromatography	Cromatografía Líquida de Alta Presión
HPβCD	Hydroxypropyl- β -cyclodextrin	Hidroxipropil- β -Ciclodextrina

IFN-γ	Interferon Gamma	Interferón Gamma
IgA	Immunoglobulin A	Inmunoglobulina A
IgE	Immunoglobulin E	Inmunoglobulina E
IgG	Immunoglobulin G	Inmunoglobulina G
IM-ConjEpi	Immortalized Conjunctival Epithelial cells	Células Epiteliales Conjuntivales Inmortalizadas
ITT	Inverse Transition Temperature	Temperatura de Transición Inversa
JNK	c-Jun N-terminal kinases	Quinasas c-Jun N-terminal
LFU	Lacrimal Functional Unit	Unidad Funcional Lagrimal
LOD	Limit of Detection	Límite de Detección
LOQ	Limit of Quantification	Límite de Cuantificación
MAA	Methacrylic acid	Ácido Metacrílico
MAPK	Mitogen-activated protein kinase	Proteína Quinasas Activadas por Mitógenos
MDA-MB-231	Human Breast Adenocarcinoma cells	Células de Adenocarcinoma de Mama Humano
MFC7	Human Breast Cancer cells	Células de Cáncer de Mama Humano
MGD	Meibomian Gland Dysfunction	Disfunción de las Glándulas de Meibomio
MW	Molecular Weight	Peso Molecular
MWCO	Molecular Weight Cut-Off	Peso Molecular Límite
NF-κB	Nuclear Factor Kappa-Light-Chain of Activated B cells	Factor Nuclear Potenciador de las Cadenas Ligeras Kappa de las células B Activadas
NMR	Nuclear Magnetic Resonance	Resonancia Nuclear Magnética
NPs	Nanoparticles	Nanopartículas
OCT	Optimal Cutting Temperature	Temperatura Óptima de Corte
PBS	Phosphate Buffer Saline	Tampón Fosfato
PdI	Polydispersivity Index	Índice de Polidispersividad
PKC-α	Protein Kinase C-alpha	Proteína Quinasa C
PLGA	Poly(Lactic-co-Glycolic acid)	Ácido poli(láctico-co-glicólico)
PMMA	Polymethylmethacrylate	Polimetacrilato
PMS	5-methylphenazinium methyl sulphate	Metosulfato de Fenazina
QUE	Quercetin	Quercetina
RGC-5	Retinal Ganglion Cells	Células Ganglionares de la Retina
ROS	Reactive Oxygen Species	Especies de Oxígeno Reactivas
RP	Reverse Phase	Fase Inversa
RSV	Resveratrol	Resveratrol
RT	Room Temperature	Temperatura Ambiente
SAS	Supercritical Antisolvent	Antidisolvente Supercrítico
SCF	Supercritical Fluid	Fluido Supercrítico
SEM	Standard Error of the Mean	Error Estándar de la Media
SEM	Scanning Electron Microscopy	Microscopía Electrónica de Barrido
TFA	Trifluoroacetic Acid	Ácido Trifluoroacético
TNF-α	Tumor Necrosis Factor Alpha	Factor de Necrosis Tumoral Alpha
UV	Ultraviolet	Ultravioleta
UV-Vis	Ultraviolet-Visible	Ultravioleta-Visible

Financial Support

This research project was funded by the European Union's Horizon 2020 research and innovation program under the Marie-Sklodowska-Curie Initial Training Network (ITN) Integrated Training in Dry Eye Disease Drug Development IT-DED³ (H2020-MSCA-ITN-2017, Grant Agreement No. 765608).



Additional funding:

Spanish Ministry of Science, Innovation and Universities and European Regional Development Fund, RTI2018-094071-B-C21.



Short *Curriculum Vitae*

Luna Krstić obtained her Master Degree in Chemistry and Pharmaceutical Technology at the University of Padova (Italy). After completing her degree, she did a post-graduate internship in the Drug Delivery Laboratory at the same university, working on bioconjugates for cancer therapy. In the late 2018, she joined the Ocular Surface Group of the IOBA, at the University of Valladolid, to embark her PhD path within a MSCA funded network (IT-DED³). She has actively participated in different projects within the consortium. Also, she took part in the inter-University Master of Research in Vision Sciences as an invited lecturer several times.

ACADEMIC EDUCATION

- PhD candidate in the PhD program in Vision Sciences, University of Valladolid, Spain (October, 2018-present)
- Master's degree in *Chemistry and Pharmaceutical Technology* from the University of Padova, Italy (October, 2012-December, 2017)

PROFESSIONAL EXPERIENCE

- Researcher in the *Ocular Surface group* of IOBA, in a Proof-of-Concept project, RETINARTEX, funded by the Ministry of Science, Innovation and Universities (May, 2023-present)
- PhD candidate (October, 2018-present)
 - Participation in different courses and trainings organised in the framework of the IT-DED³ network
 - Collaboration in 4 peer reviewed scientific articles (2 as a first author) and in 7 congress presentations (6 as a first author)
 - Invited Lecturer in the course of *Biomaterials in Ocular Therapy* (2019,2020,2021, 2022)
- Post-graduate Internship, University of Padova (January, 2018-October, 2018)

Scientific Dissemination

The research work performed in this doctoral thesis resulted in 4 JCR indexed scientific publications and 1 is under preparation.

1. **Krstić, L.**; González-García, M.J.; Diebold, Y.
Ocular Delivery of Polyphenols: Meeting the Unmet Needs.
Molecules 2021, **26**,370.
doi.org/10.3390/molecules26020370
(JCR 2021 Impact Factor-4.927-Q2 in Chemistry,Multidisciplinary)
2. Abdallah, M.M.; Leonardo, I.C.; **Krstić, L.**; Enríquez-de-Salamanca, A.; Diebold, Y.; González-García, M.J.; Gaspar, F.B.; Matias, A.A.; Bronze, M.R.; Fernández, N.
Potential Ophthalmological Application of Extracts Obtained from Tuna Vitreous Humor Using Lactic Acid-Based Deep Eutectic Systems.
Foods 2022, **11**, 342.
doi.org/10.3390/foods11030342
(JCR 2021 Impact Factor- 4.121-Q1 in Health Professions)
3. García-Posadas, L., Romero-Castillo, I., Katsinas, N., **Krstić L.**, López-García, A., Diebold, Y.
Characterization and functional performance of a commercial human conjunctival epithelial cell line.
Exp Eye Res. 2022;**223**:109220.
[doi:10.1016/j.exer.2022.109220](https://doi.org/10.1016/j.exer.2022.109220)
(JCR 2021 Impact Factor- 3.467-Q1 in Ophthalmology)
4. **Krstić, L.**, Jarho, P, Rupunen, M, Urtti, A, González-García, M.J., Diebold, Y.
Improved ocular delivery of quercetin and resveratrol: A comparative study between binary and ternary cyclodextrin complexes.
Int J Pharm. 2022;**624**:122028.
[doi:10.1016/j.ijpharm.2022.122028](https://doi.org/10.1016/j.ijpharm.2022.122028)
(JCR 2021 Impact Factor- 6.510-Q1 in Pharmaceutical Science)
5. **Krstić, L.**, Vallejo, R., Rodriguez-Rojo, S., Girotti, A., Arias, F.J., González-García, M.J., Diebold, Y.
ELR-based nanoparticles as a platform for ophthalmic delivery of quercetin and resveratrol (manuscript in preparation)

In addition, the PhD candidate participated in the following congresses:

Oral Presentations:

1. **Krstić L.**

Use of natural compounds for treatment of DED and strategies for drug delivery.
1st European Dry Eye Society Virtual Congress (EuDEC).
(June 18th-19th 2021)

2. **Krstić L.**

Development of new carriers to improve the bioavailability of natural compounds to treat ocular surface disorders.
Joint meeting OcuTher & IT-DED³, Nice, France
(October 16th, 2019)

Poster Presentations:

1. **Krstić L.;** González-García M.J., Diebold Y.

Quercetin and resveratrol in combination with HP- β -Cyclodextrin protect human conjunctival epithelial cells from oxidative stress.
1st European Dry Eye Society Virtual Congress (EuDEC).
(June 18th-19th 2021)

2. **Krstić L.,**Jarho P.; Ruponen M.; Urtti A.; González-García M.J., Diebold Y.

HP- β -Cyclodextrin: a simple but effective strategy to improve the physico-chemical characteristic of resveratrol and quercetin for ocular application.
The Controlled Release Society 2021 Virtual Annual Meeting
(July 25th-29th 2021)

3. **Krstić L.;** Vallejo R.; Rodriguez-Rojo S.; Girotti A.; Arias F.J.; González-García M.J., Diebold Y.

Topical ophthalmic delivery of quercetin and resveratrol using elastin-like recombinamer nanoparticles.
The Association for Research in Vision and Ophthalmology (ARVO) Annual Meeting
(May 1st-4th 2022)

4. Abdallah M., Leonardo I., **Krstić L.**, Gaspar FB., Enríquez-de-Salamanca A., Diebold Y., González-García M.J., Ana A. Matias, Bronze MR, Fernández N.
Extraction of bioactive compounds from fisheries waste streams using natural eutectic solvent systems for their therapeutic application.
9th IUPAC Conference on Green Chemistry
(5th-9th September 2022)

5. **Krstić L.**; Vallejo R.; Rodríguez-Rojo S.; Girotti A.; Arias FJ; González-García M.J., Diebold Y.
Encapsulation of natural polyphenols in elastin-like recombinamer nanoparticles through the use of the supercritical anti-solvent method.
4th SPLC-CRS Young Scientist Meeting
(February 6th-7th 2023)

Abstract

Polyphenols constitute one of the most widespread class of compounds throughout the plant kingdom. Among them, quercetin (QUE) and resveratrol (RSV) emerge for their extraordinary beneficial health effects. Although widely studied, currently there are no commercially available formulations of these compounds. Given their extensive potential in the treatment of diverse health disorders, including ones related with the ocular surface, the main goal of this thesis was the development of formulations capable of circumventing the physico-chemical limitations (such as poor aqueous solubility and low chemical stability) that the two molecules possess. Moreover, an advanced formulation strategy will help overcome the physiological and anatomical barriers related to the targeted tissues in the ocular surface.

The first choice for the ocular delivery of QUE and RSV were liposomes. Two distinct size-reducing methods were explored successfully. However, a problem with a low encapsulating efficiency of both molecules was found which was not possible to address with the resources that we had available. Further analysis have to be done in this regard.

Formation of inclusion complexes with hydroxypropyl- β -cyclodextrin (HP β CD) have revealed to have a favourable effect on the solubility and chemical stability of the two polyphenols. These characteristics were further improved with the addition of hyaluronic acid (HA) to the binary complex (drug:CD). Both types of complexes were biocompatible with corneal (HCE) and conjunctival (IM-ConjEpi) epithelial cell lines. Additionally, the complexes were capable of scavenging reactive oxygen species (ROS) intracellularly in the previously mentioned cell lines.

Elastin-like recombinamer (ELR) nanoparticles encapsulating QUE, RSV or both polyphenols were prepared through the supercritical antisolvent (SAS) process. *In vitro* release studies performed in simulated tear fluid unveiled the potential of ELR-NPs to control the release rate of hydrophobic active pharmaceutical ingredients (APIs). ELR-NPs carrying QUE, RSV or both did not cause any cytotoxic effect in HCE cells. Besides, all the formulations were efficacious in neutralizing ROS. *Ex vivo* studies manifested the ability of the ELR-NPs to penetrate corneal layers and deliver their payload beyond the corneal epithelium.

As a compelling delivery strategy contact lenses (CLs) embedded with micelles were explored. Hydroxyethylmethacrylate (HEMA) and HEMA/MAA (methacrylic acid) based hydrogels were prepared by thermal polymerization, while the micelles made of Pluronic[®] F127 were prepared by solvent evaporation method. Drug load-

ing into micelles resulted in an extremely high yields of encapsulation efficiency and in solubility improvement of the two compounds. Solvent uptake and light transmittance were in accordance with what reported in literature for these types of hydrogels. Problems were encountered with the loading and releasing process of the colloidal carrier from the hydrogels. Therefore, this part of the experimental procedures needs to be revised and further developed.

In conclusion, four different formulations were studied for the topical ophthalmic delivery of QUE and RSV. Two of them, inclusion complexes with HP β CD and ELR-NPs displayed promising results. These formulations were capable of positively influencing the limiting physico-chemical characteristics of the two polyphenols. Besides, they showed to be biocompatible and to protect the ocular surface epithelial cells from oxidative stress. In summary, the two systems may be considered as good candidates for the subsequent stage of drug development. Regarding liposomes and CLs loaded with micelles, further adjustment in the design and performance of the assays has to be carried out, in order to fully exploit their possibilities.

Organization of the Doctoral Thesis

The present doctoral thesis report has been prepared in the form of **standard modality**, and it applies for the International-Awarded Doctoral Thesis Degree. The scientific work presented in this thesis has been performed at the University of Valladolid (UVa), following the directives of the Doctoral School of the University of Valladolid (EsDUVa). During the doctorate training period, a three-month academic secondment was performed at the *Faculty of Health Sciences, School of Pharmacy of the University of Eastern Finland* (Kuopio, Finland). An additional one-month academic secondment was performed at the *Pharmacology, Pharmacy and Pharmaceutical Technology department of the University of Santiago de Compostela* (Santiago de Compostela, Spain).

The thesis report meets the following criteria requested by the EsDUVa to allow the candidate to publicly defend the thesis work presented:

- The thesis report has been written in English.
- A general summary in Spanish has been included.
- The thematic unit of the study conducted in the thesis has been justified.
- The objectives, methodology, results, discussions, and conclusions have been presented.
- A minimum of one publication in a peer reviewed journal between Q1 and Q3, derived from the thesis results has been published.

As a part of the appendices, four published manuscripts are presented as well as the one in preparation/revision.

The main idea of the thesis work is exposed in the preface, which contains the motivation, a general introduction about the ocular surface, DED, polyphenols, and drug

delivery systems, and a well-defined hypothesis and objectives. The scientific results are divided into four chapters, each one corresponding to a particular formulation strategy that was proposed to ease the understanding of the work. Each chapter is subsequently divided into a short introduction about the formulation strategy used, methodology, results, discussion, and conclusions.

The chapters related to the scientific results are as follows and are schematically represented in figure 1:

- **Chapter 5: Liposomes as a Potential Delivery Platform for Natural Polyphenols.**

To improve the physico-chemical characteristics of the two polyphenols of interest, liposomes were proposed as an initial formulation strategy.

- **Chapter 6: Inclusion Complexes with Cyclodextrins: Comparison Between Binary and Ternary Complexes.**

The formation of complexes with cyclodextrins is an effective way to improve the aqueous solubility of the compounds of interest, while the addition of hydrophilic polymers to already existing drug:CD complexes is a strategy to further improve chemical stability.

- **Chapter 7: ELR-based Nanoparticles: A Prospective Drug Delivery System for DED Treatment.**

The use of protein-based biopolymers, like recombinant elastin, with tunable properties appears to be a good formulation strategy for naturally occurring compounds. In addition, the manufacturing process using supercritical fluids, enables the production of a product with a minimum content of organic solvent.

- **Chapter 8: Contact Lenses Embedded with Micelles: An Innovative Approach to Ophthalmic Delivery.**

Therapeutic CLs in combination with colloidal carriers represent an interesting approach for the delivery of active principles to the ocular surface, where a significant improvement in residence time and bioavailability can be achieved.

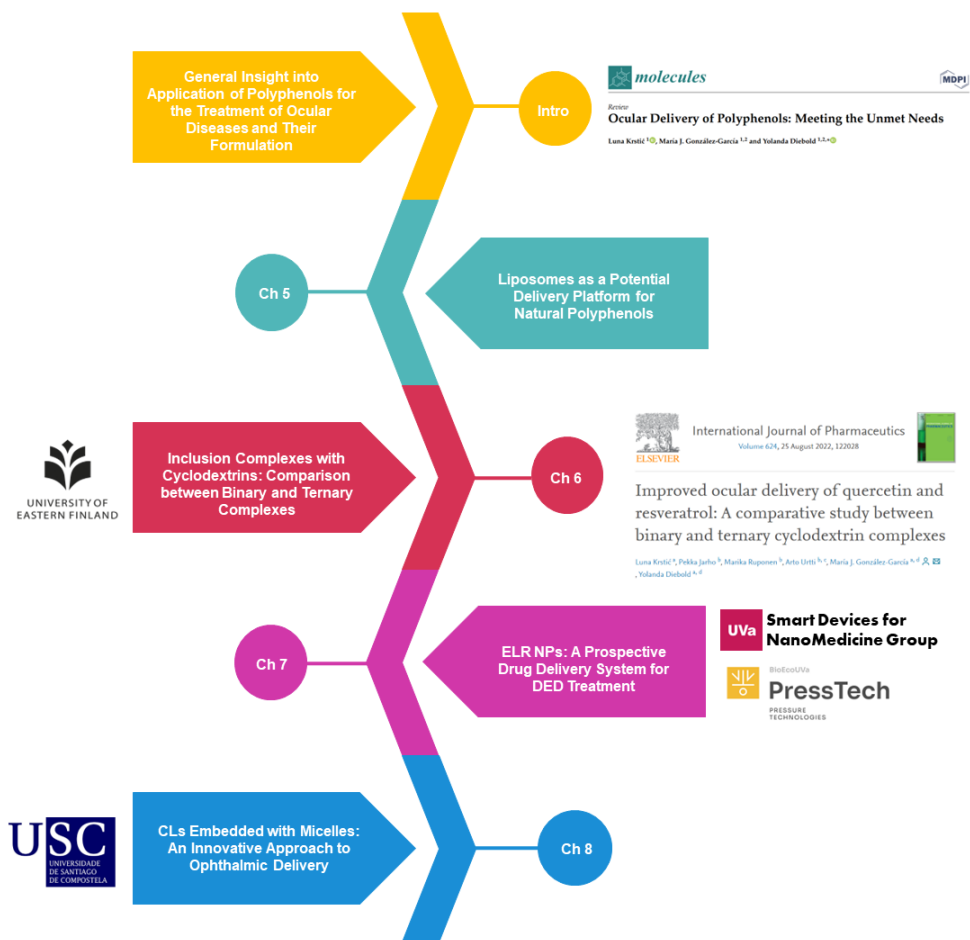


Figure 1: Schematic representation of the thesis organization.

II

Introduction

1

Introduction

The eye is a unique sensory organ with complex anatomical and physiological features. As a unit, it can be divided into two main segments: the anterior segment, which comprises the cornea, the conjunctiva, the iris, the ciliary body, and the lens, and the posterior segment, which includes the choroid, the retina, and the sclera. The light that enters the eye is refracted by the cornea, then proceeds through the lens, and finally reaches the retina, which, once the photoreceptor cells are activated, enables signal transduction to the brain and the generation of an image (Awwad *et al.*, 2017; Gipson *et al.*, 2010; Souto *et al.*, 2019).

1.1. The Ocular Surface and the Lacrimal Functional Unit

The ocular surface comprises the tissues of the eye that are more exposed to the external environment, which are the cornea, the conjunctiva, the principal and accessory lacrimal glands, the Meibomian glands, and the tear film (Thoft *et al.*, 1979). Alongside the annexed secretory glands (lacrimal and Meibomian glands) and the vast neuronal network, it forms the Lacrimal Functional Unit (LFU), as shown in **figure 1.1**. LFU controls normal tear secretion and, through this, directly influences the provision of i) a smooth optical surface needed for the correct refraction of light, ii) protection against bacterial and viral infections, and iii) the maintenance of the ocular surface equilibrium (Stern *et al.*, 2004, 2013).

1.1.1. Tear Film

The tear film represents a highly complex interface between the external environment and the corneal epithelium. Recent evidence suggests that it is made up of an external lipid layer and a continuous muco-aqueous layer, as represented in **figure 1.2** (Gipson *et al.*, 2007). The lipid layer contains a variety of lipids that are secreted in a holocrine manner by the Meibomian glands, with a modest contribution from the

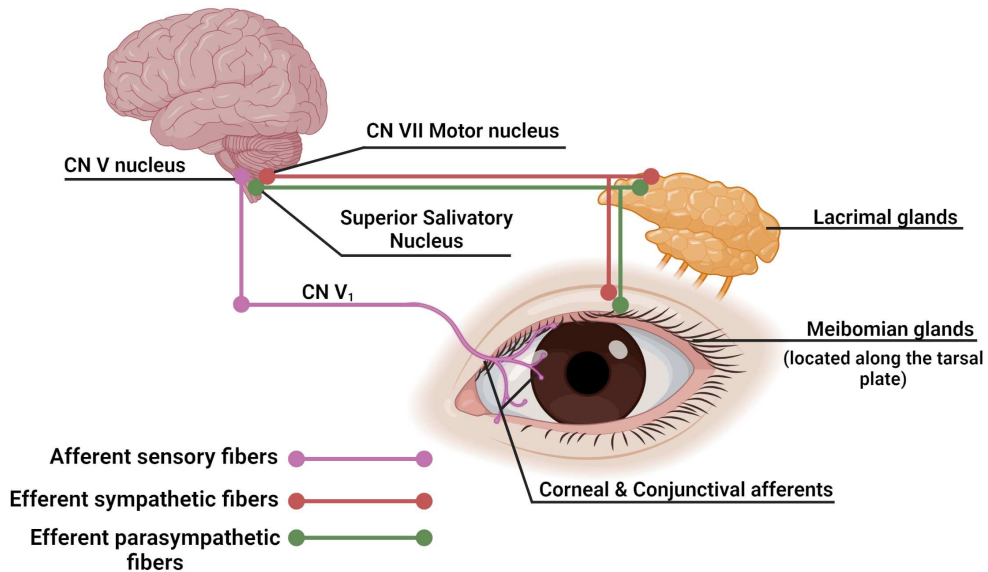


Figure 1.1 - Illustration of the Lacrimal Functional Unit. Prepared with BioRender®.

glands of Moll and Zeiss. The lacrimal glands are mainly responsible for the secretion of the aqueous fluid together with the secretion of different proteins and electrolytes, while the mucins that form the mucous part of the muco-aqueous layer originate from the goblet and non-goblet secretory epithelial cells present in the conjunctival epithelium (Dartt *et al.*, 2013; Hodges *et al.*, 2013a).

Regarding the electrolytes, a greater concentration of sodium, potassium, and chloride is found in the tear film in comparison to the plasma, which assures the maintenance of the osmotic pressure (Gilbard *et al.*, 1994). The presence of low molecular weight (MW) metabolites in the tear film depends strongly on the expression of specific transporters in the corneal and conjunctival epithelia, and this affects the concentration of glucose, lactate, and urea (Jäger *et al.*, 2022; Takahashi *et al.*, 1996; Tiffany *et al.*, 2008). Lactoferrin, lipocalin, lysozyme, and secretory IgA are the most abundant proteins in the tear film. Lipocalin, also known as specific tear pre-albumin, is a lipid-binding protein that removes the surplus of lipids from the tear film, preventing the formation of non-wettable surfaces. Lactoferrin, produced by the acinar tissue of the lacrimal gland, functions as a high-affinity iron-carrier, making this metal ion inaccessible for bacteria. Another protein with a bacteriolytic role is lysozyme, which is capable of digesting the outer cell wall of gram-positive bacteria through its muramidase activity (Tiffany *et al.*, 2008; Van Haeringen *et al.*, 1981). The primary immunoglobulin in the tear film is IgA, secreted by the interstitial plasma cells of the lacrimal gland and

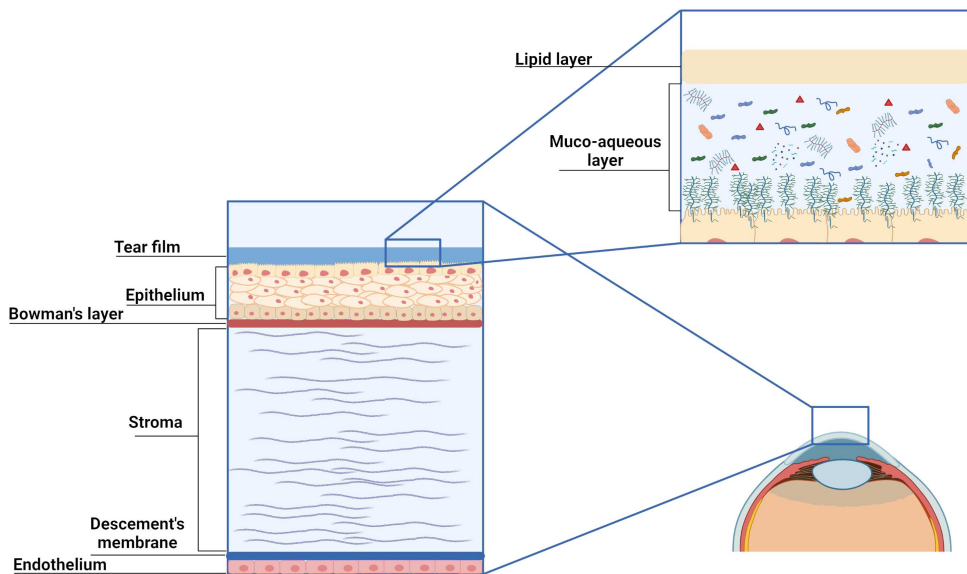


Figure 1.2 - Cross-sectional view of the corneal and tear-film layers. Prepared with BioRender®.

by the conjunctival epithelia and coupled to a secretory component before it reaches the ocular surface (Knop *et al.*, 2008). Secretory IgA offers immunological protection against viruses and microorganisms. Except for IgA, other immunoglobulins that can be found in the tear film are IgG and IgE, although in very low concentrations and following a harmful event (McClellan *et al.*, 1973). Ascorbic acid, cysteine, glutathione, tyrosine, and uric acid are described as physiological water-soluble small MW antioxidants that protect the ocular surface from oxidative stress generated by external factors (Gogia *et al.*, 1998; Venkata *et al.*, 2012).

The lipids secreted by the Meibomian glands have as a principal function to secure the preservation of a smooth optical surface, to prevent the evaporation of the underlying aqueous layer, and to lower the surface tension. All of these are achieved by the orientation of polar (tear-mucin interface) and non-polar lipids (air-tear film interface). The lipids of the tear film have been reported to belong to classes of wax and cholesterol esters, phospholipids, try-, di-, and monoglycerides, and free fatty acids (Greiner *et al.*, 1996; Wollensak *et al.*, 1990).

Mucins are produced by the conjunctival and corneal epithelia and, to a lesser extent, by the lacrimal gland and are glycoproteins with a polypeptide backbone rich in

serine and threonine, forming O-glycoside bonds with oligosaccharide molecules (?). They play an important role in the lubrication of the corneal surface and the spreading of the tear film. Two main types of mucins are distinguished: membrane-spanning and secretory. Secretory mucins are further divided into non-gel-forming and gel-forming (Paulsen *et al.*, 2006). Several membrane-spanning mucins like MUC-1, -4, -16, and -20 are found on the ocular surface. These mucins are anchored through the polypeptide backbone to the epithelial cells of the cornea and conjunctiva (Pflugfelder *et al.*, 2000; Spurr-Michaud *et al.*, 2007). Small secretory mucins such as MUC-7 are suggested to play an important role in protecting the ocular surface from bacterial expansion (Hodges *et al.*, 2013a). Goblet cells in the conjunctiva have been reported as the largest sources of gel-forming mucins; however, some of them have been found as well in the lacrimal gland and apical cells of the cornea (Spurr-Michaud *et al.*, 2007). MUC-5AC is reported as the most abundant and most studied gel-forming mucin (McKenzie *et al.*, 2000).

1.1.2. Cornea

Due to its anatomical features, the cornea represents one of the most important structures of the ocular surface for the preservation of visual function. It is a convex, transparent, and avascular tissue that together with the overspreading tear film, accounts for two-thirds of the total refractive power of the eye (Klintworth *et al.*, 1977). The direct exposure to the external environment makes it act as a primary structural barrier to exogenous substances like dust, microorganisms, or even topically applied drugs (Forrester *et al.*, 1996).

Although the cornea is continuous with the white, opaque sclera, they possess opposite internal compositions. This is justified by their distinct roles in ocular anatomy and physiology. The border of the cornea, continuous to the sclera, is called the limbus. This part of the cornea plays an important role in the corneal response to injuries since it contains the niche of cornea-specific stem cells (Schermer *et al.*, 1986; ?).

With a nerve density almost 400 times higher than the skin, the cornea is the most innervated tissue in the human body. Polymodal corneal nociceptors (sensitive to mechanical, thermal, and chemical stimulation) are free nerve endings that represent an extension of the trigeminal cranial nerve (CN V). When stimulated by exogenous factors, the afferent pathway of the CN V is activated. Subsequently, the lacrimal nucleus, through the efferent pathway of the CN VII - facial nerve, stimulates the tear secretion by the lacrimal glands (Mensher *et al.*, 1974; Zander *et al.*, 1948).

Since the cornea lacks a supply of blood vessels, the aqueous humour and the tear

film are responsible for furnishing it with nutrients and oxygen (Maurice *et al.*, 1962; Pirie *et al.*, 1955).

Histologically, the cornea can be divided into three cellular layers (epithelium, stroma, and endothelium) and two interfaces (Bowman's layer and Descemet membrane) (Teichmann *et al.*, 2013) (**figure 1.2**). The outermost epithelium is made of non-keratinized stratified squamous epithelial cells. This layer consists of superficial, wing, and columnar basal cells (Schermer *et al.*, 1986). Only the latter are capable of mitosis and function as a source of superficial and wing cells during regular physiological turnover (every 7-10 days) (Dua *et al.*, 1993). In between the epithelium and the stroma, lies the Bowman's layer, an acellular accumulation of short collagen type I fibrils. Its function is to maintain the cornea's shape. More than 85% of the corneal thickness is occupied by the stroma. The stroma is mostly made up of collagen fibres (type I), which are organised in parallel layers called lamellae (Del Monte *et al.*, 2011; Komai *et al.*, 1991). Thanks to the uniformity of the collagen fibrils and their spatial organisation, corneal transparency is preserved (Birk *et al.*, 1990; Hart *et al.*, 1969; Meek *et al.*, 2015). Keratocytes are mesenchymal-derived cells, sparse between stromal collagen lamellae. Due to the dendritic processes that they have, they form a cellular network through which they are able to communicate between each other. Upon injury, keratocytes are capable of differentiating into reparative cell phenotypes through the action of different stimuli (Hay *et al.*, 1979; Muller *et al.*, 1995; Stramer *et al.*, 2003). The Descemet membrane is an amorphous structure prior to the endothelium. The innermost stratum of the cornea is the endothelium, which consists of a single cell layer, whose density decreases throughout life. Because of its leaky nature and the presence of a vast range of ion-transporters, the corneal endothelium plays an important role in supplying the cornea with nutrients and maintaining its transparency (Bonanno *et al.*, 2003; Del Monte *et al.*, 2011; Mishima *et al.*, 1982).

1.1.3. Conjunctiva

The conjunctiva is a part of the anterior segment of the eye that covers the inner surface of the eyelids, extending from the front surface of the eyeball until the cornea. Topographically, the conjunctiva can be divided into bulbar, which overlays the sclera until the cornea; palpebral, which lines the inner surface of the upper and lower eyelids; and forniceal, which connects the palpebral and the bulbar conjunctiva (Kessing *et al.*, 1967).

Based on a histological analysis, the conjunctiva can be divided into two main layers: the epithelium and the stroma. The epithelium is made up of a few cell layers,

generally of polygonal shape, and is therefore classified as a stratified columnar cell layer (Nichols *et al.*, 1996). The apical surface of the epithelium possesses outfoldings named microvilli, whose role is to stabilise and anchor the tear film throughout the glycocalyx. Mucins produced by goblet and non-goblet conjunctival epithelial cells contribute to the generation of the mucous component of the tear film (Gipson *et al.*, 2016; Nichols *et al.*, 1996).

The conjunctival stroma is found directly under the epithelium, and it is a layer furnished with nerve endings, blood, and lymphatic vessels. The lymphatic vessels, along with the presence of B and T lymphocytes, which are diffusely present and organised in follicles, form the so-called Conjunctiva Associated Lymphoid Tissue (CALT). CALT plays an important role in maintaining the immune homeostasis of the ocular surface and in the setting off and propagation of the immune response (Cano-Suárez *et al.*, 2021; Knop *et al.*, 2005).

1.2. Ocular Surface Diseases

To preserve the homeostasis of the LFU, all the structures associated with it (cornea, conjunctiva, tear film, lacrimal and Meibomian glands, neural and lymphatic networks) respond to distinct environmental and internal threats through fine functional cooperation. In the instance that this collaborative mechanism fails, pathological conditions occur (Stern *et al.*, 1998).

Diseases of the ocular surface comprise an extensive number of anomalies that may be primarily developed or secondary to other ophthalmic or systemic disorders. Activation of the inflammatory cascades has been reported as the core etiopathological mechanism of the most prevalent ocular surface diseases such as blepharitis, ocular allergies, and DED (Bernardes *et al.*, 2010; Leonardi *et al.*, 2021; Messmer *et al.*, 2015).

1.2.1. Dry Eye Disease

The first notion of a condition affecting the tears was suggested by Schirmer back in 1903 (Schirmer *et al.*, 1903). For more than 50 years, Dry Eye Disease (DED) was recognised as keratoconjunctivitis sicca in Sjögren's syndrome. In 1995, a workshop organised by the National Eye Institute defined DED for the first time as a disorder of the tear film with consequent damage to the ocular surface (Lemp *et al.*, 1995). In 2007, an agreement between ocular care practitioners was achieved at the first International Dry Eye Workshop, where DED was defined as a multifactorial disorder of

the ocular surface and overlying tear film, in which the compromised homeostasis of the tear film leads to its instability, an inflammatory status, and damage of the corneal epithelial barrier accompanied by neurosensory abnormalities (Lee *et al.*, 2018; Lemp *et al.*, 2007).

DED patients are affected in their daily lives as recurrent symptoms comprise ocular dryness, discomfort and visual disturbance, photophobia, itching, and burning sensation (Jackson *et al.*, 2022; Wei *et al.*, 2014). Diagnostic tools such as measurement of the tear volume and break-up time and quantification of the tear osmolarity coupled with specific questionnaires serve to detect DED and assess its severity (Kojima *et al.*, 2020; Wolffsohn *et al.*, 2017).

The two main classes of DED are aqueous deficient and evaporative dry eye. These two classes can be further classified in different subgroups according to the main cause that led to the development of DED (Lemp *et al.*, 2007).

Evaporative dry eye is correlated with the dysfunction of the Meibomian glands (MGD). Subjects with MGD have an altered chemical composition of the meibum (decreased levels of cholesterol triacylglycerides and hydroxyl fatty acids) which reflects in an abnormal viscosity and appearance (Borchman *et al.*, 2010; Lee *et al.*, 2018). These alterations can be associated with age-related changes but also with a hyperkeratinization process that leads to Meibomian glands obstruction (Yeotikar *et al.*, 2014). As a result, the outermost layer of the tear film, the lipid layer, loses its functional ability to reduce the surface tension and to impede the evaporation of the tear film, thus evolving into DED (Bland *et al.*, 2019; Cwiklik *et al.*, 2016).

Aqueous-deficient dry eye occurs after impairment of the lacrimal acinar cells in the lacrimal glands. This condition can lead to a loss of the mucin producing goblet cells, vital for the maintenance of tear film stability. The indicated alterations trigger pro-inflammatory signalling cascades, which intensify the instability of the tear film and close the self-maintaining cycle of DED (Alam *et al.*, 2021; Pflugfelder *et al.*, 2017a, 2015; Rouen *et al.*, 2018).

1.2.2. Pathophysiological Mechanism of Dry Eye Disease

In the pathological process of DED, a cascade of events takes place, commencing with the tear dysfunction, developed as a consequence of a compromised component/s that are part of the LFU. A variety of starting events may cause the onset of the disease and the initiation of an inflammatory response, as shown in **figure 1.3**. This involves exposure to environmental stress and dry environments, worsening conditions of an autoimmune disease, refractive surgery, contact lens (CLs) wear, medications,

preservatives, and allergens (Perez *et al.*, 2020; Stern *et al.*, 2013).

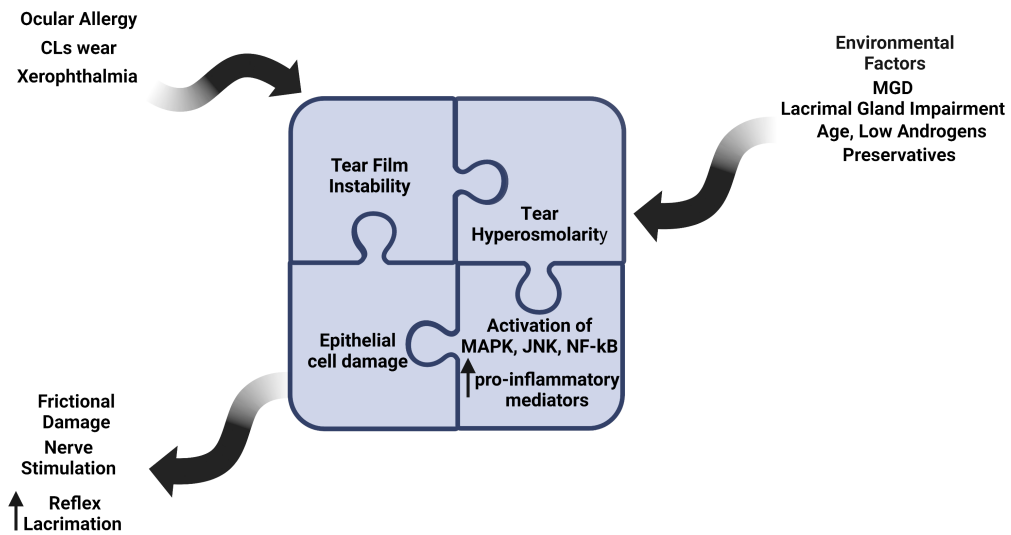


Figure 1.3 - DED vicious cycle. Prepared with BioRender®.

In response to the mentioned triggers, signalling pathways involving mitogen-activated protein kinase (MAPK), c-Jun N-terminal kinase (JNK), nuclear factor kB (NF-kB), and activator protein-1 are activated within the surface epithelial cells with the subsequent generation of inflammatory mediators (IL-1, IL-6, TNF- α , IL-8) (De Paiva *et al.*, 2006; Li *et al.*, 2004; Pflugfelder *et al.*, 2005) Consequently, goblet and non-goblet epithelial cells undergo apoptosis. The latter promotes the instability of the tear film, aggravating the already present hyperosmolarity, which in turn accentuates the inflammatory response. Like this, the self-perpetuating DED cycle is closed (Baudouin *et al.*, 2019).

It is important to emphasise the involvement of the immune response in the inflammatory process that lies behind the DED. The innate immune response on the ocular surface starts, as explained above, after the activation and secretion of different pro-inflammatory cytokines. These cytokines, in particular IL-1 and TNF- α are responsible for the activation and maturation of antigen presenting cells. Once mature, the mAPC migrate to the nearby lymph node by the afferent arm of the immune response, where they participate in the conversion of naïve TH₀ cells into effector T cells. Based on the proportion of expressed signalling molecules (IL-12, TGF- β , IL-23) specific subtypes of effector T cells will differentiate. Effector T cells infiltrate the ocular surface and annexed glands following the efferent arm of the immune response by means of blood vessels. Infiltration of T cells, especially TH₁ and TH₁₇,

with the concomitant release of inflammatory cytokines (IFN- γ , IL-17) leads to DED with chronic inflammation (Ganesalingam *et al.*, 2019; Perez *et al.*, 2020; Periman *et al.*, 2020; Pflugfelder *et al.*, 2017b; Stern *et al.*, 2004).

Oxidative stress is proposed as an additional alternative origin of the DED cycle (Li *et al.*, 2022). The generation of reactive oxygen species (ROS) and oxidative stress occurs because of a disbalance between the pro- and antioxidant systems inside the cells. This causes the damage of intracellular macromolecules such as lipids, proteins, and nucleic acids, with consequential cellular death. Choi *et al.* have described the presence of hydroxy-2-nonenal and malondialdehyde, products of lipid peroxidation and oxidative stress markers, in the tear film of DED patients (Choi *et al.*, 2016). This opens a new direction in the treatment of DED.

1.2.3. Epidemiology and Risk Factors

DED is one of the most frequent reasons for visiting ocular care practitioners. Efforts shall be invested in research labour with the aim of improving the life quality of the patients while also reducing the economic burden on the public health care system that is experiencing uninterrupted growth (Tavakoli *et al.*, 2022; Wang *et al.*, 2021).

DED has been associated with various risk factors, which include environmental, clinical (general health conditions and eye health), and personal conditions. Adverse environmental settings such as low humidity, windy, or polluted areas showed to increase the risk of DED occurrence. A study conducted in Korea on more than 16.000 participants, showed that higher ozone levels and air pollution significantly influenced the development of DED (Hwang *et al.*, 2016). In another study subjects that were regularly exposed to very low humidity (under 1 %) in their working environment were evaluated during a three-year period. At the end of the study, the prevalence of DED increased by 32.8 % (Cho *et al.*, 2014). Over the last few years, the extended use of displays (especially PC screens and mobile phones) has given rise to more DED cases among young people. It is hypothesised that in the course of display use, the rate of blinking decreases and that this consequently leads towards higher tear evaporation and therefore an unstable tear film (Argilés *et al.*, 2015; Wolkoff *et al.*, 2005).

Regarding the individual risk factors, particular emphasis should be placed on age, sex, ethnicity, and the use of CLs. Many studies have reported a correlation between advanced age and DED development. DED is more commonly developed in women than in men (Schaumberg *et al.*, 2013), especially in postmenopausal women (Stern *et al.*, 2004). According to some analysis, being of Asian ethnicity would rep-

represent a risk factor for DED. Indeed, a two-times higher incidence was detected in Asians than in Caucasians (Stapleton *et al.*, 2017). CLs wearers were reported to be four times more likely to develop severe DED (Uchino *et al.*, 2008).

There are diverse autoimmune diseases that secondarily lead to DED development, like Sjögren syndrome, rheumatoid arthritis, or sarcoidosis. Additionally, chronic clinical conditions like diabetes, Parkinson's disease, hepatitis C and thyroid abnormalities increase the risk of DED development (Rouen *et al.*, 2018; Stapleton *et al.*, 2017).

1.2.4. Current Treatments and Their Limitations

In DED management, artificial tears are often chosen as the first therapeutic approach (Nelson *et al.*, 1989). Except for their important role in lubricating the ocular surface, artificial tears are reported to decrease tear hyperosmolarity by dilution of solutes present in the tear film and therefore re-establish tear film stability (Aragona *et al.*, 2021; Kim *et al.*, 2021). Often viscosity-enhancing agents like natural (hyaluronic acid) or semi-synthetic polymers (hydroxypropyl cellulose, carboxymethyl cellulose) are added to these formulations with the aim of enhancing the lubricating effect and extending the retention time on the ocular surface (Wegener *et al.*, 2015). Although largely in use, artificial tears provide only a temporary relief from the symptoms of DED, preventing their expansion. Many artificial tear formulations contain different preservatives that, after longer use, may have an adverse effect on the ocular surface (Aragona *et al.*, 2021; Bernal *et al.*, 1991; Goldberg *et al.*, 2015).

More attention has been given to therapeutic approaches able to block the self-perpetuating vicious cycle of DED. This strategy relies on the employment of anti-inflammatory agents and, recently, anti-oxidative agents which are still in the pre- and clinical stages of research (Pellegrini *et al.*, 2020). Topical and systemic corticosteroids, fluorometholone, and hydrocortisone have been demonstrated to ameliorate both signs and symptoms in moderate and severe DED patients (Módis *et al.*, 2011; Pinto-Fraga *et al.*, 2016). Yet, protracted use of corticosteroids can lead to adverse effects like elevated intraocular pressure or cataract formation, so only short-term therapy with corticosteroids is advised (Gaballa *et al.*, 2021.).

Cyclosporine A (CsA), a cyclic peptide of fungal origin capable of inhibiting the activation of lymphocytes and the production of pro-inflammatory cytokines, is used for the management of autoimmune diseases and allergies and as an anti-rejection treatment after organ transplants (Jones *et al.*, 2017; Milner *et al.*, 2016). Due to its anti-inflammatory properties, CsA (0.05% topical solution) was approved by the FDA in

2003 as a treatment for DED (Laibovitz *et al.*, 1993; Pflugfelder *et al.*, 2004). Besides the reduction of inflammatory markers, CsA reduces tear hyperosmolarity and recovers goblet cell density in conjunctival cells (Pflugfelder *et al.*, 2008; Sall *et al.*, 2000). It has been reported that signs and symptoms of DED improved in more than 50 % of patients who were applying topical CsA (Módís *et al.*, 2011). Despite being efficacious in managing DED, some patients experience itching and eye irritation upon instillation of CsA, which represents a disadvantage in its therapeutic use (Lei *et al.*, 2011).

Lymphocyte activation and their infiltration into the ocular surface play a central role in the evolution of chronic inflammation associated with DED. Following this line, a novel drug for the treatment of dry eye, Lifitegrast, was approved by the FDA in 2016. Lifitegrast, a small integrin agonist, inhibits the adhesion of T- cells to intercellular adhesion molecule-1. This approach permits control of the T-cell-mediated inflammation linked to DED (Perez *et al.*, 2016; Thulasi *et al.*, 2017; Zhong *et al.*, 2012). Nevertheless, as in the case of CsA, patients frequently report blurred vision and discomfort associated with the use of this therapeutic agent (Lollett I. *et al.*, 2018).

Antibiotics from the classes of macrolides and tetracyclines are used for the treatment of DED related to MGD. They follow a double mechanism of action: they control the microbiome that caused MGD and exert an anti-inflammatory effect on the ocular surface. Gastro- Intestinal disturbance is often experienced by patients subjected to this treatment (Vernhardsdottir *et al.*, 2022).

A promising innovation in the therapeutic arsenal against DED is the anti-oxidative approach. As already mentioned, oxidative stress is considered to play a crucial role in the pathogenesis of DED, so its regulation could represent a revolution in the DED treatment. As potential molecules for this application, emerges the class of secondary plant metabolites, the polyphenols (Faveroet *et al.*, 2021; Nebbioso *et al.*, 2016). Even though, acclaimed for their many health effects their clinical application in ophthalmology still lacks robust evidence.

1.3. Polyphenols

This section was published as a part of the following article:

Ocular Delivery of Polyphenols: Meeting the Unmet Needs

Krstić, L., González-García, M.J.; Diebold, Y.,

Molecules **26**, 370 (2021).

Polyphenols represent one of the most abundant groups of phytochemicals present in nature; indeed, more than 10,000 different compounds can be found throughout the plant kingdom (Bungau *et al.*, 2019). As secondary metabolites, they have different roles, such as prevention of pathogen development and protection from UV radiation. Beside these, polyphenols offer protection from excessive development of reactive oxygen species (ROS), herbivores, and environmental stresses. Additionally, they are involved in physiological functions that are essential for the well-being of the plant. Higher resistance to predators, pigmentation, lignification, or increased astringency of fruit are some of these functions (El Gharras *et al.*, 2009; Fraga *et al.*, 2010).

1.3.1. Synthetic Pathways of Polyphenols

There are two main synthetic pathways through which polyphenols are built in plants, the shikimate and the malonate-acetate pathway, represented in **figure 1.4**. (Kondratyuk *et al.*, 2004). Activation of these synthetic pathway is promoted by different biotic and abiotic factors; these include adverse temperature and pH, the presence of pathogens and herbivores, and stress produced by an excessive concentration of heavy metals or salts (Francenia Santos-Sánchez *et al.*, 2019.; Mandal *et al.*, 2010). The first one comprises seven consecutive enzymatic steps that are carried out in the chloroplast. In the second pathway, the phenolic ring structure is formed under the successive addition of malonyl coenzyme A moieties to the polyketide chain; these sequential reactions characterize the malonate-acetate pathway that is mostly exploited by the plants for the synthesis of different sub-classes of flavonoids, such as flavones, isoflavones, or flavanones (Stewart *et al.*, 2008).

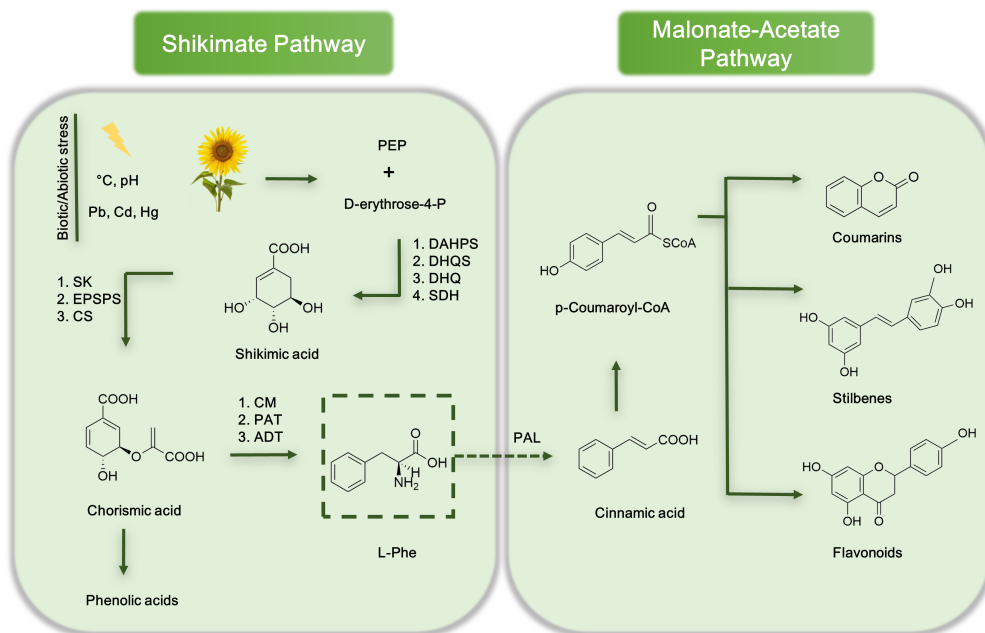


Figure 1.4 - Representation of synthetic pathways of polyphenols. Note: DAHPS-3-deoxy-D-arabino-heptulosonate-7-phosphate synthase; DHQS-3-dehydroquinase; DHQ-3-dehydroquinase dehydratase; SDH-shikimate dehydrogenase; SK-shikimate kinase; EPSPS-5-enolpyruvylshikimate 3-phosphate synthase; CS-chorismate synthase; CM-chorismate mutase; PAT-prephenate aminotransferase; ADT-arogenate dehydratase; PAL-phenylalanine ammonia-lyase; PEP-phosphoenolpyruvic acid.

1.3.2. Classification of Polyphenols

Based on their structural complexity polyphenols can be classified in different groups and subgroups. For example, certain structural patterns are typical for specific groups of polyphenols, such as the C6-C3-C6 pattern (two aromatic rings interconnected with an oxygen bearing heterocycle) representative of flavonoids (Es-Safi *et al.*, 2007). According to the level of oxidation of the central ring, flavonoids are further classified in six subgroups: flavonols, flavones, flavanones, flavanols, anthocyanins and isoflavones. Non-flavonoid polyphenols include the classes of stilbenes, phenolic acids, and lignans. Among these latter classes typical chemical “fingerprints” are found; two benzene rings joined by a methylene bridge (C6-C2-C6) are characteristic of stilbenes, while for lignans, the union of two phenyl-propanoid moieties (C6-C3) is typical, and at β and β' carbon atoms, these moieties can be joined to an ether, lactone, etc. (Pandey *et al.*, 2009). **Figure 1.5** schematically illustrates the classification of polyphenols.

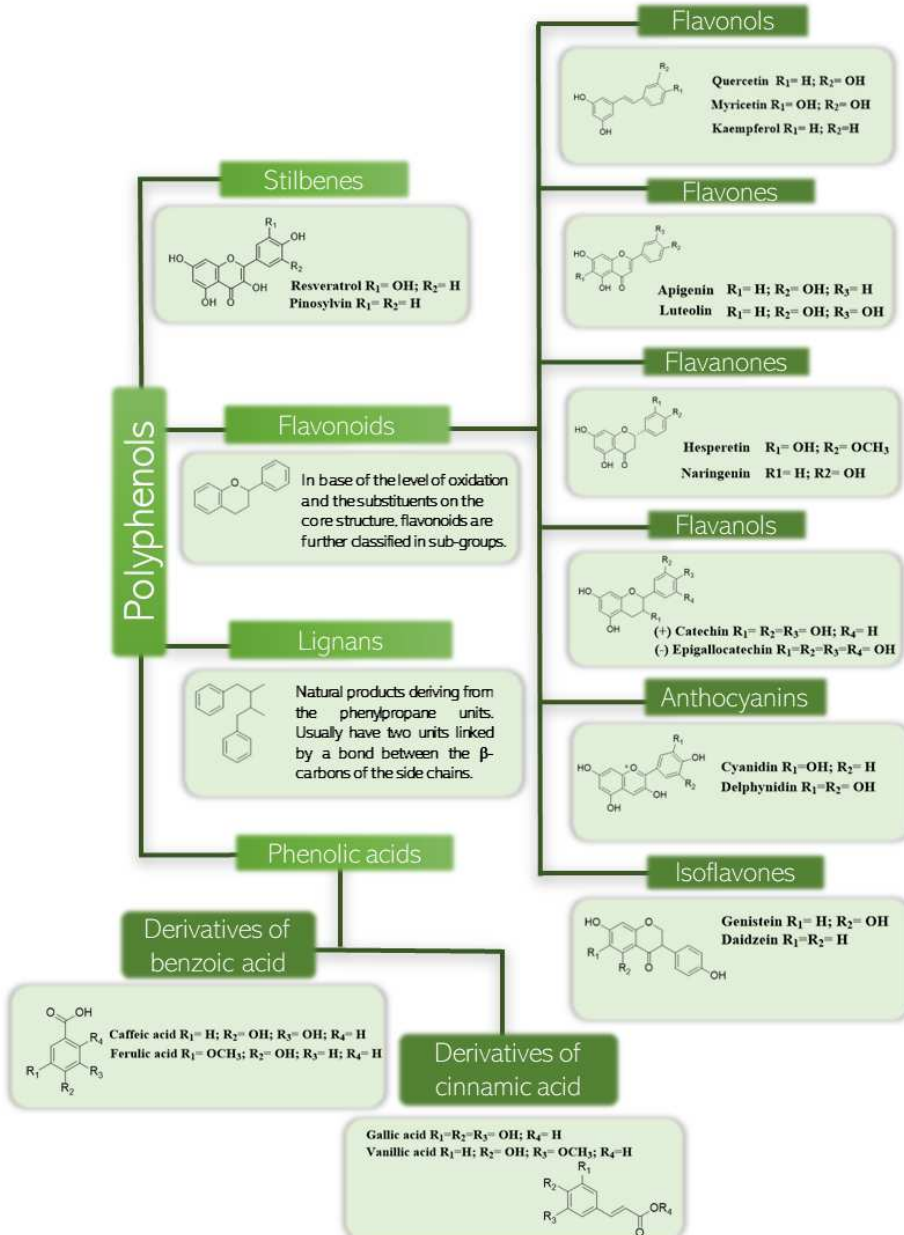


Figure 1.5 - Classification of polyphenolic compounds.

1.3.3. Sources of Polyphenols

The ubiquity of polyphenolic compounds in nature is confirmed by their presence not only in fruits and vegetables, but also in whole grain cereals, coffee, tea, and red wine (Scalbert *et al.*, 2005). Plant sources of polyphenols differ by the quantity and the variety of the polyphenolic compounds that they possess due to different factors to which these sources can be exposed. For example, environmental factors, such as soil content, sun exposure, or even the ripeness of the fruit, influence the final concentration of the polyphenols. Various studies have reported that even the storage conditions or the method of culinary preparation have a significant effect on the polyphenolic content (Manach *et al.*, 2004).

Flavonols, the most predominant sub-class of flavonoids, are mainly found in leafy vegetables such as lettuce and cabbage, onions, broccoli, and blueberries (Justesen *et al.*, 1998). These compounds usually accumulate in the part of the plants that are more exposed to sunlight since their biosynthesis is activated by light. The most abundant flavonols are quercetin and kaempferol. Celery and parsley represent a source of luteolin and apigenin, which are flavones, a less common sub-class of flavonoids. Daidzein and genistein, mostly found in leguminous plants, such as soya, are isoflavones (Franke *et al.*, 1999), are usually considered as phytoestrogens due to the high structural similarity with human estrogens. Flavanones such as hesperetin or naringenin are detected in citrus fruit, such as oranges or lemons, while chocolate and green tea are the richest sources of flavanols (Arts *et al.*, 2000; Justesen *et al.*, 1998). The latter ones can exist in both monomeric and polymeric form. Pigments, such as anthocyanins, are mostly found in fruits, usually complexed with other flavonoids, and this complexation exerts a stabilization effect on them.

The derivatives of benzoic acid and those of cinnamic acid are distinguished among other phenolic acids. The derivatives of benzoic acid, in their free form or esterified, are present in low quantities in only few edible plants and are, therefore, not considered of major nutritional and health interest. On the contrary, the derivatives of cinnamic acid, which are usually found in glycosylated or esterified forms, are more common, and fruits such as plums, kiwis, and blueberries have the highest content (Manach *et al.*, 2004).

Resveratrol, a stilbene, and the compound that is responsible for the well-known French paradox (a lower incidence of cardiovascular diseases despite a high fat diet related to the supposed high consumption of wine by French people), is found mostly in red wine (Somkuwar *et al.*, 2018). Oleaginous seeds have been identified as the primary source of lignans, while onions, asparagus, wheat, and pears have been iden-

tified as secondary sources (Catalgol *et al.*, 2012; Manach *et al.*, 2004).

It is interesting to mention that in addition to terrestrial plants, polyphenols are found in marine microalgae. Compounds such as benzoic acid and vanillic acid are extracted from the genus *Gracilaria*, while isoflavones such as daidzein or genistein are extracted from red and brown seaweeds (Cotas *et al.*, 2020; Gómez-Guzmán *et al.*, 2018).

1.3.4. Resveratrol

Resveratrol was mentioned for the first time in 1939, when Takaoka published his article: "Resveratrol, a new phenolic compound, from *Veratrum grandiflorum*" (Breuss *et al.*, 2019). Since then, the interest for this phenolic compound has grown exponentially: numerous scientific papers, book chapters, patents, symposiums, and conferences have been dedicated to it (Pezzuto *et al.*, 2019).

Resveratrol (3,5,4'-trihydroxy-*trans*-stilbene) is a phenolic compound belonging to the non-flavonoid group of stilbenes. The chemical structure of resveratrol comprises two aromatic rings that are joined by a methylene bridge, and this allows the existence of two isomeric forms of resveratrol the *cis*- and the *trans*-form. The *trans*-form is the predominant one, to which biological effects are attributed (Zhu *et al.*, 2017). When *trans*-resveratrol is exposed to sunlight or artificial UV light at wavelengths of 254 nm or 366 nm, the interconversion to *cis*-resveratrol occurs (Delmas *et al.*, 2011). External stimuli, such as UV light or pathogen invasion, stimulate the biosynthesis of resveratrol in plants. Resveratrol and other stilbene derivatives are mostly found in parts of plants that are not photosynthetically active. Indeed, it has been shown that, in active ones, they restrict ion transport and redox reactions (Keylor *et al.*, 2015).

Resveratrol (**figure 1.6**) has gained attention over the years thanks to the anti-

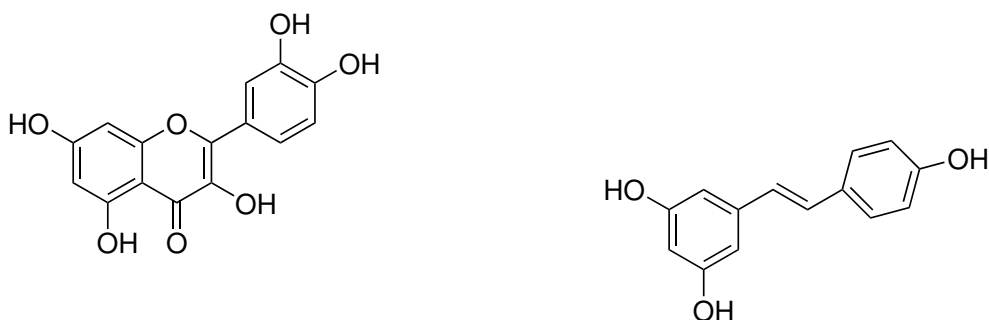


Figure 1.6 - Chemical structures of quercetin (left) and resveratrol (right).

oxidative, anti-inflammatory, anti-apoptotic, and anti-angiogenic effects attributed, among others. It has been used in the treatments of cancer, cardiovascular diseases, neurological disorders, and diabetes, among others (Lançon *et al.*, 2016). As regards ocular pathologies, resveratrol has shown its potential in the treatment of cataracts, glaucoma, and diabetic retinopathy (Koushki *et al.*, 2018).

1.3.5. Quercetin

Inside the class of flavonoids and polyphenols in general, quercetin (2-(3,4-dihydroxyphenyl)-3,5,7-trihydroxychromen-4-one) emerges as one of the most studied compounds, being a leading candidate for use in therapy. Its numerous favourable health effects are a direct consequence of its chemical structure. Two benzene rings, connected to an additional pyrone ring, represent the carbon skeletal with a typical C6-C3-C6 formation, characteristic of flavonoids (**figure 1.6**). In addition, the carbon skeleton bears five hydroxyl groups; quercetin is also referred to as pentahydroxyflavonol (Kashyap *et al.*, 2019; Khan *et al.*, 2016).

Through the involvement in individual molecular pathways and mechanisms quercetin plays a promising role in the potential treatment of a multiplicity of diseases, such as: cardiovascular diseases, hypertension, Alzheimer's disease, cancer, and allergies (Dabeek *et al.*, 2019; Mlcek *et al.*, 2016; Nam *et al.*, 2016; Salvamani *et al.*, 2014; Shafabakhsh *et al.*, 2019). The pharmacological action of quercetin has been shown by the implication in different mechanisms that regulate cell homeostasis. For example, the anticancer effect of quercetin is provided by the inhibition of proteins that are involved in cell survival signalling such as protein kinase C (PKC- α), AKT, and ERK, and the setting off cell death signals, such as PKC- σ or JNK. Quercetin is able to stimulate proapoptotic Bcl-2 proteins, such as Bax and Bad in multiple cell lines (Granado-Serrano *et al.*, 2008; Hashemzaei *et al.*, 2017; Sahpazidou *et al.*, 2014). The anti-inflammatory effect provided by quercetin is a direct consequence of its capacity of scavenging free radical species, which promotes the NF- κ B transcription factor. After activation under ROS, NF- κ B translocate into the nucleus where it functions as a gene promoter that encodes for different pro-inflammatory cytokines and chemokines (IL-1, IL-6, TNF- α) (McKay *et al.*, 2017).

1.3.6. Limitations of QUE and RSV to their Therapeutic Applications

As seen in the previous sections, quercetin and resveratrol have gained interest for their array of health-related effects. Despite this, as disclosed by the Food and

Drug Administration and European Medicinal Agency, there are currently no registered pharmaceutical products bearing as active pharmaceutical ingredients (APIs) quercetin or resveratrol. The reason for this lies in the physico-chemical properties of both polyphenols.

QUE is a highly lipophilic compound that presents a very low aqueous solubility (0.01 mg/mL). On the other hand, its solubility increases in organic solvents such as **EtOH** (4 mg/mL) or **DMSO** (150 mg/mL). This feature restricts the incorporation of high amounts of QUE in aqueous-based matrixes. It has been described that the chemical stability of QUE is pH dependent; the tendency towards degradation increases at a more alkaline pH (pH > 7). The susceptibility of QUE towards oxidation is a direct consequence of its five hydroxyl groups, since a larger number of hydroxyl groups results in a lower energy needed for oxidation (Wang *et al.*, 2016; Kumari *et al.*, 2010; Sokolová *et al.*, 2011).

According to published literature, the stability of RSV is particularly affected by light, the pH of the medium, and elevated temperatures. *Trans*-RSV, the isomer of therapeutic interest, has been reported to be unstable under alkaline conditions. In addition, prolonged exposure to oxygen may induce the oxidation of the hydroxyl groups, leading to products that could potentially complex with ions or other molecules, resulting in a probable cytotoxic effect. It has been reported that exposure to increased temperatures (> 100 °C) can influence the stability of the double C-C bond, leading to the formation of resorcinol and phenol monomers. In addition to this, its solubility in water has been reported to be low (< 0.05 mg/mL) (Delmas *et al.*, 2011; Tian *et al.*, 2020).

As pharmaceutical technology evolves, many formulation approaches have been proposed to circumvent these problems. Each of the potential drug delivery strategies has its own advantages and limitations. The selection should be made considering the specific applications to offer the best possible solution that will enable the use of QUE and RSV as relevant therapeutic molecules.

1.4. Drug Delivery Systems

A formulation or device that permits the introduction of an active substance into the organism and its transport through it, possibly with a regulated rate and site of release, is called a drug delivery system (DDS) (Kewal *et al.*, 2020). The DDS is always a combination of an active pharmaceutical ingredient (API) and non-active ingredients, the so-called excipients. The restraints of using a pure API are various: i) degradation at the site of administration; ii) sensitiveness to environmental conditions (light, tem-

perature, pH); iii) chemical instability; and iv) difficulty in accurate dosing (Adepu *et al.*, 2021). These factors directly influence the bioavailability of the API and, in consequence, its therapeutic performance. Consequently, a DDS is designed in a manner that overcomes not only the limitations of the API itself but also the limitations of the administration site, ensuring maximum safety and efficacy (Baryakova *et al.*, 2023; Laffleur *et al.*, 2020).

1.4.1. Drug Delivery to the Anterior Segment of the Eye: Barriers and Routes of Administration

Due to its peculiar anatomical and physiological features, the application of therapeutics to the eye has been and remains a challenging field in pharmaceutical technology. The diseases of the anterior segment of the eye may be treated through four different routes of administration, each of which is associated with one or multiple ocular barriers that need to be overcome to permit the drug to reach the desired pharmaceutical target (Uruti *et al.*, 2006). Both barriers and routes of administration are represented schematically in **figure 1.7**.

The presence of the blood-aqueous barrier impedes the treatment of anterior segment diseases by systemic administration (intravenous or oral). The blood-aqueous barrier is made up of ciliary epithelia and uveal capillary epithelia, and it restricts the access of drugs from the systemic circulation to the anterior chamber (Amador *et al.*, 2021; Del Amo *et al.*, 2008). The systemic administration route is often associated with toxicity issues related to the high drug doses used (Varela-Fernández *et al.*, 2020).

The direct administration of the drugs to the anterior chamber is done through intracameral injections. This local method of delivery enables to bypass the constraints offered by the cornea, the conjunctiva, and the blood-aqueous barrier (Gaudana *et al.*, 2010).

Another method of local delivery to the anterior part of the eye is subconjunctival administration. This approach places the drugs directly under the conjunctiva, which covers the eyelids or the eyeball (Rafiei *et al.*, 2020). Although it permits overcoming those inconvenients associated with precorneal factors, systemic drug loss may happen due to the high presence of conjunctival blood vessels (Ahmed *et al.*, 1987).

The most patient-friendly and least invasive route to treat diseases associated with the ocular surface is the topical one. Drugs delivered through this route are typically formulated in eyedrops, making them the most predominant ophthalmic formulation (Allyn *et al.*, 2022; Mofidfar *et al.*, 2021). However, other types of topical formulations, such as emulsions or suspensions, are also available (Addo *et al.*, 2016; Bucolo *et al.*,

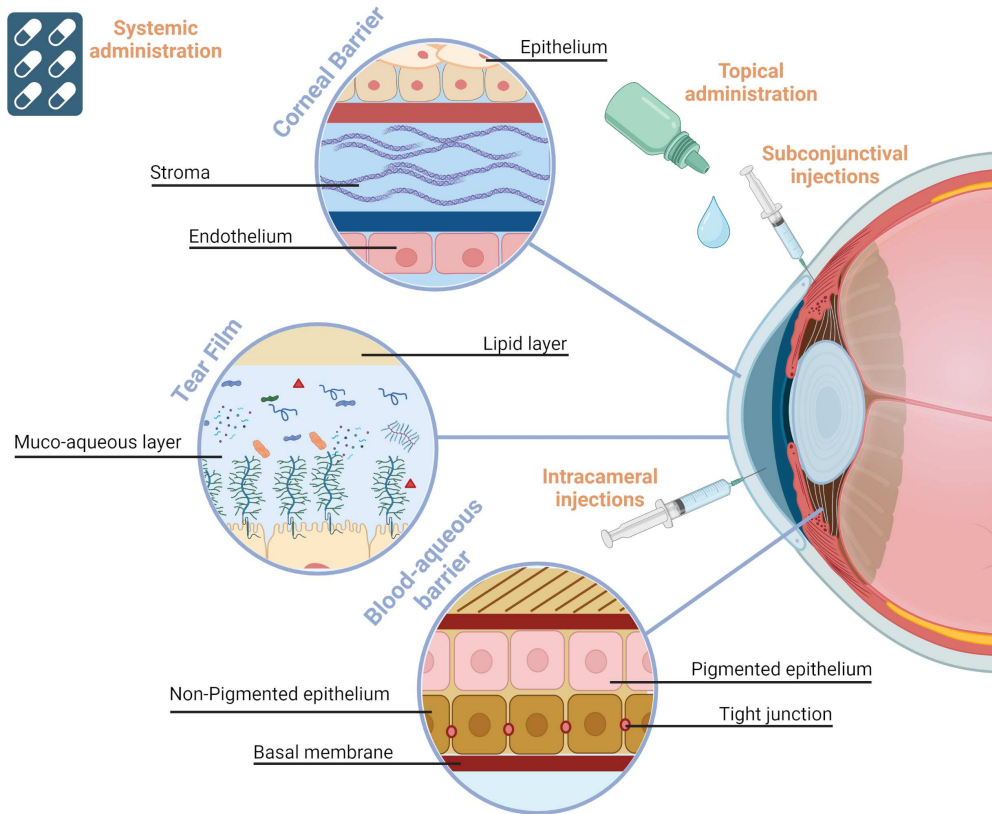


Figure 1.7 - Schematic representation of the most common routes of administration used for the treatment of the diseases of the ocular surface and the barriers associated with. Prepared with BioRender®.

2012; Janagam *et al.*, 2017).

Since the eye has developed very efficient physiological mechanisms that together with the anatomical barriers, provide an impediment towards the absorption of foreign molecules, a very low proportion of the topical applied drugs reaches intraocular tissues (Agarwal *et al.*, 2016; Gan *et al.*, 2013).

The tear film represents a first barrier for topical instilled drugs. It has a high turnover rate of 0.5 - 2.2 μL and a fast restoration time of less than 3 minutes (Ali *et al.*, 2008). If the effects of blinking and tear drainage through the nasolacrimal duct are added, the permanence of the topically applied drugs on the ocular surface is relatively short (Davies *et al.*, 2000; Yoshihisa *et al.*, 2007). To reach intraocular structures, drug molecules mostly follow the corneal pathway. Due to the contrasting nature of the corneal layers, the cornea as a unit limits the absorption of both hydrophilic and hydrophobic molecules. An additional contribution to its impermeable character is

made by the presence of tight junctions and desmosomes in the epithelial cells. These protein junctional complexes regulate the permeation of xenobiotics through the paracellular route (Barar *et al.*, 2008).

A minor absorption route is represented by the so-called conjunctival/scleral pathway. However, this route is considered non-productive since a considerable part of the drug is carried into systemic circulation by conjunctival blood vessels (Ahmed *et al.*, 1985). The sclera is structurally very similar to the corneal stroma, mostly made of collagen and negatively charged proteoglycans. This feature conditions the absorption of positively charged drug molecules (Kim *et al.*, 2007).

Besides all of these, membrane transporters like efflux pumps (P-glycoprotein and multi-drug resistance protein) present in the cornea and the conjunctiva additionally hinder the penetration of drugs in those tissues (Addo *et al.*, 2016; Yoshihisa *et al.*, 2007).

1.4.2. Drug Delivery Systems for Ophthalmic Applications

Although the eye represents an accessible site for topical drug administration, there are several constraints that diminish the effectiveness of these formulations. Efforts have been put into design of conventional and novel drug delivery systems that will permit to overcome the ocular barriers and achieve enhanced drug bioavailability.

Among conventional dosage forms, eyedrops are the most commonly used, accounting for more than 90 % of all marketed ophthalmic formulations (Gulsen *et al.*, 2004; Patel *et al.*, 2013). Eyedrops are distinguished by high patient compliance, a good cost-effectiveness ratio and scalability, and adequate product stability. Once applied, the drug permeates the ocular structures in a pulsatile manner. However, there is a quick decline in the drug concentration since the elimination process starts almost simultaneously. To reach the desired bioavailability, several modifiers can be added to the eyedrop formulation. These can be viscosity agents such as hydroxymethyl cellulose, hydroxypropyl methylcellulose, polyvinyl alcohol, and others (Kaur *et al.*, 2002). Their function is to increase the viscosity of the vehicle and therefore increase the residence time of the drug in the preocular structures, resulting in greater penetration of the drug molecule. Another type of modifiers that can be added to eyedrop formulations are penetration enhancers, which act by disrupting corneal integrity. Inclusion of these kinds of agents in formulations (benzalkonium chloride, Tween 20, Brij 35, saponins) has been associated with local toxicity, therefore, their use should be limited (Liang *et al.*, 2008; Moiseev R. *Vet al.*, 2019).

Emulsions are usually mixtures of two immiscible liquids, where one liquid is

suspended in the form of small droplets inside the other. Moreover, emulsions contain surfactants that act as stabilisers of the formulation (Peng *et al.*, 2011; Tiwari *et al.*, 2018). In ophthalmic therapeutics, emulsions of oil in water (O/W) are preferred to those of water in oil (W/O), principally because of a minor irritation of the ocular tissues (Tamilvanan *et al.*, 2004). Among diverse commercially available emulsions, Restasis[®] (Allergan, USA) was the first emulsion-based topical ophthalmic formulation approved by the FDA. Emulsions possess several assets; these include the improvement of the solubility of the active substance, which in turn improves corneal permeation and therefore ocular bioavailability. Nevertheless, emulsions are thermodynamically unstable; therefore, special attention should be put into preventing phase separation (Brito *et al.*, 2022; Singh *et al.*, 2017).

Like emulsions, suspensions are dispersion systems, defined as a mix of a solid phase suspended in a liquid one (Tadros *et al.*, 2009). Once the suspension is applied to the ocular surface, the solid particles are retained by the cul-de-sac (the lower fornical region of the conjunctiva), increasing the contact time and the duration of the therapeutic effect. The size of the particles shall be carefully evaluated; larger particles increase retention time but also increase eye irritation once instilled (Kaur *et al.*, 2002). Among the various marketed suspensions, TobraDex[®] (tobramycin 0.3 % and dexamethasone 0.1 %) is the most prescribed one for the treatment of ocular bacterial infections (Scoper S. *et al.*, 2008). The consistency of the mean administered dose depends highly on the re-dispersibility of the particles upon shaking. All this, along with the stability issues encountered during the storage time, represent the major drawbacks of suspensions (Yoshihisa *et al.*, 2007).

Ointments are semi-solid formulations based on a mixture of hydrocarbons, that has a melting temperature close to that of the ocular surface (34°C). There is a large variety of drugs to be incorporated into ointments, since even drugs with very low water solubility can be successfully delivered to the eye. Antibacterial agents, such as vancomycin are usually formulated as ophthalmic ointments. In spite of the fact that they are considered safe, ointments are not popular among patients since they cause blurred vision and irritation (Fukuda *et al.*, 2003; Lynch *et al.*, 2019; Patel *et al.*, 2013).

Conventional drug delivery systems like those already mentioned are distinguished by the lack of controlled drug release and by non-specific biodistribution, especially if administered systemically. Further constraints are represented by the need of high doses, frequent application schemes and usual low bioavailability of the active substance (Laffleur *et al.*, 2020; Liu *et al.*, 2016). To solve these issues, great efforts have been put into the development of novel delivery systems that combine the use of advanced materials and techniques. Drug formulations that can control the release

and site of action, limiting the toxicity and dosing frequencies are highly sought in the field of ophthalmic therapeutics (Wang *et al.*, 2016).

For this reason, this thesis work focuses on the development of different formulation approaches for the topical ophthalmic delivery of two promising drug candidates with unfavourable physico-chemical characteristics.

References of Chapter 1

- Addo, R.T.,
Ocular drug delivery: advances, challenges and applications,
Springer International Publishing., (2016).
- Adepu, S., and Ramakrishna, S.,
Controlled drug delivery systems: Current status and future directions,
Molecules **26**(19), 2021 (5905)
<https://doi.org/10.3390/molecules26195905>
- Agarwal, R., Iezhita, I., Agarwal, P., Abdul Nasir, N.A., Razali, N., Alyautdin, R., and Ismail, N.M.,
Liposomes in topical ophthalmic drug delivery: an update,
Drug Deliv. **23**, 2016 (1075–1091)
<https://doi.org/10.3109/10717544.2014.943336>
- Ahmed I.,
Physicochemical determinants of drug diffusion across the conjunctiva, sclera, and cornea,
J. Pharm Sci. **76**, 1987 (583–586)
<https://doi.org/10.15171/PS.2016.01>
- Ahmed, I., and Patron, T.F.,
Importance of the noncorneal absorption route in topical ophthalmic drug delivery,
IOVS **26**, 1985 (584–587).
- Alam, J., Paiva, C.S. De, Pflugfelder, S.C., and States, U.,
Immune-Goblet Cell Interaction in the Conjunctiva,
Ocul Surf. **18**, 2021 (326–334)
<https://doi.org/10.1016/j.jtos.2019.12.006>
- Ali, M., and Byrne, M.E.,
Challenges and solutions in topical ocular drug-delivery systems,
Expert Rev. Clin. Pharmacol. **1**, 2008 (145–161)
<https://doi.org/10.1586/17512433.1.1.145>
- Allyn, M.M., Luo, R.H., Hellwarth, E.B., and Swindle-Reilly, K.E.,
Considerations for polymers used in ocular drug delivery,
Front. Med. **8**, 2022 (1–25)
<https://doi.org/10.3389/fmed.2021.787644>
- Amador, C., Shah, R., Ghiam, S., Kramerov, A.A., and Ljubimov, A. V.,
Gene therapy in the anterior eye segment,
Curr. Gene Ther. **22**, 2021 (104–131)
<https://doi.org/10.2174/1566523221666210423084233>
- Aragona, P., Giannaccare, G., Mencucci, R., Rubino, P., Cantera, E., and Rolando, M.,
Modern approach to the treatment of dry eye, a complex multifactorial disease: A P.I.C.A.S.S.O. board review,
Br. J. Ophthalmol. **105**, 2021 (446–453)
<https://doi.org/10.1136/bjophthalmol-2019-315747>

- Argilés, M., Cardona, G., Pérez-Cabré, E., and Rodríguez, M.,
Blink rate and incomplete blinks in six different controlled hard-copy and electronic reading conditions,
Investig. Ophthalmol. Vis. Sci. **56**, 2015 (6679–6685)
<https://doi.org/10.1167/iovs.15-16967>
- Arts, I.C.W., Van De Putte, B., and Hollman, P.C.H.,
Catechin contents of foods commonly consumed in The Netherlands. 1. Fruits, vegetables, staple foods, and processed foods,
J. Agric. Food Chem. **48**, 2000 (1746–1751)
<https://doi.org/10.1021/jf000025h>
- Awwad, S., Mohamed Ahmed, A.H.A., Sharma, G., Heng, J.S., Khaw, P.T., Brocchini, S., and Lockwood, A.,
Principles of pharmacology in the eye,
Br. J. Pharmacol. **174**, 2017 (4205–4223)
<https://doi.org/10.1111/bph.14024>
- Barar, J., Javadzadeh, A.R., and Omidi, Y.,
Ocular novel drug delivery: Impacts of membranes and barriers,
Expert Opin. Drug Deliv. **5**, 2008 (567–581)
<https://doi.org/10.1517/17425247.5.5.567>
- Baryakova, T.H., Pogostin, B.H., Langer, R., and McHugh, K.J.,
Overcoming barriers to patient adherence: the case for developing innovative drug delivery systems,
Nat. Rev. Drug Discov **22**, 2023 (387–409)
<https://doi.org/10.1038/s41573-023-00670-0>
- Baudouin, C., Rolando, M., Benitez Del Castillo, J.M., Messmer, E.M., Figueiredo, F.C., Irkec, M., Van Setten, G., and Labetoulle, M.,
Reconsidering the central role of mucins in dry eye and ocular surface diseases,
Prog. Retin. Eye Res. **71**, 2019 (68–87)
<https://doi.org/10.1016/j.preteyeres.2018.11.007>
- Bernal, D.L., and Ubels, J.L.,
Quantitative evaluation of the corneal epithelial barrier: Effect of artificial tears and preservatives,
Curr. Eye Res. **10**, 1991 (645–656)
<https://doi.org/10.3109/02713689109013856>
- Bernardes, T.F., and Bonfioli, A.A.,
Blepharitis,
Semin. Ophthalmol. **25**, 2010 (79–83)
<https://doi.org/10.3109/08820538.2010.488562>
- Birk, D.E., Fitch, J.M., Babiarez, J.P., Doane, K.J., and Linsenmayer, T.F.,
Collagen fibrillogenesis in vitro: Interaction of types I and V collagen regulates fibril diameter,
J. Cell Sci. **95**, 1990 (649–657)
<https://doi.org/10.1242/jcs.95.4.649>
- Bland, H.C., Moilanen, J.A., Ekholm, F.S., and Paananen, R.O.,
Investigating the role of specific tear film lipids connected to dry eye syndrome: a study on O-Acyl- ω -hydroxy fatty acids and diesters,
Langmuir. **35**, 2019 (3545–3552)
<https://doi.org/10.1021/acs.langmuir.8b04182>
- Bonanno, J.A.,
Identity and regulation of ion transport mechanisms in the corneal endothelium,
Prog. Retin. Eye Res. **22(1)**, 2003 (69–94)
[https://doi.org/10.1016/S1350-9462\(02\)00059-9](https://doi.org/10.1016/S1350-9462(02)00059-9)
- Borchman, D., Yappert, M.C., and Foulks, G.N.,
Changes in human meibum lipid with meibomian gland dysfunction using principal component analysis,
Exp. Eye Res. **91**, 2010 (246–256)
<https://doi.org/10.1016/j.exer.2010.05.014>

- Breuss, J.M., Atanasov, A.G., and Uhrin, P.,
Resveratrol and its effects on the vascular system,
Int. J. Mol. Sci. **20**, 2019 (1–18)
<https://doi.org/10.3390/ijms20071523>
- Brito, F., Carvalho-Guimaraes, D., Correa, K.L., de Souza, T.P., Rodriguez Amado, J.R., Ribeiro-Costa, R.A., and Silva-Junior, J.O.,
A review of pickering emulsions: perspectives and applications,
Pharmaceuticals **15(11)**, 2022 (1413)
<https://doi.org/10.3390/ph15111413>
- Bucolo, C., Drago, F., and Salomone, S.,
Ocular drug delivery: A clue from nanotechnology,
Front. Pharmacol. **3**, 2012 (2002–2004.)
<https://doi.org/10.3389/fphar.2012.00188>
- Bungau, S., Abdel-Daim, M.M., Tit, D.M., Ghanem, E., Sato, S., Maruyama-Inoue, M., Yamane, S., and Kadosono, K.,
Health benefits of polyphenols and carotenoids in age-related eye diseases,
Oxid. Med. Cell. Longev. 2019 **2019**, ()
<https://doi.org/10.1155/2019/9783429>
- Cano-Suárez, M.T., Reinoso, R., Martín, M.C., Calonge, M., Vallelado, A.I., Fernández, I., and Corell, A.,
Epithelial component and intraepithelial lymphocytes of conjunctiva-associated lymphoid tissue in healthy children,
Histol. Histopathol. **36**, 2021 (1273–1283)
<https://doi.org/10.14670/HH-18-385>
- Catalgol, B., Batirel, S., Taga, Y., and Ozer, N.K.,
Resveratrol: French paradox revisited,
Front. Pharmacol. **3**, 2012 (1–18)
<https://doi.org/10.3389/fphar.2012.00141>
- Cho, H.A., Cheon, J.J., Lee, J.S., Kim, S.Y., and Chang, S.S.,
Prevalence of dry eye syndrome after a three-year exposure to a clean room,
Ann. Occup. Environ. Med. **26(1)**, 2014 (1–6)
<https://doi.org/10.1186/s40557-014-0026-z>
- Choi, W., Lian, C., Ying, L., Kim, G.E., You, I.C., and Park, S.H.,
Expression of lipid peroxidation markers in the tear film and ocular surface of patients with non-sjogren syndrome: potential biomarkers for dry eye disease,
Curr. Eye Res. **41(9)**, 2016 (1143–1149)
<https://doi.org/10.3109/02713683.2015.1098707>
- Cotas, J., Leandro, A., Monteiro, P., Pacheco, D., Figueirinha, A., Gonçalves, A.M.M., Da Silva, G.J., and Pereira, L.,
Seaweed phenolics: From extraction to applications,
Mar. Drugs **18(8)**, 2020 (384)
<https://doi.org/10.3390/MD18080384>
- Cwiklik, L.,
Tear film lipid layer: A molecular level view,
Biochim. Biophys. Acta - Biomembr. **1858**, 2016 (2421–2430)
<https://doi.org/10.1016/j.bbmem.2016.02.020>
- Dabeek, W.M., and Marra, M.V.,
Dietary quercetin and kaempferol: Bioavailability and potential cardiovascular-related bioactivity in humans,
Nutrients **11(10)**, 2019 (2288)
<https://doi.org/10.3390/nu11102288>
- Dartt, D.A.,
Complexity of the tear film: Importance in homeostasis and dysfunction during disease,
Exp Eye Res **117**, 2013 (1–3)
<https://doi.org/10.1016/j.exer.2013.10.008>.Complexity

- Davies, N.M.,
Biopharmaceutical considerations in topical ocular drug delivery,
Clin. Exp. Pharmacol **27**(7), 2000 (558–562)
<https://pubmed.ncbi.nlm.nih.gov/10874518/>
- De Paiva, C.S., Corrales, R.M., Villarreal, A.L., Farley, W.J., Li, D.Q., Stern, M.E., and Pflugfelder, S.C.,
Corticosteroid and doxycycline suppress MMP-9 and inflammatory cytokine expression, MAPK activation in the corneal epithelium in experimental dry eye,
Exp. Eye Res. **83**(3), 2006 (526–535)
<https://doi.org/10.1016/j.exer.2006.02.004>
- Del Amo, E.M., and Urtti, A.,
Current and future ophthalmic drug delivery systems. A shift to the posterior segment,
Drug Discov. Today **13**, 2008 (135–143)
<https://doi.org/10.1016/j.drudis.2007.11.002>
- Delmas, D., Aires, V., Limagne, E., Dutartre, P., Mazué, F., Ghiringhelli, F., and Latruffe, N.,
Transport, stability, and biological activity of resveratrol,
Ann. N. Y. Acad. Sci. **1215**, 2011 (48–59)
<https://doi.org/10.1111/j.1749-6632.2010.05871.x>
- Del Monte, D.W., and Kim, T.,
Anatomy and physiology of the cornea,
J. Cataract Refract. Surg. **37**, 2011 (588–598)
<https://doi.org/10.1016/j.jcrs.2010.12.037>
- Dua, H.S., Watson, N.J., Mathur, R.M., and Forrester, J. V.,
Corneal epithelial cell migration in humans: "hurricane and blizzard keratopathy",
Eye **7**, 1993 (53–58)
<https://doi.org/10.1038/eye.1993.12>
- El Gharras, H.,
Polyphenols: Food sources, properties and applications - A review,
Int. J. Food Sci. Technol. **44**, 2009 (2512–2518)
<https://doi.org/10.1111/j.1365-2621.2009.02077.x>
- Es-Safi, N.E., Ghidouche, S., and Ducrot, P.H.,
Flavonoids: Hemisynthesis, reactivity, characterization and free radical scavenging activity,
Molecules **12**, 2007 (2228–2258)
<https://doi.org/10.3390/12092228>
- Favero, G., Moretti, E., Krajčíková, K., Tomečková, V., and Rezzani, R.,
Evidence of polyphenols efficacy against dry eye disease,
Antioxidants **10**, 2021 (1–17)
<https://doi.org/10.3390/antiox10020190>
- Forrester, J.,
The eye-basic sciences in practice,
WB Saunders Company Ltd, London., (1996).
- Fraga, C.G., Galleano, M., Verstraeten, S. V., and Oteiza, P.I.,
Basic biochemical mechanisms behind the health benefits of polyphenols,
Mol. Aspects Med. **31**, 2010 (435–445)
<https://doi.org/10.1016/j.mam.2010.09.006>
- Francenia Santos-Sánchez, N., Salas-Coronado, R., Hernández-Carlos, B., and Villanueva-Cañongo, C.,
Shikimic acid pathway in biosynthesis of phenolic compounds,
Plant Physiol. Asp. Phenolic Compd. , 2019 (1–15)
<https://doi.org/10.5772/intechopen.83815>
- Franke, A.A., Hankin, J.H., Yu, M.C., Maskarinec, G., Low, S.H., and Custer, L.J.,
Isoflavone levels in soy foods consumed by multiethnic populations in Singapore and Hawaii,
J. Agric. Food Chem. **47**, 1999 (977–986)
<https://doi.org/10.1021/jf9808832>

- Fukuda, M., Hanazome, I., and Sasaki, K.,
The intraocular dynamics of vancomycin hydrochloride ophthalmic ointment (TN-011) in rabbits,
J. Infect. Chemother. **9**, 2003 (93–96)
<https://doi.org/10.1007/s10156-002-0219-1>
- Gaballa, S.A., Kompella, U.B., Elgarhy, O., Alqahtani, A.M., Pierscionek, B., Alany, R.G., and Abdelkader, H.,
Corticosteroids in ophthalmology: drug delivery innovations, pharmacology, clinical applications, and future perspectives,
Drug Deliv. Transl. Res. **11**, 2021 (866–893)
<https://doi.org/10.1007/s13346-020-00843-z>
- Gan, L., Wang, J., Jiang, M., Bartlett, H., Ouyang, D., Eperjesi, F., Liu, J., and Gan, Y.,
Recent advances in topical ophthalmic drug delivery with lipid-based nanocarriers,
Drug Discov. Today **18**, 2013 (290–297)
<https://doi.org/10.1016/j.drudis.2012.10.005>
- Ganesalingam, K., Ismail, S., Sherwin, T., and Craig, J.P.,
Molecular evidence for the role of inflammation in dry eye disease,
Clin. Exp. Optom. **102**, 2019 (446–454)
<https://doi.org/10.1111/cxo.12849>
- Gaudana, R., Ananthula, H.K., Parenky, A., and Mitra, A.K.,
Ocular drug delivery,
AAPS J. **12**, 2010 (348–360)
<https://doi.org/10.1208/s12248-010-9183-3>
- Gilbard, J.,
Human tear film electrolyte concentrations in health and dry-eye disease,
Int Ophthalmol Clin **34**, 1994 (27–36).
- Gipson, I.K.,
The ocular surface: the challenge to enable and protect vision-the Friedenwald lecture,
IOVS **48**, 2007 (4391–4398)
<https://doi.org/10.1167/iovs.07>
- Gipson, I.K.,
Goblet cells of the conjunctiva: A review of recent findings,
Prog. Retin. Eye Res. **54**, 2016 (49–63)
<https://doi.org/10.1016/j.preteyeres.2016.04.005>
- Gipson, I.K.,
The ocular surface: the challenge to enable and protect vision,
IOVS **48**, 2010 (4390–4398)
<https://doi.org/10.1167/iovs.07-0770>
- Gogia, R., Richer, S.P., and Rose, R.C.,
Tear fluid content of electrochemically active components including water soluble antioxidants,
Curr. Eye Res. **17**, 1994 (257–263).
- Goldberg, I., Graham, S.L., Crowston, J.G., and d’Mellow, G.,
Clinical audit examining the impact of benzalkonium chloride-free anti-glaucoma medications on patients with symptoms of ocular surface disease,
Clin. Exp. Ophthalmol. **43**(3), 2015 (214–220)
<https://doi.org/10.1111/ceo.12431>
- Gómez-Guzmán, M., Rodríguez-Nogales, A., Algieri, F., and Gálvez, J.,
Potential role of seaweed polyphenols in cardiovascular-associated disorders,
Mar. Drugs **16**, 2018 (1–21)
<https://doi.org/10.3390/md16080250>

- Granado-Serrano, A.B., Martín, M.A., Bravo, L., Goya, L., and Ramos, S.,
Time-course regulation of quercetin on cell survival/proliferation pathways in human hepatoma cells,
Mol. Nutr. Food Res. **52**, 2008 (457–464)
<https://doi.org/10.1002/mnfr.200700203>
- Greiner, J., Glonek, T., Korb, D.R., Booth, R., and Leahy, C.D.,
Phospholipids in meibomian gland secretion,
Ophthalmic Res. **28**, 1996 (44–49).
- Gulsen, D., and Chauhan, A.,
Ophthalmic drug delivery through contact lenses,
Investig. Ophthalmol. Vis. Sci. **45**, 2004 (2342–2347)
<https://doi.org/10.1167/iovs.03-0959>
- Hart, R.W., and Farrell, R.A.,
Light scattering in the cornea.,
J. Opt. Soc. Am. **59**, 1969 (766–774)
<https://doi.org/10.1364/JOSA.59.000766>
- Hashemzaei, M., Far, A.D., Yari, A., Heravi, R.E., Tabrizian, K., Taghdisi, S.M., Sadegh, S.E., Tsarouhas, K., Kouretas, D., Tzanakakis, G., Nikitovic, D., Anisimov, N.Y., Spandidos, D.A., Tsatsakis, A.M., and Rezaee, R.,
Anticancer and apoptosis-inducing effects of quercetin in vitro and in vivo,
Oncol. Rep. **38**, 2017 (819–828)
<https://doi.org/10.3892/or.2017.5766>
- Hay, E.D.,
Development of the vertebrate cornea,
Int Rev Cytol **63**, 1979 (263–322).
- Hodges, R.R., and Dartt, D.A.,
Tear film mucins: Front line defenders of the ocular surface; comparison with airway and gastrointestinal tract mucins,
Exp. Eye Res. **117**, 2013a (62–78)
<https://doi.org/10.1016/j.exer.2013.07.027>
- Hwang, S.H., Choi, Y.-H., Paik, H.J., Wee, W.R., Kim, M.K., and Kim, D.H.,
Potential importance of ozone in the association between outdoor air pollution and dry eye disease in South Korea,
JAMA Ophthalmol. **134**, 2016 (503–510)
<https://doi.org/10.1001/jamaophthalmol.2016.0139>
- Jackson, C.J., Gundersen, K.G., Tong, L., and Utheim, T.P.,
Dry eye disease and proteomics,
Ocul. Surf. **24**, 2022 (119–128)
<https://doi.org/10.1016/j.jtos.2022.03.001>
- Jäger, F., Paulsen, F., Bergua, A., Jungbauer, R., and Hammer, C.M.,
Urea transporter-B expression on the ocular surface and in the lacrimal glands,
Ann. Anat. **243**, 2022 (151954)
<https://doi.org/10.1016/j.aanat.2022.151954>
- Janagam, D.R.,
Nanoparticles for drug delivery to the anterior segment of the eye,
Adv Drug Deliv Rev **122**, 2017 (31–64)
<https://doi.org/10.1016/j.addr.2017.04.001>. Nanoparticles
- Jones, L., Downie, L.E., Korb, D., Benitez-del-Castillo, J.M., Dana, R., Deng, S.X., Dong, P.N., Geerling, G., Hida, R.Y., Liu, Y., Seo, K.Y., Tauber, J., Wakamatsu, T.H., Xu, J., Wolffsohn, J.S., and Craig, J.P.,
TFOS DEWS II Management and Therapy Report,
Ocul. Surf. **15**, 2017 (575–628)
<https://doi.org/10.1016/j.jtos.2017.05.006>

- Justesen, U., Knuthsen, P., and Leth, T.,
Quantitative analysis of flavonols, flavones, and flavanones in fruits, vegetables and beverages by high-performance liquid chromatography with photo-diode array and mass spectrometric detection,
J. Chromatogr. A **799**, 1998 (101–110)
[https://doi.org/10.1016/S0021-9673\(97\)01061-3](https://doi.org/10.1016/S0021-9673(97)01061-3)
- Kashyap, D., Garg, V.K., Tuli, H.S., Yerer, M.B., Sak, K., Sharma, A.K., Kumar, M., Aggarwal, V., and Sandhu, S.S.,
Fisetin and quercetin: Promising flavonoids with chemopreventive potential,
Biomolecules **9**, 2019 (1–22)
<https://doi.org/10.3390/biom9050174>
- Kaur, I.P., and Kanwar, M.,
Ocular preparations: The formulation approach,
Drug Dev. Ind. Pharm. **28**, 2002 (473–493)
<https://doi.org/10.1081/DDC-120003445>
- Kessing, S.V.,
A New Division Of the Conjunctiva on the basis of X-ray examination,
S.V. Acta Ophthalmol. **45**, 1967 (680–683).
- Kewal, K.J.,
Drug Delivery Systems.,
Springer Science, (2020).
- Keylor, M.H., Matsuura, B.S., Stephenson, C.R.J.,
Chemistry and Biology of Resveratrol-Derived Natural Products,
Chem. Rev. **115**, 2015 (8976–9027)
<https://doi.org/10.1021/cr500689b>
- Khan, F., Niaz, K., Maqbool, F., Hassan, F.I., Abdollahi, M., Nagulapalli Venkata, K.C., Nabavi, S.M., and Bishayee, A.,
Molecular targets underlying the anticancer effects of quercetin: An update.,
Nutrients **8**, 2016 (1–19)
<https://doi.org/10.3390/nu8090529>
- Kim, M., Lee, Y., Mehra, D., Sabater, A.L., and Galor, A.,
Dry eye: Why artificial tears are not always the answer,
BMJ Open Ophthalmol. **6**, 2021 (1–12)
<https://doi.org/10.1136/bmjophth-2020-000697>
- Kim, S.H., Lutz, R.J., Wang, N.S., and Robinson, M.R.,
Transport barriers in trans-scleral drug delivery for retinal diseases,
Ophthalmic Res. **39**, 2007 (244–254)
<https://doi.org/10.1159/000108117>
- Klintworth GK,
The cornea-structure and macromolecules in health and disease,
Am J Pathol **3**, 1977 (718–808).
- Knop, E., and Knop, N.,
The role of eye-associated lymphoid tissue in corneal immune protection,
J. Anat. **206**, 2005 (271–285)
<https://doi.org/10.1111/j.1469-7580.2005.00394.x>
- Knop, E., Knop, N., and Claus, P.,
Local production of secretory IgA in the eye-associated lymphoid tissue (EALT) of the normal human ocular surface,
Investig. Ophthalmol. Vis. Sci. **49**, 2008 (2322–2329)
<https://doi.org/10.1167/iovs.07-0691>
- Kojima, T., Dogru, M., Kawashima, M., Nakamura, S., and Tsubota, K.,
Advances in the diagnosis and treatment of dry eye,
Prog. Retin. Eye Res. **59**, 2020 (163–168)
<https://doi.org/10.1016/j.preteyeres.2020.100842>

- Komai, Y., and Ushiki, T.,
The three-dimensional organization of collagen fibrils in the human cornea and sclera,
Investig. Ophthalmol. Vis. Sci. **32**, 1991 (2244–2258).
- Kondratyuk, T.P., and Pezzuto, J.M.,
Natural product polyphenols of relevance to human health,
Pharm. Biol. **42**, 2004 (46–63)
<https://doi.org/10.1080/13880200490893519>
- Koushki, M., Amiri-Dashatan, N., Ahmadi, N., Abbaszadeh, H.A., and Rezaei-Tavirani, M.,
Resveratrol: A miraculous natural compound for diseases treatment,
Food Sci. Nutr. **6**, 2018 (2473–2490)
<https://doi.org/10.1002/fsn3.855>
- Kumari, A., Yadav, S.K., Pakade, Y.B., Singh, B., and Yadav, S.C.,
Development of biodegradable nanoparticles for delivery of quercetin,
Colloids Surfaces B Biointerfaces **80**, 2010 (184–192)
<https://doi.org/10.1016/j.colsurfb.2010.06.002>
- Laffleur, F., and Keckeis, V.,
Advances in drug delivery systems: Work in progress still needed?,
Int. J. Pharm. X **2**, 2020 (100050)
<https://doi.org/10.1016/j.ijpx.2020.100050>
- Laibovitz, R., Solch, S., Andriano, K., and O'Connell, M.,
Pilot trial of cyclosporine 1% ophthalmic ointment in the treatment of keratoconjunctivitis,
Sicca. Cornea **12**, 1993 (315–323).
- Lançon, A., Frazzi, R., and Latruffe, N.,
Anti-oxidant, anti-inflammatory and anti-angiogenic properties of resveratrol in ocular diseases,
Molecules **21**, 2016 (304)
<https://doi.org/10.3390/molecules21030304>
- Lee, L., Garrett, Q., Flanagan, J., Chakrabarti, S., and Papas, E.,
Genetic factors and molecular mechanisms in dry eye disease,
Ocul. Surf. **16**, 2018 (206–217)
<https://doi.org/10.1016/j.jtos.2018.03.003>
- Lei, H.L., Ku, W.C., Sun, M.H., Chen, K.J., Lai, J.Y., and Sun, C.C.,
Cyclosporine a eye drop-induced elongated eyelashes: A case report,
Case Rep. Ophthalmol. **2**, 2011 (398–400)
<https://doi.org/10.1159/000335281>
- Lemp, M.A.,
Report of the National Eye Institute/Industry Workshop on clinical trials in dry eyes,
CLAO J. **21**, 1995 (221–232).
- Lemp, M.A., Baudouin, C., Baum, J., Dogru, M., Foulks, G.N., Kinoshita, S., Laibson, P., McCulley, J.,
Murube, J., Pflugfelder, S.C., Rolando, M., and Toda, I.,
The definition and classification of dry eye disease: Report of the definition and classification subcommittee of the international Dry Eye Workshop (2007),
Ocul. Surf. **5**, 2007 (75–92)
[https://doi.org/10.1016/s1542-0124\(12\)70081-2](https://doi.org/10.1016/s1542-0124(12)70081-2)
- Leonardi, A., Modugno, R.L., and Salami, E.,
Allergy and dry eye disease,
Ocul. Immunol. Inflamm. **29**, 2021 (1168–1176)
<https://doi.org/10.1080/09273948.2020.1841804>
- Li, D.Q., Chen, Z., Song, X.J., Luo, L., and Pflugfelder, S.C.,
Stimulation of matrix metalloproteinases by hyperosmolarity via a JNK pathway in human corneal epithelial cells,
Investig. Ophthalmol. Vis. Sci. **45**, 2004 (4302–4311)
<https://doi.org/10.1167/iovs.04-0299>

- Li, S., Lu, Z., Huang, Y., Wang, Y., Jin, Q., Shentu, X., Ye, J., Ji, J., Yao, K., and Han, H.,
Anti-Oxidative and anti-inflammatory micelles: break the dry eye vicious cycle,
Adv. Sci. **9**, 2022 (1–16)
<https://doi.org/10.1002/advs.202200435>
- Liang, H., Brignole-Baudouin, F., Rabinovich-Guilatt, L., Mao, Z., Riancho, L., Faure, M.O., Warnet, J.M., Lambert, G., and Baudouin, C.,
Reduction of quaternary ammonium-induced ocular surface toxicity by emulsions: An in vivo study in rabbits,
Mol. Vis. **14**, 2008 (204–216).
- Liu, D., Yang, F., Xiong, F., and Gu, N.,
The smart drug delivery system and its clinical potential,
Theranostics **6**, 2016 (1306–1323)
<https://doi.org/10.7150/thno.14858>
- Lollett, I. V., and Galor, A.,
Dry eye syndrome: Developments and lifitegrast in perspective,
Clin. Ophthalmol. **12**, 2018 (125–139)
<https://doi.org/10.2147/OPTH.S126668>
- Lynch, C., Kondiah, P.P.D., Choonara, Y.E., du Toit, L.C., Ally, N., and Pillay, V.,
Advances in biodegradable nano-sized polymer-based ocular drug delivery,
Polymers (Basel). **11**, 2019 (1371)
<https://doi.org/10.3390/polym11081371>
- Manach, C., Scalbert, A., Morand, C., Rémésy, C., and Jiménez, L.,
Polyphenols: Food sources and bioavailability,
Am. J. Clin. Nutr. **79**, 2004 (727–747)
<https://doi.org/10.1093/ajcn/79.5.727>
- Mandal, S.M., Chakraborty, D., and Dey, S.,
Phenolic acids act as signaling molecules in plant-microbe symbioses,
Plant Signal. Behav. **5**, 2010 (359–368).
- Maurice, D.M.,
The cornea and sclera, vegetative physiology and biochemistry,
Academic Press Inc. **1962**, 1962 (289–368)
<https://doi.org/10.1016/b978-1-4832-3090-0.50013-7>
- McClellan, B.H., Whitney, C.R., Newman, L.P., and Allansmith, M.R.,
Immunoglobulins in tears,
Am. J. Ophthalmol. **76**, 1973 (89–101)
[https://doi.org/10.1016/0002-9394\(73\)90015-9](https://doi.org/10.1016/0002-9394(73)90015-9)
- McKay, T.B., and Karamichos, D.,
Quercetin and the ocular surface: What we know and where we are going,
Exp. Biol. Med. **242**, 2017 (565–572)
<https://doi.org/10.1177/1535370216685187>
- McKenzie, R.W., Jumblatt, J.E., and Jumblatt, M.M.,
Quantification of MUC2 and MUC5AC transcripts in human conjunctiva,
Investig. Ophthalmol. Vis. Sci. **41**, 2000 (703–708).
- Meek, K.M., and Knupp, C.,
Corneal structure and transparency,
Prog. Retin. Eye Res. **49**, 2015 (1–16)
<https://doi.org/10.1016/j.preteyeres.2015.07.001>
- Mensher, J.H.,
Corneal nerves,
Surv. Ophthalmol. **19**, 1974 (1–18).

- Messmer, E.M.,
The pathophysiology, diagnosis and treatment of dry eye disease,
Dtsch Arztebl Int **112**, 2015 (71–82)
<https://doi.org/10.3238/arztebl.2015.0071>
- Milner, M.S., Beckman, K.A., and Luchs, J.I., and Yeu, E.,
Dysfunctional tear syndrome: dry eye disease and associated tear film disorders - new strategies for diagnosis and treatment,
Curr Opin Ophthalmol. **28**, 2016 (1–44)
<https://doi.org/10.1097/ICU.0000000000000355>
- Mishima, S.,
Clinical investigations on the corneal endothelium,
Am. J. Ophthalmol. **93**, 1982 (1–29)
[https://doi.org/10.1016/0002-9394\(82\)90693-6](https://doi.org/10.1016/0002-9394(82)90693-6)
- Mlcek, J., Jurikova, T., Skrovankova, S., and Sochor, J.,
Quercetin and its anti-allergic immune response,
Molecules **21**, 2016 (1–15)
<https://doi.org/10.3390/molecules21050623>
- Módis, L., and Szalai, E.,
Dry eye diagnosis and management,
Expert Rev. Ophthalmol. **6**, 2011 (67–79)
<https://doi.org/10.1586/eop.10.89>
- Mofidfar, M., Abdi, B., Ahadian, S., Mostafavi, E., Desai, T.A., Abbasi, F., Sun, Y., Manche, E.E., Ta, C.N., and Flowers, C.W.,
Drug delivery to the anterior segment of the eye: A review of current and future treatment strategies,
Int. J. Pharm. **607**, 2021 (120924)
<https://doi.org/10.1016/j.ijpharm.2021.120924>
- Moiseev, R. V, Morrison, P.W.J., Steele, F., and Khutoryanskiy, V. V.,
Penetration enhancers in ocular drug delivery,
Pharmaceutics. **11**, 2019 (321)
<https://doi:10.3390/pharmaceutics11070321>
- Muller, L.J., Pels, L., and Vrensen, G.F.,
Novel aspects of the ultrastructural organization of human corneal keratocytes,
Invest Ophthalmol Vis Sci **36**, 1995 (2557–2567).
- Nam, J.S., Sharma, A.R., Nguyen, L.T., Chakraborty, C., Sharma, G., and Lee, S.S.,
Application of bioactive quercetin in oncotherapy: From nutrition to nanomedicine,
Molecules **21**, 2016 (1–23)
<https://doi.org/10.3390/molecules21010108>
- Nebbioso, M., Fameli, V., Gharbiya, M., Sacchetti, M., Zicari, A.M., and Lambiase, A.,
Investigational drugs in dry eye disease,
Expert Opin. Investig. Drugs **25**, 2016 (1437–1446)
<https://doi.org/10.1080/13543784.2016.1249564>
- Nelson, J.D.,
Managing the dry eye Accurate diagnosis is the key,
Postgrad. Med. , (5481)
<https://doi.org/10.1080/00325481.1989.11700594>
- Nichols, B.A.,
Conjunctiva,
Microsc. Res. Tech. **33**, 1996 (296–319).
- Pandey, K.B., and Rizvi, S.I.,
Plant polyphenols as dietary antioxidants in human health and disease,
Oxid. Med. Cell. Longev. **2**, 2009 (270–278)
<https://doi.org/10.4161/oxim.2.5.9498>

- Patel, A.,
Ocular drug delivery systems: An overview,
World J. Pharmacol. **2**, 2013 (47)
<https://doi.org/10.5497/wjp.v2.i2.47>
- Paulsen, F.P., and Berry, M.S.,
Mucins and TFF peptides of the tear film and lacrimal apparatus,
Prog. Histochem. Cytochem. **41**, 2006 (1–53)
<https://doi.org/10.1016/j.proghi.2006.03.001>
- Pellegrini, M., Senni, C., Bernabei, F., Cicero, A.F.G., Vagge, A., Maestri, A., Scordia, V., and Giannaccare, G.,
The role of nutrition and nutritional supplements in ocular surface diseases,
Nutrients **12**, 2020 (1–16).
- Peng, C.C., Bengani, L.C., Jung, H.J., Leclerc, J., Gupta, C., and Chauhan, A.,
Emulsions and microemulsions for ocular drug delivery,
J. Drug Deliv. Sci. Technol. **21**, 2011 (111–121)
[https://doi.org/10.1016/S1773-2247\(11\)50010-3](https://doi.org/10.1016/S1773-2247(11)50010-3)
- Perez, V.L., Pflugfelder, S.C., Zhang, S., Shojaei, A., and Haque, R.,
Lifitegrast, a novel integrin antagonist for treatment of dry eye disease,
Ocul. Surf. **14**, 2016 (207–215)
<https://doi.org/10.1016/j.jtos.2016.01.001>
- Perez, V.L., Stern, M.E., and Pflugfelder, S.C.,
Inflammatory basis for dry eye disease flares,
Exp Eye Res **201**, 2020 ()
<https://doi.org/10.1016/j.exer.2020.108294>. Inflammatory
- Periman, L.M., Perez, V.L., Saban, D.R., Lin, M.C., and Neri, P.,
The immunological basis of dry eye disease and current topical treatment options,
J. Ocul. Pharmacol. Ther. **36**, 2020 (137–146)
<https://doi.org/10.1089/jop.2019.0060>
- Pezzuto, J.M.,
Resveratrol: twenty years of growth, development and controversy,
Biomol. Ther. **27**, 2019 (1–14)
<https://doi.org/10.4062/biomolther.2018.176>
- Pflugfelder, S.C.,
Antiinflammatory therapy for dry eye,
Am. J. Ophthalmol. **137**, 2004 (337–342)
<https://doi.org/10.1016/j.ajo.2003.10.036>
- Pflugfelder, S.C., and de Paiva, C.S.,
The pathophysiology of dry eye disease,
Ophthalmology **124**, 2017a (S4–S13)
<https://doi.org/10.1016/j.optha.2017.07.010>
- Pflugfelder, S.C., and de Paiva, C.S.,
The pathophysiology of dry eye disease: what we know and future directions for research,
Ophthalmology **124**, 2017b (S4–S13)
<https://doi.org/10.1016/j.optha.2017.07.010>
- Pflugfelder, S.C., De Paiva, C.S., Tong, L., Luo, L., Stern, M.E., and Li, D.Q.,
Stress-activated protein kinase signaling pathways in dry eye and ocular surface disease,
Ocul. Surf. **3**, 2005 (S154–S157)
[https://doi.org/10.1016/s1542-0124\(12\)70244-6](https://doi.org/10.1016/s1542-0124(12)70244-6)

- Pflugfelder, S.C., De Paiva, C.S., Villarreal, A.L., and Stern, M.E.,
Effects of sequential artificial tear and cyclosporine emulsion therapy on conjunctival goblet cell density and transforming growth factor- β 2 production,
Cornea **27**, 2008 (64–69)
<https://doi.org/10.1097/IC0.0b013e318158f6dc>
- Pflugfelder, S.C., Liu, Z., Monroy, D., Li, D.Q., Carvajal, M.E., Price-Schiavi, S.A., Idris, N., Solomon, A., Perez, A., and Carraway, K.L.,
Detection of sialomucin complex (MUC4) in human ocular surface epithelium and tear fluid,
Investig. Ophthalmol. Vis. Sci. **41**, 2000 (1316–1326).
- Pflugfelder, S.C., Paiva, C.S. De, Moore, Q.L., Volpe, E.A., Li, D., Gumus, K., Zaheer, M.L., and Corrales, R.M.,
Aqueous tear deficiency increases conjunctival interferon expression and goblet cell loss,
Cornea **56**, 2015 (7545–7550)
<https://doi.org/10.1167/iovs.15-17627>
- Pflugfelder, S.C., and Stern, M.E.,
Biological functions of tear film,
Exp. Eye Res. **197**, 2020 (1–7)
<https://doi.org/10.1016/j.exer.2020.108115>
- Pinto-Fraga, J., Lopez-Miguel, A., Gonzalez-Garcia, M.J., Fernandez, I., Lopez-De-La-Rosa, A., Enriquez-De-Salamanca, A., Stern, M.E., and Calonge, M.,
Topical fluorometholone protects the ocular surface of dry eye patients from desiccating stress: a randomized controlled clinical trial,
Ophthalmology **123**, 2016 (141–153)
<https://doi.org/10.1016/j.ophtha.2015.09.029>
- Pirie, A.,
The biochemistry of the eye,
Symp. Proc. **19**, 1955 (73–78).
- Rafei, F., Tabesh, H. and Farzad, F.,
Sustained subconjunctival drug delivery systems: current trend and future perspectives,
Int. Ophthalmol. **40**, 2020 (2385–2401)
<https://doi.org/10.1007/s10792-020-01391-8>
- Rouen, P.A., and White, M.L.,
Dry eye disease: prevalence, assessment, and management,
Home Healthc. Now **36**, 2018 (74–83)
<https://doi.org/10.1097/NHH.0000000000000652>
- Sahpazidou, D., Geromichalos, G.D., Stagos, D., Apostolou, A., Haroutounian, S.A., Tsatsakis, A.M., Tzanakakis, G.N., Hayes, A.W., and Kouretas, D.,
Anticarcinogenic activity of polyphenolic extracts from grape stems against breast, colon, renal and thyroid cancer cells,
Toxicol. Lett. **230**, 2014 (218–224)
<https://doi.org/10.1016/j.toxlet.2014.01.042>
- Sall, K., Stevenson, O.D., Mundorf, T.K., and Reis, B.L.,
Two multicenter randomized studies of the efficacy and safety of cyclosporine ophthalmic emulsion in moderate to severe dry eye disease,
Ophthalmology **107**, 2000 (631–639)
[https://doi.org/10.1016/S0161-6420\(99\)00176-1](https://doi.org/10.1016/S0161-6420(99)00176-1)
- Salvamani, S., Gunasekaran, B., Shaharuddin, N.A., Ahmad, S.A., and Shukor, M.Y.,
Antiatherosclerotic effects of plant flavonoids,
Biomed Res. Int. **2014**, 2014 (1–11)
<https://doi.org/10.1155/2014/480258>

- Scalbert, A., Manach, C., Morand, C., Rémésy, C., and Jiménez, L.,
Dietary polyphenols and the prevention of diseases,
Crit. Rev. Food Sci. Nutr. **45**, 2005 (287–306)
<https://doi.org/10.1080/1040869059096>
- Schaumberg, D.A., Uchino, M., Christen, W.G., Semba, R.D., Buring, J.E., and Li, J.Z.,
Patient reported differences in dry eye disease between men and women: impact, management, and patient satisfaction,
PLoS One **8**, 2013 (1–11)
<https://doi.org/10.1371/journal.pone.0076121>
- Schermer, A., Galvin, S., and Sun, T.T.,
Differentiation-related expression of a major 64K corneal keratin in vivo and in culture suggests limbal location of corneal epithelial stem cells,
J. Cell Biol. **103**, 1986 (49–62)
<https://doi.org/10.1083/jcb.103.1.49>
- Schirmer, O.,
Studien zur Physiologie und Pathologie der Tränenabsonderung und Tränenabfuhr,
Albr. von Graefe's Arch. für Ophthalmol. **56**, 1903 (197–291)
<https://doi.org/10.1007/BF01946264>
- Scoper, S. V., Kabat, A.G., Owen, G.R., Stroman, D.W., Kabra, B.P., Faulkner, R., Kulshreshtha, A.K., Rusk, C., Bell, B., Jamison, T., Bernal-Perez, L.F., Brooks, A.C., and Nguyen, V.A.,
Ocular distribution, bactericidal activity and settling characteristics of TobraDex® ST ophthalmic suspension compared with TobraDex® ophthalmic suspension,
Adv. Ther. **25**, 2008 (77–88)
<https://doi.org/10.1007/s12325-008-0019-9>
- Shafabakhsh, R., and Asemi, Z.,
Quercetin: A natural compound for ovarian cancer treatment,
J. Ovarian Res. **12**, 2019 (1–9)
<https://doi.org/10.1186/s13048-019-0530-4>
- Singh, Y., Meher, J.G., Raval, K., Khan, F.A., Chaurasia, M., Jain, N.K., and Chourasia, M.K.,
Nanemulsions: concepts, development and applications in drug delivery,
J. Control. Release **17**, 2017 ()
<https://doi.org/10.1016/j.jconrel.2017.03.008>
- Sokolová, R., Degano, I., Ramešová, Š., Bulíčková, J., Hromadová, M., Gál, M., Fiedler, J., and Valášek, M.,
The oxidation mechanism of the antioxidant quercetin in nonaqueous media,
Electrochim. Acta **56**, 2011 (7421–7427)
<https://doi.org/10.1016/j.electacta.2011.04.121>
- Somkuwar, R.G., Bhange, M.A., Oulkar, D.P., Sharma, A.K., and Ahammed Shabeer, T.P.,
Estimation of polyphenols by using HPLC–DAD in red and white wine grape varieties grown under tropical conditions of India,
J. Food Sci. Technol. **55**, 2018 (4994–5002)
<https://doi.org/10.1007/s13197-018-3438-x>
- Souto, E.B., Dias-Ferreira, J., López-Machado, A., Ettcheto, M., Cano, A., Espuny, A.C., Espina, M., Garcia, M.L., and Sánchez-López, E.,
Advanced formulation approaches for ocular drug delivery: State-of-the-art and recent patents,
Pharmaceutics **11**, 2019 (1–29)
<https://doi.org/10.3390/pharmaceutics11090460>
- Spurr-Michaud, S., Argüeso, P., and Gipson, I.,
Assay of mucins in human tear fluid,
Exp. Eye Res. **84**, 2007 (939–950)
<https://doi.org/10.1016/j.exer.2007.01.018>

- Stapleton, F., Alves, M., Bunya, V.Y., Jalbert, I., Lekhanont, K., Malet, F., Na, K.S., Schaumberg, D., Uchino, M., Vehof, J., Viso, E., Vitale, S., and Jones, L.,
TFOS DEWS II Epidemiology Report,
Ocul. Surf. **15**, 2017 (334–365)
<https://doi.org/10.1016/j.jtos.2017.05.003>
- Stern, M.E., Beuerman, R.W., Fox, R.I., Gao, J., Mircheff, A.K., and Pflugfelder, S.C.,
The pathology of dry eye: the interaction between the ocular surface and lacrimal glands,
Cornea **17**, 1998 (584).
- Stern, M.E., Gao, J., Siemasko, K.F., Beuerman, R.W., and Pflugfelder, S.C.,
The role of the lacrimal functional unit in the pathophysiology of dry eye,
Exp. Eye Res. **78**, 2004 (409–416)
<https://doi.org/10.1016/j.exer.2003.09.003>
- Stern, M.E., Schaumburg, C.S., and Pflugfelder, S.C.,
Dry eye as a mucosal autoimmune disease,
Int. Rev. Immunol. **32**, 2013 (19–41)
<https://doi.org/10.3109/08830185.2012.748052>
- Stewart, A.J., and Stewart, R.F.,
Phenols,
Ecotoxicology **2008**, 2008 (2682–2689)
<https://doi.org/10.1017/cbo9780511615276.028>
- Stramer, B.M., Zieske, J.D., Jung, J.C., Austin, J.S, and Fini, M.E.,
Molecular mechanisms controlling the fibrotic repair phenotype in cornea: implications for surgical outcomes,
Invest Ophthalmol Vis Sci **44**, 2003 (4237–4246).
- Tadros, T.,
Polymeric surfactants in disperse systems,
Adv. Colloid Interface Sci. **147–148**, 2009 (281–299)
<https://doi.org/10.1016/j.cis.2008.10.005>
- Takahashi, H., Kaminski, A.E., and Zieske, J.D.,
Glucose transporter 1 expression is enhanced during corneal epithelial wound repair,
Exp. Eye Res. **63**, 1996 (649–659)
<https://doi.org/10.1006/exer.1996.0159>
- Tamilvanan, S., and Benita, S.,
The potential of lipid emulsion for ocular delivery of lipophilic drugs,
Eur. J. Pharm. Biopharm. **58**, 2004 (357–368)
<https://doi.org/10.1016/j.ejpb.2004.03.033>
- Tavakoli, A., and Flanagan, J.L.,
Dry eye disease: an (in)convenient truth,
Clin. Exp. Optom. **105**, 2022 (222–229)
<https://doi.org/10.1080/08164622.2021.1945410>
- Teichmann, J., Valtink, M., Nitschke, M., Gramm, S., Funk, R., Engelmann, K., and Werner, C.,
Tissue engineering of the corneal endothelium: a review of carrier materials,
J. Funct. Biomater. **4**, 2013 (178–208)
<https://doi.org/10.3390/jfb4040178>
- Thoft, R.A., and Friend, J.,
International ophthalmology clinics,
Little, Brown and Company, Boston, (1979).
- Thulasi, P., and Djalilian, A.R.,
Update in current diagnostics and therapeutics of dry eye disease,
Ophthalmology **124**, 2017 (S27–S33)
<https://doi.org/10.1016/j.optha.2017.07.022>

- Tian, B., and Liu, J.,
Resveratrol: a review of plant sources, synthesis, stability, modification and food application,
J. Sci. Food Agric. **100**, 2020 (1392–1404)
<https://doi.org/10.1002/jsfa.10152>
- Tiffany, J.M.,
The normal tear film, in: development in ophthalmology,
Karger, Basel **41**, 2008 (1–20).
- Tiwari, R., Pandey, V., Asati, S., Soni, V., and Jain, D.,
Therapeutic challenges in ocular delivery of lipid based emulsion,
J. Basic Appl. Sci. **5**, 2018 (121–129)
<https://doi.org/10.1016/j.ejbas.2018.04.001>
- Uchino, M., Dogru, M., Uchino, Y., Fukagawa, K., Shimmura, S., Takebayashi, T., Schaumberg, D.A., and Tsubota, K.,
Japan ministry of health study on prevalence of dry eye disease among japanese high school students,
Am. J. Ophthalmol. **146**, 2008 (925–929)
<https://doi.org/10.1016/j.ajo.2008.06.030>
- Urtti, A.,
Challenges and obstacles of ocular pharmacokinetics and drug delivery,
Adv. Drug Deliv. Rev. **58**, 2006 (1131–1135)
<https://doi.org/10.1016/j.addr.2006.07.027>
- Van Haeringen, N.,
Clinical biochemistry of tears,
Surv. Ophthalmol. **26**, 1981 (84–96).
- Varela-Fernández, Díaz-Tomé, V., Luaces-Rodríguez, A., Conde-Penedo, A., García-Otero, X., Luzardo-Álvarez, A., Fernández-Ferreiro, A., and Otero-Espinar, F.J.,
Drug delivery to the posterior segment of the eye: biopharmaceutic and pharmacokinetic considerations,
Pharmaceutics **12**, 2020 (1–39)
<https://doi.org/10.3390/pharmaceutics12030269>
- Venkata, A., Fowjana, J., Madhumathi, S., and Rajeshwari, M.,
Tear fluid small molecular antioxidants profiling shows lowered glutathione in keratoconus,
Exp Eye Res **103**, 2012 (41–46)
<https://doi.org/10.1016/j.exer.2012.07.010>
- Vernhardsdottir, R.R., Magno, M.S., Hynnekleiv, L., Lagali, N., Dartt, D.A., Vehof, J., Jackson, C.J., and Utheim, T.P.,
Antibiotic treatment for dry eye disease related to meibomian gland dysfunction and blepharitis – A review,
Ocul. Surf. **26**, 2022 (211–221)
<https://doi.org/10.1016/j.jtos.2022.08.010>
- Wang, M.T.M., Muntz, A., Mamidi, B., Wolffsohn, J.S., and Craig, J.P.,
Modifiable lifestyle risk factors for dry eye disease,
Contact Lens Anterior Eye **44**, (101409)
<https://doi.org/10.1016/j.clae.2021.01.004>
- Wang, W., Sun, C., Mao, L., Ma, P., Liu, F., Yang, J., and Gao, Y.,
The biological activities, chemical stability, metabolism and delivery systems of quercetin: A review,
Trends Food Sci. Technol. **56**, 2016 (21–38)
<https://doi.org/10.1016/j.tifs.2016.07.004>
- Wang, X., Wang, S., and Zhang, Y.,
Advance of the application of nano-controlled release system in ophthalmic drug delivery,
Drug Deliv. **23**, 2016 (2897–2901)
<https://doi.org/10.3109/10717544.2015.1116025>

- Wegener, A.R., Meyer, L.M., and Schönfeld, C.L.,
Effect of viscous agents on corneal density in dry eye disease,
J. Ocul. Pharmacol. Ther. **31**, 2015 (504–508)
<https://doi.org/10.1089/jop.2014.0157>
- Wei, Y., and Asbell, P.A.,
The core mechanism of dry eye disease is inflammation,
Eye Contact Lens **40**, 2014 (248–256)
<https://doi.org/10.1097/ICL.0000000000000042>
- Wolffsohn, J.S., Arita, R., Chalmers, R., Djalilian, A., Dogru, M., Dumbleton, K., Gupta, P.K., Karpecki, P., Lazreg, S., Pult, H., Sullivan, B.D., Tomlinson, A., Tong, L., Villani, E., Yoon, K.C., Jones, L., and Craig, J.P.,
TFOS DEWS II Diagnostic Methodology report,
Ocul. Surf. **15**, 2017 (539–574)
<https://doi.org/10.1016/j.jtos.2017.05.001>
- Wolkoff, P., Nøjgaard, J.K., Troiano, P., and Piccoli, B.,
Eye complaints in the office environment: Precorneal tear film integrity influenced by eye blinking efficiency,
Occup. Environ. Med. **62**, 2005 (4–12)
<https://doi.org/10.1136/oem.2004.016030>
- Wollensak, G., Mur, E., Mayr, A., Baier, G., Göttinger, W., and Stöffler, G.,
Effective methods for the investigation of human tear film proteins and lipids,
Graefe's Arch. Clin. Exp. Ophthalmol. **228**, 1990 (78–82)
<https://doi.org/10.1007/BF02764296>
- Yeotikar, N.S.,
The natural history of meibomian glands: age-related changes in an asymptomatic population,
Invest Ophthalmol Vis Sci **55**, 2014 (21).
- Yoshihisa Shirasaki,
Molecular design for enhancement of ocular penetration,
J. Pharm. Sci. **97**, 2007 (2462–2496)
<https://doi.org/10.1002/jps>
- Zander, B.E., and Weddell, G.,
Observations on the innervation of the cornea,
J. Anat. **85**, 1948 (68–99).
- Zhong, M., Gadek, T.R., Bui, M., Shen, W., Burnier, J., Barr, K.J., Hanan, E.J., Oslob, J.D., Yu, C.H., Zhu, J., Arkin, M.R., Evanchik, M.J., Flanagan, W.M., Hoch, U., Hyde, J., Prabhu, S., Silverman, J.A., and Wright, J.,
Discovery and development of potent LFA-1/ICAM-1 antagonist SAR 1118 as an ophthalmic solution for treating dry eye,
ACS Med. Chem. Lett. **3**, 2012 (203–206)
<https://doi.org/10.1021/m12002482>
- Zhu, X.D., Lei, X.P., Dong and W. Bin,
Resveratrol as a potential therapeutic drug for respiratory system diseases,
Drug Des. Devel. Ther. **11**, 2017 (3591–3598)
<https://doi.org/10.2147/DDDT.S148868>

2

Motivation

Dry eye disease (DED) is a complex pathological state that affects the ocular surface. DED emerges because of a dysfunctional Lacrimal Functional Unit (LFU), which is no longer capable of preserving the homeostasis of the ocular surface. Although the causes of the dysfunction of the LFU are not clearly understood, it is suggested that it mostly develops due to exogenous stress. This causes the activation of acute inflammatory pathways, with the consequent development of a chronic inflammatory condition typical of DED. The therapeutic options are wide and distinct: from topical application of corticosteroids and other anti-inflammatory compounds to lid hygiene and thermal and massage treatments. However, all of these have in common that they do not represent a permanent therapeutic solution for DED patients. As a result, efforts have been put into finding new potential molecules that could meet the unmet needs in the treatment of DED. One of the emerging classes of molecules that has gained particular interest are polyphenols. Polyphenols are natural plant metabolites that have been granted a large variety of therapeutic effects, among them the anti-inflammatory and antioxidative ones. In previous studies conducted by our research group, quercetin and resveratrol, two compounds from the group of polyphenols, have come out as good candidates for the treatment of DED. Unfortunately, broader therapeutic applications have been restrained by their poor physico-chemical characteristics, such as low water solubility and chemical instability.

Therefore, the aim of this thesis work was the development of different formulation strategies that could overcome the issues related to these molecules and bring them closer to a commercially available treatment for DED.

3

Hypothesis

For the development of this thesis, the following hypothesis was formulated:

Quercetin and resveratrol are natural polyphenolic compounds with potential applications as ophthalmological therapeutics. Since their application is limited by their poor physico-chemical characteristics, they are likely to be improved by the employment of advanced drug delivery strategies.

4

Objectives

To support the hypothesis, the following objectives were established:

General Objective

To develop different formulation strategies for quercetin (QUE) and resveratrol (RSV) to improve their physico-chemical characteristics and, consequently, their bioavailability for ocular surface cells.

Specific Objectives

1. To design four different types of formulations for QUE and RSV, namely liposomes, inclusion complexes with cyclodextrins, elastin-like recombinamer-based nanoparticles and contact lenses embedded with micelles in order to improve their solubility and chemical stability.
2. To test the biocompatibility of the formulations *in vitro* using ocular surface cell lines.
3. To test the antioxidant and anti-inflammatory abilities of the formulations *in vitro*.
4. To evaluate the penetration capacity of the developed formulations in *in vitro* and *ex vivo* ocular surface models.

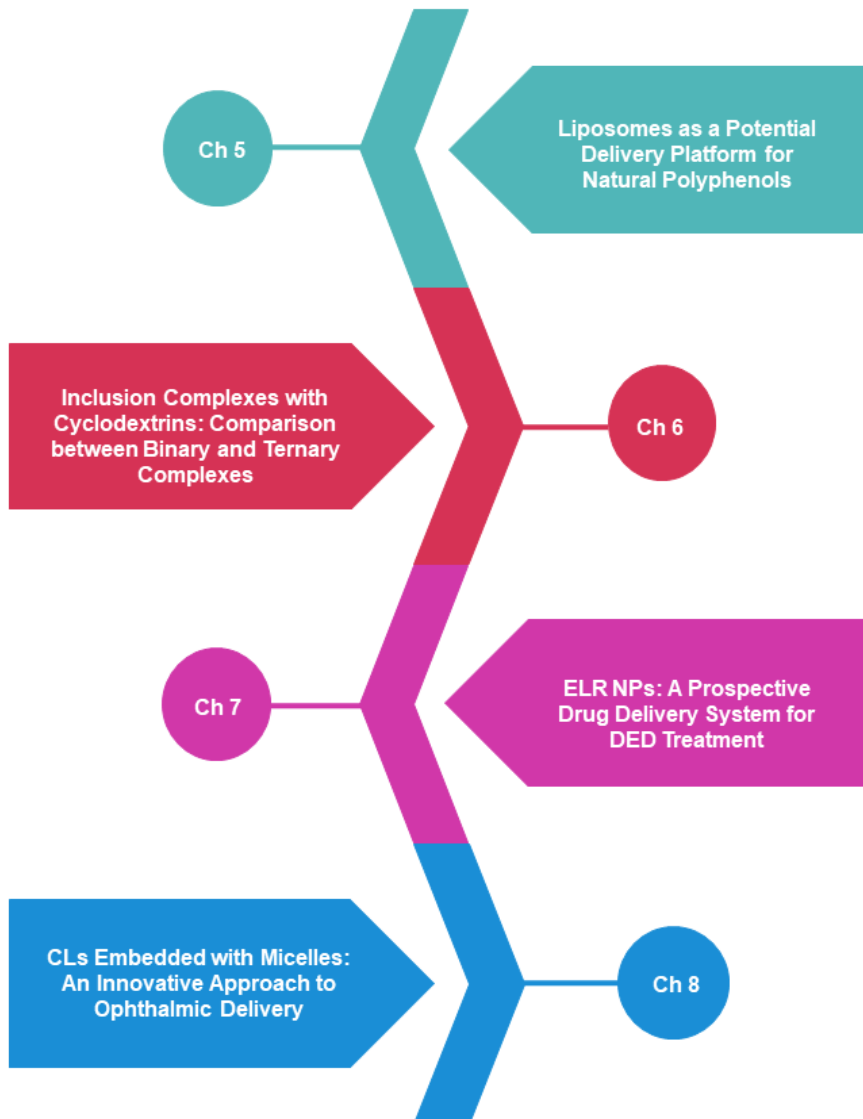


Figure 4.1: A schematic representation of the chapters and the delivery strategy covered in each one of it.

III

Development

5

Liposomes as a Potential Delivery Platform for Natural Polyphenols

Liposomes are lipid-based vesicles first discovered in the 1960s by the British hematologist Dr. Alec D. Bangham (Bangham *et al.*, 1964). At present, liposomes represent one of the most studied delivery systems for biomedical applications. Their unique architecture consisting of one or more lipid bilayers (*lamellae*) surrounding an aqueous interior offers them the versatility to serve as a carrier for different types of molecules like small drugs, proteins, nucleic acids, and imaging agents (Al-Amin *et al.*, 2023; Gao *et al.*, 1994; Portnoy *et al.*, 2019, 2011)

Due to their similarity with the cellular membrane, liposomes possess excellent biocompatibility. Additionally, they are listed as a biodegradable, non-toxic and non-immunogenic carriers, suitable for administration through different routes (Guimar *et al.*, 2021; Łukawski *et al.*, 2019; Mehta *et al.*, 2020; Shah *et al.*, 2020; Taha *et al.*, 2014). Furthermore, the drugs loaded into liposomes are protected from enzymatic degradation and potential chemical inactivation. In addition, the contact of the drug with the healthy tissues prior the drug release is limited, reducing the appearance of adverse effects (Bozzutto *et al.*, 2015). The surface properties of the liposomes can be easily modulated by decorating them with PEG or different ligands, which confer stealth or targeting properties (Kapoor *et al.*, 2017).

Phospholipids used for the preparation of liposomes can be divided into natural and synthetic ones. Natural phospholipids are mostly obtained from soy bean and egg yolk (Monteiro *et al.*, 2014), while the synthetic ones result from modifications of the naturals. These modifications usually involve changes in the aliphatic chain, head, or alcohol group, regulating the properties of the phospholipid, usually conferring it higher stability (Guimar *et al.*, 2021; Lombardo *et al.*, 2016). Liposomes and

phospholipid general structures are shown in **figure 5.1**.

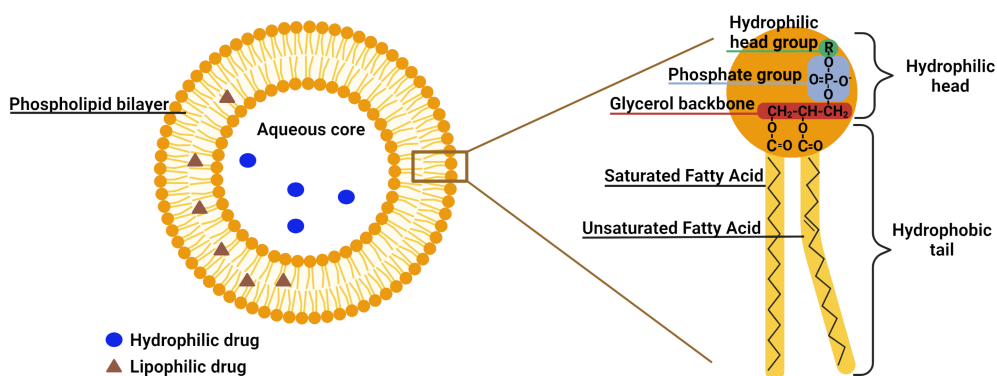


Figure 5.1 - Schematic representation of the liposomal and phospholipid structure. The figure was created with BioRender®.

In 1995, the first nanomedicine formulation was approved by the FDA. This was Doxil®, a liposomal formulation of doxorubicin that significantly reduces the toxic effects associated with its administration while maintaining the efficiency of free doxorubicin (Patel *et al.*, 1996; Popilski *et al.*, 2020). For ophthalmic applications, Visudyne®, a formulation based on conventional liposomes for the treatment of age-related macular degeneration was approved in the 2000 (Kim *et al.*, 2021). The aim of this part of the thesis was the development and physico-chemical characterization of a liposomal formulation for the topical ocular delivery of small naturally occurring molecules, QUE and RSV. Part of the physico-chemical characterization was done as a part of an academic secondment, at the University of Eastern Finland (Kuopio, Finland).

5.1. Materials and Methods

5.1.1. Materials

Quercetin, resveratrol, 1,2-Dioctadecanoyl-*sn*-glycero-3-phosphocholine (DSPC), cholesterol and Spectra-Por® Float-A-Lyzer® G2 MWCO 100 kDa were obtained from Merck Life Sciences (St. Louis, MO, USA). Chloroform and round-bottom flasks were purchased from Quimilid (Valladolid, Spain). Avanti mini extruder equipped with a 200-nm cut-off polycarbonate membrane was acquired from Avanti Polar Lipids Inc. (Alabaster, Alabama, USA).

5.1.2. Methods

Preparation of the Liposomes

Liposomes were prepared by the thin rehydration technique proposed by Bangham (Bangham *et al.*, 1965). Two types of liposomes with different lipidic composition were prepared: DSPC:cholesterol in a 1:1 molar ratio and DSPC:cholesterol in a 6:4 ratio. All the reagents were dissolved in anhydrous chloroform, which was evaporated under reduced pressure using a rotary evaporator (Hei-VAP Core, Heidolph, Schwabach, Germany). The lipidic film formed on the bottom of the flask was rehydrated with 200 μL of Phosphate Buffer Saline (PBS) (pH 7.4) and subjected to ten freeze-thaw cycles. The final volume was adjusted to 1 mL, corresponding to a final concentration of 10 mg/mL of lipids.

For the size adjustment, two different approaches were explored. The first one relies on the application of ultrasounds. Liposomal suspensions were exposed to ultrasounds using a probe sonicator (40 % power, 55 kHz, J.P. Selecta, Abrera, Spain), for a total of 10 minutes with alternating one minute pulse and one minute off (Silva *et al.*, 2010).

In the second one, a classical approach involves extruding (11 times) the liposomal suspension through an extruder (Avanti mini extruder, Avanti Polar Lipids Inc. Alabaster, Alabama, USA) having a 200-nm cut-off polycarbonate membrane (Wenche *et al.*, 2015).

Liposomes loaded with QUE or RSV were prepared by adding the drug solutions (500 μM , dissolved in CHCl_3) to the initial lipid mixture. To remove the non-loaded drug, dialysis against 1 L of PBS was performed for 2 hours.

Characterization of Liposomal Formulations

Dynamic Light Scattering (Malvern Panalytical, Malvern, Worcestershire, UK) was used to determine the size and polydispersity index (PDI) of blank (empty) and loaded liposomes. For this purpose, liposomes were diluted to a concentration of 0.5 mg/mL in PBS.

The calibration curves of both molecules were prepared using a UV-Vis spectrophotometer (DeNovix DS-11 FX+, Wilmington, DE, USA) and measuring the absorbances at 306 and 370, for RSV and QUE, respectively. The concentration ranges for the calibration curves were 2.5-100 μM for RSV, $R^2=0.9984$ and of 2.5-80 μM for QUE, $R^2=0.9954$, prepared in MeOH/ H_2O (50:50 v/v). To measure the entrapment efficacy of QUE and RSV, liposomes were broken using pure MeOH and subsequently

sonicated for 10 minutes. The amount of both drugs was calculated using the calibration lines previously prepared.

Statistical Analysis

Experimental data is reported as mean \pm standard error of the mean (SEM). Data means were compared using an independent Student's t-test, preceded by Shapiro-Wilk normality test. All analysis were done with SPSS software (SPSS 20.0; SPPS, Inc., Chicago, IL, USA).

5.2. Results and Discussion

5.2.1. Characterization of Liposomal Formulations

In this study, we prepared liposomes made from the combination of DSPC, a zwitterionic long-alkyl chain phospholipid, and cholesterol, a sterol derivative. DSPC is one of the most common synthetic phospholipids used in liposomal preparations, while cholesterol is a natural constituent of cell membranes with important physiological functions (Bennett *et al.*, 2018; Monteiro *et al.*, 2014). The introduction of cholesterol in the liposomal bilayer has several beneficial functions, such as: i) improving the liposomal stability; ii) increasing the packing of phospholipid molecules; iii) modulating bi-layer fluidity (Gregoriadis *et al.*, 1979; Plessis *et al.*, 1996). A maximum of 50 % (of the total liposomal composition) of cholesterol can be incorporated into reconstituted bilayers, as suggested by several studies. Likewise, the 1:1 molar ratio (phospholipid:cholesterol) is one of the most commonly used (Nakhaei *et al.*, 2021). The 6:4 molar ratio was chosen to see its effect on the entrapment efficacy of the polyphenols and its potential behavior in *in vitro* studies, as well as because it is frequently reported in the literature for liposomal formulations (Bruglia *et al.*, 2015; Semple *et al.*, 1996; Su *et al.*, 2018).

The size and PDI of the liposomes obtained from two different size reduction methods were studied by DLS, and the results are summarised in **table 5.1**. Blank liposomes treated with ultrasounds had a mean diameter of 146.55 ± 17 nm for the composition DSPC:Chol = 1:1 and of 133.12 ± 13 nm for DSPC:Chol = 6:4. In both cases, the PDI was below 0.3, indicating that a good size homogeneity inside the samples was achieved. Regarding the liposomes that were extruded through the Mini Extruder, the DSPC:Chol = 1:1 had a size of 144.7 ± 10 nm while the DSPC:Chol = 6:4 were 137.89 ± 11 nm, with PDI values below 0.2 for both liposome preparations. Liposomes prepared with a 1:1 ratio displayed a moderately larger size than the ones made

with a 6:4 ratio. This is in accordance with the finding that the higher the amount of cholesterol in the liposome, the higher is its mean size (Lee *et al.*, 2005). Although the two methods used for liposomal size reduction gave optimal and comparable results, we decided to proceed with the extrusion method. This is because extrusion has proven to be a simpler and faster method, with the advantage of being highly efficient and reproducible in the size reduction of the liposomes.

Table 5.1: Summary of the size (nm), Pdl, and encapsulation efficiency (%) of QUE and RSV. Values are reported as means \pm SEM.

	Composition	Size (nm)	Pdl	% QUE	% RSV
Ultrasounds	DSPC:Chol = 1:1	146.55 \pm 17	0.28 \pm 0.078	N/D	N/D
	DSPC:Chol = 6:4	133.12 \pm 13	0.25 \pm 0.043	N/D	N/D
Extruded	DSPC:Chol = 1:1	144.7 \pm 10	0.18 \pm 0.013	-	-
	DSPC:Chol = 6:4	137.89 \pm 11	0.22 \pm 0.10	-	-
	DSPC:Chol = 1:1	156.9 \pm 09	0.15 \pm 0.12	12.26 \pm 5.39	-
	DSPC:Chol = 6:4	142.9 \pm 03	0.12 \pm 0.072	1.35 \pm 0.36	-
	DSPC:Chol = 1:1	164.05 \pm 12	0.21 \pm 0.034	-	2.25 \pm 1.68
	DSPC:Chol = 6:4	131.56 \pm 04	0.20 \pm 0.028	-	0.24 \pm 0.94

N/D = not determined.

Concerning the encapsulation efficiency of QUE and RSV, this was exceptionally low. For the lipidic composition DSPC:Chol=1:1 only 12.26 \pm 5.39 % of initial QUE was loaded, and for RSV this was 2.25 \pm 1.68 %. The results did not differ for the DSPC:Chol=6:4 liposomes, in which 1.35 \pm 0.36 % and 0.24 \pm 0.94 % of QUE and RSV were loaded, respectively. Statistical analysis of the data was performed, however there were no significant differences among the groups compared ($p > 0.05$). The poor loading of the polyphenols in our liposomal formulations may have diverse explanations. QUE and RSV were loaded into the liposomes through the passive loading method, where drug loading and liposome formation take place at the same time. Although, this is a preferred method for loading of poorly soluble drugs (such as QUE and RSV), cases with insufficient drug entrapment may occur because of poor interaction between the drug(s) and the liposomes, or because of concomitant interfering events such as burst release (Pauli *et al.*, 2019).

To solve this issue active (remote) loading can represent an alternative. In this method, the drug is loaded into preformed liposomes, exploiting a transmembrane

gradient (Bally *et al.*, 1988). Nevertheless, solubilisation of the compound of interest occurs in the outer aqueous phase, with possible limitations emerging in the loading of a hydrophobic drug. Besides the method of preparation, the entrapment efficiency of a drug into the liposomes may also be affected by the size and lamellarity of the lipid vesicles (Immordino *et al.*, 2006). Liposomes can be divided into different groups according to their size and the lipid layers present in the liposome architecture. The liposomes prepared in this work are classified as large unilamellar vesicles (100-400 nm), containing one lipid bilayer surrounding an aqueous core (Arcuri *et al.*, 1999). Multilamellar vesicles, made from several concentric lipid bilayers, have a larger lipidic portion suitable for hosting higher quantities of hydrophobic drugs. However, they possess a greater diameter (micrometric size range) as well, and are consequently not suitable for topical ophthalmic applications (Walde *et al.*, 2001).

No examples of liposomes loaded with QUE and RSV for ophthalmic applications were found in the literature. However, formulations aimed for the treatment of non-ocular diseases have been developed. For example, Cadena *et al.* proposed a formulation of elastic liposomes, where the formation of an inclusion complex with HP β CD enabled the loading of QUE and RSV into the inner core of the liposome (Cadena *et al.*, 2013). Caddeo and co-workers suggested the co-delivery of QUE and RSV for the treatment of skin cancer using a commercially available lipid mixture for the preparation of liposomes. Small unilamellar vesicles were formed by sonicating the starting mixture of drug(s) and lipids, with an excellent entrapment efficacy of above 60 % for both polyphenols (Caddeo *et al.*, 2016). These examples suggest that it is possible to achieve an elevated loading of the therapeutic agent inside the liposomes using the passive loading method. A potential solution could be adopting a solubilization technique (salt or prodrug formation, complexation with cyclodextrins, etc.) combined with a refinement of the liposomal composition.

5.3. Conclusions

The aim of this chapter was the generation of a potential liposomal formulation for ophthalmic delivery of QUE and RSV. Different methods of size reduction of liposomes were explored successfully; however, the encapsulation of QUE and RSV led to issues related to the efficiency of the loading process. As already mentioned, several parameters lacked proper adjustment to be able to obtain a promising liposomal formulation capable of delivering therapeutic concentrations of natural substances of interest.

References of Chapter 5

- Al-Amin, M.D., Mastrotto, F., Subrizi, S, Sen, M. ,Turunen, T. , Arango-Gonzalez, B., Ueffing, M., Urtti, A., Salmaso, S., and Caliceti, P.,
Tailoring surface properties of liposomes for dexamethasone intraocular administration,
J. Control. Release **354**, 2023 (323–336)
<https://doi.org/10.1016/j.jconrel.2023.01.027>
- Arcuri, B.F., Vechetti, G.F., and Chehi, R.N.,
Protein-induced fusion of phospholipid vesicles of heterogeneous sizes,
Biochem. Biophys. Res. Commun. **590**, 586–590 (1999).
- Bally, B., and Cullis, R.,
Dopamine accumulation in large unilamellar vesicle systems induced by transmembrane ion gradients,
Chem. Phys. Lipids **47**, 97–107 (1988).
- Bangham, A.D., and Horne, R.W.,
Negative staining of phospholipids and their structural modification by surface-active agents as observed in the electron microscope,
J. Mol. Biol. **8**, 1964 (660–668)
[https://doi.org/10.1016/S0022-2836\(64\)80115-7](https://doi.org/10.1016/S0022-2836(64)80115-7)
- Bangham, A.D., Standish, M.M., and Watkins, J.C.,
Diffusion of univalent ions across the lamellae of swollen phospholipids,
J. Mol. Biol. **13**, 1965 (238–252)
[https://doi.org/10.1016/S0022-2836\(65\)80093-6](https://doi.org/10.1016/S0022-2836(65)80093-6)
- Bennett, W.F.D., Shea, J., and Tieleman, D.P.,
Phospholipid chain interactions with cholesterol drive domain formation in lipid membranes,
Biophys. J. **114**, 2018 (2595–2605)
<https://doi.org/10.1016/j.bpj.2018.04.022>
- Bozzuto, G., and Molinari, A.,
Liposomes as nanomedical devices,
Int. J. Nanomedicine **10**, 2018 (975–999)
<https://doi.org/10.1016/j.bpj.2018.04.022>
- Bruglia, ML., Rotella, C. , McFarlane, A. , and Lamprou, D.A.,
Influence of cholesterol on liposome stability and on in vitro drug release,
Drug Deliv. Transl **3**, 231–242 (2015).
- Caddeo, C., Nacher, A., Vassallo, A., Francesca, M., Pons, R., Fernández-Busquets, X., Carbone, C., Valenti, D., Maria, A., and Manconi, M.,
Effect of quercetin and resveratrol co-incorporated in liposomes against inflammatory / oxidative response associated with skin cancer,
Int. J. Pharm. **513**, 2016 (153–163)
<https://doi.org/10.1016/j.ijpharm.2016.09.014>

- Cadena, P.G., Pereira, M.A., Cordeiro, R.B.S., Cavalcanti, I.M.F., Barros, B., Pimentel, C.C.B., Luiz, J., Filho, L., Silva, V.L., and Santos-Magalhães, N.S.,
Nanoencapsulation of quercetin and resveratrol into elastic liposomes,
BBA-Biomembr. **1828**, 2013 (309–316)
<https://doi.org/10.1016/j.bbamem.2012.10.022>
- Gao, X., Noda, Y., Rubinstein, I., and Paul, S.,
Vasoactive intestinal peptide encapsulated in liposomes: effects on systemic arterial blood pressure,
Pharmacol. Lett. **54**, 247–252 (1994).
- Gregoriadis, G., and Davis, C.,
Stability of liposomes in vivo and in vitro is promoted by their cholesterol content and the presence of blood cells,
Biochem. Biophys. Res. Commun. **89**, 1287–1293 (1979).
- Guimar, D., and Cavaco-Paulo, A.,
Design of liposomes as drug delivery system for therapeutic applications,
Int. J. Pharm. **601**, 2021 (309–316)
<https://doi.org/10.1016/j.ijpharm.2021.120571>
- Immordino, M.L., and Cattell, L.,
Stealth liposomes: review of the basic science, rationale, and clinical applications, existing and potential,
Int. J. Nanomedicine **3**, 297–315 (2006).
- Kapoor, M., Lee, S.L., and Tyner, K.M.,
Liposomal drug product development and quality: current US experience and perspective,
AAPS J. **19**, 2017 (632–641)
<https://doi.org/10.1208/s12248-017-0049-9>
- Kim, E., and Jeong, H.,
Liposomes: Biomedical Applications,
CMJ **57**, 27–35 (2021).
- Lee, S., Lee, K., Kim, J., and Lim, S.,
The effect of cholesterol in the liposome bilayer on the stabilization of incorporated retinol,
Liposome Res. **15**, 2005 (157–166)
<https://doi.org/10.1080/08982100500364131>
- Lombardo, D., Calandra, P., Barreca, D., Magazù, S., and Kiselev, M.A.,
Soft interaction in liposome nanocarriers for therapeutic drug delivery,
Nanomaterials **6**, 2016 (125–151)
<https://doi.org/10.3390/nano6070125>
- Łukawski, M., Dałek, P., Borowik, T., Foryś, A., Witkiewicz, W., Przybyło, M., Maciej, Ł., Da, P., Borowik, T., and Fory, A.,
New oral liposomal vitamin C formulation: properties and bioavailability,
J.Liposome Res. **6**, 2019 (1–8)
<https://doi.org/10.1080/08982104.2019.1630642>
- Mehta, P.P., Ghoshal, D., Pawar, A.P., Kadam, S.S., and Dhapte-Pawar, V.S.,
Recent advances in inhalable liposomes for treatment of pulmonary diseases: Concept to clinical stance,
J. Drug Deliv. Sci. Technol. **6**, 2020 (1–53)
<https://doi.org/10.1016/j.jddst.2020.101509>
- Monteiro, N., Martins, A., Reis, R.L., and Neves, N.M.,
Liposomes in tissue engineering and regenerative medicine,
J. R. Soc. Interface. **11**, 2014 (1–24)
<https://doi.org/10.1098/rsif.2014.0459>
- Nakhaei, P., Margiana, R., Bokov, D.O., Abdelbasset, W.K., Amin, M., Kouhbanani, J., Varma, R.S., Maro, F., and Sarani, M.,
Liposomes: structure, biomedical applications, and stability parameters with emphasis on cholesterol,
Front. Bioeng. Biotechnol. **9**, 2021 (1–23)
<https://doi.org/10.3389/fbioe.2021.705886>

- Patel, J.,
Liposomal doxorubicin: Doxil®,
J Oncol Pharm Practice. **2**, 201–210 (1996).
- Pauli, G., Tang, W., and Li, S.,
Development and characterization of the solvent-assisted active loading technology (SALT) for liposomal loading of poorly water-soluble compounds,
Pharmaceutics **57**, 27–35 (2019).
- Plessis, J., and Ramachandran, C.,
The influence of lipid composition and lamellarity of liposomes on the physical stability of liposomes upon storage,
Int J. Pharma. **127**, 273–278 (1996).
- Popilski, H., Feinshtein, V., Kleiman, S., Mattarei, A., Garofalo, M., Salmaso, S., and Stepensky, D.,
Doxorubicin liposomes cell penetration enhancement and its potential drawbacks for the tumor targeting efficiency,
Int. J. Pharm. **592**, 2020 (1–10)
<https://doi.org/10.1016/j.ijpharm.2020.120012>
- Portnoy, E., Lecht, S., Lazarovici, P., Danino, D., and Magdassi, S.,
Cetuximab-labeled liposomes containing near-infrared probe for in vivo imaging,
Nanomedicine Nanotechnology, Biol. Med. **7**, 2011 (480–488)
<https://doi.org/10.1016/j.nano.2011.01.001>
- Rodrigues, S., Banerjee, A., Kanekiyo, T., and Singh, J.,
Functionalized liposomal nanoparticles for efficient gene delivery system to neuronal cell transfection,
Int. J. Pharm. **7**, 2019 (1–56)
<https://doi.org/10.1016/j.ijpharm.2019.06.026>
- Simple, S.C., Chonn, A., and Cullis, P.R.,
Influence of cholesterol on the association of plasma proteins with liposomes,
Int J. Pharma. **35**, 2521–2525 (1996).
- Shah, S., Dhawan, V., Holm, R., Nagarsenker, M.S., and Perrie, Y.,
Liposomes: Advancements and innovation in the manufacturing process,
Adv. Drug Deliv. Rev. **154**, 2020 (102–122)
<https://doi.org/10.1016/j.addr.2020.07.002>
- Silva, R., Ferreira, H., Little, C., and Cavaco-Paulo, A.,
Ultrasonics sonochemistry effect of ultrasound parameters for unilamellar liposome preparation,
Ultrason. - Sonochemistry. **17**, 2010 (628–632)
<https://doi.org/10.1016/j.ultsonch.2009.10.010>
- Su, F., Chen, J., Son, H., Kelly, A.M., Convertine, A.J., and Daniel, M.,
Polymer-augmented liposomes enhancing antibiotic delivery against intracellular infections,
Biomater. Sci. **6**, 2018 (1976–1985)
<https://doi.org/10.1039/c8bm00282g>
- Taha, E.I., El-anazi, M.H., El-bagory, I.M., and Bayomi, M.A.,
Design of liposomal colloidal systems for ocular delivery of ciprofloxacin,
Saudi Phar. J. **22**, 2014 (231–239)
<https://doi.org/10.1016/j.jsps.2013.07.003>
- Walde, P., and Ichikawa, S.,
Enzymes inside lipid vesicles: preparation, reactivity and applications,
Biomol. Eng. **18**, 143–177 (2001).
- Wenche, M., Acharya, G., and Basnet, P.,
Resveratrol-loaded liposomes for topical treatment of the vaginal inflammation and infections,
Eur.J. Pharm. Sci. **79**, 2015 (112–121)
<https://doi.org/10.1016/j.ejps.2015.09.007>

6

Inclusion Complexes with Cyclodextrins: Comparison Between Binary and Ternary Complexes

This chapter was published as a part of the following article:

Improved ocular delivery of quercetin and resveratrol: A comparative study between binary and ternary cyclodextrin complexes,

Krstić, L., Jarho, P, Ruponen, M, Urtili, A, González-García, M.J., Diebold, Y.,
Int J Pharm. **624**, 122028 (2022)

Cyclodextrins (CDs) are cyclic oligosaccharides broadly used in pharmaceutical, cosmetic and food industries (Del Valle, 2004). The enzymatic conversion of starch produces the most abundant naturally occurring CDs which contain 6 (α -CD), 7 (β -CD) or 8 (γ -CD) glucopyranose units (Lachowicz *et al.*, 2020; Loftsson & Stefánsson, 1997). Apart from these, synthetic derivatives produced by alkylation or hydroxyalkylation of the hydroxyl groups of the parent CDs are widely used (Varan *et al.*, 2017).

The cone shaped structure of CDs, with the hydroxyl groups pointing towards the external environment enables them to host hydrophobic molecules inside the internal cavity. The driving force towards the complex formation is the replacement of energy-rich water molecules with a guest molecule that is capable of forming a complex through non-covalent weak forces (electrostatic interaction, hydrogen bonding, van der Waals forces, hydrophobic interactions, relief of conformational strain) and therefore lower the energy of the system (Liu & Guo, 2002; Loftsson & Stefánsson,

1997). Once complexed, many of the physicochemical properties of the guest molecule will be affected. This is the reason why inclusion complexes with CDs find wide applications. Regarding commercially available products, several eyedrop formulations contain CDs. For example, Indocollyre[®] (Bausch & Lomb, Rochester, USA) include Indomethacin and HP β CDs. Another example of eyedrops is Chlorocil[®] (Laboratorio Edol, Lisbon, Portugal), where chloramphenicol is complexed with methyl- β -CD (Loftsson & Stefánsson, 2021). Different authors have studied the formation of inclusion complexes between distinct CD and QUE and RSV. For example, Venuti *et al.* (2014) reported a potential anticancerogenic effect in human breast cancer cells (MFC7) of RSV/sulfobutylether- β -cyclodextrin complexes. The same authors outlined the exceptional improvement in RSV solubility once complexed (Venuti *et al.*, 2014). In the case of QUE, Başaran *et al.* (2022) prepared complexes between QUE and hydroxypropyl- β -cyclodextrin (HP β CD) and tested them in 3T3 mouse fibroblast for the evaluation of their potential cytotoxicity and in Human Breast Adenocarcinoma (MDA-MB-231) and Human Lung Carcinoma (A549) to evaluate their anticancer activity. The authors as well described that complexation with HP β CD did not affected the antioxidant capacity of the flavonol of interest (Başaran *et al.*, 2022).

In various studies it was observed that the addition of certain excipients, like hydrophilic polymers, to the drug:CD complexes can promote their complexation efficiency and stabilization. These supramolecular nano-assemblies rely on mutual interactions between the CD, drug, and the polymer (Loftsson and Duchêne, 2007; Saokham *et al.*, 2018). The formation of ternary complexes represents a novel and promising approach for delivery of therapeutic agents. Hyaluronic acid is a natural polysaccharide, found in our bodies, mostly in the joints and eyes. It is a linear polymer made up of repeating units of N-acetyl-glucosamine and D-glucuronic acid. Due to its excellent biocompatibility and non-toxicity, it is often used as a material for medical purposes, such as eye-surgeries or in drug delivery (Bayer, 2020).

HP β CD was chosen for this study since it is a well-tolerated β CD derivative, approved by regulatory authorities, and already present in commercially available topical ophthalmic products. For the best of our knowledge there are no studies reported in literature that describe the complexation of QUE and RSV with HP β CD nor formation of ternary complexes with HP β CD/HA for ophthalmic applications (**figure 6.1**). Therefore, the objective of this study was to improve the solubility and stability of QUE and RSV using hydroxypropyl- β -cyclodextrin (HP β CD) and the combination of HP β CD with HA. The formulations were physicochemically characterized, and their biocompatibility and intracellular antioxidant activity was evaluated in human corneal and conjunctival cell lines.

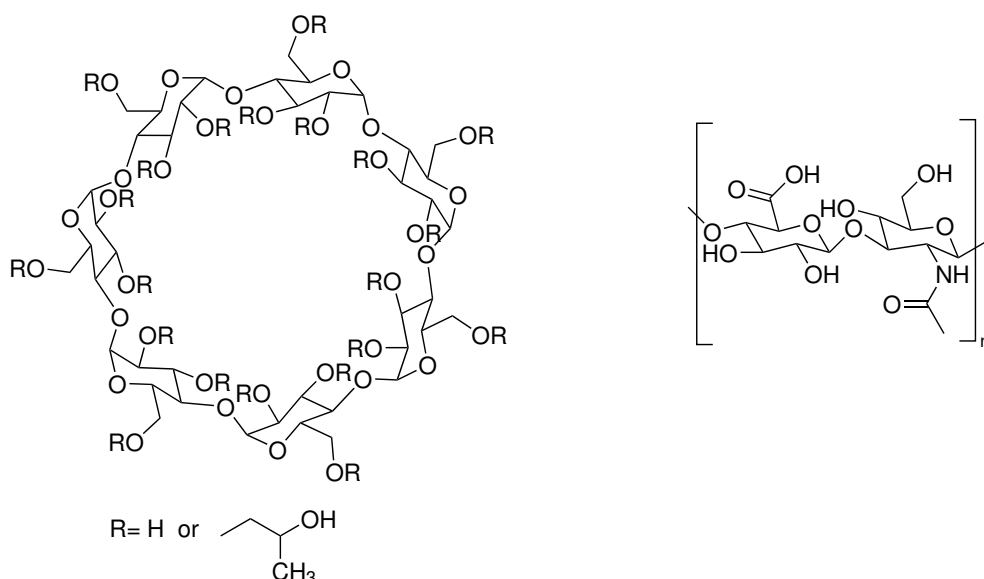


Figure 6.1 - Chemical structures of (a) hydroxypropyl- β -cyclodextrin (HP β CD) and (b) repeating disaccharide unit of hyaluronic acid (HA).

6.1. Materials and Methods

6.1.1. Materials

Hydroxypropyl- β -cyclodextrin (HP β CD) (Av. Mw 1396 Da) (Degree of substitution: 0.67 hydroxypropyl groups per glucose unit), quercetin (QUE), resveratrol (RSV), 2',7'-dichlorofluorescein diacetate (H₂DCFDA), trifluoroacetic acid (TFA), penicillin/streptomycin, human epithelial growth factor (hEGF), hyaluronic acid sodium salt (MW range 1.5–1.8 MDa), 5-methylphenazinium methyl sulphate (PMS) and bovine insulin were obtained from Merck Life Sciences (St. Louis, MO, USA). Cell culture medium Dulbecco's modified Eagle's medium/Nutrient Mixture F-12 (DMEM/F-12) + GlutaMax, DMEM/F12 without phenol red, Dulbecco's phosphate buffered saline (DPBS), foetal bovine serum (FBS), XTT ((2,3-Bis-(2-methoxy-4-nitro-5-sulfophenyl)-2H-tetrazolium-5-carboxanilide), human insulin, BCA Protein Assay kit and all the plastic material (tips, pipettes, culture flask and plates) were purchased from ThermoFisher Scientific (Rockford, IL, USA). MilliQ water was obtained from the Millipore unit. Acetonitrile of HPLC grade was obtained from PanReac (Darmstadt, Germany). Human IL-6 ELISA kit was purchased from Diaclone SAS (Besançon, France). Recombinant Human TNF- α was obtained from PeproTech (Neuilly-sur-Seine, France).

6.1.2. Physicochemical Characterization of the Formulations

Quantitative Analysis of QUE and RSV

For quantitation of QUE and RSV a chromatographic method was developed based on reversed-phase high-pressure liquid chromatography (RP-HPLC) Waters e2695 separation module equipped with an autosampler and a quaternary pump, connected to a Waters 2998 photodiode array detector provided with an UV detector. A C18 Mediterranean Sea column (250×4.6 mm, 5 μm) (Teknokroma Analítica S.A., Barcelona, Spain) with an OptiGuard 1 mm guard column (Sigma-Aldrich, San Luis, Missouri, USA) was used for the separation. The flow rate was set to 1 mL/min and the injection volume was 20 μL . The mobile phase consisted of milliQ water/0.05% (v/v) TFA (A) and acetonitrile/0.05% (v/v) TFA (B) which were eluted in a gradient mode as follows: 4 min 10% B, 6 min 30% B, 16 min 60% B, 17 min 95% B, 18 min 95% B, 19 min 10% B, 22 min 10% B. The retention time for QUE was 15.6 min, while for RSV was 14.7 min, and the wavelengths used for detection were 370 nm and 306 nm, respectively. For the acquisition and processing of data Empower[®] 3 software (Waters[®], Ireland, UK) was used. Standard solutions of QUE (range: 1.5-30 $\mu\text{g}/\text{mL}$, linearity R^2 : 0.9968; LOD- 1.87 $\mu\text{g}/\text{mL}$; LOQ- 2.13 $\mu\text{g}/\text{mL}$) and RSV (range: 1-35 $\mu\text{g}/\text{mL}$, linearity R^2 : 0.9984; LOD- 3.12 $\mu\text{g}/\text{mL}$; LOQ- 4.82 $\mu\text{g}/\text{mL}$) were prepared in ACN: H₂O 50:50 (v/v) and analysed with the same conditions as the samples.

Chemical Stability

The chemical stability of QUE and RSV in PBS (pH 7.4) in the presence of 5% w/v of HP β CD was assessed under controlled temperature (25 °C). Additionally, the possible stabilizing effect of 0.1 %, 0.25% and 0.5% w/v of HA was evaluated. Solutions of free QUE and RSV were used as controls. Samples were protected from light. The clarity of all formulations was visually inspected prior to each analysis. At scheduled time points aliquots of the samples were withdrawn and quantified by RP-HPLC. Data are expressed as percentage of the initial compound concentration (C_0) at the initial time (t_0), and was properly fitted to first order degradation kinetics using the equation below:

$$\log(C_t/C_0) = -kt \quad (6.1)$$

The half-life of compound degradation, $t_{1/2}$, represents the period in which the initial concentration of the samples is reduced by half, and was calculated as follows:

$$t_{1/2} = \frac{1}{k} \log(2) \quad (6.2)$$

Shelf-life of a compound (t_{90}) is the time in which its initial concentration decreases to 90% of the initial one, it is calculated as shown:

$$t_{90} = \frac{0.105}{k} \quad (6.3)$$

Solubility Studies

The solubility of QUE and RSV in the presence of HP β CD was studied in PBS (pH 7.4). Briefly, an excess amount of QUE or RSV was added to increasing concentrations of HP β CD up to 12.5% (w/v). The saturated drug suspensions were left in agitation overnight at 25 °C protected from light. After this time the suspensions were centrifuged (6000 rpm, 10 min) to remove any undissolved drug and analysed for QUE and RSV concentration by RP-HPLC. Phase solubility profiles were established following the method proposed by Higuchi and Connors (Higuchi and Connors, 1965). The apparent stability constant ($K_{1:1}$) and complexation efficiencies (CE) were calculated using equations 6.4 and 6.5, starting from the slopes of the phase solubility diagrams, where S_0 represents the solubility of the drug (Messner et al., 2010). In a specific complexation media, CE can be used for calculating the molar ratio between drug-cyclodextrin as reported in equation 6.6.

$$K_{1:1} = \frac{\text{slope}}{S_0(1 - \text{slope})} \quad (6.4)$$

$$CE = \frac{[\frac{D}{CD}]}{[CD]} = S_0 \times K_{1:1} = \frac{\text{slope}}{S_0(1 - \text{slope})} \quad (6.5)$$

$$D : CD_{\text{molar ratio}} = 1 : \frac{CE + 1}{CE} \quad (6.6)$$

Additionally, the same studies were repeated in the presence of 0.1% w/v HA to evaluate the effect of this polymer on QUE and RSV solubilization by HP β CD complexation.

Preparation of the Formulations

Complexes were prepared by dissolving QUE or RSV in a solution of HP β CD in PBS under agitation. After equilibration at room temperature (RT), any undissolved drug was eliminated through centrifugation (6000 rpm, 10 min). Solid state characterization was performed on freeze-dried solutions (24 h, - 50 °C) (Lyoquest, Telstar, Terassa, Spain). The quantities used were chosen based on previously conducted

phase solubility and stability studies. The composition of all inclusion complexes prepared is listed in **table 6.1**.

Table 6.1: Composition of binary and ternary complexes; ingredient amounts are expressed as % w/v.

Ingredient	Formulations			
	F1	F2	F3	F4
Quercetin	0.065	0.065	-	-
Resveratrol	-	-	0.35	0.35
HP β CD	5	5	5	5
HA	-	0.1	-	0.1

Fourier Transform Infrared Spectra Analysis

The Fourier-Transform Infra-Red (FT-IR) spectra of pure QUE, RSV, CD and HA and their lyophilized complexes were acquired with a FT-IR Bruker ALPHA spectrometer (Ettlingen, Germany). All analyses were performed at RT. Data were collected in the range of 400–4000 cm^{-1} with a spectral resolution of 4 cm^{-1} with an average of 60 scans. Data were collected and processed by OPUS software (version 7.2, Bruker Optik GmbH, Ettlingen, Germany).

Dynamic Light Scattering Measurements

Dynamic light scattering (DLS) was used for the characterization of the particle size within the formulations. All measurements were performed using a Zetasizer Pro (Malvern Panalytical, Malvern, Worcestershire, United Kingdom) in triplicate at RT with a scattering angle at 173°. Possible larger aggregates were eliminated through filtration using a 0.45 μm filter before each measurement.

Atomic Force Microscopy

Surface topography and the size of the complexes were analysed by atomic force microscopy (AFM) (Asylum Research MFP3D BIO; Oxford Instruments, Abingdon, Oxfordshire, United Kingdom). The measurements were performed in tapping mode with 240AC-NA OPUS tips (MikroMasch). Samples were prepared by placing 20 μL of the sample on a recently cleaved mica surface and letting it evaporate at room temperature. Quantitative data, like particle size were obtained through the Gwyd-

dion software (version 2.55, Department of Nanometrology, Czech Metrology Institute, Brno, Czech Republic).

6.1.3. Biological Assays

Cell Lines and Culture Conditions

Human corneal epithelial (HCE) (Araki-Sasaki *et al.*, 1995) and immortalized human conjunctival epithelial (IM-ConjEpi) (Innoprot, Derio, Spain) cell lines were used to evaluate the biocompatibility and functional performance of formulations. Both cell lines are SV-40 Large T antigen immortalized cell lines.

HCE cells were cultured in DMEM/F-12 + GlutaMax cell medium supplemented with 10% FBS, 5 $\mu\text{g}/\text{mL}$ human insulin, 10 ng/mL EGF and with 100 U/mL of penicillin and 0.1 mg/mL of streptomycin. The passages used were from 35 to 45.

IM-ConjEpi cells were cultured in DMEM/ F-12 + GlutaMax which was completed with 10% FBS, 10 ng/mL EGF, 1 $\mu\text{g}/\text{mL}$ bovine insulin and 5000 U/mL of penicillin and 5000 $\mu\text{g}/\text{mL}$ of streptomycin. The passages used were from 7 to 15.

The two cell lines were cultured at controlled temperature and atmosphere (37°C, 5% CO₂). Quotidian inspection of the cells was performed under the phase contrast microscope, while the cell medium was exchanged on every second day.

Cell Viability

To determine cell viability of HCE and IM-ConjEpi cells after exposure to the different formulations a XTT cell viability assay was performed. Cells were seeded in 96-well plates (1×10^4 cells/well) and grown in supplemented medium until 90% of confluence was reached. Cells were then maintained in supplement-free medium for 24 hours. Afterwards, cells were exposed to the formulations (**table 6.1**) for 24 hours. In all cases final concentrations of the polyphenols in the complexes were adjusted in accordance with our previous study (Abengózar-Vela *et al.*, 2015). Concentration range of QUE was 5-50 μM and 25-300 μM for RSV in the complexes. As positive and negative controls, cells were exposed to cell culture medium or 0.005% benzalkonium chloride (BAK), respectively. After 24 hours exposure, cell viability was measured as follows. In brief, cell culture supernatants were discarded, and the wells were loaded with 100 μL of DMEM/F-12 without phenol red. Then, 25 μL of PMS/XTT reaction mixture (10 μL of 3 mg/mL of PMS in 0.25 mg/mL of XTT) prepared just before use was added to each well. After the addition of the reaction mixture the cells were incubated at 37°C for 3 hours. UV/Vis spectrophotometer (SpectraMax M5; Molecular

Devices, Sunnyvale, CA, USA) was used for the measurement of the absorbance at 450 and 660 nm, respectively. The percentage of living cells was calculated relative to the values of the positive control. Six replicates were performed in three independent experiments for each formulation.

Intracellular ROS Scavenging Activity

Intracellular ROS scavenging capacity of the formulations was measured using H₂DCF-DA. HCE and IM-ConjEpi cells were cultured into 24-well plates (6×10^4 cells/well) until 90 % of confluence was reached. After this, the cells were maintained in non-supplemented medium for 24 hours. Subsequently, the cells were pre-treated with 500 μ L of the formulations and left for 1 hour at 37°C. The formulations were then removed, and the cells were incubated for 30 minutes with 500 μ L of a 10 μ M solution of H₂DCF-DA. After 30 minutes the H₂DCF-DA solution was removed, and the cells were treated again with the formulations (at the same concentration as before) and exposed to 8-W V-B lamp (Bio-Rad, Inc., Hercules, CA, USA) for 15 seconds. Control cells were not irradiated. After the UV-B exposure the cells were cultured for 1 hour. The intracellular fluorescence intensity was measured at 488 nm (excitation) and 522 nm (emission). The data obtained from the fluorescence measurements were normalized by the total protein content. The latter was measured in adherent cells using the BCA assay, following the manufacturer's instructions. For each treatment two replicates were performed in three independent experiments for each formulation.

***In Vitro* Evaluation of the Anti-Inflammatory Activity**

Human corneal epithelial (HCE) cells were seeded in 24-well plates at a density of 6×10^4 cells/well. Once the confluence was reached (90 %), the cells were maintained in supplement-free medium for 24 hours. Subsequently, the medium was discarded, and the cells were treated with inclusion complexes of CDs containing QUE (5 - 25 μ M of QUE) or RSV (25 - 100 μ M of RSV) for 2 hours. Then, the supernatants were discarded, and the cells were stimulated with 25 ng/mL of TNF- α for 24 hours. As controls, cells treated with the formulations but not stimulated with TNF- α were used. The supernatants were then collected and centrifuged (18.000g for 10 minutes). The concentration of IL-6 in the supernatants was measured through an Enzyme-linked immunosorbent assay (ELISA) performed following the manufacturer's instructions. Protein extraction was performed on the plates with adherent cells. The concentration of IL-6 was normalised by the total protein content. For every condition, two replicates were made in three independent experiments.

Statistical Analysis

All experiments were performed in triplicate ($n=3$) and data are represented as mean \pm standard error of the mean (SEM). The SPSS software was used (SPSS 20.0; SPSS, Inc., Chicago, IL, USA) for the statistical analysis applying one-way analysis of variances (ANOVA) followed by Tukey's or Games-Howell post-hoc tests.

6.2. Results and Discussion

6.2.1. Chemical Stability of Complexed QUE and RSV

To study the short-term chemical stability of complexed and pure QUE and RSV, all samples were placed in glass vials, protected from light, and kept in a controlled environment room. Additionally, the possible stabilizing effects of different concentrations of HA were evaluated. One-week stability profiles are reported in **figure 6.2**. **Table 6.2** summaries of the kinetic parameters of the degradation reactions.

Pure QUE was unstable in aqueous solutions at 25°C. The calculated kinetic parameters showed that the half-life ($t_{1/2}$) is 3.66 hours, meaning that basically all QUE degrades in one day. The degradation was slower when QUE was complexed with HP β CD and HP β CD:HA. The degradation half-life of QUE was prolonged to about one day for the complexes with HP β CD. The stabilizing effect of HA was inversely proportional to its concentration as the best stabilization of QUE was seen at the lowest HA concentrations (0.1% w/v). Chromatograms of pure QUE showed the onset of lower retention peaks than the one of QUE after 24 h, meaning that the degradation products formed are more hydrophilic than pure QUE. Although these products were not determined in detail (beyond the scope of this study) this finding corroborates the theory that the main pathways of degradation of QUE are oxidation and hydroxylation.

In the case of RSV, the pure compound showed to be more stable than pure QUE, having a degradation half-life of 97.6 hours. Complexes of RSV with HP β CD and HP β CD:HA showed to enhance stability of the polyphenol and this improvement was dependent on the HA concentration.

Various authors reported that the stability of QUE is influenced by the temperature and pH of solution. For example, Wang & Zhao (2016) showed that QUE followed a first-order kinetics of degradation upon incubation at 37°C. The same authors reported that the degradation rate decreased at lower pH (6 and 6.8). Some authors proposed the addition of proteins, like casein (Wang & Zhao, 2016; Wang *et al.*, 2016) as a potential strategy to stabilize QUE. In addition to the exposure to UV or visi-

Table 6.2: Summary of the first order degradation constant (k), half-time degradation period ($t_{1/2}$), shelf-life (t_{90}) and the correlation coefficient (R^2) for pure QUE and RSV and complexes with HP β CD and HP β CD:HA in PBS (pH 7.4) at 25°C. All concentrations are expressed as % w/v and all samples contained 5% w/v HP β CD.

Sample	Additive	k (h ⁻¹)	$t_{1/2}$ (h)	t_{90} (h)	R^2
	HA				
Pure QUE	-	0.188	3.66	0.55	0.987
QUE: HP β CD	-	0.029	23.57	3.57	0.940
QUE: HP β CD:HA	0.1%	0.012	55.45	8.75	0.967
	0.25%	0.015	44.71	6.77	0.946
	0.5%	0.016	43.05	6.52	0.941
Pure RSV	-	0.0071	97.62	14.78	0.967
RSV: HP β CD	-	0.0009	770.16	116.66	0.819
RSV: HP β CD:HA	0.1%	0.0008	866.43	131.25	0.900
	0.25%	0.0013	533.19	80.76	0.908
	0.5%	0.0018	385.08	58.33	0.613

ble light, which triggers the conversion from *trans*- to *cis*-RSV, other environmental factors, like pH and temperature, influence the RSV stability. The phenolic groups of RSV ionize at basic pH leading to the formation of the phenate ions more prone to oxidation compared to the protonated form of RSV. Therefore, at more acidic pH (< 6.8) RSV seems to be stable since all the phenolic groups are in their non-ionized form (Robinson, 2015; Zupanč *et al.*, 2015). The higher instability of QUE compared to that of RSV can be explained by the comparison of their chemical structure: QUE possesses more hydroxyl groups (5 groups) than RSV (3 groups). A greater number of hydroxyl groups leads to an easier oxidation (Sokolová *et al.*, 2011). This explains well the stability profiles of the pure compounds observed in our studies. All subsequent studies were performed with 0.1% w/v HA as it displayed the higher stabilizing capacity in the case of both polyphenolic compounds. It is interesting to notice that a higher stabilization of the two polyphenolic compounds was achieved at the lowest concentration of HA (0.1% w/v) in solution. This can be justified by the fact that a

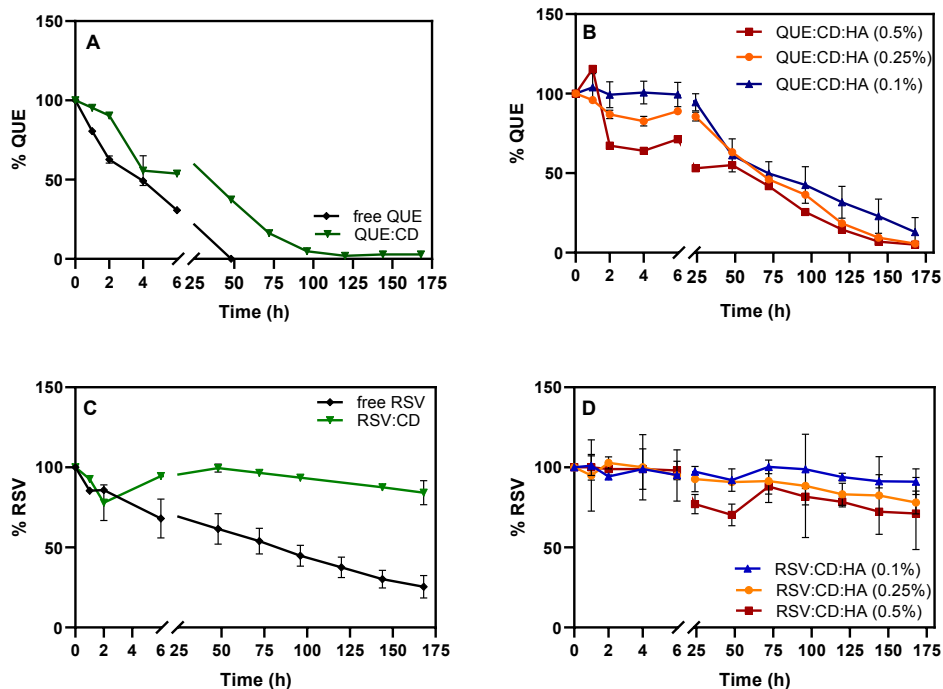


Figure 6.2 - Stability profiles (25°C, pH 7.4) of A-pure QUE, with HP β CD; B-QUE with HP β CD:HA: 0.1% of HA, 0.25% of HA and 0.5% of HA w/v. Stability profiles of C-pure RSV, with HP β CD; D-RSV with HP β CD:HA: 0.1% of HA, 0.25% of HA and 0.5% of HA w/v. Each point represents the % of QUE or RSV at a given time point in respect to the initial concentration and these are means of three measurements \pm SEM.

higher concentrations HA is able to form intra- or intermolecular hydrogen bonds leading to the formation of a three-dimensional polymeric web. In this case less HA is accessible to interact and stabilize the polyphenolic compounds (Snetkov *et al.*, 2020).

Formation of binary or tertiary complexes of QUE or RSV with CD or CD:hydrophilic polymers, respectively, has emerged as an interesting approach to enhance the stability profiles of these compounds and we are not aware of the previous drug stability reports in this respect.

6.2.2. Solubility of QUE and RSV in the Formulations

The effect of increasing concentrations of HP β CD (0-12.5% w/v) on the solubility of QUE and RSV in PBS (pH 7.4) was investigated in phase-solubility experiments (figure 6.3). Among different CDs, we selected HP β CD due to its safety in eyedrop formulations and by ability to increase absorption of hydrophobic drugs to the eye (Challa *et al.*, 2005).

The phase solubility profiles of QUE indicate linear solubility improvement with increasing concentration of HP β CD. Thus, the profile is in accordance with the AL type complexation in the classification of Higuchi and Connors. Stability constant $K_{1:1}$ of the association between QUE and HP β CD was 2609 M^{-1} . However, in the case of poorly soluble drugs like QUE, the determination of intrinsic solubility (S_0) is not always accurate. Since this value is used for the calculation $K_{1:1}$ this can lead to an over- or underestimation of the complexation capacity. Calculation of CE represents a more exact parameter of the estimation of the solubilizing efficiency of the CDs (Loftsson & Brewster, 2012). This value (eq. 6.5) is independent of S_0 . In this case, CE was calculated to be 0.04 and the drug:CD molar ratio 1:25. If the formation of 1:1 drug:CD soluble complex is assumed, one out of every twenty-five cyclodextrin molecules is involved in the complex formation (Loftsson *et al.*, 2005). In the case of RSV, the values of $K_{1:1}$, CE, and drug:CD ratio were 9808 M^{-1} , 1.24 and 1.8. This suggests that the complexation of RSV with CD is more efficient than in the case of QUE. The introduction of excipients, such as hydrophilic polymers has been indicated to improve the solubilization capacity of CDs. In addition, this promotes formation of complexed particle-like structures.

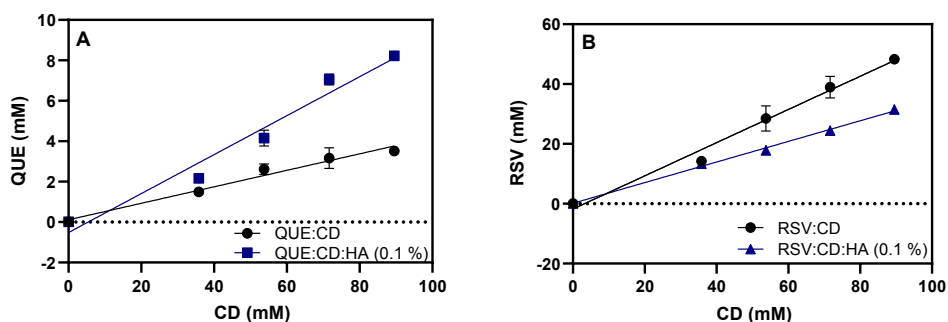


Figure 6.3 - Phase solubility studies (25°C, pH 7.4) of QUE with A: HP β CD and HP β CD:HA. B: RSV with HP β CD and HP β CD:HA.

The addition of hyaluronic acid (HA) resulted in further improvement in the solubility of QUE. For example, at the highest concentration of HP β CD (12.5% w/v) the solubilized quantity of QUE increased from 0.44 mg/mL to 1.06 mg/mL. This was reflected in the values of $K_{1:1}$ and CE, which were 7940 M^{-1} and 0.1, respectively. Greater CE values indicate that smaller number of CD molecules are required in QUE solubilization, and that the complexation is more effective. On the contrary, the presence of HA slightly reduced the solubilization and complexation of RSV. In this case $K_{1:1}$ and CE were 7299 M^{-1} and 0.52, i.e. values moderately lower than without HA. **Table 6.3** summarizes all the parameters calculated from the phase solubility diagrams.

Table 6.3: Results from the phase-solubility studies measured at 25°C and pH 7.4 (mean \pm SEM; n=3).

Polyphenol	HA (% w/v)	Type	$K_{1:1}$ (M^{-1})	CE	Drug:CD molar ratio	Solubility (mg/mL) ^a	Solubility (mg/mL) ^b
QUE ^c	-	A _L	2609	0.04	1:24	0.44 \pm 0.09	1.06 \pm 0.28
QUE ^c	0.1	A _L	7940	0.10	1:10	0.65 \pm 0.03	2.48 \pm 0.99
RSV ^c	-	A _L	9808	1.24	1:1.8	3.24 \pm 0.41	11 \pm 3.60
RSV ^c	0.1	A _L	7299	0.52	1:2.9	3.04 \pm 0.78	7.17 \pm 1.25

^a in the presence of 5% (w/v) CD^b in the presence of 12.5% (w/v) CD^c all complexes were prepared with HP β CD (0-12.5% w/v)

6.2.3. Fourier Transformed Infrared Spectroscopy

Fourier transformed infra-red (FT-IR) spectroscopy was used to confirm the presence of both host and guest molecules in the inclusion complexes. **Figure 6.4** illustrates the spectra of free QUE, RSV, HP β CD and HA, together with the spectra of the complexes. The spectrum of pure QUE shows the characteristic bands: stretching of the hydroxyl groups was detected in the region between 3400 and 3200 cm^{-1} . The intense bending of the phenolic hydroxyl was observed at around 1380 cm^{-1} . The bands corresponding to the in and out- of plane bending of the aromatic C-H were identified in the region from 950 to 600 cm^{-1} . The signal from the ketone was detectable at 1660 cm^{-1} . With regard to the signals of pure RSV the stretching of the aromatic double C-C bonds was visible at 1600 cm^{-1} , whereas a strong signal at 960 cm^{-1} indicates stretching of the olefinic C-H. At 3200 cm^{-1} a strong broad peak of -OH group is visible.

The spectra of the pure compounds were compared with the complexed form in which we can observe different changes. It is evident the masking of the signals of the fingerprint region (1500-900 cm^{-1}) of both compounds upon complexation. The spectra of both complexes (QUE: HP β CD and RSV: HP β CD) are similar with the one of free HP β CD, with the broad and intense band of the hydroxyl groups at 3400-3200 cm^{-1} and the stretching of the -CH and -CH₂ groups at 2800 cm^{-1} . FT-IR spectrum of pure HA shows the bands of -OH and -NH stretching at 3400 cm^{-1} , while the medium band intensity at 2900 cm^{-1} indicates the stretching of the -CH and -CH₂, as in the spectrum of the pure HP β CD. The wide band in the region of 1600-1500 cm^{-1} is representative of the amide functional group present in the backbone of N-acetylglucosamine. In the complexes where HA was present these bands were conserved. The spectra of QUE and RSV when complexed with either HP β CD or HP β CD:HA represent major changes in the fingerprint region, indicating that the complexation has occurred.

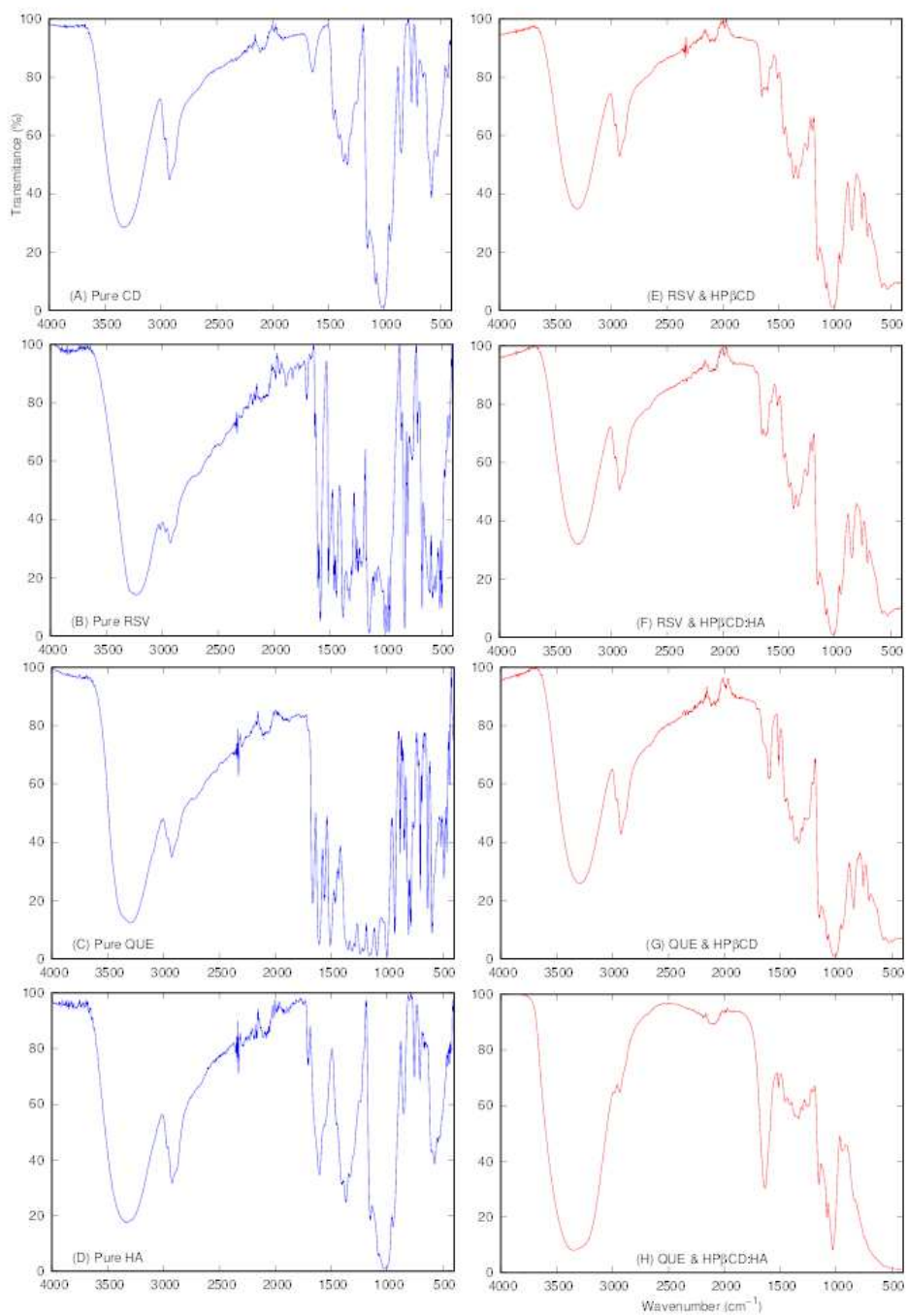


Figure 6.4 - FT-IR spectra of pure HPβCD (A), RSV (B), QUE (C), HA (D) and complexes of RSV with HPβCD (E) and HPβCD:HA (F) and QUE with HPβCD (G) and HPβCD:HA (H).

6.2.4. Particle Size Characterization

The size distributions of the formulations are shown in the **Table 6.4**. Binary complexes between the polyphenols and HP β CD displayed a uniform size distribution, all in the range of 2-3 nm. On the contrary, complexes containing HA exhibited bimodal particle size distribution, with an intensity peak at around 2 nm, which as in the binary complexes probably represents the monomeric complex between the drug: HP β CD, while the second intensity peak that appears represents larger complex aggregates. In addition, QUE-containing complexes were able to form slightly larger aggregates than those formed in RSV-containing complexes, 103.6 and 82.14 nm respectively. These results suggest that HA triggers formation of nanoaggregates in drug:CD complexes. The size of these aggregates are clearly below the acceptable size limit (diameter of 10 μ m) in topical suspension delivery (Kassem *et al.*, 2007).

Table 6.4: Hydrodynamic diameter (*d*); the intensity distribution (%I); and *d*₁₀, *d*₅₀ and *d*₉₀ values for all the formulations measured by DLS (mean \pm SEM; n=3).

Formulation	<i>d</i> (nm)	%I	<i>d</i> ₁₀	<i>d</i> ₅₀	<i>d</i> ₉₀
QUE: HP β CD complexes	2.81 \pm 0.23 3647 \pm 418.8	93.1 6.86	1.645 \pm 0.099	2.735 \pm 0.18	303.29 \pm 0.51
QUE: HP β CD:HA complexes	2.08 \pm 0.006 103.6 \pm 1.31	63 34.78	1.47 \pm 0.026	2.58 \pm 0.02	135.76 \pm 0.89
RSV: HP β CD complexes	2.74 \pm 0.1 3804 \pm 211.5	98.65 2.024	1.50 \pm 0.082	2.54 \pm 0.088	4.49 \pm 0.30
RSV: HP β CD:HA complexes	2.22 \pm 0.005 82.14 \pm 1.32	61.38 36.13	1.62 \pm 0.072	2.80 \pm 0.03	109.53 \pm 3.24

6.2.5. Atomic Force Microscopy

The images of the surface morphology of drug: HP β CD complexes and their aggregates were acquired with AFM. Que:HP β CD formed spherical particle-like aggregates (**figure 6.5A and 6.5B**), while the addition of HA in the complex, induced the formation of larger aggregates (**figure 6.5C and 6.5D**) of around 200 nm in diameter. Regarding the formulations containing RSV, no aggregate formation (**figure 6.5E**) occurred in the inclusion complexes with CD, while the ones including HA had a regular spherical shape and a diameter in the range of 40-70 nm (**figure 6.5F**). Size data obtained by AFM imaging confirmed the size distribution of the complexes and their aggregates previously obtained by the dynamic light scattering.

The formation of nanoaggregate structures may indicate that the improvement of solubility and stability of the two polyphenols occurs through the formation of non-inclusion complexes or micellar-like structures (Jansook *et al.*, 2019). This could be positively reflected on the potential topical administration of the formulations since a higher corneal retention and thus an increased ocular bioavailability of QUE and RSV might be observed (Jóhannsdóttir *et al.*, 2015).

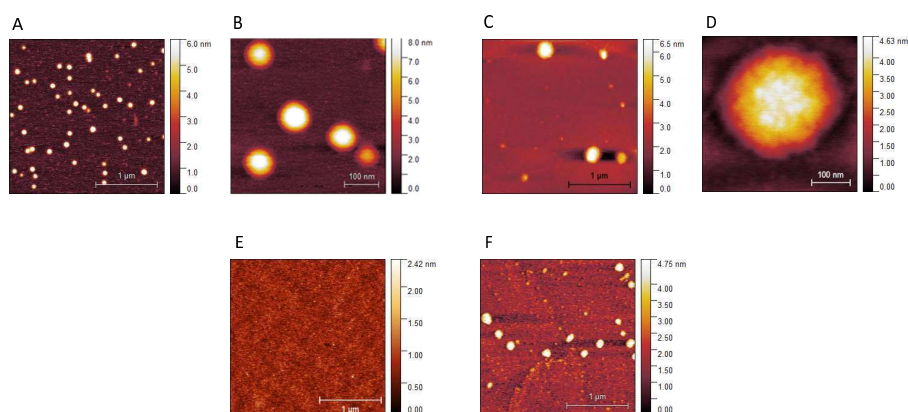


Figure 6.5 - AFM images of QUE in complex with HP β CD (A and B) and with HP β CD:HA (C and D); RSV in complex with HP β CD (E) and with HP β CD:HA (F). Horizontal (length) and vertical (height) scales are reported on the images.

6.2.6. *In Vitro* Biocompatibility of Inclusion Complexes

The *in vitro* biocompatibility of the inclusion complexes of QUE and RSV on two human ocular surface cell lines, HCE (corneal) and IM-ConjEpi (conjunctival) after a 24-hour exposure was assessed using the XTT cell viability assay. Cell viability after exposure to all complexes are shown in **figure 6.6**. None of the formulations reduced the cell viability of the two cell lines, that was maintained around 100%. As expected, BAK, which was used as a positive control of toxicity, significantly decreased the viability of both cell lines ($p < 0.001$).

RSV-containing inclusion complexes seem to stimulate cell proliferation. Similar behaviour of HCEs cells was noticed by Li *et al.* (2020) when investigating the cytotoxicity of a micellar-based formulation of RSV (Li *et al.*, 2020). On the other hand, the IM-ConjEpi cells seem to be more susceptible to stimulation of cell proliferation than HCE cells. It is interesting to observe that the formulations with HA promoted cell proliferation more than those without HA. This might be explained by the presence of HA specific CD44 receptor, present on the surface of human corneal and conjunctival epithelial cells (Contreras-Ruiz *et al.*, 2011). Besides being implied in physiological processes like haematopoiesis and lymphocyte activation, HA also stimulates cell proliferation and adhesion (Jordan *et al.*, 2015). Even though the possible generation of degradation products that can arise in QUE containing complexes, they did not affect the cellular viability of HCE and IM-ConjEpi cells in our experiments.

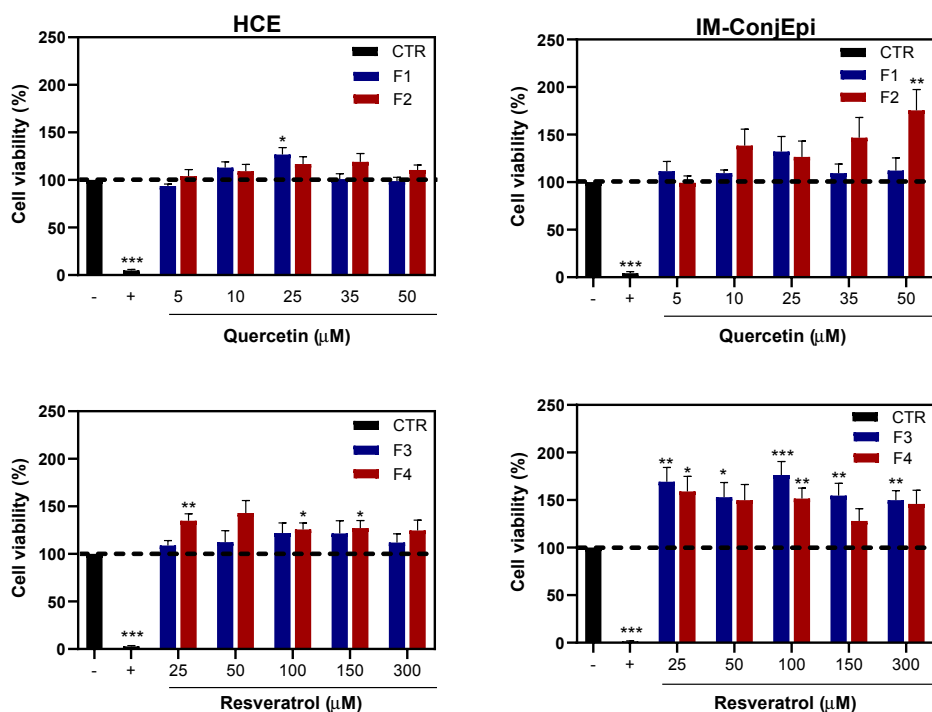


Figure 6.6 - Viability of HCE and IM-ConjEpi cells after treating with the formulations: F1-QUE:HP β CD, F2-QUE:HP β CD:HA, F3-RSV:HP β CD and F4-RSV:HP β CD:HA complexes, negative CTR-cell culture medium, positive CTR-BAK (0.005%). The data represent the mean of three independent experiments \pm SEM. * $p < 0.05$, ** $p < 0.01$, *** $p < 0.001$ compared with control cells treated with culture medium.

6.2.7. Intracellular Antioxidant Activity of Formulations

H₂DCF-DA, a fluorogenic dye sensitive to ROS, was used to assess the potential intracellular ability of the complexes (table 6.1). H₂DCF-DA can passively diffuse into the cells, where the acetyl groups are cleaved through the action of intracellular esterase yielding a non-fluorescent compound (DCFH). DCFH is subsequently oxidized to DCF, emitting a fluorescent signal proportional to ROS levels in the cytosol (Kim & Xue, 2021). Figure 6.7 illustrates the production of ROS in HCE and IM-ConjEpi cells after treatment with the formulations. The results are expressed as percentages, taking as 100% of ROS production cells exposed to culture medium.

Binary complexes of QUE and RSV were capable to scavenge cytosolic ROS in HCE cells in a dose dependent manner. A marked reduction of ROS was observed from the lowest concentrations tested ($p < 0.05$). Regarding tertiary complexes, the addition of HA did not affect the antioxidant ability of the complexes, maintaining it to levels comparable to the ones in binary complexes. In contrast, inclusion complex with QUE reached a plateau in their antioxidant scavenging capacity when the IM-ConjEpi cells were treated with a concentration of 10 μ M or

higher. Inclusion complexes containing RSV, were able to reduce intracellular ROS levels with a considerably effect. In fact, statistically significant differences were observed when comparing the antioxidant effect between the highest (300 μM) and the lowest concentrations (25 μM) tested ($p < 0.005$) of RSV:HP β CD complexes, and between 50 μM and 300 μM concentrations ($p < 0.001$), as well.

All formulations demonstrated scavenging capacity of ROS. QUE and RSV exert their antioxidant activities through specific moieties and functional groups present in their chemical structure like the catechol group and the chromen-4-one nucleus in QUE, and the phenolic groups present in RSV (Amorati *et al.*, 2017; Salehi *et al.*, 2018). Except the alteration of the physiological balance between antioxidant enzymes and ROS, matrix-remodelling and inflammatory factors contribute to the oxidative stress in DED (Favero *et al.*, 2021). Consequently, natural therapeutic agents capable of counterbalance this type of stress would represent a novel potential line of treatments for DED.

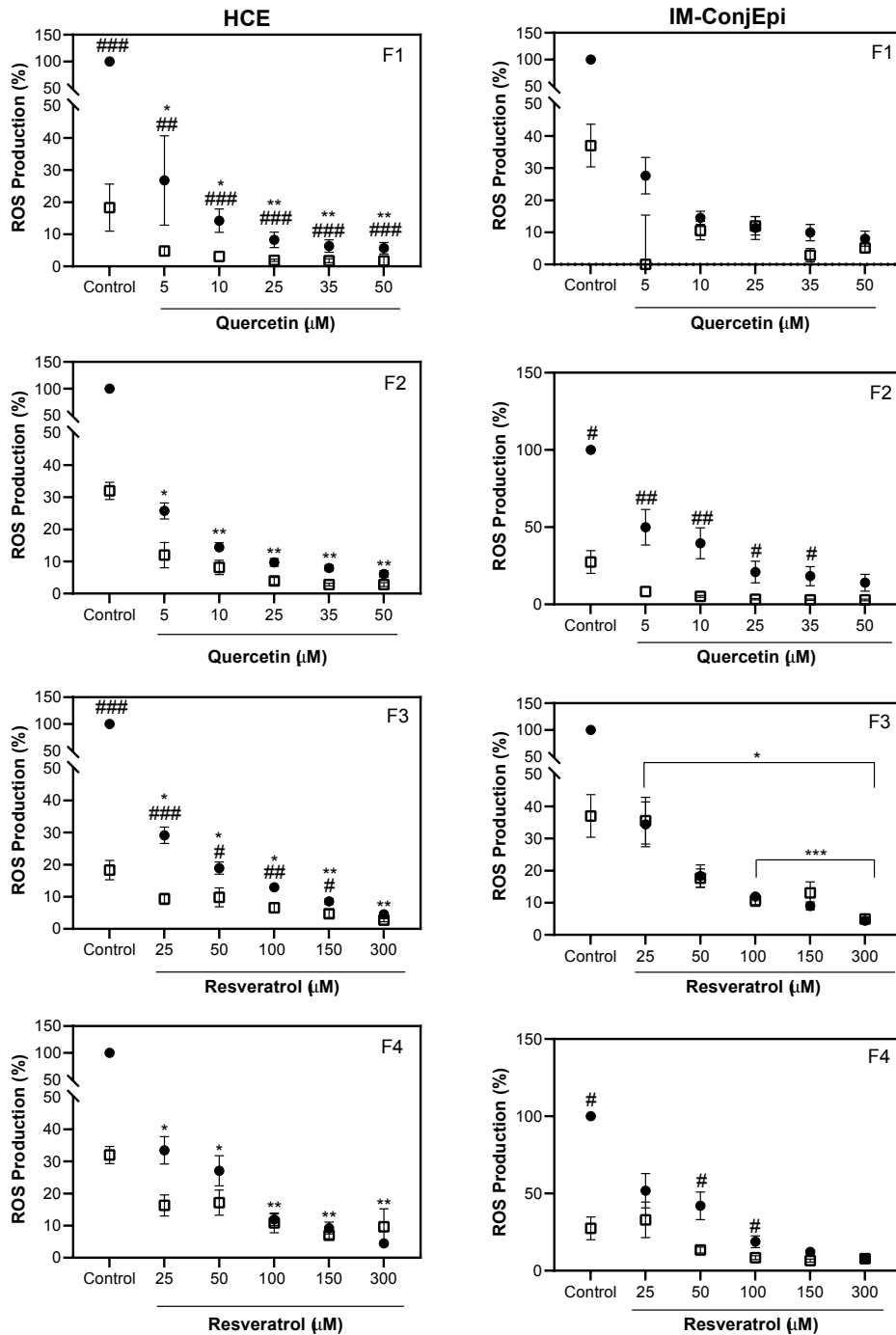


Figure 6.7 - Antioxidant ability of the formulations in HCE and IM-ConjEpi cells: F1-QUE:HPβCD, F2-QUE:HPβCD:HA, F3-RSV:HPβCD and F4-RSV:HPβCD:HA complexes, CTR-cell culture medium. (●) Exposed to UV-B; (□) Unexposed to UV-B. The data represent the mean of three independent experiments ± SEM. * $p < 0.05$, ** $p < 0.01$, *** $p < 0.001$, compared with UV-B exposed cells; # $p < 0.05$, ## $p < 0.01$, ### $p < 0.001$, intergroup comparison.

6.2.8. *In Vitro* Evaluation of the Anti-Inflammatory Activity

Since inflammation is at the core of DED etiopathological mechanisms, pharmaceutical formulations that could counteract this physiological response would be a beneficial treatment option. Interleukin-6 (IL-6) is a pro-inflammatory cytokine whose levels were found to be increased in patients with mild or moderate DED (Enruez-de-Salamanca *et al.*, 2010; Na *et al.*, 2012; Pinazo-Durn *et al.*, 2010). The anti-inflammatory activity was evaluated in terms of IL-6 production after cell stimulation with TNF- α . Thus, a decrease of IL-6 concentration indicates an *in vitro* inhibition of the inflammatory pathways that lead to the production of this pro-inflammatory cytokine. From **figure 6.8**, it can be observed that inclusion complexes of CD with QUE had relatively modest anti-inflammatory activity. This response was not statistically significant when compared to the control cells just treated with cell culture medium. In the case of the complexes with RSV, an opposite effect to the one expected was observed. It seems that these complexes elicit an inflammatory response. However, it has to be pointed out that a decrease in the concentrations of IL-6 is observed at increasing concentrations of RSV. This could mean that higher concentrations of this polyphenol are necessary to obtain the desired anti-inflammatory effect. In the case of both types of complexes, the stimulation with TNF- α worked well, generating a distinction between inflammatory and non-inflammatory conditions ($p < 0.001$).

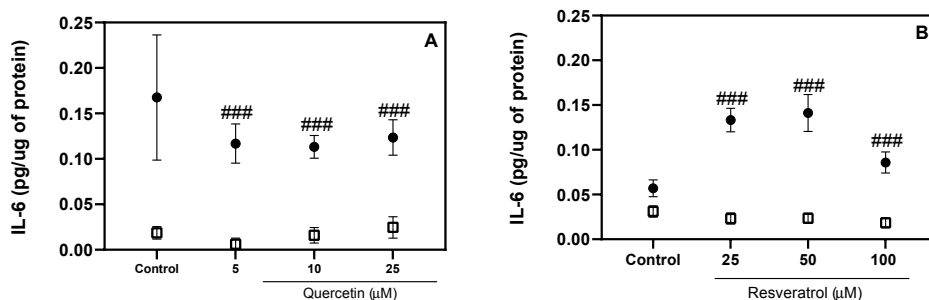


Figure 6.8 - IL-6 Production after stimulation with TNF- α and treatment with A: QUE:HP β CD and B: RSV:HP β CD. (●) Exposed to TNF- α ; (□) Unexposed to TNF- α . The data represent the mean of three independent experiments \pm SEM. * $p < 0.05$, ** $p < 0.01$, *** $p < 0.001$, compared with TNF- α exposed cells; # $p < 0.05$, ## $p < 0.01$, ### $p < 0.001$, intergroup comparison.

A previous study from our group demonstrated that both QUE and RSV are capable of decreasing the concentrations of pro-inflammatory cytokines like IL-6 in corneal and conjunctival cell lines. This effect was observed at low concentrations of both molecules ($\leq 20 \mu$ M) (Abengzar-Vela *et al.*, 2015). However, inclusion complexes with QUE or RSV were not capable of eliciting the same effect. Indeed, between the two studies, there was a slight difference in the experimental design. Abengzar-Vela *et al.* (2015) has used an *in vitro* inflammatory model involving a pre-treatment step (with the drugs) before inducing pro-inflammatory stimulus with

TNF- α . In this manner, the preventive potential of the polyphenols against inflammatory development is emphasized. In the assay performed as a part of this thesis, the pre-treatment step was omitted, focusing instead on the formulations' anticipated ability to reduce inflammation. The effect of increasing the exposure time of the formulations and the concentrations of the two compounds in the complexes should be evaluated. Possible adjustments in the experimental design or the use of another inflammatory model shall be considered as well.

6.3. Conclusions

Due to many beneficial health effects of QUE and RSV, their potential applicability in the treatment of ophthalmic diseases, especially those affecting the ocular surface like DED was proposed in this study. Issues related to their physico-chemical characteristics, like poor water solubility were successfully solved through the formation of binary or ternary complexes with HP β CD and HP β CD:HA. Also, the formation of tertiary complexes with HP β CD:HA showed to be more advantageous in terms of chemical stability improvement of the two compounds. Therefore, it should be considered as a good starting point for future formulation solutions. In the case of QUE the stability improvement observed was of modest extent and additional efforts in stabilising it are needed. For RSV, a greater stabilising effect was achieved. The shelf-lives (t_{90}) found for ternary complexes were 8.75 h for QUE:HP β CD:HA and 131.25 h (5.5 days) for RSV:HP β CD:HA. These results suggest that slight modifications of some parameters like the pH or the addition of chelating agents, such as EDTA, could lead to an adequate stability period, which for eye drops formulation should be around one year (considering the allowed limit of degradation of 10%). An alternative approach involves lyophilized powder, if the stability after reconstitution can be maintained for at least one month. It has to be underlined that due to the low chemical stability of the two compounds, especially QUE, the results in many literature studies may represent the effects of the degradation products, instead of biological effects of QUE.

Although the properties of both compounds improved through the formation of complexes, we think that the ones containing RSV have a higher potential applicability in the treatment of DED, since they are more stable and less challenging for the formulator and further prospective scale-up.

References of Chapter 6

- Abengózar-Vela, A., Calonge, M., Stern, M.E., González-García, M.J. and Enríquez-De-Salamanca, A.,
Quercetin and resveratrol decrease the inflammatory and oxidative responses in human ocular surface epithelial cells,
Investig. Ophthalmol. Vis. Sci. **56**, 2709 (2015)
<https://doi.org/10.1167/iovs.15-16595>
- Amorati, R., Baschieri, A., Cowden, A. and Valgimigli, L.,
The antioxidant activity of quercetin in water solution,
Biomimetics **2**, 6–9 (2017)
<https://doi.org/10.3390/biomimetics2030009>
- Araki-Sasaki, K., Ohashi, Y., Sasabe, T., Hayashi, K., Watanabe, H., Tano, Y. and Handa, H.,
An SV40-immortalized human corneal epithelial cell line and its characterization,
Investig. Ophthalmol. Vis. Sci. **36**, 614–621 (1995).
- Başaran, E., Öztürk, A.A., Şenel, B., Demirel, M. and Sarica, Ş.,
Quercetin, rutin and quercetin-rutin incorporated hydroxypropyl β -cyclodextrin inclusion complexes,
Eur. J. Pharm. Sci. **172**, 106153 (2022)
<https://doi.org/10.1016/j.ejps.2022.106153>
- Bayer, I.S.,
Hyaluronic acid and controlled release: A review,
Molecules **25**, 2649 (2020)
<https://doi.org/10.3390/molecules25112649>
- Challa, R., Ahuja, A., Ali, J. and Khar, R.K.,
Cyclodextrins in drug delivery: An updated review,
AAPS PharmSciTech **6**, 329–357 (2005)
<https://doi.org/10.1208/pt060243>
- Contreras-Ruiz, L., de la Fuente, M., Párraga, J.E., López-García, A., Fernández, I., Seijo, B., Sánchez, A.,
Calonge, M. and Diebold, Y.,
Intracellular trafficking of hyaluronic acid-chitosan oligomer based nanoparticles in cultured human ocular surface cells,
Mol. Vis. **17**, 279–290 (2011).
- Del Valle, E.M.M.,
Cyclodextrins and their uses: A review,
Process Biochem. **39**, 1033–1046 (2004)
[https://doi.org/10.1016/S0032-9592\(03\)00258-9](https://doi.org/10.1016/S0032-9592(03)00258-9)
- Enríquez-de-Salamanca, A., Castellanos, E., Stern, M.E., Fernández, I., Carreño, E., García-Vázquez, C.,
Herreras, J.M., Calonge, M.,
Tear cytokine and chemokine analysis and clinical correlations in evaporative-type dry eye disease,
Mol. Vis. **16**, 862–873 (2010).

- Favero, G., Moretti, E., Krajčíková, K., Tomečková, V. and Rezzani, R.,
Evidence of polyphenols efficacy against dry eye disease,
Antioxidants **10**, 1–17 (2021)
<https://doi.org/10.3390/antiox10020190>
- Jansook, P., Kulsirachote, P., Asasutjarit, R. and Loftsson, T.,
Development of celecoxib eye drop solution and microsuspension: A comparative investigation of binary and ternary cyclodextrin complexes,
Carbohydr. Polym. **225**, 115209 (2019)
<https://doi.org/10.1016/j.carbpol.2019.115209>
- Jóhannsdóttir, S., Jansook, P., Stefánsson, E. and Loftsson, T.,
Development of a cyclodextrin-based aqueous cyclosporin A eye drop formulations,
Int. J. Pharm. **493**, 86–95 (2015)
<https://doi.org/10.1016/j.ijpharm.2015.07.040>
- Jordan, A.R., Racine, R.R., Hennig, M.J.P. and Lokeshwar, V.B.,
The role of CD44 in disease pathophysiology and targeted treatment,
Front. Immunol. **6**, 1–14 (2015)
<https://doi.org/10.3389/fimmu.2015.00182>
- Kassem, M.A., Abdel Rahman, A.A., Ghorab, M.M., Ahmed, M.B. and Khalil, R.M.,
Nanosuspension as an ophthalmic delivery system for certain glucocorticoid drugs,
Int. J. Pharm. **340**, 126–133 (2007)
<https://doi.org/10.1016/j.ijpharm.2007.03.011>
- Kim, H. and Xue, X.,
Detection of total reactive oxygen species in adherent cells by 2',7'-dichlorodihydrofluorescein diacetate staining,
J Vis Exp. (2021)
DOI: 10.3791/60682-v
- Lachowicz, M., Stańczyk, A. and Kołodziejczyk, M.,
Characteristic of cyclodextrins: their role and use in the pharmaceutical technology,
Curr. Drug Targets **21**, 1495–1510 (2020)
<https://doi.org/10.2174/1389450121666200615150039>
- Li, M., Zhang, L., Li, R. and Yan, M.,
New resveratrol micelle formulation for ocular delivery: characterization and in vitro/in vivo evaluation,
Drug Dev. Ind. Pharm. **46**, 1960–1970 (2020)
<https://doi.org/10.1080/03639045.2020.1828909>
- Liu, L. and Guo, Q.X.,
The driving forces in the inclusion complexation of cyclodextrins,
J. Incl. Phenom. **42**, 1–14 (2002)
<https://doi.org/10.1023/A:1014520830813>
- Loftsson, T. and Brewster, M.E.,
Cyclodextrins as functional excipients: methods to enhance complexation efficiency,
J. Pharm. Sci. **101**, 2271–2280 (2012)
<https://doi.org/10.1002/jps>
- Loftsson, T. and Duchêne, D.,
Cyclodextrins and their pharmaceutical applications,
Int. J. Pharm. **329**, 1–11 (2007)
<https://doi.org/10.1016/j.ijpharm.2006.10.044>
- Loftsson, T., Hreinsdóttir, D. and Másson, M.,
Evaluation of cyclodextrin solubilization of drugs,
Int. J. Pharm. **302**, 18–28 (2005)
<https://doi.org/10.1016/j.ijpharm.2005.05.042>

- Loftsson, T. and Stefánsson, E.,
Aqueous eye drops containing drug/cyclodextrin nanoparticles deliver therapeutic drug concentrations to both anterior and posterior segment,
Acta Ophthalmol. **100**, 7–25 (2021)
<https://doi.org/10.1111/aos.14861>
- Loftsson, T. and Stefánsson, E.,
Effect of cyclodextrins on topical drug delivery to the eye,
Drug Dev. Ind. Pharm. **23**, 473–481 (1997)
<https://doi.org/10.3109/03639049709148496>
- Na, K.S., Mok, J.W., Kim, J.Y., Rhe Rho, C., and Joo, C.K.,
Correlations between tear cytokines, chemokines, and soluble receptors and clinical severity of dry eye disease,
IOVS **53**, 5443–5450 (2012).
- Pinazo-Durán, M.D., Galbis-Estrada, C., Pons-Vázquez, S., Cantú-Dibildox, J., Marco-Ramírez, C., and Benítez-del-Castillo, J.,
Effects of a nutraceutical formulation based on the combination of antioxidants and ω -3 essential fatty acids in the expression of inflammation and immune response mediators in tears from patients with dry eye disorders,
Clin Interv Aging **16**, 862–873 (2013).
- Robinson, K.,
Pre-formulation studies of resveratrol,
Drug Dev. Ind. Pharm. **41**, 1464–1469 (2015)
<https://doi.org/10.3109/03639045.2014.958753>
- Salehi, B., Mishra, A.P., Nigam, M., Sener, B., Kilic, M., Sharifi-Rad, M., Fokou, P.V.T., Martins, N. and Sharifi-Rad, J.,
Resveratrol: A double-edged sword in health benefits,
Biomedicines **6**, 1–20 (2018)
<https://doi.org/10.3390/biomedicines6030091>
- Saokham, P., Muankaew, C., Jansook, P. and Loftsson, T.,
Solubility of cyclodextrins and drug/cyclodextrin complexes,
Molecules **23**, 1–15 (2018)
<https://doi.org/10.3390/molecules23051161>
- Snetkov, P., Zakharova, K., Morozkina, S., Olekhovich, R. and Uspenskaya, M.,
Hyaluronic acid: The influence of molecular weight on structural, physical, physico-chemical, and degradable properties of biopolymer,
Polymers (Basel) **12**, 1800 (2020)
<https://doi.org/10.3390/polym12081800>
- Sokolová, R., Degano, I., Ramešová, Š, Bulíčková, J., Hromadová, M., Gál, M., Fiedler, J. and Valášek, M.,
The oxidation mechanism of the antioxidant quercetin in non-aqueous media,
Electrochim. Acta **56**, 7421–7427 (2011)
<https://doi.org/10.1016/j.electacta.2011.04.121>
- Varan, G., Varan, C., Erdoğar, N., Hincal, A.A. and Bilensoy, E.,
Amphiphilic cyclodextrin nanoparticles,
Int. J. Pharm. **531**, 457–469 (2017)
<https://doi.org/10.1016/j.ijpharm.2017.06.010>
- Venuti, V., Cannavà, C., Cristiano, M.C., Fresta, M., Majolino, D., Paolino, D., Stancanelli, R., Tommasini, S. and Ventura, C.A.,
A characterization study of resveratrol/sulfobutyl ether- β -cyclodextrin inclusion complex and in vitro anticancer activity,
Colloids Surfaces B Biointerfaces **115**, 22–28 (2014)
<https://doi.org/10.1016/j.colsurfb.2013.11.025>

- Wang, J. and Zhao, Xi.H.,
Degradation kinetics of fisetin and quercetin in solutions affected by medium pH, temperature and co-existing proteins,
J. Serbian Chem. Soc. **81**, 243–253 (2016)
<https://doi.org/10.2298/JSC150706092W>
- Wang, W., Sun, C., Mao, L., Ma, P., Liu, F., Yang and J., Gao, Y.,
The biological activities, chemical stability, metabolism and delivery systems of quercetin: A review,
Trends Food Sci. Technol. **56**, 21–38 (2016)
<https://doi.org/10.1016/j.tifs.2016.07.004>
- Zupančič, Š., Lavrič, Z. and Kristl, J.,
Stability and solubility of trans-resveratrol are strongly influenced by pH and temperature,
Eur. J. Pharm. Biopharm. **93**, 196–204 (2015)
<https://doi.org/10.1016/j.ejpb.2015.04.002>

7

ELR-based Nanoparticles: A Prospective Drug Delivery System for DED Treatment

The evolution of drug delivery systems capable of temporal and spatial control of drug release has increased the demand for advanced materials (Kohane *et al.*, 2010). A classical approach for the generation of new materials is chemical synthesis. However, obtaining materials with elevated structural and functional complexity via this method is time- and cost-consuming. Alternatively, the field of recombinamers offers a solution, taking inspiration from the world around us. Recombinamers are protein-based polymers produced by means of genetic engineering with a precisely defined and controlled amino acid sequence (Girotti *et al.*, 2011). This allows the obtaining of a greatly monodisperse material with desired functional properties (Navarro *et al.*, 2012). Biomaterials like recombinamers offer outstanding biocompatibility and biodegradability, without evoking an immune response (Girotti *et al.*, 2020; Price *et al.*, 2014). Additionally, the production of these materials is easily scalable (Vallejo *et al.*, 2021).

Recombinant polymers resembling natural silk, collagen, or resilin have been proposed as potential starting materials for drug carriers (Desai *et al.*, 2015). Among these, elastin-like recombinamers (ELR) have gained significant interest in recent years. ELRs are designed based on repeating sequences of tropoelastin, a precursor of natural elastin. Elastin is one of the major proteic constituents of the extracellular matrix, characterised by exceptional elasticity and resistance to stress (Rodríguez-Cabello *et al.*, 2018; Shi *et al.*, 2014). One of the most commonly used repeated motifs for ELRs is the pentapeptide Valine-Proline-Glycine-X-Glycine (VPGXG). By modulating X, which can be any amino acid except proline, many properties of the recombinamer can be tuned. An example of tunable property is represented by the inverse temperature transition (ITT). ITT determines the transition temperature (Tt), below which the chains of the polymer remain in a disordered, soluble random-coil state; above the Tt, the polymer suffers a structural reorganisation and finally adopts an ordered β -spiral structure stabilised by hydrophobic interactions (Gonzalez-Valdivieso *et al.*, 2021; Quintanilla-Sierra *et al.*, 2019). Application of ELRs in the production of (nano)-particulate systems for the delivery of poorly soluble drugs and peptides has proven to be a versatile strategy, considering the wide range of

administration routes through which they can be administered (Hu *et al.*, 2015; Ryu *et al.*, 2014; Wang *et al.*, 2014).

Supercritical fluids (SCF) are all substances at a pressure and temperature above their critical point (De Marco *et al.*, 2022). Among SCF, supercritical carbon dioxide (scCO₂) assumes its supercritical state at mild conditions (7.38 MPa and 33.1°C), making its use for the production of drug delivery systems extremely feasible (Cocero *et al.*, 2009). Additional benefits include the fact that it can be recycled and is non-flammable and non-toxic (Santos *et al.*, 2013). The use of SCF in the production of micro- and nano-particulate systems has been proposed as an attempt to overcome the limits of traditional micronization techniques (e.g., spray drying, jet-milling, or solvent evaporation). These limits include a non-negligent residual of organic solvent in the final product and elevated temperatures that can cause thermal degradation of sensible active principles. Additionally, when using traditional micronization techniques, it is more difficult to control the final size of the particles produced (Franco *et al.*, 2020).

One of the methods that employs scCO₂ for the production of particulate systems is the supercritical anti-solvent (SAS) method (Campardelli *et al.*, 2015). During this process, scCO₂ acts as an anti-solvent by decreasing the solubility of the solute in the *solute-organic solvent* mixture, supersaturating it. This leads to nucleation and the subsequent formation of the nano- or microparticles (Reverchon *et al.*, 2002). Particle size and morphology can be adjusted by modulating the parameters of the process, like the concentration of the solution, nozzle geometry, or flow rate (Martín *et al.*, 2008, 2009).

For that reason, the SAS technique was used as a green method to produce ELR-particulate-based systems for the ophthalmic delivery of QUE and RSV. Physico-chemical characterization, together with *in vitro* biocompatibility and functional assays of the system, were performed. Also, the ability of the formulations to penetrate *ex vivo* porcine corneas was evaluated. The work was done in collaboration with Reinaldo Vallejo Vicente, a PhD student from *Smart Devices for NanoMedicine* Group, and from *PressTech* Group, both from the University of Valladolid, and under the supervision of professors Javier F. Arias Vallejo, Alessandra Girotti and Soraya Rodríguez-Rojo.

7.1. Synthesis of the Outcomes Obtained in Collaboration

The following section represents a summary of the methods and results obtained in collaboration with the *Smart Devices for NanoMedicine* Group and the *PressTech* Group from the University of Valladolid.

The biopolymer (EI)₂ used in this work was obtained through standard genetic engineering techniques. It consists of a tetra-block configuration. Two hydrophilic blocks contain glutamic acid (E) as a guest amino acid in the VPGXG sequence, while the hydrophobic ones contain isoleucine (I). To perform the encapsulation of QUE and RSV through the SAS process, initial operating parameters were established as follows: pressure and temperature were fixed at 11 MPa and 308 K. The CO₂ flow was set at 0.5 kg/h and the solution (drug:polymer) flow in the

reactor was set at 10.8 mL/min. Additionally, a 6:1 ratio was established between the polymer and the polyphenols. In the case where both polyphenols were encapsulated, the molar ratio between them was established at 1:1, and then 6:1 between ELR:QUE/RSV.

Nuclear Magnetic Resonance (NMR) analysis was used to confirm the ratio stabilised between the polymer and the polyphenolic compounds, as well as the encapsulation and the potential presence of EtOH in the final product. As a reference for QUE signals at 6.4 ppm and 6.2 ppm were taken, while for RSV the reference was at 6.13 ppm. In both cases, signals were from CH-groups.

As for the results, the NMR analysis disclosed that the ratio between the polymer and the compounds was as initially stabilised in all cases, 6:1. Furthermore, it confirmed that both compounds were successfully encapsulated in the particles obtained from the SAS process. Regarding the residual EtOH, whose peak was identified at 1.20 ppm, it had a very low intensity in all the samples, thus indicating a very pure product.

ELR-NPs obtained from the SAS process were dispersed in an aqueous medium at 37°C and subsequently analysed by DLS. All ELR-NPs formulations (containing QUE, RSV, or both) showed consistent size in the range of 56.7 ± 1.0 - 61.5 ± 2.6 nm. The ζ potential recorded in all cases was above -30 mV, indicating a stable particle dispersion. No significant changes in these parameters were recorded during the 5-day monitoring period.

Additionally, fluorescent-labelled ELR-NPs were prepared modifying the (EI)₂ polymer with an amine-fluorescein derivate through the formation of a stable amidic bond. The fluorescein-modified polymer was used for the preparation of ELR-NPs loaded with Nile red, a fluorescent compound used as a model of hydrophobic drugs. ELR-NPs bearing a double fluorescent tag were subsequently used in the *in vitro* cellular uptake and *ex vivo* corneal permeation experiments, as described in the following chapters of this thesis work.

7.2. Materials and Methods

7.2.1. Materials

Quercetin (QUE), 2',7'-dichlorofluorescein diacetate (H₂DCF-DA), trifluoroacetic acid (TFA), Nile Red, penicillin/streptomycin, human epithelial growth factor (hEGF), 5-methylphenazinium methyl sulphate (PMS), dialysis membranes with Molecular Weight Cut-Off (MWCO) of 14 kDa, and bovine insulin were obtained from Merck Life Sciences (St. Louis, MO, USA). Resveratrol (RSV) was purchased to Acros Organics (Geel, Belgium). Cell culture medium Dulbecco's modified Eagle's medium/Nutrient Mixture F-12 (DMEM/F12) + GlutaMax, DMEM/F12 without phenol red, Dulbecco's phosphate buffered saline (DPBS), foetal bovine serum (FBS), (2,3-Bis-(2-methoxy-4-nitro-5-sulfophenyl)-2H-tetrazolium-5-carboxanilide) (XTT), human insulin, BCA Protein Assay kit, and all the plastic materials (tips, pipettes, culture flask and plates) were purchased from ThermoFisher Scientific (Rockford, IL, USA). MilliQ water was obtained from the Millipore unit. Acetonitrile of HPLC grade was obtained from PanReac (Darm-

stadt, Germany). Fluoromonunt-G[®] mounting medium was purchased from SouthernBiotech (Birmingham, AL, USA). Tissue-Tek Compound O.C.T. was purchased from Sakura Finetek (Torrance, CA, USA). ELRs employed in this work were obtained as described previously in Vallejo *et al.* (2021).

7.2.2. Methods

Quantitative Analysis of Encapsulated QUE and RSV

The Reverse-Phase High-Pressure Liquid Chromatography (RP-HPLC) Waters e2695 module (Waters Corporation, MA, USA) was used for the development of a separation method to quantify QUE and RSV. The module was provided with a quaternary pump, an autosampler, and a photodiode array detector connected to an UV detector, which was set at 370 and 306 nm for the detection of QUE and RSV, respectively. For the separation a C18 Mediterranean Sea column (250 × 4.6 mm, 5 μm) (Teknokroma Analítica S.A., Barcelona, Spain) was used, connected to an OptiGuard 1 mm guard column (Sigma-Aldrich, San Luis, Missouri, USA). In each run, 20 μL of the sample were injected. For the mobile phase, milliQ water and acetonitrile were used, both with the addition of 0.05 % TFA (v/v). The flow rate was set at 1 mL/min. The gradient, as well as the range of the calibration lines and the LOD and LOQ, were previously mentioned in *Chapter 2* of this thesis work (page 64).

Particle Morphology and Size Analysis

Scanning Electron Microscopy (SEM) was used to analyse the morphology and size of the microparticles obtained from the SAS process. Before the analysis, the particles were placed under argon atmosphere at room temperature (25°C). The measurements were performed at the Advanced Microscopy Laboratory (Parque Científico, University of Valladolid) using an ESEM QUANTA 200 FEG instrument (FEI Company, Hillsboro, OR, USA). The analysis was performed applying 1 kV of accelerating voltage, enough to provide sufficient resolution without damaging the sample. 2011 ZEN 2.3 blue edition (Carl Zeiss GmbH, Jena, Germany) software was used to measure the particles size in the photomicrographs.

Release Studies

To determine the release kinetics of QUE and RSV from the ELR-NPs, 1.5 mL of all formulations were placed in separate dialysis bags (MWCO 12.4 kDa) sealed on both ends. The dialysis bags were then put in vials with 20 mL of Simulated Tear Fluid (composition: 0.67 g of NaCl, 0.008 g of CaCl₂, 0.2 g of NaHCO₃, and milliQ water up to 100 mL; pH 7.4) with the addition of 1 mM of ascorbic acid and placed in an incubator under controlled conditions. At scheduled time points (0, 0.25, 0.5, 1, 2, 4, 6, 8, and 24 hours) the releasing medium from the corresponding vials was collected and analysed by RP-HPLC as previously reported (*Chapter 2*, page 64). Samples were prepared in three separate vials for each time point.

The Korsmeyer-Peppas model was used to elucidate the mechanism of drug release from the ELR-NPs. Drug release data was fitted to the following equation:

$$\frac{M_t}{M_\infty} = kt^n \quad (7.1)$$

Where the fraction $\frac{M_t}{M_\infty}$ represents the amount of drug(s) released at time t ; k is the rate constant giving information about the geometry of the drug delivery system; and the value of n describes the mechanism of drug transport from the system of interest. For a system having a spherical geometry, a value of $n \leq 0.43$ suggests a Fickian transport; a value of n between 0.43 and 0.85 indicates a non-Fickian, anomalous transport proposing a combination of diffusion and erosion/rearrangement; $n = 0.85$ indicates Case II governed by zero-order kinetics; while $n > 0.85$ designates a Super Case II transport described by a relaxation mechanism of drug release. For the determination of n , only the $\frac{M_t}{M_\infty} < 0.60$ part of the release data is used.

Corneal Cell Line and Culture Conditions

A SV-40 immortalised human corneal epithelial cell line (HCE) (Araki-Sasaki *et al.*, 1995) was used for the *in vitro* evaluation of the formulations. The passages used for the experiments were from 31 to 41. The cells were cultured at 37°C in a 5% CO₂ atmosphere in DMEM/F12 + GlutaMax cell medium with the addition of 10% FBS, 5 µg/mL human insulin, 10 ng/mL EGF, and 100 U/mL of penicillin and 0.1 mg/mL of streptomycin. Cell inspection under a phase microscope was done daily, while the cell-medium was changed on alternate days.

In Vitro Biocompatibility of ELR-NPs

To evaluate ELR-NPs biocompatibility, HCE cells were seeded into 96-well plates (1x10⁴ cells/well) and grown in supplemented medium until 90% confluence. Once the desired confluence was reached, the cells were maintained for 24 hours in a supplement-free medium. Subsequently, cells were incubated with ELR-NPs solubilized in DMEM/F12 without phenol red for 1 and 3 hours at the following concentrations: i) for the QUE- ELR-NPs from 5 to 50 µM of encapsulated QUE; ii) for the RSV-ELR-NPs 25-300 µM of encapsulated RSV; iii) for the ELR-NPs containing both polyphenols (1:1 molar ratio), the concentrations used were 5-50 µM in total; and iv) blank ELR-NPs in the range of 0.025-0.5 mg/mL. Negative control of cell toxicity consisted of cells exposed to culture medium, while cells exposed to 0.005% benzalkonium chloride (BAK) were used as a positive control. After the exposure time, supernatants were discarded and loaded with 100 µL of DMEM/F12 without phenol red and 25 µL of reaction mixture (10 µL of 3 mg/mL of PMS in 0.25 mg/mL of XTT). Cells were left in incubation for 3 hours at 37°C. Absorbance was collected at 450 and 660 nm using an UV/Vis spectrophotometer (SpectraMax M5; Molecular Devices, Sunnyvale, CA, USA). For each formulation, six replicates in three independent experiments were performed. The percentage (%) of living cells was calculated relative to the values of the negative control of toxicity (100 %).

Intracellular Antioxidant Activity of ELR-NPs Formulations

The capacity of the different ELR-NPs formulations to neutralise intracellular ROS was evaluated utilising H₂DCF-DA, a fluorescent probe sensitive to ROS presence. HCE cells were seeded into 24-well plates with a 6x10⁴ cells/well density. Once the confluence of 90 % was reached, the cells were maintained in supplement free medium for 24 hours. Afterwards, 500 μ L of the formulations were applied to the cells as pre-treatments and incubated for 1 hour at 37°C. The concentration ranges of ELR-NPs used in this assay were the same as those used in the cell viability assay. Then, pretreatments were removed, and the cells were loaded with 500 μ L of a 10 μ M H₂DCF-DA solution for 30 minutes. The cells were again treated with the formulations at the same concentrations as before and subsequently exposed for 15 seconds to an 8-W UV-B lamp (Bio-Rad, Inc., Hercules, CA, USA). The control plate was not irradiated. After 1 hour of incubation, fluorescence was collected at 488 and 522 nm (excitation and emission, respectively). The total protein content of the adherent cells was measured using the BCA assay, following the instructions of the manufacturer. This measurement was used to normalise the fluorescence values. Three independent experiments were performed, with two replicates for each type of formulation.

Cellular Uptake of Fluorescent-Labelled ELR-NPs

In vitro cellular uptake of fluorescent-labelled ELR- NPs was monitored by a confocal microscope Leica TCS SP5X equipped with a 63x oil immersion objective (Wetzlar, Germany). Fluorescent-labelled ELR-NPs used in this study, bore a double fluorescent tag. One was fluorescein conjugated to the ELR biopolymer, and the other was Nile red encapsulated in the ELR-NPs. The ELR-NPs were prepared in PBS and subsequently diluted in phenol red free DMEM/F12 medium to a final concentration of 2 mg/mL, equivalent to 10 μ g/mL of Nile red. HCE cells were seeded in 8-well Permanox[®] multi-chamber slides at a density of 15x10³ cells/well. Before the addition of the formulations, the cells were washed twice with PBS. Following this, 200 μ L ELR-NPs were added to each well and incubated for a predetermined time intervals (5, 15, 30, 60, and 90 minutes). Once the formulations were removed, the cells were fixed with ice-cold methanol for 15 minutes. Cell nuclei were counterstained with DAPI (10 μ g/mL in PBS). To remove the excess dye, the cells were washed three times with PBS. The slides were mounted with the mounting medium Fluoromount-G[®] (Southern Biotech, Birmingham, AL, USA). Control cells were treated with phenol red free DMEM/F12 or with 10 μ g/mL Nile red diluted in the same solvent. The collected images were analysed through Image J software (LOCI, University of Wisconsin, Madison, WI, USA).

Penetration of ELR-NPs through *Ex Vivo* Porcine Corneal Tissues

To assess the *ex vivo* corneal penetration of fluorescent ELR-NPs, porcine eyeballs were obtained from the local slaughterhouse (Matadero Justino Gutiérrez SL., Laguna de Duero, Val-

ladolid, Spain). Enucleated eyeballs were disinfected and cleaned from the annexed muscular and connective tissues, washed in PBS, and placed in 12-well plates. To avoid spilling of the ELR-NPs solutions upon instillation, a 12-mm silicon ring was placed over the cornea of the porcine eyeballs. Eyes were incubated with 300 μL of a 2 mg/mL fluorescent-labelled ELR-NPs solution. As controls, Nile red dissolved in olive oil and PBS were used. After predefined times (5, 15, 30, and 60 minutes), the globes were washed in PBS to remove the formulations, then the corneas were dissected and included in OCT medium at -20°C . Cryostat cutting was used to obtain 5 μm tissue sections that were subsequently placed on slides, coverslipped, and viewed under an inverted fluorescence microscope (Leica DMI 6000B, Wetzlar, Germany). Images were collected from two independent experiments. As previously, the images obtained were analysed with Image J software (LOCI, University of Wisconsin, Madison, WI, USA).

Statistical Analysis

The fitting of the experimental results with the mathematical model of drug release was performed through non-linear curve fitting using OriginPro Software (OriginLab Corporation, Northampton, MA, USA). For cell-based assays, all data is expressed as the mean \pm standard error of the mean (SEM). Statistical analysis of the data was done using one-way analysis of variances (ANOVA) followed by Tukey's or Games-Howell post-hoc tests. This was performed using the SPSS software (SPSS 20.0; SPPS, Inc., Chicago, IL, USA).

7.3. Results and Discussion

7.3.1. ELR-NPs Morphology and Size

Following the encapsulation procedure, the ELR-NPs in solid form were submitted to SEM analysis to explore the morphology and size range obtained. Concerning the morphology, as shown in **figure 7.1**, all particles prepared were spherical and presented a smooth surface. Also, there was no significant aggregation between the particles. Nonetheless, a heterogenous range of sizes was observed, ranging from 4 – 8.5 μm (**table 7.1**). The comparable velocities of the CO_2 and of the working solution (drug-polymer) at the nozzle's outflow could be one explanation for these results. The approximate values of the velocities causes a less uniform pulverisation, which in turn generates the formation of different microdroplets and, as a consequence, a heterogeneous nucleation. Additionally, it has been suggested that the initial concentration of the drug solution may have an impact on particle size, since it influences the processes of supersaturation and nucleation (Kalani *et al.*, 2011). Thus, for this particulate population, the heterogeneous size distribution is a consequence of the combination of the two phenomena before mentioned.

Prior to each subsequent experiment, solid ELR-NPs were dispersed in PBS at 37°C , allowing the microparticles to rearrange and assume nanometric dimensions.

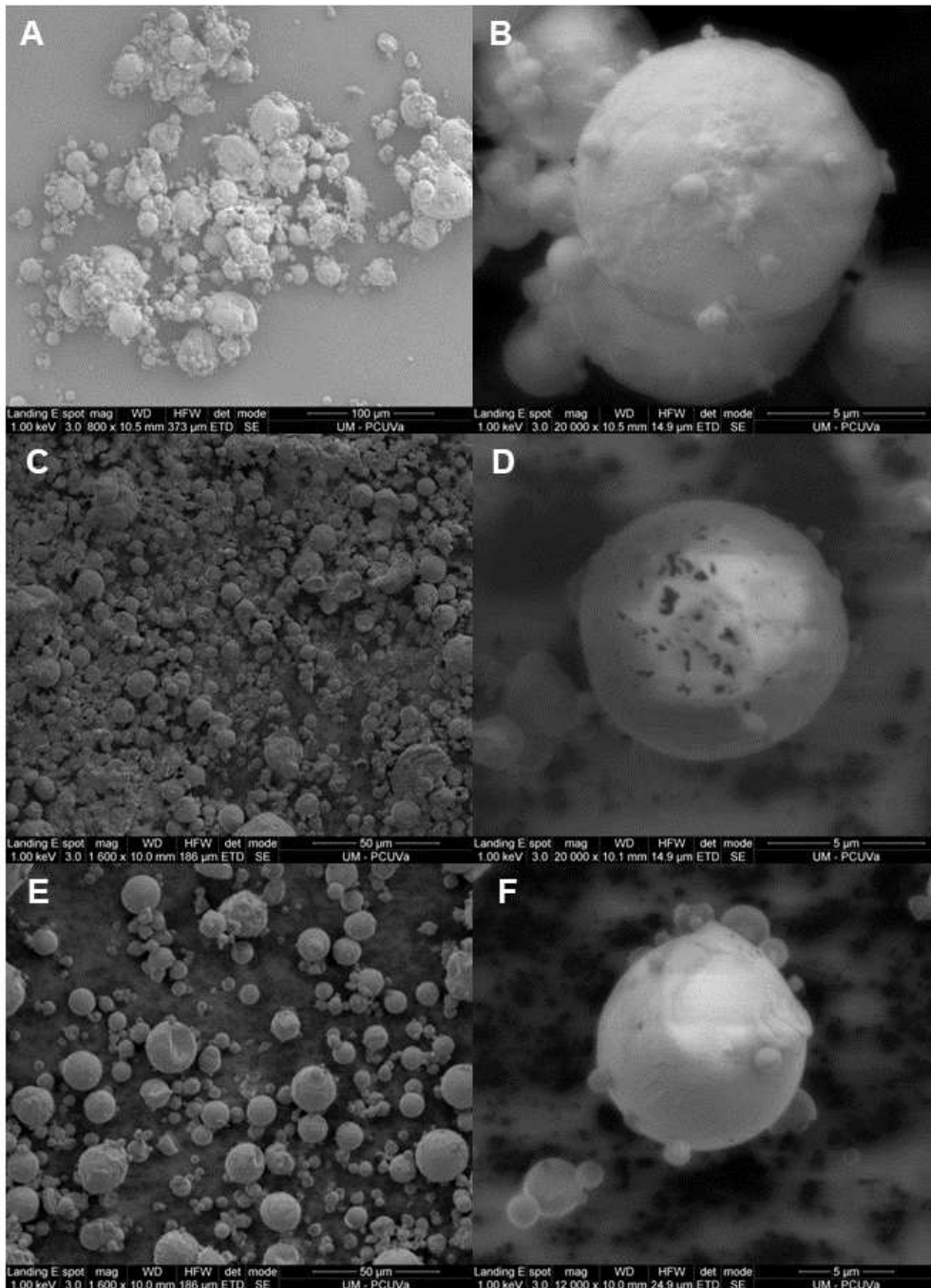


Figure 7.1 - SEM microphotographs showing low magnification (A, C, and E) and high magnification (B, D, and F) morphology of: A) QUE-ELR-NPs, scale bar 100 μm ; C) RSV-ELR-NPs, scale bar 50 μm ; and E) QUE/RSV-ELR-NPs, scale bar 50 μm . Detailed views: B) QUE-ELR-NPs, scale bar 5 μm ; D) RSV-ELR-NPs, scale bar 5 μm ; and F) QUE/RSV-ELR-NPs, scale bar 5 μm .

Table 7.1: Average diameter and median particle diameter (D (0.5)) determined from the images obtained by SEM (n>200) of QUE-ELR-NPs, RSV-ELR-NPs and QUE/RSV-ELR-NPs. All values are shown as mean \pm SEM.

Sample	Average Diameter (μm)	D (0.5)
QUE-ELR-NPs	8.5 ± 0.18	5.9
RSV-ELR-NPs	4.0 ± 0.09	2.6
QUE/RSV-ELR-NPs	6.0 ± 0.20	3.7

7.3.2. Release Studies

To reduce dosing frequencies and improve patient compliance to adhere to certain therapeutic regimens, efforts have been put into the development of formulations that are able to achieve sustained release of the active principle (Juliano *et al.*, 1978). For this reason, a study of the release kinetics from the ELR-NPs containing QUE, RSV, or both polyphenolic compounds was performed. The obtained release profiles were compared to the release profiles of free drugs. **Figure 7.2** illustrates the release profiles of the formulations studied in this work over a period of 24 hours.

For the RSV-ELR-NPs, 47.6 ± 2.73 % of the polyphenol was released during the first hour, reaching the 88.2 ± 0.07 % by the end of the study. During the first hour, 67.2 ± 1.10 % of free RSV was released, concluding that a modest retention in the release of RSV is reached upon encapsulation in ELR-NPs. QUE-ELR-NPs liberated only 13.7 ± 5.65 % and 43 ± 1.38 % of QUE in 1 and 24 hours, respectively. This was only a decent deceleration in the release of QUE in comparison to free QUE, which in the same time span had a release of 23.8 ± 0.39 % and 52.71 ± 0.22 %. In the case of ELR-NPs where both drugs were encapsulated, only 1.44 ± 0.88 % of QUE and 28.4 ± 3.17 % of RSV were released in the first hour of the study. This data indicates that an appreciable delay in the release profiles of both drugs occurs when compared to the control release profiles of non-encapsulated polyphenols. These findings are probably the result of a tighter packing of the core of the NPs due to the presence of the two hydrophobic molecules.

It should be kept in mind that QUE is a compound prone to degradation, especially by oxidation, and that this fact could have significantly impacted the measurement of the release profile of QUE in all three cases. The chemical instability of QUE was the object of a study conducted as a part of this thesis (*Chapter 2*), where it was observed that in solution at RT, QUE has a $t_{1/2}$ of 3.66 hours (see page 69).

To have a more comprehensive insight into the mechanism of the releasing process, experimental data obtained from the release study were fitted to the Korsmeyer-Peppas model. This model is commonly used to analyse the drug release from polymeric NPs, and the results are summarised in **table 7.2**.

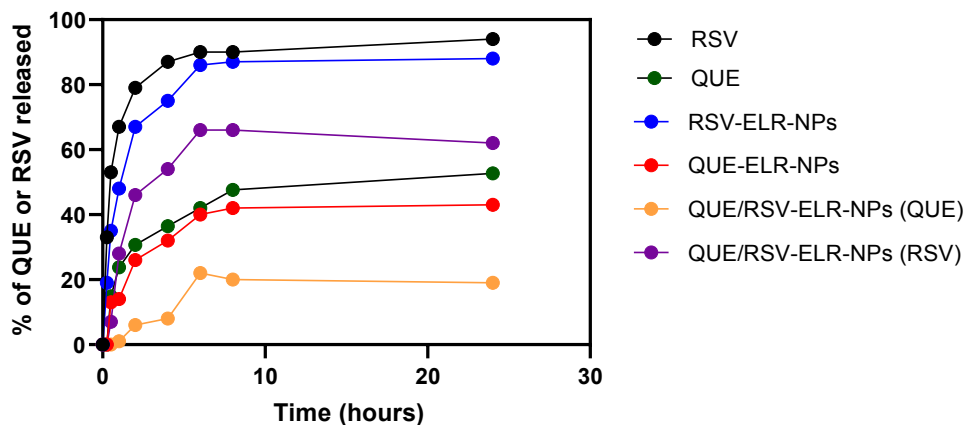


Figure 7.2 - Release profiles of QUE and RSV from ELR-NPs in STF. All data are mean \pm SEM of three independent experiments.

Table 7.2: Kinetic parameters n (release exponent), k (rate constant), and R^2 (correlation coefficient) resulted from the fitting of the drug release data to the Korsmeyer-Peppas model.

Formulation	n	k	R^2	Transport mechanism
RSV-ELR-NPs	0.53	0.46	0.993	Diffusion/Pol. Rearrangement
QUE-ELR-NPs	0.32	0.18	0.85	Diffusion
QUE/RSV-ELR-NPs (QUE)	0.52	0.04	0.82	Diffusion/Pol. Rearrangement
QUE/RSV-ELR-NPs (RSV)	0.22	0.69	0.900	Diffusion

The values of n found in the cases of QUE-ELR-NPs and QUE/RSV-ELR-NPs (RSV) were lower than 0.43, thus indicating a spherical-shaped system from which drug release occurs primarily through a diffusion process. A non-Fickian n exponent ($0.43 \leq n \leq 0.85$) was observed for the RSV-ELR-NPs and QUE/RSV-ELR NPs (QUE), proposing an anomalous transport, where apart from drug diffusion, a rearrangement of the ELR polymeric chains occurs, influencing the rate of the drug liberation. A generally high correlation coefficient ($R^2 > 0.9$) was observed, suggesting a good correspondence between the experimental data and the Korsmeyer-Peppas equation. A slightly poorer values of R^2 were observed in the data obtained from QUE related samples, again indicating the issues encountered in determining the release profile of this polyphenol.

7.3.3. *In Vitro* Biocompatibility of ELR-NPs

Since our final goal would be to use the ELR- NPs as topical treatment for DED, which affects the ocular surface, the cell viability of a human corneal epithelial cell line (HCE cells) after short-term exposure to the formulations was evaluated. Exposure times of one and three hours were selected considering the reduced contact time that an eyedrop formulation has with the ocular surface once applied. As seen in **figure 7.3**, neither type of ELR-NPs negatively impacted the cell viability of corneal cells, as viability percentages of formulation-exposed cells were always close to 100 %. Thus, all formulations may be considered safe.

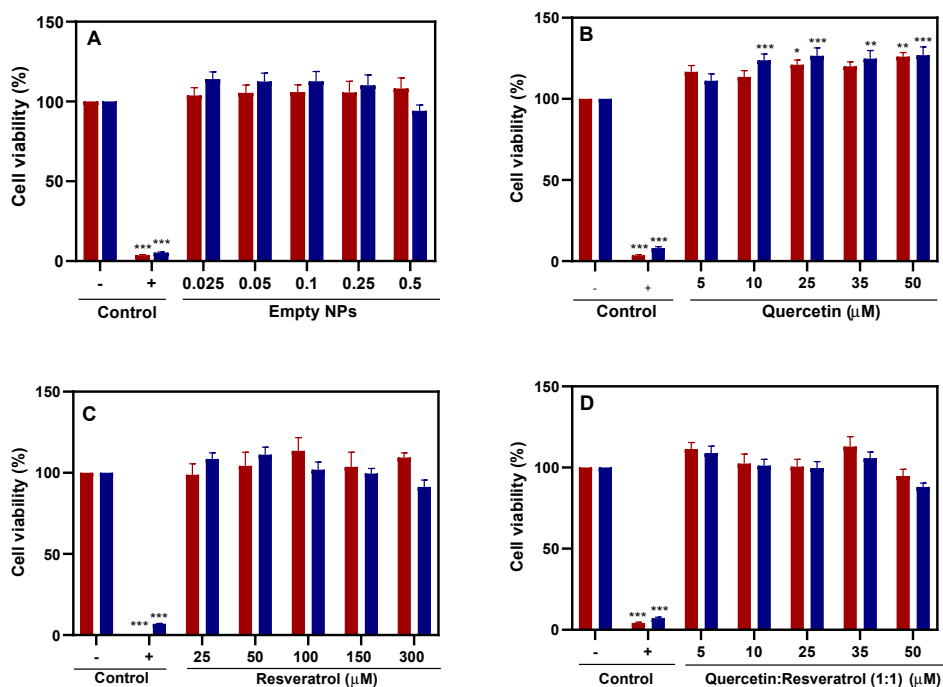


Figure 7.3 - Viability of HCE cells upon treatment with (A) empty and loaded ELR-NPs with (B) QUE; (C) RSV; and (D) QUE/RSV after 1 (red bars) and 3 hours (blue bars) of exposure. The reported concentration ranges refer to the concentrations of encapsulated polyphenol inside the ELR-NPs. Negative controls was cell culture medium, positive control was BAK (0.005%). The data represent the mean of three independent experiments \pm SEM. * $p < 0.05$, ** $p < 0.01$, *** $p < 0.001$ compared to control cells treated with culture medium.

Thanks to their valuable health effects, QUE and RSV are well-studied natural compounds. A literature review describes different attempts of their formulation in polymer-based particulate systems for ocular delivery. The studies conducted on different ocular cell lines, such as ARPE-19 (retinal pigmented epithelium) and RGC-5 (retinal ganglion cells), evinced a very good biocompatibility of QUE and RSV-bearing carriers, as was the case with our ELR-NPs. Additionally, the cytotoxic effect of pure QUE and RSV found at higher dosages, was dimin-

ished as a result of their encapsulation in PLGA-NPs and solid lipid nanoparticles . (Bhatt *et al.*, 2020; Liu *et al.*, 2015). Moreover, the co-administration of the two polyphenols did not have a negative impact on HCE cell viability either, which is interesting because this combination could be used to obtain a more pronounced biological response (e.g., antioxidant or anti-inflammatory).

Besides, blank ELR-NPs without any drug encapsulated did not compromise the viability of the HCE cells, highlighting the elevated biocompatibility of the material used for the preparation of the NPs. This important aspect of ELR-based NPs was supported by research done by other authors as well. Gonzalez-Valdivieso *et al.* reported that an elastin-like biopolymer composed of a combination of hydrophobic-hydrophilic blocks joined to a penetration promoting sequence did not induce cell death in three different pancreatic cells lines (PANC-1, PDX354, and PDX185) during a 3-hour exposure period (Gonzalez-Valdivieso *et al.*, 2021). In another published work, the same author outlined the safety of the ELR-NPs in three human primary cell lines (HFF-1 fibroblast, mesenchymal stem cells (hMSCs), and HUVEC endothelial cells) (Gonzalez-Valdivieso *et al.*, 2019).

Finally, as expected, 0.005% BAK induced a significant reduction in HCE cell viability ($p < 0.001$) at both time intervals.

7.3.4. Intracellular Antioxidant Activity of ELR-NPs

The capacity of the ELR-NPs loaded with polyphenols to neutralise free radical species developed intracellularly was evaluated using H₂DCF-DA, a compound that, in the presence of ROS, is converted into a fluorescent metabolite (Leutner *et al.*, 2001). **Figure 7.4** shows the development of intracellular ROS after treatment with the ELR-NPs. Control cells treated with culture medium are taken as 100 %, so values below 100 % indicate that ROS have been neutralised. Among the formulations loaded with the polyphenolic compounds, the one containing QUE showed to be the most efficient in scavenging radical species. QUE-ELR-NPs significantly decreased ROS at 5 μ M of encapsulated QUE ($p < 0.05$). This effect maintained a constant significant response at concentrations equal to or higher than 25 μ M of QUE inside the ELR-NPs ($p < 0.01$). With respect to the RSV-ELR-NPs, they were able to decrease ROS in a dose-dependent manner, obtaining an important reduction at a 150 μ M RSV ($p < 0.05$). Although carrying both polyphenolic molecules, QUE/RSV-ELR-NPs did not appear to be the most effective formulation in counteracting the development of ROS. Blank NPs did not exhibit any scavenging activity, indicating that all the effects observed with the ELR-NPs loaded with the polyphenolic compounds are obtained thanks to them.

Phenolic compounds are well known for their antioxidant activity. This activity results from the presence of hydroxyl or phenolic groups in their chemical structure, since free radicals are inhibited by the transfer of a hydrogen atom from these chemical moieties. The higher antioxidative effect of ELR-NPs carrying QUE is related to the greater number of hydroxyl groups present in its structure compared to the ones in RSV. Also, hydroxyl groups that are

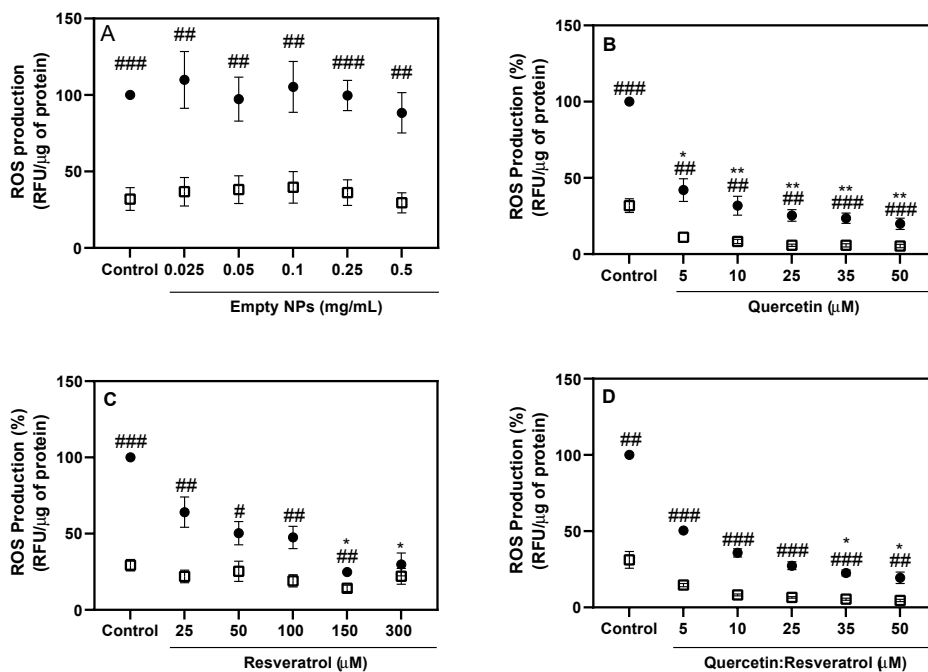


Figure 7.4 - Intracellular ROS production in HCE cells exposed to UV-B light for 15 seconds. The scavenging capacity of the (A) empty ELR-NPs and containing: (B) QUE; (C) RSV; and (D) QUE/RSV is shown in exposed and control cells (exposed just to cell-culture medium). (●) Cells exposed to UV-B; (□) Cells unexposed to UV-B. The data represent the mean of three independent experiments \pm SEM. * $p < 0.05$, ** $p < 0.01$, *** $p < 0.001$, compared with UV-B exposed cells; # $p < 0.05$, ## $p < 0.01$, ### $p < 0.001$ intergroup comparison.

adjacent in the ring, as in the case of QUE, can form a resonance stabilised quinone structure capable of interacting with free radicals in a more pronounced way (Francenia Santos-Sánchez *et al.*, 2019.; Tu *et al.*, 2015). Abengonzar *et al.* confirmed the greater antioxidant capacity of QUE in respect to RSV in an *in vitro* study conducted on HCE and IOBA-NHC cells (Abengózar-Vela *et al.*, 2015). In comparison to the scavenging ability of other natural compounds, Stoddard *et al.* revealed that QUE have the lowest EC_{50} value of $2.98 \mu\text{M}$ among epigallocatechin gallate, n-propyl gallate, and gallic acid. This was measured by the $\text{H}_2\text{DCF-DA}$ assay in human corneal limbal epithelial cells (Stoddard *et al.*, 2013). Unfortunately, an equivalent ocular cell-based study comparing the antioxidant activity of RSV with other polyphenolic compounds than QUE has not been reported yet. However, an investigation carried out by Gülçin evaluated the ability of RSV to scavenge free radical species by chemical antioxidant assays like as 2,2-diphenyl-1-picrylhydrazyl (DPPH•) and 2,2'-azino-bis(3-ethylbenzothiazoline-6-sulfonic acid (ABTS•+). Gülçin reports that $30 \mu\text{g}/\text{mL}$ of RSV were capable of neutralising 99.1 % of the free radicals generated in solution. The observed effect was comparable to the ones of butylated hydroxyanisole (BHA) and 2,6-bis(1,1-dimethylethyl)-

4-methylphenol (BHT), antioxidants used in pharmaceutical, food, and cosmetic industries. Also, this effect was higher than the one of α -tocopherol which was capable of scavenging only 55.9 % of free radical species (Gülçin *et al.*, 2010). Another study estimating the antioxidant capacity of one hundred compounds through the same chemical assays as the one before mentioned listed QUE among the seventeen substances with the most potent antioxidant ability (Lee *et al.*, 2015).

Combining QUE and RSV did not significantly potentiate the anti-oxidant response; however, other possible benefits of this combination may be expected. This may include the improvement of RSV bioavailability since QUE is capable of competitively inhibiting the P-gp efflux pump present in corneal epithelial cells (Choi *et al.*, 2011; Dey *et al.*, 2003).

7.3.5. Cellular Uptake of ELR-NPs

Drug-loaded ELR-NPs must be internalised by target cells in order to produce a therapeutic effect. Therefore, uptake of ELR-NPs bearing a double fluorescent-tag by corneal epithelial cells was studied using confocal microscopy. Nile red, encapsulated in the ELR-NPs, was used as a model for hydrophobic drugs. This compound was chosen because of its significant hydrophobicity and low solubility in water (Snipstad *et al.*, 2014). As observed in **figure 7.5**, the ELR-NPs efficiently accessed the intracellular compartment after just 5 minutes of contact with the cells. The Nile red used as a payload (red), together with the ELR-NPs (green spots), are mainly located in the cytosol in proximity to the cell membrane. An increased red fluorescence over time confirmed a time-dependent uptake of Nile red loaded ELR-NPs. On the contrary, the green fluorescence corresponding to the ELR-NPs decreased, indicating that after the release of Nile red, the biopolymer was probably degraded due to presence of intracellular proteases (Lim *et al.*, 2003). In contrast, non-encapsulated Nile red dissolved in PBS exhibited very poor cell uptake, as shown in **figure 7.6**.

The internalisation process of the ELR-NPs may occur following different active endocytic mechanisms. These include clathrin or caveolin-mediated endocytosis, clathrin/caveolin-independent endocytosis, or micropinocytosis. As well, cell internalisation may take place by passive diffusion across cell membranes following the concentration gradient (Foroozandeh *et al.*, 2018; Mitchell *et al.*, 2021). Nanoparticle-related parameters such as size, shape, surface charge and chemistry, are crucial in determining the rate of cell uptake (Treuel *et al.*, 2013). In general, smaller NPs in the range of 10-60 nm, like the ones used in this work, are better taken up by cells than larger NPs. This is because smaller NPs form more interactions with biological membranes due to their larger surface area. Also, different studies showed that they had a shorter uptake time (Chithrani *et al.*, 2007; Sabourian *et al.*, 2020; Salatin *et al.*, 2017). Regarding the surface charge, positively charged NPs favourably interact with the negatively charged phospholipid membrane layer. Despite this attractive interaction, damage of the cell membrane may occur, causing cytotoxicity (Goodman *et al.*, 2004; Lovric *et al.*, 2005). On the other hand, the repulsive forces between the negatively charged NPs and the

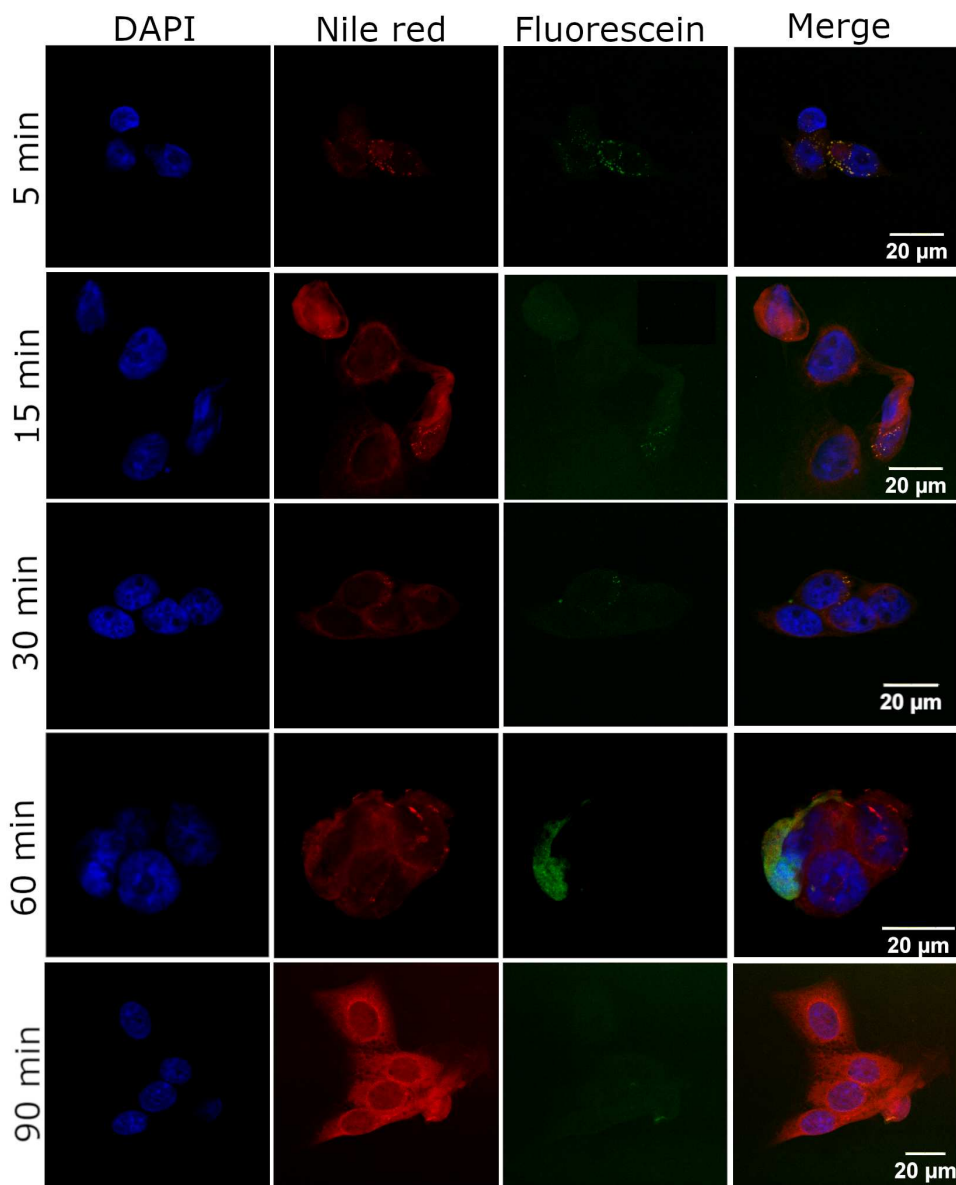


Figure 7.5 - Confocal microphotographs of fluorescein labelled ELR-NPs loaded with Nile red and taken up by HCE cells after exposure for 5, 15, 30, 60, and 90 minutes. Nile red is observed in red; cell nuclei in blue, counterstained with DAPI; ELR-NPs in green. Scale bar 20 μm .

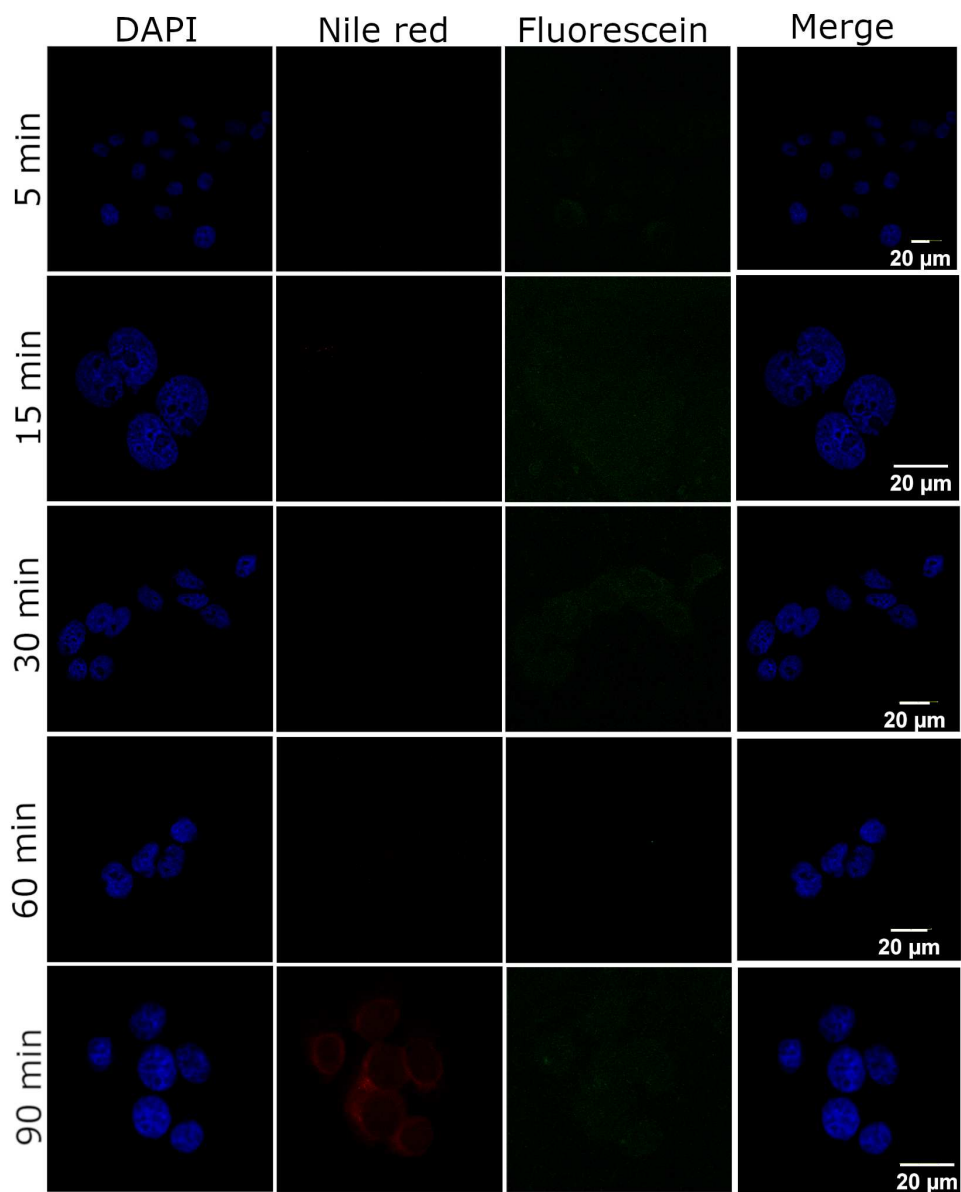


Figure 7.6 - Confocal microphotographs of non-encapsulated Nile red taken up by HCE cells after exposure for 5, 15, 30, 60, and 90 minutes. Nile red is observed in red; cell nuclei in blue, counterstained with DAPI; scale bar 20 μm .

cell membrane may be counteracted through the interaction with positively charged membrane proteins (Mazumdar *et al.*, 2020). This scenario is likely to occur in our case, considering that the ELR-NPs possess a negative charge (~ -30 mV). Additionally, it has been seen that non-cationic (slightly neutral or anionic) NPs manifest a higher biocompatibility (Wai *et al.*, 2019). In spite of the fact that there is not a firm consensus on the predominant internalisation pathway based on the particle shape, spherical NPs seem to be more readily taken up by non-phagocytic cells compared to rod-shaped ones (Han *et al.*, 2016; Zhang *et al.*, 2019). Along with the characteristics of the nanosystem employed, the extent of the uptake strongly depends on the cell line used (Mitchell *et al.*, 2021). During prolonged exposure to NPs, passive routes of internalisation may play a key role; however, it would be interesting to use specific inhibitors to elucidate the endocytic pathway(s) of ELR-NPs internalisation in corneal epithelial cells.

7.3.6. Penetration of ELR-NPs in *Ex Vivo* Porcine Corneas

Fluorescence intensities in porcine corneal cross-sections were used to estimate the distribution of fluorescein-labelled ELR-NPs loaded with Nile red across corneal layers.

At the shortest contact time of the ELR-NPs with the porcine corneal tissues (5 minutes), a modest red fluorescence was already observed over the corneal epithelium. This signal corresponds to Nile red (**figure 7.7**). Additionally, a green fluorescence signal, given by the fluorescein-labelled ELR polymer of the NPs, is observed on the apical part of the corneal epithelium. After 15 minutes, the red fluorescence signal was homogeneously distributed throughout the corneal epithelium. This signal overlapped with a less intense green signal corresponding to the carrier. Although the green signal had its highest intensity at the superficial epithelial layers, less intense fluorescence was also observed across the epithelium. This indicates that most of the ELR-NPs are retained on the corneal surface, but also that some of them distribute into the epithelium, where they release Nile red. The fluorescence intensity in the corneal epithelium, corresponding to the payload, increased with the increasing contact time of the ELR-NPs.

This suggests a time-dependent penetration pattern. Regarding the non-formulated Nile red, dissolved in olive oil, no fluorescence signal was detected until 30 minutes of incubation. At 30 minutes, low intensity signal started to appear. This intensity increased after 60 minutes of incubation. Although a red fluorescence signal was observed in corneal tissues exposed to non-formulated Nile red, it was clearly of lesser extent than the one found in corneal tissues exposed to ELR-NPs (**figure 7.8**). Moreover, it must be highlighted that the corneal epithelium and stroma did not suffer any alternation upon contact with the fluorescein-labelled ELR-NPs, as shown in **figure 7.9**.

Together with the precorneal factors, the cornea represents the main obstacle for drug permeation into intra-ocular tissues (Ramsay *et al.*, 2018). Once the drug is topically instilled onto the ocular surface, the first barrier that is encountered is the corneal epithelium. The corneal epithelium is a highly lipophilic structure, formed of several cell layers and sealed by tight junctions. These characteristics impede the absorption of any molecule that is not small and

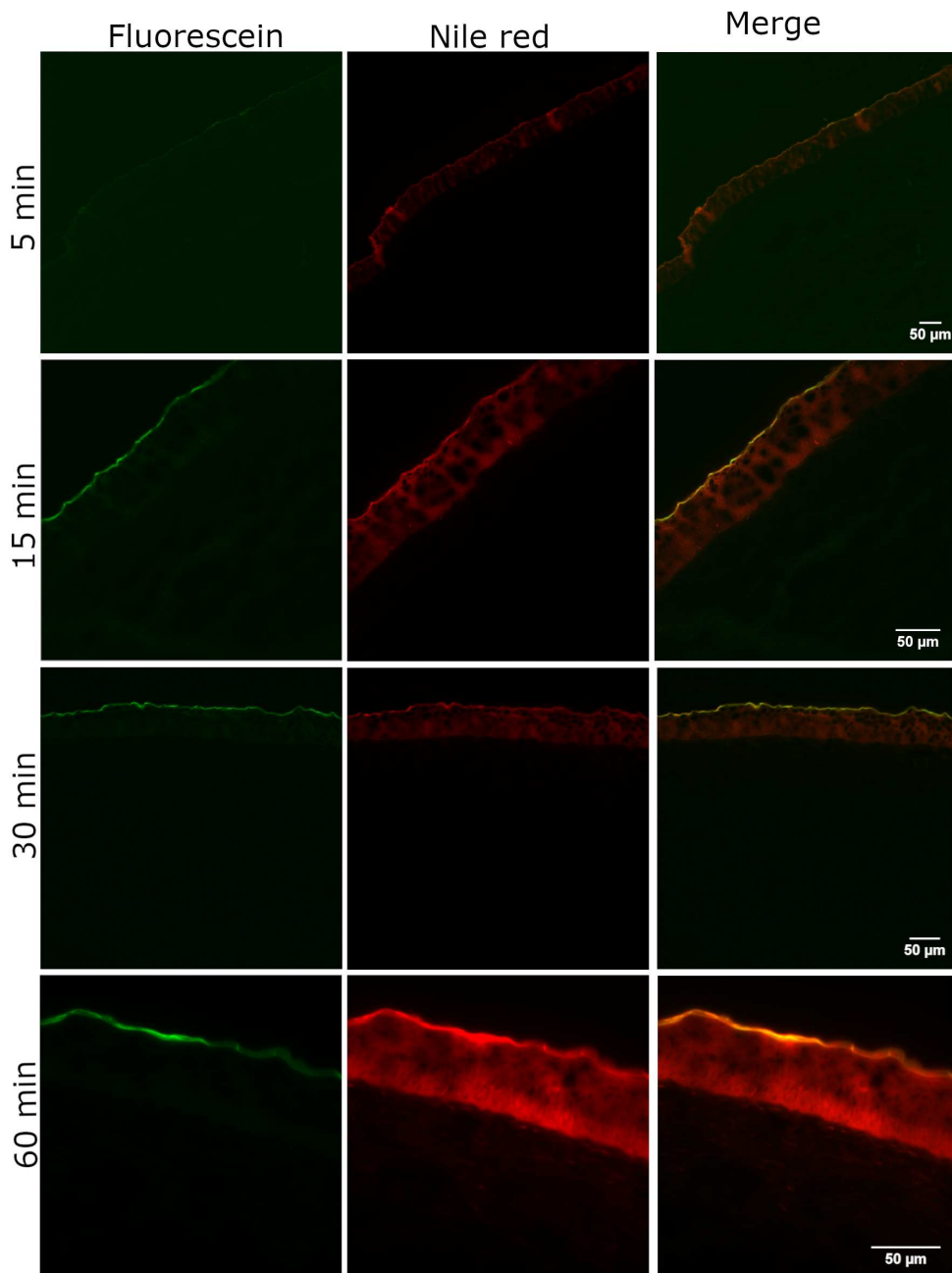


Figure 7.7 - Fluorescence microphotographs of *ex vivo* penetration of corneal tissues of fluorescein labelled ELR-NPs loaded with Nile red. Red-Nile red, green-fluorescein; scale bar 50 μm. E-corneal epithelium; S-stroma.

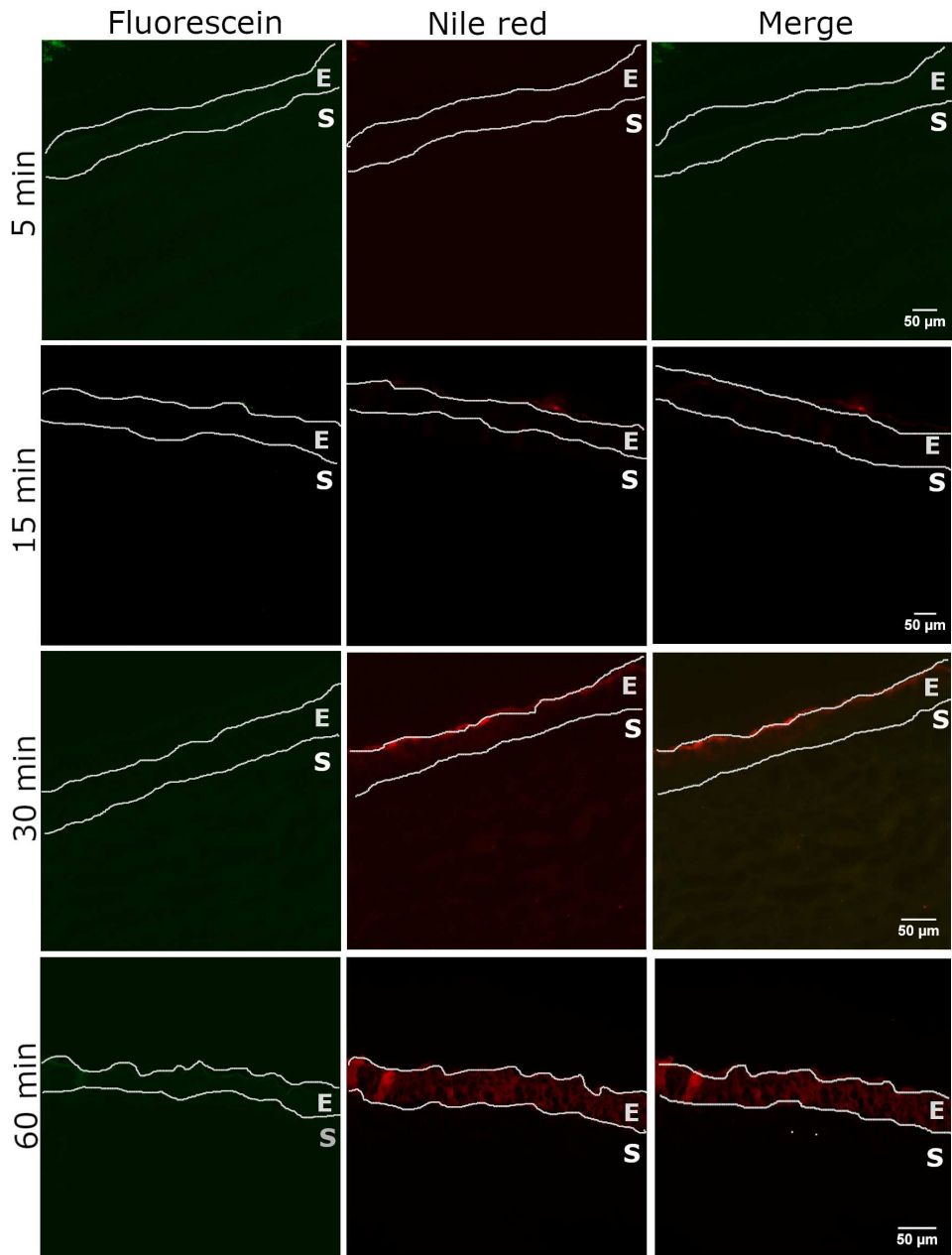


Figure 7.8 - Fluorescence microphotographs of *ex vivo* penetration of corneal tissues of Nile red dissolved in olive oil. Red-Nile red, green-fluorescein; scale bar 50 μm. E-corneal epithelium; S-stroma.

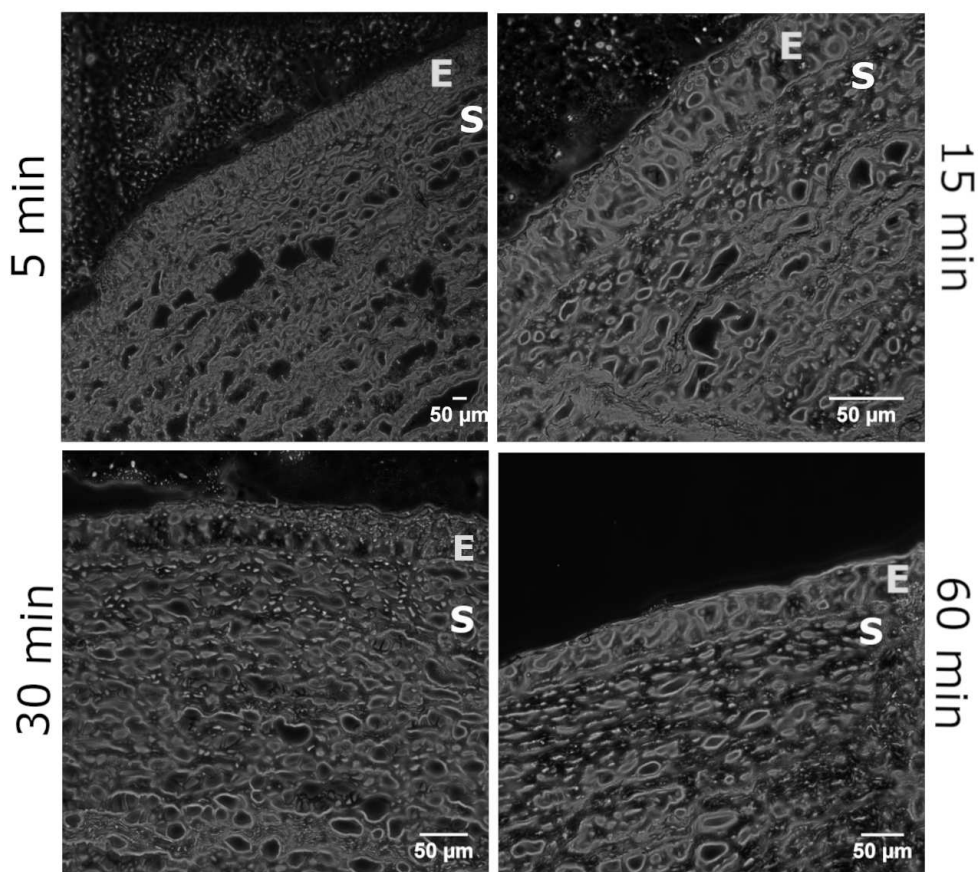


Figure 7.9 - Phase-contrast microphotographs of *ex vivo* after contact with fluorescein labelled ELR-NPs loaded with Nile red at different times (5, 15, 30, and 60 minutes); scale bar 50 μm . E-corneal epithelium; S-stroma.

lipophilic (Prausnitz *et al.*, 1998). Due to the contrasting nature of the underlying stromal layer, hydrophobic drugs accumulate in the epithelium and are only slowly released to the stroma (Agrahari *et al.*, 2016).

Notably, after 60 minutes of contact time with the ELR-NPs, some red fluorescence was observed in the corneal stroma. As mentioned, the corneal epithelium acts as a reservoir for hydrophobic drugs. This notion, combined with the general fact that NPs can enhance epithelial uptake, results in an increased concentration gradient between the epithelium and the stroma, therefore promoting the diffusion of the payload to stromal layers (Agarwal *et al.*, 2018). The result of the combination of these two factors may be noticed in our case as well.

According to our results, the ELR-NPs improved the *ex vivo* corneal penetration of Nile red, compared to the non-encapsulated Nile red, which confirms the utility of this platform for topical ophthalmic delivery of hydrophobic compounds.

7.4. Conclusions

In this work, we used a specifically designed biomaterial to encapsulate two natural compounds of interest using a one-step green SAS process. The operating conditions of the SAS process and the amphiphilic nature of the ELR polymer used showed to be adequate for the formulation of hydrophobic molecules such as QUE and RSV. Thanks to the properties of the biopolymer the microparticles obtained were capable of rearranging into nanoparticles once dispersed in solution at physiological temperature. All types of ELR-NPs prepared were biocompatible with human corneal epithelial cells. Also, the formulations exerted an excellent scavenging activity of intracellular ROS species. Additional experiments using fluorescent-labelled ELR-NPs assessed the cellular uptake and penetration of the formulations in *ex vivo* porcine corneas that followed a time-dependent process.

ELR-NPs represent a promising strategy for the ocular delivery of polyphenolic compounds such as QUE and RSV. Following steps may involve evaluation of the stability, mandatory to prepare topical ophthalmic formulations. As well, *in vivo* studies on DED-mice models.

References of Chapter 7

- Abengózar-Vela, A., Calonge, M., Stern, M.E., González-García, M.J. and Enríquez-De-Salamanca, A.,
Quercetin and resveratrol decrease the inflammatory and oxidative responses in human ocular surface epithelial cells,
Investig. Ophthalmol. Vis. Sci. **56**, 2709 (2719–2015)
<https://doi.org/10.1167/iovs.15-16595>
- Agarwal, P., Scherer, D., Günther, B., and Rupenthal, I.D.,
Semi fluorinated alkane based systems for enhanced corneal penetration of poorly soluble drugs,
Int. J. Pharm. **538**, 2018 (119–129)
<https://doi.org/10.1016/j.ijpharm.2018.01.019>
- Agrahari, V., Mandal, A., Agrahari, V., Trinh, H.M., Joseph, M., Ray, A., Hadji, H., Mitra, R., Pal, D., and Mitra, A.K.,
A comprehensive insight on ocular pharmacokinetics,
Drug Deliv. Transl. Res. **6**, 2016 (735–754)
<https://doi.org/10.1007/s13346-016-0339-2>
- Araki-Sasaki, K., Ohashi, Y., Sasabe, T., Hayashi, K., Watanabe, H., Tano, Y. and Handa, H.,
An SV40-immortalized human corneal epithelial cell line and its characterization,
Investig. Ophthalmol. Vis. Sci. **36**, 614–621 (1995).
- Bhatt, P., Fnu, G., Bhatia, D., Shahid, A., and Sutariya, V.,
Nanodelivery of resveratrol-Loaded PLGA nanoparticles for Age-Related Macular Degeneration,
AAPS PharmSciTech **21**, 2020 (1–9)
<https://doi.org/10.1208/s12249-020-01836-4>
- Campardelli, R., Baldino, L., and Reverchon, E.,
Supercritical fluids applications in nanomedicine,
J. Supercrit. Fluids **101**, 2015 (193–214)
<https://doi.org/10.1016/j.supflu.2015.01.030>
- Chithrani, B.D., and Chan, W.C.W.,
Elucidating the mechanism of cellular uptake and removal of protein-coated gold nanoparticles of different sizes and shapes,
Nano Lett. **7**, 1542–1550 (2007).
- Choi, J.S., Piao, Y.J., and Kang, K.W.,
Effects of quercetin on the bioavailability of doxorubicin in rats: Role of CYP3A4 and P-gp inhibition by quercetin,
Arch. Pharm. Res. **34**, 2011 (607–613)
<https://doi.org/10.1007/s12272-011-0411-x>
- Cocero, M.J., Martín, Á., Mattea, F., and Varona, S.,
Encapsulation and co-precipitation processes with supercritical fluids: Fundamentals and applications,
J. Supercrit. Fluids. **47**, 2009 (546–555)
<https://doi.org/10.1016/j.supflu.2008.08.015>

- De Marco, I.,
Supercritical fluids and nanoparticles in cancer therapy,
Micromachines **13**, 2022 (1309–1449)
<https://doi.org/10.3390/mi13091449>
- Desai, M.S., and Lee, S.W.,
Protein-based functional nanomaterial design for bioengineering applications,
Wiley Interdiscip. Rev. Nanomedicine Nanobiotechnology **7**, 2015 (69–97)
<https://doi.org/10.1002/wnan.1303>
- Desai, M.S., and Lee, S.W.,
P-Glycoprotein (MDR1) in human and rabbit cornea and corneal epithelial cell lines,
IOVS **44**, 2003 (2909–2918)
<https://doi.org/10.1002/wnan.1303>
- Foroozandeh, P., and Aziz, A.A.,
Insight into cellular uptake and intracellular trafficking of nanoparticles,
Nanoscale Res. Lett. **6**, 2018 (317–339)
<https://doi.org/10.1186/s11671-018-2728-6>
- Foroozandeh, P., and Aziz, A.A.,
Insight into cellular uptake and intracellular trafficking of nanoparticles,
Nanoscale Res. Lett. **6**, 2018 (317–339)
<https://doi.org/10.1186/s11671-018-2728-6>
- Francenia Santos-Sánchez, N., Salas-Coronado, R., Hernández-Carlos, B., and Villanueva-Cañongo, C.,
Shikimic Acid Pathway in Biosynthesis of Phenolic Compounds,
Plant Physiol. Asp. Phenolic Compd., 2019 (1–15)
<https://doi.org/10.5772/intechopen.83815>
- Franco, P. and De Marco, I.,
Supercritical antisolvent process for pharmaceutical applications: a review,
Processes **8**, 2020 (938–968)
<https://doi.org/10.3390/pr8080938>
- Girotti, A., Fernández-Colino, A., López, I.M., Rodríguez-Cabello, J.C., and Arias, F.J.,
Elastin-like recombinamers: Biosynthetic strategies and biotechnological applications,
Biotechnol. J. **6**, 2011 (1174–1186)
<https://doi.org/10.1002/biot.201100116>
- Girotti, A., Gonzalez-Valdivieso, J., Santos, M., Martin, L., and Arias, F.J.,
Functional characterization of an enzymatically degradable multi-bioactive elastin-like recombinamer,
Int. J. Biol. Macromol. **164**, 2020 (1640–1648)
<https://doi.org/10.1016/j.ijbiomac.2020.08.004>
- Gonzalez-Valdivieso, J., Garcia-Sampedro, A., Hall, A.R., Girotti, A., Arias, F.J., Pereira, S.P., Acedo, P.,
Smart nanoparticles as advanced Anti-Akt kinase delivery systems for pancreatic cancer therapy,
ACS Appl. Mater. Interfaces **13**, 2021 (55790–55805)
<https://doi.org/10.1021/acsami.1c14592>
- Gonzalez-Valdivieso, J., Girotti, A., Muñoz, R., Rodriguez-Cabello, J.C., Arias, F.J.,
Self-Assembling ELR-based nanoparticles as smart drug-delivery systems modulating cellular growth via Aktr,
Biomacromolecules **20**, 2019 (1996–2007)
<https://doi.org/10.1021/acs.biomac.9b00206>
- Goodman, C.M., Mccusker, C.D., Yilmaz, T., and Rotello, V.M.,
Toxicity of gold nanoparticles functionalized with cationic and anionic side chains,
Bioconjugate Chem. **15**, 897–900 (2004).
- Gülçin, İ.,
Antioxidant properties of resveratrol: A structure – activity insight,
IFSET **11**, 2010 (210–218)
<https://doi.org/10.1016/j.ifset.2009.07.002>

- Han, H., Nazanin, and H.,
The effect of nanoparticle size on in vivo pharmacokinetics and cellular interaction,
Nanomedicine **11**, 673–692 (2016).
- Hu, J., Xie, L., Zhao, W., Sun, M., Liu, X., and Gao, W.,
Design of tumor-homing and pH-responsive polypeptide-doxorubicin nanoparticles with enhanced anticancer efficacy and reduced side effects,
Chem. Commun. **51**, 2015 (11405–11408)
<https://doi.org/10.1039/c5cc04035c>
- Juliano, R.,
Drug delivery systems: A brief review,
Can J Physiol Pharmacol **56**, 683–690 (1978).
- Kalani, M., and Yunus, R.,
Application of supercritical antisolvent method in drug encapsulation: a review,
Int. J. Nanomedicine. **6**, 2011 (1429–1442)
<https://doi.org/10.2147/ijn.s19021>
- Kohane, D.S., and Langer, R.,
Biocompatibility and drug delivery systems,
Chem. Sci. **1**, 2010 (441–446)
<https://doi.org/10.1039/c0sc00203h>
- Lee, K.J., Oh, Y.C., Cho, W.K., and Ma, J.Y.,
Antioxidant and anti-inflammatory activity determination of one hundred kinds of pure HPLC compounds using offline and online screening HPLC assay,
eCAM **2015**, 2015 (1–13)
<https://doi.org/10.1155/2015/165457>
- Leutner, S., Eckert, A., and Müller, W.E.,
ROS generation, lipid peroxidation and antioxidant enzyme activities in the aging brain,
J. Neurol. **248**, 2001 (955–967)
<https://doi.org/10.1007/s007020170015>
- Lim, M., Goldstein, M.H., Tuli, S., and Schultz, G.S.,
Growth factor, cytokine and protease interactions during corneal wound healing,
Lab. Sci. **1**, 2003 (53–65)
[https://doi.org/10.1016/S1542-0124\(12\)70128-3](https://doi.org/10.1016/S1542-0124(12)70128-3)
- Liu, C., Huang, Y., Jhang, J., Liu, Y., and Wu, W.,
Quercetin delivery to porcine cornea and sclera by solid lipid nanoparticles and nanoemulsion,
J. Neurol. **5**, 2015 (100923–100933)
<https://doi.org/10.1039/C5RA17423F>
- Lovric, J., Yan, S.B., Fortin, G.R.A., and Winnik, F.M.,
Differences in subcellular distribution and toxicity of green and red emitting CdTe quantum dots,
J Mol Med **83**, 2015 (377–385)
<https://doi.org/10.1007/s00109-004-0629-x>
- Martín, A., and Cocero, M.J.,
Micronization processes with supercritical fluids: Fundamentals and mechanisms,
Adv. Drug Deliv. Rev. **60**, 2008 (339–350)
<https://doi.org/10.1016/j.addr.2007.06.019>
- Martín, Á., Scholle, K., Mattea, F., Meterc, D., and Cocero, M.J.,
Production of polymorphs of ibuprofen sodium by supercritical antisolvent (SAS) precipitation,
Cryst. Growth Des. **9**, 2009 (2504–2511)
<https://doi.org/10.1021/cg900003m>
- Mazumdar, S., Chitkara, D., and Mittal, A.,
Exploration and insights into the cellular internalization and intracellular fate of amphiphilic polymeric nanocarriers,
Acta Pharm. Sin. B **11**, 2020 (903–924).

- Mitchell, M.J., Billingsley, M.M., Haley, R.M., Wechsler, M.E., Peppas, N.A., and Langer, R.,
Engineering precision nanoparticles,
Nat. Rev. Drug Discov. **20**, 2021 (101–124)
<https://doi.org/10.1038/s41573-020-0090-8>
- Navarro, M., and Planell, J.A.,
Nanotechnology in regenerative medicine,
Springer Life Sciences, (2012).
- Prasnitz, M.,
Permeability of cornea, sclera, and conjunctiva: A literature analysis for drug delivery to the eye,
J. Pharm. Sci. **87**, 1479–1488 (1998).
- Price, R., Poursaid, A., and Ghandehari, H.,
Controlled release from recombinant polymers,
J. Control. Release. **190**, 2014 (304–313)
<https://doi.org/10.1016/j.jconrel.2014.06.016>
- Quintanilla-Sierra, L., García-Arévalo, C., and Rodríguez-Cabello, J.C.,
Self-assembly in elastin-like recombinamers: a mechanism to mimic natural complexity,
Mater. Today Bio **2**, 2014 (1–17)
<https://doi.org/10.1016/j.mtbio.2019.100007>
- Ramsay, E., del Amo, E.M., Toropainen, E., Tengvall-Unadike, U., Ranta, V.P., Urtili, A., and Ruponen, M.,
Corneal and conjunctival drug permeability: Systematic comparison and pharmacokinetic impact in the eye,
Mater. Today Bio **119**, 2018 (83–89)
<https://doi.org/10.1016/j.ejps.2018.03.034>
- Reverchon, E.,
Supercritical-assisted atomization to produce micro- and/or nanoparticles of controlled size and distribution,
Ind. Eng. Chem. Res. **41**, 2002 (2405–2411)
<https://doi.org/10.1021/ie010943k>
- Rodríguez-Cabello, J.C., González de Torre, I., Ibañez-Fonseca, A., and Alonso, M.,
Bioactive scaffolds based on elastin-like materials for wound healing,
Adv. Drug Deliv. Rev. **129**, 2018 (118–133)
<https://doi.org/10.1016/j.addr.2018.03.003>
- Ryu, J.S., and Raucher, D.,
Anti-tumor efficacy of a therapeutic peptide based on thermo-responsive elastin-like polypeptide in combination with gemcitabine,
Cancer Lett. **348**, 2014 (177–184)
<https://doi.org/10.1016/j.canlet.2014.03.021>
- Sabourian, P., Yazdani, G., Ashraf, S.S., Frounchi, M., Mashayekhan, S., Kiani, S., and Kakkar, A.,
Effect of physico-chemical properties of nanoparticles on their intracellular uptake,
Int. J. Mol. Sci. **21**, 1–20 (2020).
- Salatin, S., and Khosroushahi, A.Y.,
Overviews on the cellular uptake mechanism of polysaccharide colloidal nanoparticles Mechanisms of nanoparticle endocytosis,
J Cell Mol Med **21**, 2017 (1668–1868)
<https://doi.org/10.1111/jcmm.13110>
- Santos, D.T., and Meireles, M.A.A.,
Micronization and encapsulation of functional pigments using supercritical carbon dioxide,
J. Food Process Eng. **36**, 2013 (36–49)
<https://doi.org/10.1111/j.1745-4530.2011.00651.x>
- Snipstad, S., Westrom, S., Morch, Y., Afadzi, M., Aslun, A.K., and Lange Davis, C.,
Contact-mediated intracellular delivery of hydrophobic drugs from polymeric nanoparticles,
J. Ocul. Pharmacol. Ther. **29**, 2013 (681–867).

- Shi, P., Gustafson, J.A., and Andrew MacKay, J.,
Genetically engineered nanocarriers for drug delivery,
Int. J. Nanomedicine **9**, 2014 (1617–1626)
<https://doi.org/10.2147/IJN.S53886>
- Stoddard, A.R., Koetje, L.R., Mitchell, A.K., Schotanus, M.P. and Ubels, J.L.,
Bioavailability of antioxidants applied to stratified human corneal epithelial cells,
JOPT **29**, 2013 (681–687)
[https://DOI: 10.1089/jop.2013.0014](https://DOI:10.1089/jop.2013.0014)
- Treuel, L., Jiang, X., and Nienhaus, G.U.,
New views on cellular uptake and trafficking of manufactured nanoparticles,
J. R. Soc. Interface **10**, 2013 (1–14).
- Treuel, L., Jiang, X., and Nienhaus, G.U.,
New views on cellular uptake and trafficking of manufactured nanoparticles,
J. R. Soc. Interface **10**, 2013 (1–14).
- Tu, B., Liu, Z.J., Chen, Z.F., Ouyang, Y., and Hu, Y.J.,
Understanding the structure-activity relationship between quercetin and naringenin: In vitro,
RSC Adv. **5**, 2015 (106171–106181)
<https://doi.org/10.1039/c5ra22551e>
- Vallejo, R., Gonzalez-Valdivieso, J., Santos, M., Rodriguez-Rojo, S., and Arias, F.J.,
Production of elastin-like recombinamer-based nanoparticles for docetaxel encapsulation and use as smart drug-delivery systems using a supercritical anti-solvent process,
J.Ind.Eng.Chem. **93**, 2015 (361–374)
<https://doi.org/10.1016/j.jiec.2020.10.013>
- Wai, L.C.H., Liu, Y., Ruifang, H., Bai, Q., and Choi, C.H.Y.,
Nano-Cell interactions of non-cationic bionanomaterials,
Acc. Chem. Res. **6**, 2019 (1519–1530).
- Wang, W., Despanie, J., Shi, P., Edman, M.C., Lin, Y.A., Cui, H., Heur, M., Fini, M.E., Hamm-Alvarez, S.F., and Mackay, J.A.,
Lacritin-mediated regeneration of the corneal epithelia by protein polymer nanoparticles,
J. Mater. Chem. B **2**, 2014 (8131–8141)
<https://doi.org/10.1039/c4tb00979g>
- Zhang, L., Wang, Y., Yang, D., Huang, W., Hao, P., Feng, S., Appelhans, D., Zhang, T., and Zan, X.,
Shape effect of nanoparticles on tumour penetration in monolayers versus spheroids,
Mol. Pharm. **2**, 2014 (1–27)
<https://doi.org/10.1021/acs.molpharmaceut.9b00107>

8

Contact Lenses Embedded with Micelles: An Innovative Approach to Ophthalmic Delivery

Contact lenses (CLs) are medical devices placed on the ocular surface (over the cornea and sclera) with the final purpose of correcting ametropias. The first prototype of CLs was developed in the 16th century by Leonardo da Vinci (Pillay *et al.*, 2020). During the 20th century, the field of CLs significantly expanded, and nowadays more than 140 million people wear them every day (Nichols *et al.*, 2013). Depending on the material used for their production, CLs can be grouped into soft and rigid. Initially, rigid CLs were made of polymethylmethacrylate (PMMA), a stiff polymer that is not permeable to O₂. The introduction of low-modulus components (cellulose acetate butyrate, fluoro-siloxane-methacrylates, and others) allowed the flexibilization of the CLs and a significant improvement of their O₂ permeation, developing the rigid gas-permeable (RGP) lenses available today in the market (Ruben *et al.*, 1994). In the 1970s, the evolution of materials and the development of hydrogel polymers capable of absorbing large amounts of water favoured the introduction of soft CLs. Nowadays, soft CLs are mostly made of HEMA- and silicone-based hydrogels (McDermott *et al.*, 1989; Nichols *et al.*, 2018). The choice of an appropriate material and manufacturing process for the CLs production is of critical importance since parameters such as transparency, oxygen permeability, or water content might be greatly affected by them (Musgrave *et al.*, 2019; Rykowska *et al.*, 2021).

The potential of delivering therapeutics to the eye with the aid of CLs was first proposed by Sedláček, in 1965 (Sedláček *et al.*, 1965). Since the 2000s, there have been major efforts to develop appropriate materials and preparation processes that will allow fine control of the delivery kinetics of the therapeutic agent while preserving the biocompatibility and optical properties of the CLs (Alvarez-Lorenzo *et al.*, 2019; González-Chomón *et al.*, 2013). Therapeutic CLs can overcome the key drawbacks of topical ophthalmic formulations. The prolonged contact time of the CLs with the ocular structures results in enhanced bioavailability of the therapeutic agent

up to 50%, while the modulation of release rates significantly reduces the dosing frequencies (Choi *et al.*, 2018; Grassiri *et al.*, 2021).

By far, several drug loading techniques of the CLs have been proposed. The simplest one involves the soaking of CLs in a drug solution with the subsequent entrapment of drug molecules into the hydrogel matrix (Fan *et al.*, 2020; Maulvi *et al.*, 2016). Although this is the most cost-effective method, limitations such as poor drug loading and initial burst release, increased the need for alternative approaches (Desai *et al.*, 2020; Maulvi *et al.*, 2018). An efficacious strategy to control the release kinetics is the incorporation of colloidal nanostructures, like liposomes, nanoparticles, or micelles. This of course involves the previous drug loading into the nanostructures (Maulvi *et al.*, 2021). The latter exploits the entrapment of the nanostructure in the meshes of the CLs, where it can act as a reservoir and therefore assure a sustained release of the therapeutic agent (González-Chomón *et al.*, 2013).

Once the (medicated) CLs are applied to the eye, drug molecules are delivered to tear film between the CLs and the cornea, where they can be retained for a longer period due to the lower tear-turnover. Thanks to the sink effect, a constant release of the drug from the CLs is obtained. This effect is a direct consequence of the active corneal drug penetration, which always maintains a lower drug concentration in the post-lens tear film than the one in the CLs. Similarly, intraocular accumulation of the active substance is possible, enabling a better pharmacological response due to the achievement of therapeutic concentrations (Bengani *et al.*, 2013; Carvalho *et al.*, 2015; Li *et al.*, 2006).

Polyoxyethylene (PEO)-polyoxypropylene (PPO)-polyoxyethylene (PEO) is a non-ionic triblock copolymer commercialised under the names Pluronic[®] / Poloxamer[®] (Kadam *et al.*, 2009) widely used as a pharmaceutical excipient. Owing to its amphiphilic nature, Pluronic[®] is capable of spontaneous self-assembling in solution into core-shell structures called micelles (Maulvi *et al.*, 2020, 2016). Pluronic[®] micelles are extensively employed as nanocarriers because of their ability to improve the solubility of hydrophobic compounds as well as modulate the drug release rate in body fluids (Stammet *et al.*, 2010). An additional advantage for their use is represented by their high drug loading and low immunogenicity, which marks them as safe (Patel *et al.*, 2022).

Accordingly, the objective of this chapter was to improve the solubility of QUE and RSV through encapsulation into Pluronic[®] F127 micelles and posterior loading of the nanocarrier into HEMA or HEMA/MAA- based hydrogels to obtain novel potential therapeutic CLs for DED treatment (**figure 8.1**). The micelles were characterised in terms of size, ζ -potential, and entrapment efficiency of QUE and RSV. Critical properties of the hydrogels such as solvent uptake, transparency, and the capability of loading and releasing pure drug molecules and micelles, were assessed. The work done in this chapter was performed as a part of a one-month secondment in the *I+D Farma* group, Department of Pharmacology, Pharmacy and Pharmaceutical Technology at the University of Santiago de Compostela (Spain).

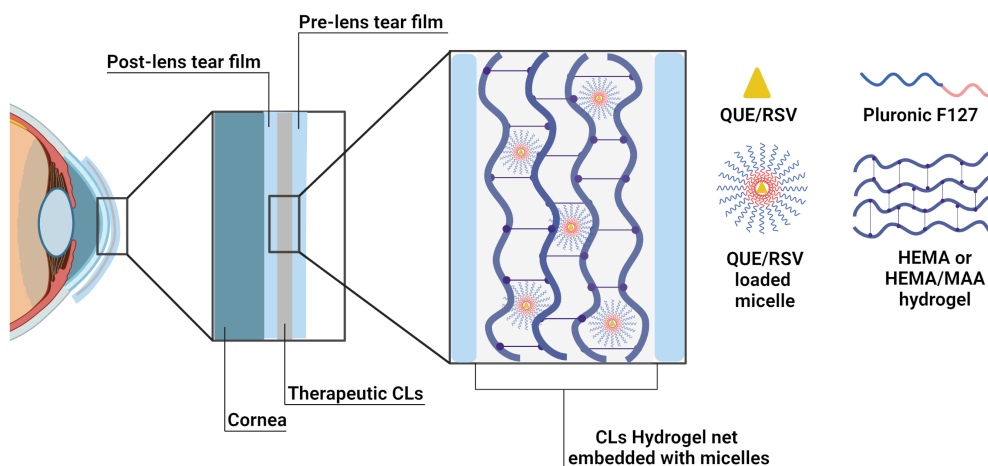


Figure 8.1 - Schematic representation of the system proposed in this chapter, based on the combination of CLs and micelles. Created with BioRender®.

8.1. Materials and Methods

8.1.1. Materials

2-Hydroxyethyl methacrylate (HEMA) was from Merck KGaA (Merck KGaA, Darmstadt, Germany); resveratrol, quercetin, ethylene glycol dimethacrylate (EGDMA), dichlorodimethylsilane, 2,2'-azobis(2-methylpropionitrile) (AIBN), methacrylic acid (MAA) were from Sigma-Aldrich (Sigma-Aldrich, St. Louis, MO, USA). Sodium chloride (NaCl) was acquired from Scharlab S.L. (Scharlab S.L., Barcelona, Spain). Absolute ethanol was bought from VWR Chemicals (VWR Chemicals, Fontenay, Sous-Bois, France). Ultrapure water (resistivity > 18.2 MΩcm) was obtained by reverse osmosis (MilliQ®, Millipore Ibérica, Madrid, Spain).

8.1.2. Methods

Hydrogel Preparation

For the present study, HEMA-based or HEMA copolymerized with MAA hydrogels were prepared by thermal polymerization (**table 8.1**). Monomer solutions, together with the crosslinker (EGDMA) and the initiator (AIBN) were mixed at room temperature (150 rpm) before the filling of the moulds (**figure 8.2**). Then the mixture was injected into the moulds made from presilanized glass plates with dimensions of 10 cm x 14 cm (**figure 8.3**). The width of hydrogels was controlled with the use of teflon marks, which were placed between the glass plates, those were respectively 0.2 mm.

The polymerization process was carried out for the first 12 hours at 50°C and for another 24

Table 8.1: Hydrogel composition

Hydrogel type	HEMA (mL)	MAA (μL)	AIBN (mg)	EGDMA (μL)
HEMA	3	-	14.48	12.10
HEMA/MAA	3	25.83	14.78	12.10

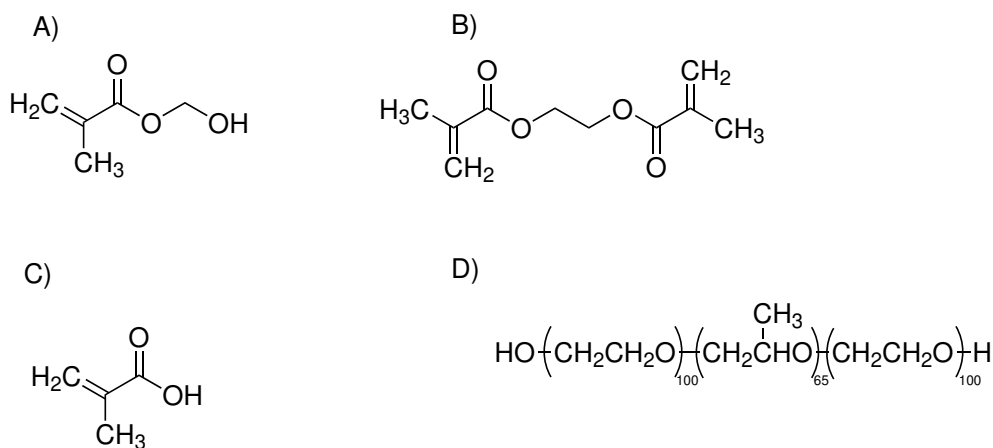


Figure 8.2 - Chemical structures of (A) 2-hydroxyethyl methacrylate (HEMA); (B) ethylene glycol dimethacrylate (EGDMA); (C) methacrylic acid (MAA); (D) Pluronic® F127.

hours at 70°C. After the polymerization, the hydrogels were carefully demoulded and washed in boiling water for 15 minutes. Considering the needs of each planned test, the hydrogels were cut into discs (10 mm and 14 mm) of different diameters and placed into 500 mL of milliQ water to complete the washing procedure (figure 8.4). The unreacted monomers were removed in a purifying process alternatively placing the hydrogels in milliQ water and NaCl solution (0.9%) at least four times a day. The complete removal of free monomers was monitored by UV-Vis spectroscopy.

Quantification of QUE and RSV by UV-Vis Spectroscopy

Quantification of QUE and RSV was done using calibration lines prepared employing an UV-Vis spectrophotometer (Agilent 8534, Waldbronn, Germany). Standard solutions of QUE or RSV (0.5-12 μM) were prepared in 50:50 EtOH:H₂O (v/v) and placed into a quartz cuvette. Absorbance was measured at 370 nm and 306 nm for QUE and RSV solutions, respectively. For both calibration lines the correlation coefficient (R^2) was 0.9997.

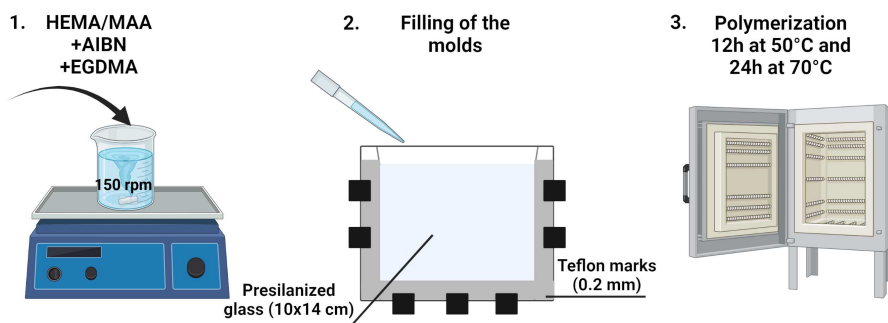


Figure 8.3 - Illustrative representation of the hydrogel preparation. Created with BioRender®.



Figure 8.4 - Hydrogel disc during preparation in the laboratory.

Micelles Preparation

Micelles were prepared by solvent casting using a 5% (w/v) solution of Pluronic® F127. Stock solutions of both drugs were prepared in ethanol with a final concentration of 1 mg/mL. QUE-containing micelles were prepared by mixing 8 mL of an ethanolic stock solution of QUE, 4 mL of ethanol and 4 gr of Pluronic® F127. The mixture was left to stir for one hour at 300 rpm at room temperature. Following, 80 mL of milliQ water were added and the mixture was left to stir for 12 hours for the evaporation of the organic solvent.

For RSV-containing micelles a slightly modified method was used, a 5% (w/v) solution of Pluronic® F127 was prepared by dissolving 4 gr of the polymer into 80 mL of milliQ water. Once the polymer was completely dissolved, 8 mL of RSV stock solution were added. As in the previous case, the solution was left to stir for 12 hours. This moderately different method of preparation of RSV-loaded micelles has been adopted since preparing them, as in the case of QUE, resulted in RSV oxidation during the first passage, as observed by the change in the solution colour.

The non-encapsulated drug was removed through centrifugation at 4000 rpm, 5°C for 30 minutes. Micelles without drug molecules (blank) were prepared using the same methods. The encapsulation efficiency of the micelles was calculated using the following equation (Patra *et al.*, 2018):

$$EE (\%) = \frac{W_t}{W_i} \times 100 \quad (8.1)$$

Where W_t represents the total amount of the drug that was incorporated into the carrier and W_i is the initial amount of the drug added during the preparation.

Micelles Characterization by Dynamic Light Scattering (DLS)

Dynamic Light Scattering (DLS) was used to measure the size, ζ -potential, and polydispersity of the micelles. Measurements were carried out at a 173° scattering angle on a Zetasizer Pro (Malvern Panalytical, Malvern, Worcestershire, United Kingdom) in triplicate at room temperature (RT).

Solvent Uptake

Before performing the planned tests and to assure the complete dryness of the hydrogel discs (10 mm in diameter), they were placed in a stove at 37 °C overnight. Then, dry discs were weighted, placed into vials, and 4 mL of aqueous micellar dispersion (micelles loaded with QUE or RSV), or of free drug solutions (0.100 mg/mL) in EtOH:water (50:50 v/v) were added. The vials were then left at room temperature and protected from light. At scheduled time points (0.5, 1, 2, 4, 6, and 24 hours) the discs were delicately dried with absorbent paper and weighted. The water uptake of the hydrogels was calculated through the increase in weight using the following equation:

$$\text{Solvent uptake (\%)} = \frac{W_t - W_0}{W_0} \times 100 \quad (8.2)$$

In the equation, W_0 and W_t represent the weight of dry and swollen hydrogel, respectively, at a certain time (t) point.

Light Transmittance of Hydrogels

The light transmittance (%) of swollen hydrogels loaded with micelles or free drug solutions was measured using a UV-Vis spectrophotometer. The transmittance was measured from 200 to 700 nm with 1 nm intervals.

Loading and Release of Pluronic[®] F127 Micelles and Free Drugs from Hydrogels

HEMA-hydrogel-dried discs (10 mm diameter, average weight 17.67 mg) and HEMA/MAA-hydrogel-dried discs (10 mm diameter, average weight 15.73 mg), all dried overnight at 37°C, were placed in separated vials and added of 7 mL of one of the following solutions: i) QUE/Pluronic[®] F127 micellar solution (0.092 mg/mL of QUE loaded), or ii) RSV/Pluronic[®] F127 micellar solution (0.096 mg/mL of RSV loaded) or iii) 0.100 mg/mL QUE or RSV solutions prepared in EtOH:H₂O (50:50 v/v).

The vials were protected from light and maintained under controlled stirring and temperature (180 rpm and 36°C). Aliquots of 250 µL of the loading solutions were withdrawn at predefined time points (2, 4, 6, 8, and 24 hours), and after 1:20 dilution in EtOH:H₂O (50:50 v/v) the absorbance at 306 and 370 nm was measured using a UV-Vis spectrophotometer (Agilent 8534, Waldbronn, Germany). The amount of QUE or RSV that was absorbed by the hydrogels in both micelles and in free form was calculated using a validated calibration curve.

Release experiments were performed placing the discs loaded with micelles or free drugs into vials containing 6 mL of NaCl (0.9%). The vials were then placed into an incubator, protected from light, and left in agitation (180 rpm) at 36°C. The release of QUE and RSV was monitored each hour by measuring the absorbance of the releasing medium at 306 and 370 nm using a UV-Vis spectrophotometer. The aliquots that were used for measuring the release were immediately returned to the corresponding vial after the measurement. Also, the same method of release was repeated with other release media, made of NaCl (0.9%) with the addition of Lysozyme (2.68 mg/mL) or BSA (2.68 mg/mL), respectively.

8.2. Results and Discussion

8.2.1. Hydrogel Synthesis

Table 8.2 summarises hydrogel types and their loading, as well as the coding used for each formulation prepared in this chapter. To try to resemble the thickness of CLs (0.1 mm), all hydrogel discs were prepared with the minimum possible thickness using 0.2 mm moulds.

For the current study, HEMA-based hydrogels were chosen as HEMA is one of the most common structural monomers used for the preparation of soft CLs (Nicolson *et al.*, 2001; Refojo *et al.*, 1973). Since pHEMA based soft CLs are distinguished by moderate water content and oxygen permeability (Ruben *et al.*, 1994) these characteristics may be refined by copolymerizing HEMA with different monomers such as methacrylic acid (MAA) (Chhabra *et al.*, 2009). Additionally, the introduction of a functional monomer may improve drug loading when preparing medicated CLs (Kim *et al.*, 1992). At physiological pH, MAA is ionised, bearing a negative charge and therefore capable of establishing electrostatic interactions with carriers/drugs (Alvarez-Lorenzo *et al.*, 2002). Several soft CLs that are commercially available are made from HEMA or a combination of HEMA/MAA hydrogels. These include, for example, the ACUVUE

Moist[®] (Johnson & Johnson, New Brunswick, NJ, USA) and the Biomedics 1-day[®] (Cooper Vision, San Ramon, CA, USA) (Fan *et al.*, 2020).

Table 8.2: Summary of formulation coding and loading.

Form. Code	Hydrogel Type	Loading	Form. Code	Hydrogel Type	Loading
HMR	HEMA	RSV/Pluronic [®] F127 micelles	MMR	HEMA/MAA	RSV/Pluronic [®] F127 micelles
HR	HEMA	Free RSV	MR	HEMA/MAA	Free RSV
HMQ	HEMA	QUE/Pluronic [®] F127 micelles	MMQ	HEMA/MAA	QUE/Pluronic [®] F127 micelles
HQ	HEMA	Free QUE	MQ	HEMA/MAA	Free QUE

8.2.2. Micelles Characterization

Owing to their capacity to form core-shell structures that can encapsulate drug molecules, micelles have been broadly used as an approach to improve the physico-chemical characteristics of hydrophobic drugs (Kelishady *et al.*, 2015). The concentration of Pluronic[®] F127 used for the preparations was 5% (w/v), which was above the CMC value ($0.26 \pm 0.03\%$ w/v measured in H₂O) and therefore enough to assure the formation of the micelles. Conversely, this concentration was low enough to avoid temperature-induced gelification of the polymer (Gilbert *et al.*, 1987; Sharma *et al.*, 2005). Blank and drug-loaded micelles (either QUE or RSV) were characterised in terms of size, polydispersion index (PDI) and ζ -potential, and the values obtained are summarised in **table 8.3**.

Size analysis revealed that blank micelles have a mean diameter of 5.52 ± 0.40 nm, while the ones loaded with QUE or RSV, had 4.94 ± 0.05 nm or 5.17 ± 0.09 nm, respectively. These were close to the values found in the literature (Sezgin *et al.*, 2006). All samples showed a unimodal size distribution with low values of PDI. A slightly lower micellar size after drug loading, may indicate that the incorporation of QUE or RSV into the micellar core intensifies the hydrophobic interactions, making them more closely packed. The surface charge of the micelles was close to zero, compatible with the non-ionic nature of the polymer used for their preparation (Gao *et al.*, 2011). Excellent encapsulation efficacy was observed for both polyphenols: $92.38\% \pm 2.85$ of QUE and $96.14\% \pm 1.49$ of RSV were loaded. Various authors have employed Pluronic[®] F127 for micelle preparation, obtaining an outstanding loading of the bioactive molecule. For example, Sahu *et al.* found an encapsulation efficiency of 95.57% of curcumin in a Pluronic[®]

F127 micelles prepared in a 1:50 drug/polymer molar ratio. Similarly, Zheng *et al.* managed to load 99.2% of honokiol, a phytochemical with several pharmacologically recognised activities, using the same polymer for micelles preparation (Sahu *et al.*, 2011; Zheng *et al.*, 2010).

Table 8.3: Summary of the physico-chemical characterization properties of blank and drug-loaded micelles (mean \pm SEM; n=3).

Micelles Loading ^a	Size (nm)	ζ -potential (mV)	EE (%)	PdI	pH
Blank	5.52 \pm 0.40	-4.95 \pm 2.78	N/A	0.38 \pm 0.04	7 \pm 0.02
QUE	4.94 \pm 0.05	-4.85 \pm 2.24	92.38 \pm 2.85	0.33 \pm 0.03	6.98 \pm 0.01
RSV	5.17 \pm 0.09	-3.88 \pm 0.90	96.14 \pm 1.49	0.36 \pm 0.04	6.96 \pm 0.02

N/A- not applicable; EE-encapsulation efficiency; PdI- polydispersity index;

^a All micellar formulations were prepared with Pluronic[®] F127 (5% w/v)

Regarding the pH values, all dispersion exhibited very similar values, close to the physiological tear value (6.8-8.2), guaranteeing good tolerance once in contact with the ocular structures (Willcox *et al.*, 2017).

8.2.3. Hydrogel Characterization

All hydrogels used in this work were characterised in terms of solvent uptake and light transmittance. A greater capacity of CLs to absorb solvents (e.g., water) implies higher oxygen and ion permeability to the ocular structures. Consequently, this feature of CLs conditions the comfort of the CLs for the wearer. Therefore, solvent uptake by the hydrogels was evaluated in water for micelles formulations and in 50:50 EtOH:H₂O (v/v) for free drug solutions and the results are summarised in **table 8.4**. As observed in **figure 8.5**, both types of hydrogels soaked up the loading solutions quickly, reaching the equilibrium after one hour. A solvent uptake of up to 80% was registered with both types of hydrogels studied (HEMA or HEMA/MAA) when immersed in aqueous micellar dispersions. On the contrary, a higher percentage of solvent absorption was observed in hydrogels that were submerged in free drug solutions (50:50 EtOH:H₂O (v/v)). The presence of an organic solvent in the loading solution, in our case EtOH, improves the solubility of the hydrophobic groups (α -methyl groups of the repeating units in the backbone of the polymeric network) in pHEMA by disrupting non-covalent interactions among them, inducing a greater swelling of the hydrogel in respect to its swelling capacity in water (Refojo *et al.*, 1967).

Some characteristics of the hydrogel, like drug and solvent absorption, can be improved through copolymerization of HEMA with various functional monomers (Weeks *et al.*, 2012). The introduction of an ionizable monomer like MAA should allow the hydrogel matrix to absorb more water. However, as observed in our results, this effect was of very limited extent.

Table 8.4: Solvent uptake at 24 h of HEMA and HEMA/MAA hydrogels loaded with micelle formulations or with free drugs (mean \pm SEM; n=2).

Formulation Code ^a	Solvent Uptake (%)	Formulation Code ^a	Solvent Uptake (%)
HMR	62.55 \pm 0.82	MMR	70.22 \pm 3.12
HR	160.47 \pm 8.06	MR	236.69 \pm 7.94
HMQ	75.74 \pm 2.01	MMQ	87.91 \pm 8.42
HQ	195.094 \pm 2.37	MQ	188.88 \pm 7.69

^aFormulation codes are listed in Table 8.2 in page 122.

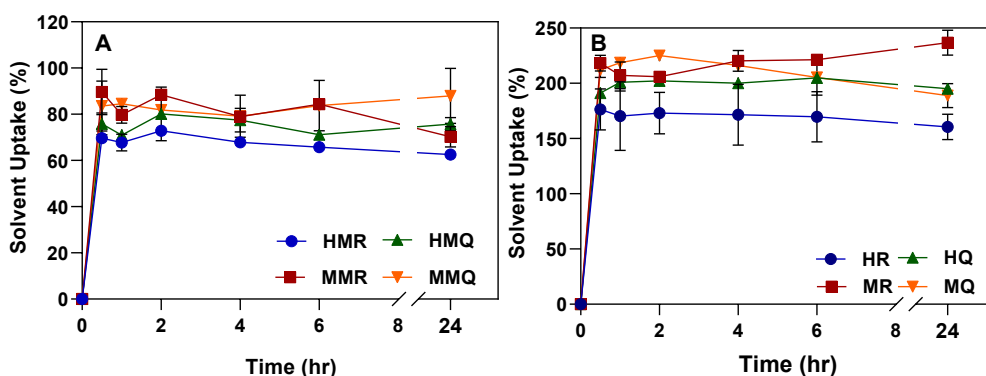


Figure 8.5 - Solvent uptake (%) of all hydrogels. A) Hydrogels loaded with QUE/Pluronic[®] F127 or RSV Pluronic[®] F127 micelles; A) free QUE or RSV dissolved in 50:50 EtOH:H₂O v/v(mean \pm SEM; n=2). Hydrogel coding is listed in 8.2.

CLs must have a light transmission rating more than 90% in the visible spectrum (400-700 nm) in order to meet safety and performance criteria specified by ISO[®] standards. **Figure 8.6** shows that all of the studied hydrogels in combination with micelles or free drugs fulfilled the above-mentioned criteria and that the inclusion of colloidal systems like micelles in the hydrogel network did not significantly alter this property (Nguyen *et al.*, 2021). Hydrogels loaded with RSV/Pluronic[®] F127 micelles or with free RSV solution appear to have the ability to block up to 80% of ultraviolet radiation (UVR) in certain regions of the UV-A/UV-B spectrum, from 290 to 320 nm. CLs capable of UVR absorption could help reduce the negative effects caused by the continuous exposure of the eye to this type of radiation. This ability of RSV to be used as a UVR blocker was confirmed in a study conducted by Vivero-Lopez *et al.* where the stilbene compound loaded in a HEMA/MPC hydrogel efficiently screened radiation in the range 200-360 nm (Vivero-Lopez *et al.*, 2022).

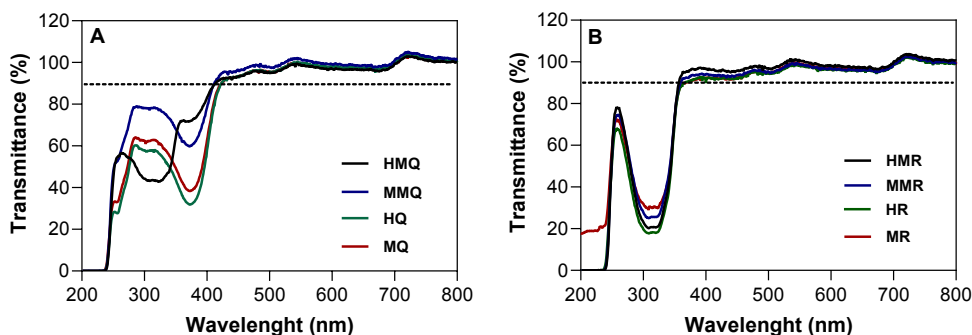


Figure 8.6 - Transmittance spectrum of hydrogel discs loaded with: **A)** QUE and QUE/Pluronic[®] F127 micelles, and **B)** RSV and RSV/Pluronic[®] F127 micelles. The requested 90% of transmittance is indicated with a dashed line. Hydrogel coding is listed in 8.2.

8.2.4. Loading and Release of Pluronic[®] F127 Micelles and Free Drugs from Hydrogels

To estimate the capacity of the hydrogels to load QUE or RSV or drug-loaded colloidal systems, dried hydrogel discs were placed into free drug solutions or micellar dispersion that had been previously prepared. The classical *soaking method* for hydrogel loading was chosen since loading during the polymerization process was impracticable due to the temperature-induced degradation of both QUE and RSV (Wang *et al.*, 2016; Zupančič *et al.*, 2015).

For the free drug solutions, no loading of the hydrogels was observed. This is not completely unexpected considering that QUE and RSV are hydrophobic molecules and are thus preferably partitioned in a solution media that contains more of a less polar organic solvent (50:50 EtOH:H₂O (v/v)) than water. The behaviour of pure compounds straightens out our initial premise that a colloidal carrier is needed for the improvement of i) the aqueous solubility of QUE and RSV, and ii) the loading of QUE and RSV into the hydrogel matrix.

All micelle-based formulations were loaded into HEMA/MAA or HEMA based hydrogels following an analogous pattern (**figure 8.7**). Rapid hydrogel soaking was observed, reaching its peak in the uptake of drug-loaded micelles after 6 hours. After 24 hours, no remarkable difference in loading of RSV/Pluronic[®] F127 micelles was observed between HEMA and HEMA/MAA hydrogels. HEMA-based hydrogels were able to load 1.77 mg of RSV per gram of hydrogel, while HEMA/MAA loaded 1.64 mg/g. In contrast, the loading of QUE-micelles was different depending on the hydrogel used. HEMA-based hydrogels were able to incorporate 3.62 mg/g of QUE, while the one containing MAA as a functional monomer incorporated 4.26 mg/g. The co-polymerization of HEMA with MAA did not enhance the loading capacity of the hydrogels.

Release studies were carried out in different releasing media (0.9% NaCl, 0.9% NaCl + Lysozyme, 0.9% NaCl + BSA) under slight stirring at 180 rpm. However, it was not possible to record any release profiles. To explain this, two hypotheses were suggested. The first is that

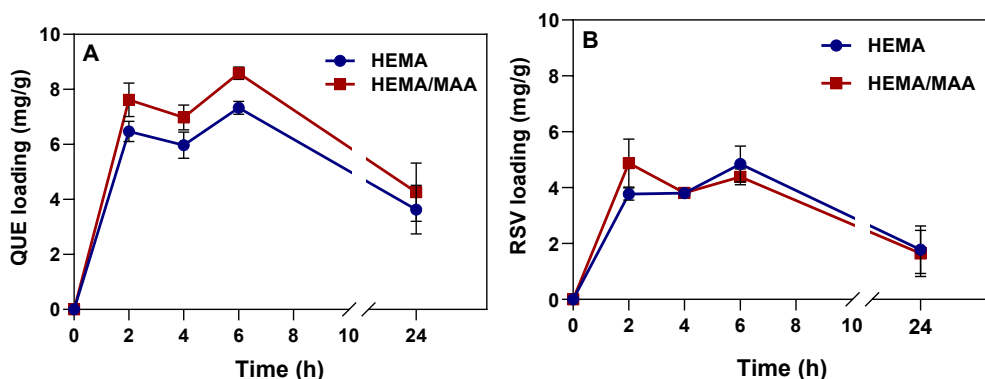


Figure 8.7 - Loading profiles of all hydrogels. Hydrogels loaded with **A)** loaded with QUE/Pluronic[®] F127 micelles **B)** RSV/ Pluronic[®] F127 micelles (mean \pm SEM; n=4. Hydrogel coding is listed in table 8.2.

an overlapping of the releasing and loading process occurred, with extremely rapid releasing kinetics under which all the nanocarriers were liberated even before the possibility of starting the release study. This explanation is supported by the fact that during the loading, the amount of the micelles formulation entrapped in the hydrogel reached a peak, and after that, it started decreasing. The second hypothesis is that the loading method employed was not appropriate for the type of carrier and hydrogel used. Despite the addition of two of the most prevalent proteins in tear fluid, lysozyme and BSA, to the releasing media, no progress was made in the release studies.

8.3. Conclusions

HEMA-based soft CLs are generally advised for daily use. Hence, developing therapeutic equivalents would considerably improve dosing regimens and patient compliance, offering in this way a valid replacement for eyedrops. The combination of hydrogel-based CLs and colloidal systems has been proposed by the scientific community as a prospective solution for the formulation of hydrophobic drugs and their delivery to the structures of the anterior part of the eye. Pluronic[®] F127 micelles show to be able to improve the aqueous solubility of both compounds in exam, additionally exhibiting excellent encapsulation efficiency.

The major concerns regarding the proposed formulations relate to the drug/micelles loading process. Due to an anomalous loading process, the observed response for the light transmission studies for QUE/RSV loading solutions is actually a result of the interaction of the solvent (50:50 EtOH:H₂O (v/v)) with the hydrogel discs. The same problem is related to the inexistent release profiles of the colloidal system. It is obvious that the loading procedure must be revised.

A feasible approach could be the preparation of charge-bearing micelles capable of an attractive electrostatic interaction with the charges present on the hydrogel due to the introduction of a functional monomer. A second option could be the shifting of the loading process from

the soaking method currently employed to one of molecular imprinting. This would imply a slight adjustment in the materials employed. However, it has to be underlined that the available time frame in which these experiments took place hugely influenced their output and the application of any possible improvement strategy.

References of Chapter 8

- Abengózar-Vela, A., Calonge, M., Stern, M.E., González-García, M.J. and Enríquez-De-Salamanca, A.,
Quercetin and resveratrol decrease the inflammatory and oxidative responses in human ocular surface epithelial cells,
Investig. Ophthalmol. Vis. Sci. **56**, 2709 (2719–2015)
<https://doi.org/10.1167/iovs.15-16595>
- Abengózar-Vela, A., Schaumburg, C.S., Stern, M.E., Calonge, M., Enríquez-De-Salamanca, A and González-García, M.J.,
Topical quercetin and resveratrol protect the ocular surface in experimental dry eye disease,
Investig. Ophthalmol. Vis. Sci. **27**, 2019 (1023–1032)
<https://doi.org/10.1080/09273948.2018.1497664>
- Alvarez-Lorenzo, C., Anguiano-Igea, S., Varela-García, A., Vivero-Lopez, M., and Concheiro, A.,
Bioinspired hydrogels for drug-eluting contact lenses,
Acta Biomater. **84**, 49–62 (2019)
<https://doi.org/10.1002/jps.10209>
- Alvarez-Lorenzo, C., Hiratani, H., Gómez-Amoza, J.L., Martínez-Pacheco, R., Souto, C., and Concheiro, A.,
Soft contact lenses capable of sustained delivery of timolol,
J.Pharm.Sci. **91**, 2182–2192 (2002)
<https://doi.org/10.1002/jps.10209>
- Bengani, L.C., Hsu, K.H., Gause, S., and Chauhan, A.,
Contact lenses as a platform for ocular drug delivery,
Expert Opin. Drug Deliv. **10**, 1483–1496 (2013)
<https://doi.org/10.1517/17425247.2013.821462>
- Carvalho, I.M., Marques, C.S., Oliveira, R.S., Coelho, P.B., Costa, P.C., and Ferreira, D.C.,
Sustained drug release by contact lenses for glaucoma treatment - A review,
J. Control. Release **202**, 76–82 (2015)
<https://doi.org/10.1016/j.jconrel.2015.01.023>
- Chhabra, P., Gupta, R., Suri, G., Tyagi, M., Seshadri, G., Sabharwal, S., Niyogi, U.K., Khandal, R.K.,
Studies on development of polymeric materials using gamma irradiation for contact and intraocular lenses,
Int. J. Polym. Sci. **2009**, 1–9 (2009)
<https://doi.org/10.1016/j.jconrel.2015.01.023>
- Choi, S.W., and Kim, J.,
Therapeutic contact lenses with polymeric vehicles for ocular drug delivery: A review,
Materials **11**, 1125–1145 (2018)
<https://doi.org/10.3390/ma11071125>
- Desai, A.R., Maulvi, F.A., Desai, D.M., Shukla, M.R., Ranch, K.M., Vyas, B.A., Shah, S.A., Sandeman, S., and Shah, D.O.,
Multiple drug delivery from the drug-implants-laden silicone contact lens: Addressing the issue of burst drug release,
Mater. Sci. Eng. C **112**, 1–13 (2018)
<https://doi.org/10.1016/j.msec.2020.110885>

- Fan, X., Torres-Luna, C., Azadi, M., Domszy, R., Hu, N., Yang, A., and David, A.E.,
Evaluation of commercial soft contact lenses for ocular drug delivery: A review,
Acta Biomater **115**, 60–74 (2020)
<https://doi.org/10.1016/j.actbio.2020.08.025>
- Gao, Q., Liang, Q., Yu, F., Xu, J., Zhao, Q., and Sun, B.,
Synthesis and characterization of novel amphiphilic copolymer stearic acid-coupled F127 nanoparticles for nano-technology based drug delivery system,
Colloids Surfaces B Biointerfaces **88**, 741–748 (2011)
<https://doi.org/10.1016/j.colsurfb.2011.08.010>
- Gilbert, J.C., Richardson, J.L., Davies, M.C., Palin, K.J., and Hadgraft, J.,
The effect of solutes and polymers on the gelation properties of pluronic F-127 solutions for controlled drug delivery,
J. Control. Release **5**, 113–118 (1987)
[https://doi.org/10.1016/0168-3659\(87\)90002-2](https://doi.org/10.1016/0168-3659(87)90002-2)
- González-Chomón, C., Concheiro, A., and Alvarez-Lorenzo, C.,
Soft contact lenses for controlled ocular delivery: 50 years in the making,
Ther. Deliv. **4**, 1141–1161 (2013)
<https://doi.org/10.4155/tde.13.81>
- Grassiri, B., Zambito, Y., and Bernkop-Schnürch, A.,
Strategies to prolong the residence time of drug delivery systems on ocular surface,
Adv. Colloid Interface Sci. **288**, 1–15 (2021)
<https://doi.org/10.1016/j.cis.2020.102342>
- Kadam, Y., Yerramilli, U., and Bahadur, A.,
Solubilization of poorly water-soluble drug carbamazepine in Pluronic® micelles: Effect of molecular characteristics, temperature and added salt on the solubilizing capacity,
Colloids Surfaces B Biointerfaces. **72**, 141–147 (2009)
<https://doi.org/10.1016/j.colsurfb.2009.03.027>
- Kelishady, P.D., Saadat, E., Ravar, F., Akbari, H., and Dorkoosh, F.,
Pluronic F127 polymeric micelles for co-delivery of paclitaxel and lapatinib against metastatic breast cancer: Preparation, optimization and in vitro evaluation,
Pharm. Dev. Technol. **20**, 1009–1017 (2015)
<https://doi.org/10.3109/10837450.2014.965323>
- Kim, S.W., Bae, Y.H., and Okano, T.,
Hydrogels: swelling, drug loading, and release,
Pharm. Res. An Off. J. Am. Assoc. Pharm. Sci. **20**, 1009–1017 (1992)
<https://doi.org/10.1023/A:1015887213431>
- Li, C.C., and Chauhan, A.,
Modeling ophthalmic drug delivery by soaked contact lenses,
Ind. Eng. Chem. Res. **45**, 3718–3734 (1992)
<https://doi.org/10.1021/ie0507934>
- Maulvi, F.A., Desai, D.T., Shetty, K.H., Shah, D.O., and Willcox, M.D.P.,
Advances and challenges in the nanoparticles-laden contact lenses for ocular drug delivery,
Int. J. Pharm. **608**, 1–9 (2021)
<https://doi.org/10.1016/j.ijpharm.2021.121090>
- Maulvi, F.A., Parmar, R.J., Desai, A.R., Desai, D.M., Shukla, M.R., Ranch, K.M., Shah, S.A., and Shah, D.O.,
Tailored gatifloxacin Pluronic® F-68-loaded contact lens: Addressing the issue of transmittance and swelling,
Int. J. Pharm. **581**, 1–39 (2021)
<https://doi.org/10.1016/j.ijpharm.2020.119279>
- Maulvi, F.A., Singhania, S.S., Desai, A.R., Shukla, M.R., Tannk, A.S., Ranch, K.M., Vyas, B.A., and Shah, D.O.,
Contact lenses with dual drug delivery for the treatment of bacterial conjunctivitis,
Int. J. Pharm. **548**, 139–150 (2018)
<https://doi.org/10.1016/j.ijpharm.2018.06.059>

- Maulvi, F.A., Soni, T.G., and Shah, D.O.,
A review on therapeutic contact lenses for ocular drug delivery,
Drug Deliv **23**, 3017–3026 (2016)
<https://doi.org/10.3109/10717544.2016.1138342>
- McDermott, M.L., and Chandler, J.W.,
Therapeutic use of contact lenses,
Drug Deliv **33**, 381–394 (1987).
- Musgrave, C.S.A., and Fang, F.,
Contact lens materials: A materials science perspective,
Materials **12**, 1–35 (2019)
<https://doi.org/10.3390/ma12020261>
- Nguyen, D.C.T., Dowling, J., Ryan, R., McLoughlin, P., and Fitzhenry, L.,
Pharmaceutical-loaded contact lenses as an ocular drug delivery system: A review of critical lens characterization methodologies with reference to ISO standards,
Contact Lens Anterior Eye **44**, 1–17 (2021)
<https://doi.org/10.1016/j.clae.2021.101487>
- Nichols, J.J.,
Continuing upward trends in daily disposable prescribing and other key segments maintained a healthy industry,
Contact Lens Spectr. **33**, 20–25 (2018)
<https://doi.org/10.1016/j.clae.2021.101487>
- Nichols, J.J., Willcox, M.D.P., Bron, A.J., Belmonte, C., Ciolino, J.B., Craig, J.P., Dogru, M., Foulks, G.N., Jones, L., Nelson, J.D., Nichols, K.K., Purslow, C., Schaumberg, D.A., Stapleton, F., and Sullivan, D.A.,
The TFOS international workshop on contact lens discomfort: executive summary,
Investig. Ophthalmol. Vis. Sci. **54**, 1–7 (2013)
<https://doi.org/10.1167/iovs.13-13212>
- Nicolson, P.C., and Vogt, J.,
Soft contact lens polymers: An evolution,
Biomaterials **22**, 3273–3283 (2001)
<https://doi.org/10.1007/s12010-021-03691-w>
- Patel, H.S., Shaikh, S.J., Ray, D., Aswal, V.K., Vaidya, F., Pathak, C., and Sharma, R.K.,
Formulation, solubilization, and in vitro characterization of quercetin-incorporated mixed micelles of PEO-PPO-PEO block copolymers,
Appl. Biochem. Biotechnol. **194**, 445–463 (2022)
<https://doi.org/10.1007/s12010-021-03691-w>
- Patra, A., Satpathy, S., Shenoy, A.K., Bush, J.A., Kazi, M., and Hussain, M.D.,
Formulation and evaluation of mixed polymeric micelles of quercetin for treatment of breast, ovarian, and multidrug resistant cancers,
Int. J. Nanomedicine **13**, 2869–2881 (2018)
<https://doi.org/10.2147/IJN.S153094>
- Pillay, R., Hansrai, R., and Rampersad, N.,
Historical development, applications and advances in materials used in spectacle lenses and contact lenses,
Clin. Optom. **12**, 157–167 (2020).
- Refojo, M.F.,
Contact lens materials.,
5, (1973). 313-331
- Refojo, M.F.,
Hydrophobic interaction in poly(2-hydroxyethyl methacrylate) homogeneous hydrogel,
J. Polym. Sci. **5**, 3103–3113 (2018)
<https://doi.org/10.1002/pol.1967.150051211>

- Ruben, M., and Guillon, M.,
Contact lens practice,
London, Champan & Hall Medical, (1994).
- Rykowska, I., Nowak, I., and Nowak, R.,
Soft contact lenses as drug delivery systems: A review,
Molecules **26**, 1–31 (2021)
<https://doi.org/10.3390/molecules26185577>
- Sahu, A., Kasoju, N., Goswami, P., and Bora, U.,
Encapsulation of curcumin in pluronic block copolymer micelles for drug delivery applications,
J. Biomater. Appl. **25**, 619–639 (2011)
<https://doi.org/10.1177/0885328209357110>
- Sedláček, J.,
Possibility of the application of ophthalmic drugs with the use of gel contact lenses,
Cesk. Oftalmol. **21**, 509–512 (1965).
- Sezgin, Z., Yüksel, N., and Baykara, T.,
Preparation and characterization of polymeric micelles for solubilization of poorly soluble anticancer drugs,
Eur. J. Pharm. Biopharm. **64**, 261–268 (2006)
<https://doi.org/10.1016/j.ejpb.2006.06.003>
- Sharma, P.K., Matthew, J.E., and Bhatia, S.R.,
Structure and assembly of PEO-PPO-PEO co-polymers in mammalian cell-culture media,
J. Biomater. Sci. Polym. Ed. **16**, 1139–1158 (2005)
<https://doi.org/10.1163/1568562054798545>
- Stammet, M., Kwon, G.S., and Rao, D.A.,
Drug loading in Pluronic® micelles made by solvent casting and equilibrium methods using resveratrol as a model drug,
J. Control. Release **148**, 50–51 (2010)
<https://doi.org/10.1016/j.jconrel.2010.07.056>
- Vivero-lopez, M., Pereira-da-mota, A.F., Carracedo, G., Huete-toral, F., Parga, A., Otero, A., Concheiro, A., and Alvarez-lorenzo, C.,
Phosphorylcholine-based contact lenses for sustained release of resveratrol: design, antioxidant and antimicrobial performances, and in vivo behaviour,
ACS Appl. Mater. Interfaces **14**, 55431–55446 (2022)
<https://doi.org/10.1021/acsami.2c18217>
- Wang, W., Sun, C., Mao, L., Ma, P., Liu, F., Yang, J., and Gao, Y.,
The biological activities, chemical stability, metabolism and delivery systems of quercetin: A review,
Trends Food Sci. Technol. **56**, 21–38 (2016)
<https://doi.org/10.1016/j.tifs.2016.07.004>
- Weeks, A., Subbaraman, L.N., Jones, L., and Sheardown, H.,
The competing effects of hyaluronic and methacrylic acid in model contact lenses,
J. Biomater. Sci. Polym. Ed. **23**, 1021–1038 (2012)
<https://doi.org/10.1163/092050611X569060>
- Willcox M, and Argüeso P.,
TFOS DEWS II Tear Film Report,
Ocul Surf. **15**, 366–403 (2017)
<https://doi.org/10.1016/j.jtos.2017.03.006>
- Zheng, X., Wang, X., Gou, M., Zhang, J., Men, K., Chen, L., Luo, F., Zhao, X., Wei, Y., and Qian, Z.,
A novel transdermal honokiol formulation based on Pluronic F127 copolymer,
Drug Deliv. **17**, 138–144 (2010)
<https://doi.org/10.3109/10717541003604874>
- Zupančič, Š., Lavrič, Z., and Kristl, J.,
Stability and solubility of trans-resveratrol are strongly influenced by pH and temperature,
Eur. J. Pharm. Biopharm. **93**, 196–204 (2015)
<https://doi.org/10.1016/j.ejpb.2015.04.002>

IV

Concluding Remarks

9

Limitations of the Present Study and Future Work

This thesis work has some limitations. These are listed below, along with the proposals for their resolution:

1. Liposomes are a versatile type of carrier for the delivery of a variety of therapeutic agents. Despite this, there were different challenges that we encountered during our formulation development, such as the extremely poor loading efficiency of the APIs, which rendered the formulation inefficient in terms of therapeutic effect and production. Due to these limitations, a complete physico-chemical characterization was not possible to perform. For the upcoming studies, we propose an extensive revision of the liposomal composition and loading method of the API(s).
2. Inclusion complexes with cyclodextrins represent a very versatile method of formulating hydrophobic compounds. Additionally, the manufacturing process is straightforward. Nonetheless, to have a candidate formulation, extended stability studies following the ICH guidelines shall be performed. This could cover the addition of other types of excipients that could further improve the stability of the formulations. All products for topical ocular applications need to be sterile; to accomplish this, several sterilisation methods can be used (thermal, radiation, etc.). These have the risk of inducing degradation of the API. Although biocompatibility and intracellular antioxidant activity were proved, there is a lack of confirmation of their effect on other biological functions, such as blocking the inflammatory cascade. The *in vitro* experiments were performed on cell culture monolayers; although these models are very reliable, they do not represent the realistic behaviour and architecture of living tissues or organs. Hence, for future studies is proposed: i) to perform long-term stability studies following the ICH guidelines; ii) to investigate the effect of the sterilisation process on the formulations; iii) to carry out *in vitro* studies on stratified or 3D culture models of the cornea or conjunctiva; and iv) to re-perform biological assays related to the directed assessment of the anti-inflammatory activity. Furthermore, it would be significant to test the optimised formulations in well-established DED-murine models. These models, which include the development of DED through

environmental stress or by administering damaging substances such as benzalkonium chloride, may help in the understanding of the safety and efficacy of the proposed formulation platform.

3. Nanoparticles made from recombinant elastin emerged as a very interesting and versatile formulation strategy. Even though the production process results in the formation of a powder, stability issues may represent a point of concern. Release studies shall be redesigned in a manner to be able to determine all the quercetin that has been released since a possible degradation of the latter has occurred, making impossible the truthful determination of the releasing kinetics. As in the case of cyclodextrins, more complex substrates for *in vitro* studies shall be used. Even though an efficient cellular uptake of ELR-NPs was observed, it would be interesting to study more in depth the mechanism by which this uptake occurs. Therefore, for the improvement of this type of formulation, it is suggested: i) to perform stability studies on both solid and in solution ELR-NPs; ii) to redefine the release studies; iii) to carry out *in vitro* studies on stratified or 3D culture models of the cornea or conjunctiva; iv) to perform biological assays related to the assessment of the anti-inflammatory activity; and v) to assess the mechanism of cell uptake of ELR-NPs. As in the case of inclusion complexes with cyclodextrins, the efficiency of the delivery platform should be proven on *in vivo* validated DED models.
4. Contact lenses embedded with micelles present a promising approach to ophthalmic delivery, especially for the possibility to extend the contact time and the control of the release of the API. Still, we have faced problems during the loading process of the hydrogel base of the contact lenses. This in part limited the characterization studies and the performance of potential *in vitro* assays. Besides, limited time for performance and improvement of the experiments conditioned the results of this study. Future work should consider the subsequent proposals: i) to re-formulate the original idea based on loading micelles into the hydrogels; ii) to consider other methods of hydrogel loading procedures; iii) to perform physico-chemical characterization of the improved system; and iv) to perform *in vitro* studies.

10

Conclusions

This thesis work was centred on the development of formulation strategies for naturally occurring compounds quercetin and resveratrol, with the purpose of their therapeutic application as topical ophthalmic treatments for dry eye disease and other disorders affecting the ocular surface. The focus on formulation development was necessary, since the beneficial effects of the compounds of interest have been proven previously both *in vitro* and *in vivo*, but their use was limited due to their poor intrinsic characteristics, such as susceptibility to degradation or poor aqueous solubility. This study demonstrates that it is possible, through the application of different formulation approaches, to improve the characteristics of the two API candidates.

Following are the main conclusions of this thesis work, that correspond to the objectives set at the beginning of the work.

1. The four formulation strategies proposed in this thesis work have reached different levels of development. With respect to the liposomal formulation, the main challenge was the extremely low encapsulation efficiency of the two polyphenols, which made them ineffective for delivering therapeutic dosages. In the case of the inclusion complexes with cyclodextrins, the solubility of QUE and RSV improved linearly with the increase in the concentration of cyclodextrin in solution. Also, a considerable improvement in the stability of both compounds was achieved. Further improvement of both solubility and stability of QUE and RSV was observed with the addition of hyaluronic acid to the preformed binary complexes CD:drug. Since the formulations of ELR-NPs were produced as solids, their stability was considered sufficient for the duration of the present study. Additionally, ELR-NPs offered sustained release for both QUE and RSV. The incorporation of micelles into the contact lenses resembling hydrogels did not alter crucial parameters of the hydrogels, such as light transmittance and water uptake. However, complications emerged with the release studies, which shall be revised.
2. The formulations of QUE and RSV in binary inclusion complexes with cyclodextrins and ternary complexes with the addition of hyaluronic acid were biocompatible with human corneal and conjunctival epithelial cells. In addition, ELR-NPs, bearing QUE, RSV or both polyphenols did not alter the cell viability of human corneal epithelial cells and are therefore considered biocompatible with this cell line.

3. Cyclodextrin and ELR-NPs formulations exhibited excellent ability to scavenge intracellular ROS species in two ocular surface cell lines. The anti-inflammatory activity of the inclusion complexes was studied. However, no consistent results were obtained. Further adjustments in the *in vitro* inflammatory model have to be considered.
4. Fluorescein labelled ELR-NPs carrying nile red have been shown to be able to enter and release their payload into human corneal epithelial cells. Also, the same system exhibited excellent penetration in an *ex vivo* corneal model. The cell uptake and *ex vivo* studies of the other formulations presented in this work were not studied due to limitations of time and the production of an efficient, fluorescent-marked system.

As a general conclusion, it can be stated that the inclusion complexes with cyclodextrins (binary and ternary) and ELR-NPs have given the most promising results for a possible future development of a topical ophthalmic formulation. Both formulations influenced positively crucial properties of the two polyphenolic compounds. However, in both cases more profound studies are required.

V

Resumen

11

Resumen en Español

11.1. Motivación del estudio

La enfermedad del ojo seco (EOS) es un estado patológico complejo que afecta a la superficie ocular. El estilo de vida actual de la mayoría de las personas, con una exposición prolongada a pantallas y largos periodos en oficinas con aire acondicionado, ha aumentado la prevalencia de este problema entre la población. Además, otros factores de riesgo relacionados con el sexo o la etnia pueden actuar como promotores de la EOS. La causa principal de su aparición radica en la disfunción de las glándulas lagrimales y/o de Meibomio. Esta disfunción conduce a una película lagrimal inestable y el consiguiente desarrollo de un estado inflamatorio crónico. Las opciones terapéuticas de esta enfermedad son amplias y variadas, desde la aplicación tópica de corticosteroides y otros compuestos de base lipídica, hasta la higiene palpebral y los tratamientos térmicos y de masaje en los párpados. Sin embargo, todas ellas tienen en común que no representan una solución terapéutica permanente para los pacientes con EOS.

En consecuencia, se han dedicado muchos esfuerzos a la búsqueda de nuevas moléculas potenciales que puedan satisfacer las necesidades no cubiertas en el tratamiento de la EOS. Uno de los tipos de moléculas emergentes que ha cobrado especial interés es el de los polifenoles. Los polifenoles son metabolitos naturales de plantas, a los que se ha otorgado una gran variedad de efectos terapéuticos, entre ellos los antiinflamatorios y los antioxidantes. En investigaciones previas realizadas por nuestro grupo de investigación, la quercetina (QUE) y el resveratrol (RSV), dos compuestos del grupo de los polifenoles, han resultado ser potenciales candidatos para el tratamiento de la EOS. Desafortunadamente, sus aplicaciones terapéuticas más amplias se han visto limitadas por sus pobres características fisicoquímicas, como son su baja solubilidad en agua y su inestabilidad química.

Por lo tanto, como objetivo de esta tesis doctoral se propuso el desarrollo de diferentes estrategias de formulación que pudieran superar los problemas relacionados con estas moléculas y acercarnos al desarrollo de un tratamiento disponible comercialmente para el tratamiento de la EOS.

11.2. Organización de la tesis doctoral

La presente tesis doctoral se plantea en la modalidad normalizada, y opta a la Mención Internacional para el Título de Doctor. El trabajo científico que se presenta en esta tesis ha sido realizado en la Universidad de Valladolid, siguiendo las directrices de la Escuela de Doctorado de la Uva. Durante el periodo de doctorado se realizó una estancia académica de tres meses en la Facultad de Ciencias de la Salud, Escuela de Farmacia de la Universidad de Finlandia Oriental (Kuopio, Finlandia). Además, se realizó una estancia académica adicional de un mes en el departamento de Farmacología, Farmacia y Tecnología Farmacéutica de la Universidad de Santiago de Compostela (Santiago de Compostela, España). Para poder ser presentada, esta tesis ha cumplido los siguientes criterios:

- El manuscrito de la tesis ha sido redactado en inglés.
- Se ha incluido un resumen general en español.
- Se ha justificado la unidad temática del estudio realizado en la tesis.
- Se han redactado los objetivos, la metodología, los resultados, la discusión y las conclusiones.
- Se ha presentado una aportación de calidad consistente en una publicación en una revista científica revisada por pares con factor de impacto y ubicada entre Q1 y Q3 en el área de ciencias farmacéuticas.

Además, como parte de los apéndices, se presentan otros cuatro manuscritos publicados, así como el que está en preparación/revisión.

La idea principal de la Tesis Doctoral se expone en el prefacio que contiene la motivación, una introducción general sobre la superficie ocular, la EOS, los polifenoles y los sistemas de liberación de fármacos, además de una hipótesis y unos objetivos bien definidos. Los resultados científicos se estructuran en cuatro capítulos, cada uno de los cuales corresponde a una estrategia de formulación concreta, que pretenden facilitar la comprensión del trabajo. Cada capítulo se divide a su vez en una breve introducción sobre la estrategia de formulación utilizada, la metodología empleada, los resultados obtenidos y su discusión, y las conclusiones. Los capítulos relacionados con los resultados científicos de este trabajo son los siguientes:

- **Capítulo 5: Liposomas como plataforma potencial de administración de polifenoles naturales.**

Se propusieron los liposomas como estrategia inicial de formulación para mejorar las características fisicoquímicas de los dos polifenoles de interés.

- **Capítulo 6: Complejos de inclusión con ciclodextrinas (CD): Comparación entre Complejos Binarios y Ternarios.**

La formación de complejos con ciclodextrinas es una forma eficaz de mejorar la solubilidad acuosa de los compuestos de interés, mientras que la adición de polímeros hidrófilos a los complejos fármaco:CD ya existentes es una estrategia para mejorar aún más la estabilidad química.

- **Capítulo 7: Nanopartículas basadas en elastina recombinante (ELR-NPs): Potencial sistema de administración de fármacos para el tratamiento de la EOS.**

El uso de biopolímeros basados en proteínas, como la elastina recombinante, con propiedades modulables, parece una buena estrategia de formulación para compuestos de origen natural. Además, el proceso de fabricación mediante fluidos supercríticos permite obtener un producto con el mínimo contenido de disolvente orgánico.

- **Capítulo 8: Micelas embebidas en lentes de contacto (LC): Un enfoque innovador para la administración oftálmica.**

Las lentes a contacto terapéuticas en combinación con portadores coloidales representan un enfoque interesante para la administración del principio activo en la superficie ocular, donde se puede conseguir una mejora significativa de su tiempo de residencia y de su biodisponibilidad.

Adicionalmente, hay un capítulo donde se presentan las limitaciones y propuestas para el trabajo futuro, así como las conclusiones de la tesis.

11.3. Hipótesis

Para el desarrollo de esta tesis se formuló la siguiente hipótesis: La quercetina y el resveratrol son compuestos polifenólicos naturales con potencial aplicación como terapéuticos en oftalmología. Dado que esta aplicación está limitada por sus pobres características fisicoquímicas, es probable que se mejoren mediante el empleo de estrategias avanzadas de administración de fármacos.

11.4. Objetivos

Para comprobar la hipótesis, se establecieron los siguientes objetivos:

Objetivo general

Desarrollar diferentes estrategias de formulación de quercetina (QUE) y resveratrol (RSV) para mejorar sus características fisicoquímicas y, en consecuencia, su biodisponibilidad para las células de la superficie ocular.

Objetivos específicos

1. Diseñar cuatro tipos diferentes de formulaciones para QUE y RSV, en concreto, liposomas, complejos de inclusión con ciclodextrinas, nanopartículas basadas en recombinafos de elastina y lentes de contacto embebidas con micelas, con el fin de mejorar su solubilidad y estabilidad química.
2. Comprobar la biocompatibilidad de las formulaciones *in vitro* utilizando líneas celulares de la superficie ocular.
3. Comprobar la capacidad antioxidante y anti-inflamatoria de las formulaciones *in vitro*.
4. Evaluar la capacidad de penetración de las formulaciones desarrolladas en modelos de superficie ocular *in vitro* y *ex vivo*.

A continuación, se presentan de forma resumida los resultados más relevantes de cada capítulo junto con la metodología aplicada para su obtención.

11.5. Los Liposomas como Plataforma de Administración de Polifenoles Naturales

11.5.1. Objetivo

Gracias a la similitud con la membrana celular y la capacidad de poder ser portadores de distintos tipos de moléculas (fármacos pequeños, proteínas, ácidos nucleicos o agentes de contraste) los liposomas se caracterizan por una excelente biocompatibilidad y versatilidad, y hoy en día representan uno de los sistemas de administración de fármacos más estudiados. Los liposomas son vesículas lipídicas, que consisten en una o más bicapas lipídicas (láminas) que

rodean un interior acuoso (Al-Amin *et al.*, 2023; Gao *et al.*, 1994; Portnoy *et al.*, 2019). Además de ser capaces de la vehiculización de fármacos hidrofóbicos e hidrofílicos, confieren protección a los mismos y previenen su inactivación química. Igualmente, limitan el contacto del fármaco con los tejidos sanos antes de su liberación, lo que reduce la aparición de efectos adversos (Bozzutto *et al.*, 2015).

El objetivo de esta parte de la tesis fue el desarrollo de una formulación liposomal para la administración tópica ocular de pequeñas moléculas de origen natural, QUE y RSV.

11.5.2. Metodología

Preparación de los liposomas

Los liposomas se prepararon mediante la técnica de rehidratación fina propuesta por Bangham (Bangham *et al.*, 1965). Se prepararon dos tipos de liposomas con diferente composición lipídica: DSPC:colesterol en una proporción molar 1:1 y DSPC:colesterol en una proporción molar 6:4.

Para el ajuste del tamaño de los liposomas se probaron dos enfoques diferentes; el primero se basó en la aplicación de ultrasonidos y el segundo, más clásico, consistió en la extrusión (11 veces) de la suspensión liposomal a través de un extrusor Avanti mini extruder (Avanti Polar Lipids Inc. Alabaster, Alabama, EE.UU.) con una membrana de policarbonato de 200 nm de corte (Silva *et al.*, 2010; Wenche *et al.*, 2015).

Los liposomas cargados con QUE o RSV se prepararon añadiendo las soluciones de los fármacos (500 μM , disueltos en cloroformio) junto con los lípidos. Para eliminar el fármaco no cargado se realizó diálisis contra 1 L de tampón fosfato (PBS) durante 2 horas.

Caracterización de las formulaciones liposomales

Se utilizó el Malvern Zetasizer (Malvern, Reino Unido) para determinar el tamaño y el índice de polidispersidad (Pdl) de los liposomas vacíos y cargados. Para determinar el tamaño y el índice de polidispersidad, los liposomas se diluyeron en PBS hasta una concentración de 0,5 mg/mL.

Para la determinación de la eficacia de encapsulación, los liposomas se rompieron utilizando MeOH puro y la cantidad encapsulada de QUE y RSV se determinó utilizando un espectrofotómetro UV-Vis (Agilent Cary 60 UV- Vis, Waldbronn, Alemania) utilizado previamente para la preparación de las curvas de calibración de ambas moléculas (2,5-80 μM para QUE, $R^2=0,9954$ y 2,5-100 μM para RSV, $R^2=0,9984$).

Análisis estadístico

Los datos experimentales se presentan como media \pm error estándar de la media (SEM). Las medias de los datos se compararon mediante la prueba t de Student independiente, precedida

de la prueba de normalidad de Shapiro-Wilk. Todos los análisis se realizaron con el programa informático SPSS (SPSS 20.0; SPSS, Inc., Chicago, IL, EE.UU.).

11.5.3. Resultados

Caracterización de las formulaciones liposomales

El tamaño y el PDI de los liposomas, obtenidos a partir de dos métodos distintos de reducción de tamaño, se analizaron mediante dispersión dinámica de la luz (DLS), y los resultados están resumidos en la **tabla 11.1**. Los liposomas tratados con ultrasonidos presentaron un diámetro medio de $146,55 \pm 17$ nm para la composición DSPC:Chol = 1:1 y de $133,12 \pm 13$ nm para DSPC:Chol = 6:4. En ambos casos el PDI fue inferior a 0,3, lo que indica que se consiguió una buena homogeneidad de tamaño en el interior de las muestras. En cuanto a los liposomas que fueron extruidos a través del mini extrusor, el DSPC:Chol = 1:1 obtuvieron un tamaño de $144,7 \pm 10$ nm mientras que el DSPC:Chol = 6:4 obtuvo $137,89 \pm 11$ nm con valores de PDI por debajo de 0,2 para ambas formulaciones. Aunque los dos métodos utilizados para la reducción del tamaño de los liposomas dieron resultados óptimos y comparables, decidimos proceder con el método de extrusión. Esto se debe a que la extrusión ha demostrado ser un método más sencillo y rápido, con la ventaja de ser altamente eficiente y reproducible en la reducción de tamaño de los liposomas.

Sin embargo, la eficacia de encapsulación de QUE y RSV fue excepcionalmente baja. En el caso de la composición lipídica DSPC:Chol = 1:1, sólo se cargó el $12,26 \pm 5,39$ % de la QUE inicial, mientras que en el caso del RSV fue del $2,25 \pm 1,68$ %. Los resultados no fueron diferentes para los liposomas DSPC:Chol = 6:4, que se cargaron con el $1,35 \pm 0,36$ % y el $0,24 \pm 0,94$ % de QUE y RSV, respectivamente. Se realizó un análisis estadístico de los datos, pero no hubo diferencias significativas entre los grupos comparados ($p > 0,05$).

Por lo tanto, aunque se exploraron con éxito diferentes métodos de reducción del tamaño de los liposomas; la encapsulación de QUE y RSV dio lugar a problemas relacionados con la eficacia del proceso de carga. Estos problemas de carga de los compuestos de interés pueden tener distintas explicaciones. Tanto QUE como RSV se cargaron en los liposomas mediante el método de carga pasiva, en el que la carga del fármaco y la formación del liposoma tienen lugar al mismo tiempo. Para obviar a este problema, podría utilizarse la carga activa (a distancia). En este método, el fármaco se carga en liposomas preformados aprovechando un gradiente transmembrana (Bally *et al.*, 1988). Sin embargo, la solubilización del compuesto de interés se produce en la fase acuosa externa, surgiendo posibles limitaciones en la carga de un fármaco hidrófobo. Además del método de preparación, la eficacia de atrapamiento de un fármaco en los liposomas puede verse afectada también por el tamaño y el número de láminas de las vesículas lipídicas (Immordino *et al.*, 2006). Las vesículas multilamelares, a contrario de las vesículas unilamelares preparadas en este trabajo, están formadas por varias bicapas lipídicas concéntricas, y por eso tienen una porción lipídica mayor, adecuada para alojar mayores cantidades de fármacos hidrófobos. Con el incremento de la laminaridad se incrementa también el tamaño

Table 11.1: Resumen del tamaño, PDI y eficacia de encapsulación (%) de QUE y RSV. Los valores están presentados como media \pm SEM

	Composición	Tamaño (nm)	PdI	% QUE	% RSV
Ultrasonidos	DSPC:Chol = 1:1	146,55 \pm 17	0,28 \pm 0,078	N/D	N/D
	DSPC:Chol = 6:4	133,12 \pm 13	0,25 \pm 0,043	N/D	N/D
Extrusion	DSPC:Chol = 1:1	144,7 \pm 10	0,18 \pm 0,013	-	-
	DSPC:Chol = 6:4	137,89 \pm 11	0,22 \pm 0,10	-	-
	DSPC:Chol = 1:1	156,9 \pm 09	0,15 \pm 0,12	12,26 \pm 5,39	-
	DSPC:Chol = 6:4	142,9 \pm 03	0,12 \pm 0,072	1,35 \pm 0,36	-
	DSPC:Chol = 1:1	164,05 \pm 12	0,21 \pm 0,034	-	2,25 \pm 1,68
	DSPC:Chol = 6:4	131,56 \pm 04	0,20 \pm 0,028	-	0,24 \pm 0,94

N/D = No determinado.

del sistema, lo cual puede hacer el sistema inadecuado para la aplicación tópica ocular.

11.5.4. Conclusiones

Como conclusión, la metodología aplicada para la preparación y carga de los liposomas no ha resultado adecuada a los objetivos planteados. Quizá el ajuste adecuado de varios parámetros podría llevar a la obtención de una formulación liposomal prometedora capaz de suministrar concentraciones terapéuticas de las sustancias naturales de interés en este trabajo.

11.6. Complejos de inclusión con ciclodextrinas: comparación entre complejos binarios y ternarios

11.6.1. Objetivo

La conversión enzimática del almidón produce unos oligosacáridos cíclicos, las ciclodextrinas (CD), ampliamente utilizados en las industrias farmacéutica, cosmética y alimentaria. A parte de las CDs naturales que contienen 6 (α -CD), 7 (β -CD) y 8 (γ -CD) unidades de glucopiranososa, existen unos derivados sintéticos producidos por alquilación o hidroxialquilación de los grupos hidroxilo de las CDs naturales (Del Valle, 2004; Lachowicz *et al.*, 2020; Loftsson & Stefánsson, 1997; Varan *et al.*, 2017). Gracias a su característica forma de cono, las CDs son capaces de albergar moléculas hidrofóbicas dentro de la cavidad interna del cono. La formación de complejos sucede mediante formación de fuerzas débiles no covalentes, como la interacción electrostática, el enlace de hidrogeno y las interacciones hidrofóbicas, entre otras, entre las CDs

y la molécula de fármaco (Liu & Guo, 2002; Loftsson & Stefánsson, 1997). Una vez formados los complejos, muchas de las propiedades fisicoquímicas de la molécula huésped se ven afectadas. Esta es la razón por la que los complejos de inclusión con CDs encuentran innumerables aplicaciones. En diversos estudios se observó que la adición de determinados excipientes, como polímeros hidrófilos a los complejos fármaco:CD puede favorecer su eficacia de complejación y su estabilización. Estos ensamblajes supramoleculares se basan en interacciones mutuas entre el CD, el fármaco y el polímero (Loftsson & Duchêne, 2007; Saokham *et al.*, 2018).

Por lo tanto, el objetivo de este estudio fue mejorar la solubilidad y la estabilidad de QUE y RSV utilizando hidroxipropil- β -ciclodextrina (HP β CD) y la combinación de HP β CD con ácido hialurónico (HA). Las formulaciones se caracterizaron fisicoquímicamente y se evaluó su biocompatibilidad y su actividad antioxidante intracelular en líneas celulares humanas de córnea y de conjuntiva. Parte de la caracterización físico-química se realizó durante una estancia académica en la Universidad de Finlandia Oriental (Kuopio, Finlandia).

11.6.2. Metodología

Análisis cuantitativo de QUE y RSV

Para la cuantificación de QUE y RSV se desarrolló un método cromatográfico basado en cromatografía líquida de alta presión en fase reversa (RP-HPLC) Waters e2695 con un módulo de separación equipado con un automuestreador y una bomba cuaternaria, ambos conectados a un detector de matriz de fotodiodos Waters 2998 provisto de un detector UV. La fase móvil consistió en agua miliQ/ 0,05 % (v/v) ácido tricloroacético (TFA) (A) y acetonitrilo/0,05 % (v/v) TFA (B), que se eluyeron en un modo de gradiente como sigue: 4 min 10 % B, 6 min 30 % B, 16 min 60 % B, 17 min 95 % B, 18 min 95 % B, 19 min 10 % B, 22 min 10 % B. El tiempo de retención para QUE fue de 15,6 min, mientras que para RSV fue de 14,7 min, y las longitudes de onda utilizadas para la detección fueron 370 nm y 306 nm, respectivamente.

Estabilidad química

Se evaluó la estabilidad química de QUE y RSV en PBS (pH 7,4) en presencia de un 5 % p/v de HP β CD a temperatura controlada (25° C). Además, se evaluó el posible efecto estabilizador del 0,1 %, 0,25 y 0,5 % p/v de HA. En los momentos predefinidos se extrajeron alícuotas de las muestras y se cuantificaron por RP-HPLC. Los datos se expresan como porcentaje de la concentración inicial del compuesto (C_0) en el momento inicial (t_0), y se ajustaron adecuadamente a la cinética de degradación de primer orden mediante la siguiente ecuación (Ec.):

$$\ln(C_t/C_0) = -kt \quad (11.1)$$

La vida media de degradación del compuesto ($t_{1/2}$) representa el periodo en el que la concentración inicial de las muestras se reduce a la mitad, y se calculó de la siguiente forma:

$$t_{1/2} = \frac{1}{k} \ln(2) \quad (11.2)$$

La vida útil de un compuesto (t_{90}) es el tiempo en el que su concentración inicial disminuye hasta el 90 % de la inicial, se calcula como se indica:

$$t_{90} = \frac{0,105}{k} \quad (11.3)$$

Estudios de solubilidad

Se estudió la solubilidad de QUE y RSV en presencia de HP β CD en PBS (pH 7,4). Brevemente, se agregó una cantidad excesiva de QUE o RSV a concentraciones crecientes de HP β CD hasta 12,5% (p/v). Las suspensiones de fármaco saturadas se dejaron en agitación durante la noche a 25°C protegidas de la luz. Después de este tiempo las suspensiones fueron centrifugadas (6000 rpm, 10 min) para eliminar los restos de fármaco no disuelto y se analizó mediante RP-HPLC para determinar las concentraciones de QUE y RSV. Los perfiles de solubilidad en fase se establecieron siguiendo el método propuesto por Higuchi y Connors. La constante de estabilidad aparente ($K_{1:1}$) y las eficiencias de complejación (CE) se calcularon mediante las ecuaciones 11.4 y 11.5 a partir de las pendientes de los diagramas de solubilidad de fase, donde S_0 representa la solubilidad del fármaco. En un medio de complejación específico, el CE puede utilizarse para calcular la relación molar entre el fármaco y la CD, como se indica en la Ec. 11.6.

$$K_{1:1} = \frac{\text{pendiente}}{S_0(1 - \text{pendiente})} \quad (11.4)$$

$$CE = \frac{[\frac{D}{CD}]}{[CD]} = S_0 \times K_{1:1} = \frac{\text{pendiente}}{S_0(1 - \text{pendiente})} \quad (11.5)$$

$$D : CD_{\text{razon molar}} = 1 : \frac{CE + 1}{CE} \quad (11.6)$$

Además, se repitieron los mismos estudios en presencia de HA al 0,1 % p/v para evaluar el efecto de este polímero en la solubilización de QUE y RSV por complejación con HP β CD.

Viabilidad celular

Para determinar la viabilidad de las células de las líneas de Epitelio Corneal Humano (HCE) y de Epitelio Conjuntival Humano (IM-ConjEpi) tras la exposición a las diferentes formulaciones se realizó el ensayo de viabilidad celular utilizando el compuesto XTT, capaz de ser transformado en un metabolito colorado solo mediante conversión enzimática en células viables. Las células se sembraron en placas de 96 pocillos (1×10^4 células/pocillo) y se cultivaron en medio suplementado (suero fetal bovino al 10 %, factor de crecimiento epitelial al 10 ng/mL, Insulina al 5 μ g/mL, penicilina-estreptomomicina al 100 U/mL y 100 μ g/mL, respectivamente)

hasta alcanzar el 90 % de confluencia. En todos los casos, las concentraciones finales de los polifenoles en los complejos se ajustaron de acuerdo con un estudio anterior de nuestro grupo (Abengózar-Vela *et al.*, 2015). El rango de concentración de QUE en los complejos fue de 5-50 μM y de 25-300 μM para RSV. Las células se expusieron a medio de cultivo celular o a cloruro de benzalconio (BAK) al 0,005 %, como controles positivo y negativo de la viabilidad celular, respectivamente. Tras 24 horas de exposición: se descartaron los sobrenadantes del cultivo celular y se cargaron los pocillos con 100 μL de DMEM/F-12 sin rojo de fenol. A continuación, se añadieron a cada pocillo 25 μL de mezcla de reacción PMS/XTT (10 μL de 3 mg/mL de PMS en 0,25 mg/mL de XTT). El porcentaje de células vivas se calculó en relación con los valores del control positivo. Se realizaron seis réplicas en tres experimentos independientes para cada formulación.

Actividad antioxidante intracelular

La capacidad de eliminación intracelular de Especies Reactivas de Oxígeno (ROS) de las formulaciones se midió utilizando 2',7'-diclorodihidrofluoresceína ($\text{H}_2\text{DCF-DA}$). Las células HCE e IM-ConjEpi se cultivaron en placas de 24 pocillos (6×10^4 células/pocillo) hasta alcanzar el 90 % de confluencia. Después, las células se mantuvieron en medio no suplementado durante 24 horas. Posteriormente, las células se pretrataron con 500 μL de las formulaciones y se dejaron durante 1 hora a 37°C . A continuación, se retiraron las formulaciones y las células se incubaron durante 30 minutos con 500 μL de una solución 10 μM de $\text{H}_2\text{DCF-DA}$. Transcurridos 30 minutos, se retiró la solución de $\text{H}_2\text{DCF-DA}$ y las células se volvieron a tratar con las formulaciones (a la misma concentración que antes) y se expusieron a una lámpara UV-B de 8 W (Bio-Rad, Inc., Hercules, CA, EE.UU.) durante 15 segundos. Las células del grupo control no fueron irradiadas. Tras la exposición a UV-B, las células se cultivaron durante 1 hora. La intensidad de la fluorescencia intracelular se midió a 488 nm (excitación) y 522 nm (emisión). Los datos obtenidos de las mediciones de fluorescencia se normalizaron por el contenido total de proteínas. Este último se midió en células adherentes mediante el ensayo del ácido bicinonínico (BCA), siguiendo las instrucciones del fabricante. Para cada tratamiento se realizaron tres experimentos independientes para cada formulación por duplicado.

Análisis estadístico

Todos los experimentos se realizaron por triplicado ($n=3$) y los datos se representan como media \pm error estándar de la media (EEM). Se utilizó el software SPSS (SPSS 20.0; SPSS, Inc., Chicago, IL, EE.UU.) para el análisis estadístico aplicando el análisis de varianzas de una vía (ANOVA) seguido de las pruebas post-hoc de Tukey o Games-Howell.

11.6.3. Resultados

Estabilidad química de los complejos de inclusión con QUE y RSV

Para estudiar la estabilidad química a corto plazo de la QUE y del RSV, en complejos con las CDs y puros, todas las muestras se colocaron en viales de vidrio, se protegieron de la luz y se mantuvieron en una sala de ambiente controlado. Además, se evaluaron los posibles efectos estabilizadores de diferentes concentraciones de HA. En la **tabla 11.2** se resumen los parámetros cinéticos de las reacciones de degradación.

Table 11.2: Resumen de la constante de degradación de primer orden (k), el periodo de degradación de medio tiempo ($t_{1/2}$), la vida útil (t_{90}) y el coeficiente de correlación (R^2) para QUE y RSV puros y complejos con HP β CD y HP β CD:HA en PBS (pH 7,4) a 25°C. Todas las concentraciones se expresan en % p/v y todas las muestras contenían un 5% w/v HP β CD.

Muestra	Aditivo	k (h ⁻¹)	$t_{1/2}$ (h)	t_{90} (h)	R^2
	HA				
QUE	-	0,188	3,66	0,55	0,987
QUE: HP β CD	-	0,029	23,57	3,57	0,940
QUE: HP β CD:HA	0,1%	0,012	55,45	8,75	0,967
	0,25%	0,015	44,71	6,77	0,946
	0,5%	0,016	43,05	6,52	0,941
RSV	-	0,0071	97,62	14,78	0,967
RSV: HP β CD	-	0,0009	770,16	116,66	0,819
RSV: HP β CD:HA	0,1%	0,0008	866,43	131,25	0,900
	0,25%	0,0013	533,19	80,76	0,908
	0,5%	0,0018	385,08	58,33	0,613

La QUE pura era inestable en soluciones acuosas a 25°C. Los parámetros cinéticos calculados mostraron que la vida media ($t_{1/2}$) es de 3.66 horas, lo que significa que, básicamente, toda la QUE se degrada en un día. La degradación fue más lenta cuando la QUE se complejó con HP β CD y HP β CD:HA.

En el caso de RSV, el compuesto puro demostró ser más estable que la QUE pura, teniendo una vida media de degradación de 97,6 horas. Los complejos de RSV con HP β CD y HP β CD:HA mostraron una mayor estabilidad del polifenol y esta mejora dependió de la concentración de

HA.

El efecto estabilizador del HA fue inversamente proporcional a su concentración, ya que una mejor estabilización de ambos compuestos (QUE y RSV) se observó con las concentraciones más bajas de HA (0,1 % p/v). Esto se puede justificar por el hecho de que, a mayores concentraciones, el HA es capaz de formar enlaces de hidrógeno intra o intermoleculares que conducen a la formación de una red polimérica tridimensional. En este caso, hay menos HA accesible para interactuar y estabilizar los compuestos polifenólicos. Todo los estudios posteriores se realizaron con 0,1% p/v de HA, ya que mostró la mayor capacidad estabilizadora en el caso de ambos compuestos polifenólicos.

Estudio de solubilidad

Se investigó el efecto de concentraciones crecientes de HP β CD (0-12,5 % p/v) en la solubilidad de QUE y RSV en PBS (pH 7,4) en experimentos de solubilidad en fase. Entre las diferentes CD, se seleccionó HP β CD debido a su seguridad en formulaciones tópicas oftálmicas y por su capacidad de aumentar la absorción de fármacos hidrófobos en el ojo (Challa *et al.*, 2005).

En el caso de ambos polifenoles, se ha visto que los perfiles de solubilidad de fase tienen un andamento lineal, es decir que solubilidad de los compuesto aumenta linealmente al aumentar la concentración de HP β CD en la solución. Además, se ha demostrado que la introducción de excipientes, como polímeros hidrófilos, mejora la capacidad de solubilización de las CD. Esto favorece la formación de estructuras complejas similares a partículas. En nuestros experimentos, la adición de HA dio lugar a una mejora adicional de la solubilidad de la QUE y del RSV. En la **tabla 11.3** se resumen todos los parámetros calculados a partir de los diagramas de solubilidad de las fases.

Table 11.3: Resultados de los estudios de solubilidad en fase medidos a 25°C y pH 7,4 media \pm SEM; n=3

Polifenol	HA (% w/v)	Tipo	$K_{1:1}$ (M ⁻¹)	CE	Fármaco:CD razón molar	Solubilidad (mg/mL) ^a	Solubilidad (mg/mL) ^b
QUE ^c	-	A _L	2609	0,04	1:24	0,44 \pm 0,09	1,06 \pm 0,28
QUE ^c	0,1	A _L	7940	0,10	1:10	0,65 \pm 0,03	2,48 \pm 0,99
RSV ^c	-	A _L	9808	1,24	1:1,8	3,24 \pm 0,41	11 \pm 3,6
RSV ^c	0,1	A _L	7299	0,52	1:2,9	3,04 \pm 0,78	7,17 \pm 1,25

^a en presencia de 5% (p/v) CD

^b en presencia de 12,5 % (p/v) CD

^c todos los complejos se prepararon con HP β CD (0-12,5 % p/v)

Biocompatibilidad *in vitro* de los complejos de inclusión

Se evaluó la biocompatibilidad *in vitro* de los complejos de inclusión de QUE y RSV en dos líneas celulares de la superficie ocular humana, las HCE (epitelio de córnea) y la IM-ConjEpi (epitelio de conjuntiva) tras una exposición de 24 horas a las formulaciones de los polifenoles con las CDs. En la **figura 11.1** se muestra la viabilidad celular tras la exposición a todos los complejos de inclusión. Ninguna de las formulaciones redujo la viabilidad celular de las dos líneas celulares, que se mantuvo en torno al 100 %. Como era de esperar, el BAK, que se utilizó como control positivo de la toxicidad celular, redujo significativamente la viabilidad de ambas líneas celulares ($p < 0,001$).

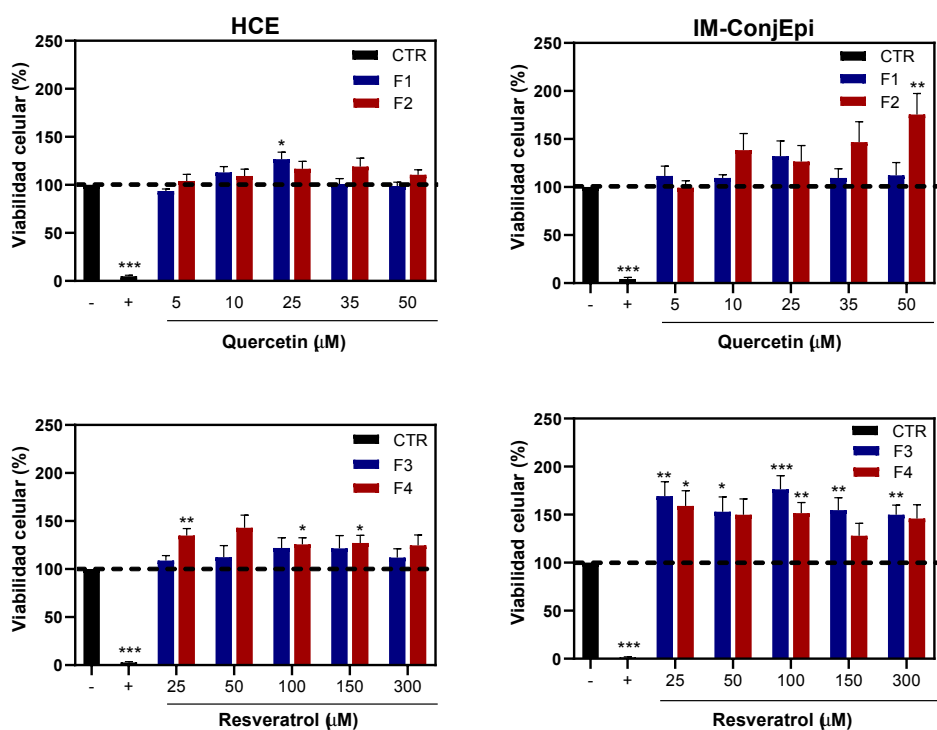


Figure 11.1 - Viabilidad de las células HCE e IM-ConjEpi tras el tratamiento con las formulaciones: F1-QUE:HP β CD, F2-QUE:HP β CD:HA, F3-RSV:HP β CD y F4-RSV:HP β CD:HA, medio de cultivo de células CTR negativo, CTR-BAK positivo (0,005%). Los datos representan la media de tres experimentos independientes \pm SEM. * $p < 0,05$, ** $p < 0,01$, *** $p < 0,001$ en comparación con las células de control tratadas con medio de cultivo.

Actividad antioxidante intracelular de las formulaciones

Se utilizó H₂DCF-DA, un colorante fluorogénico sensible a las ROS, para evaluar la capacidad antioxidante intracelular de los complejos. El H₂DCF-DA puede difundirse pasivamente

en las células y tras exposición a los ROS sufre un cambio en su estructura química, la cual permite generación de fluorescencia. La **figure 11.2** muestra la producción de ROS en células HCE e IM-ConjEpi tras el tratamiento con las formulaciones. Los resultados se expresan en porcentajes, tomando como 100 % de producción de ROS las células expuestas al medio de cultivo. Los porcentajes por debajo de 100 %, indican una neutralización de los ROS por parte de las formulaciones.

Los complejos binarios entre la CD y la QUE o el RSV fueron capaces de eliminar las ROS citoplasmáticas en las células HCE de forma dependiente de la dosis. Se observó una marcada reducción de ROS a partir de las concentraciones más bajas ensayadas ($p < 0,05$). En cuanto a los complejos terciarios, la adición de HA no afectó a la capacidad antioxidante de los complejos, manteniéndola a niveles comparables con los de los complejos binarios. En contraste, los complejos de inclusión con QUE alcanzaron un plateau en su capacidad de barrido antioxidante cuando las células IM-ConjEpi fueron tratadas con una concentración de $10 \mu\text{M}$ o superior. Los complejos de inclusión que contenían RSV, fueron capaces de reducir los niveles intracelulares de ROS con un efecto considerable. De hecho, se observaron diferencias estadísticamente significativas al comparar el efecto antioxidante entre las concentraciones más altas ($300 \mu\text{M}$) y más bajas ($25 \mu\text{M}$) ensayadas ($p < 0,005$) de los complejos RSV:HP β CD, y también entre las concentraciones de $50 \mu\text{M}$ y $300 \mu\text{M}$ ($p < 0,001$).

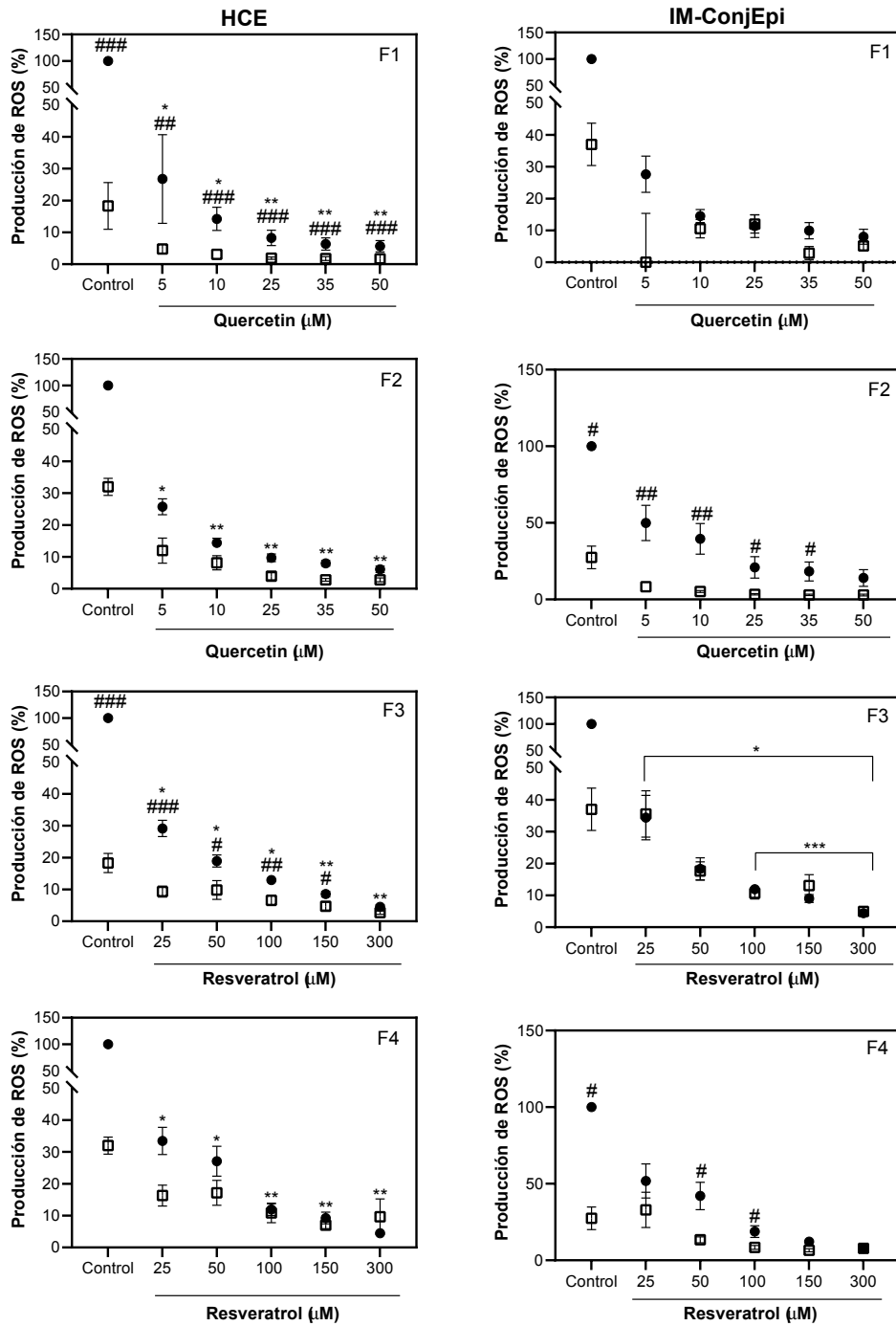


FIGURA 11.2 - Capacidad antioxidante de las formulaciones en células HCE e IM-ConjEpi: F1-QUE: HPβCD, F2-QUE: HPβCD:HA, F3-RSV:HPβCD and F4-RSV:HPβCD:HA complejos, CTR-medio de cultivo de células. (●) Expuestos a UV-B; (□) No expuestos a UV-B. Los datos representan la media de tres experimentos independientes ± SEM. * p < 0.05, ** p < 0.01, *** p < 0.001, en comparación con células expuestas a UV-B; # p < 0.05, ## p < 0.01, ### p < 0.001, comparación intergrupos.

11.6.4. Conclusiones

Para concluir, las características fisicoquímicas de QUE y RSV, como la escasa solubilidad en agua se resolvieron con éxito mediante la formación de complejos binarios o ternarios con HP β CD y HP β CD:HA. Además, la formación de complejos ternarios con HP β CD:HA demostró ser más ventajosa en términos de mejora de la estabilidad química de los dos compuestos. En el caso de la QUE, la mejora de la estabilidad observada fue modesta y se necesitan esfuerzos adicionales para estabilizarla. En el caso de RSV, se logró un mayor efecto estabilizador. Ambos tipos de complejos han mostrado de ser biocompatibles con las líneas celulares empleadas, además de demostrar una excelente capacidad neutralizadora de ROS intracelulares. Por lo tanto, esta estrategia de formulación ha resultado exitosa para estabilizar QUE y RSV de forma que puedan desarrollar su acción antioxidante en células de la superficie ocular *in vitro* tras su administración tópica.

11.7. Nanopartículas basadas en ELR: potencial sistema de administración de fármacos para el tratamiento de la EOS

11.7.1. Objetivo

Los recombinámeros son polímeros a base de proteínas producidos mediante ingeniería genética con una secuencia aminoacídica definida y controlada con precisión (Girotti *et al.*, 2011). Esto permite obtener un material con las propiedades funcionales deseadas. Además, estos biopolímeros ofrecen una biocompatibilidad y biodegradabilidad extraordinarias, sin evocar una respuesta inmunitaria (Girotti *et al.*, 2020; Price *et al.*, 2014). Una ventaja adicional es la fácil escalabilidad de la producción de estos materiales (Vallejo *et al.*, 2021). En los últimos años, los recombinámeros similares a la elastina (ELR) han despertado un gran interés. Los ELR se diseñaron a partir de secuencias repetitivas de tropoelastina, que es un precursor de la elastina natural (Rodríguez-Cabello *et al.*, 2018; Shi *et al.*, 2014). Uno de los motivos repetidos más utilizados en los ELR es el pentapéptido Valina-Prolina-Glicina-X-Glicina (VPGXG). Modulando X, que puede ser cualquier aminoácido excepto prolina, se pueden ajustar muchas propiedades del recombinámero. La aplicación de los ELR en la producción de sistemas (nano)-particulados para la administración de fármacos y de péptidos poco solubles ha demostrado ser una estrategia versátil, teniendo en cuenta la amplia gama de vías de administración a través de las cuales se pueden administrar (Hu *et al.*, 2015; Ryu *et al.*, 2014; Wang *et al.*, 2014).

El uso de fluidos supercríticos, como el CO₂ supercrítico, en la preparación de sistemas particulados representa una buena alternativa al uso de disolventes orgánicos, debido a su naturaleza no inflamable y no tóxica (Santos *et al.*, 2013). Uno de los métodos que emplea scCO₂ para la producción de sistemas particulados es el método del anti-disolvente supercrítico (SAS) (Campardelli *et al.*, 2015). Durante este proceso, el scCO₂ actúa como antisolvente disminuyendo la solubilidad del soluto en la mezcla soluto-disolvente orgánico, sobresaturándolo, permitiendo así la formulación de las partículas (Reverchon *et al.*, 2002). Modulando los parámetros

del proceso SAS, como la concentración de la solución, la geometría de la boquilla o el flujo, se puede ajustar el tamaño y la morfología de las partículas (Cocero *et al.*, 2009; Martín *et al.*, 2008).

Por este motivo, se empleó el CO₂ supercrítico para la obtención de partículas basadas en ELR mediante el proceso anti-disolvente supercrítico (SAS) para la administración oftálmica de QUE y RSV. Se realizó la caracterización físicoquímica, junto con ensayos de biocompatibilidad *in vitro* y funcionales del sistema. También se evaluó la penetración *ex vivo* en córneas porcinas. El trabajo se realizó en colaboración con Reinaldo Vallejo Vicente, estudiante de doctorado del Grupo de Dispositivos Inteligentes para NanoMedicina y del Grupo PressTech, ambos de la Universidad de Valladolid y con la supervisión de los profesores Javier F. Arias Vallejo, Alessandra Girotti y Soraya Rodríguez-Rojo.

11.7.2. Metodología

Preparación de las ELR-NPs

Para llevar a cabo la encapsulación de QUE y RSV utilizando el polímero (EI)₂ se establecieron los siguientes parámetros operativos iniciales del proceso SAS: la presión y la temperatura se fijaron en 11 MPa, 308 K; el flujo de CO₂ fue de 0,5 kg/h y el bombeo del flujo de la solución (fármaco:polímero) en el reactor de 10,8 mL/min. Además, la proporción entre el polímero y los polifenoles (QUE o RSV) se fijó en 6:1. En el caso en que se encapsularon ambos polifenoles, la relación molar entre ellos se estableció en 1:1, y luego en 6:1 entre ELR:QUE/RSV. Para la obtención de las nanopartículas, el sólido obtenido tras el proceso de SAS se disolvió en PBS (pH 7,4) a 37°C, lo cual comportó una reorganización de las cadenas biopoliméricas y la formación de las nanopartículas.

Viabilidad celular

La influencia de las ELR-NPs sobre la viabilidad celular de células epiteliales derivadas de córnea humana (línea celular HCE) se evaluó con la misma metodología descrita para los complejos de inclusión con ciclodextrinas en el capítulo 6.

De forma muy breve, se usó el ensayo de XTT, el cual consiste en la exposición de las células a las formulaciones de ELR-NPs por un cierto periodo de tiempo (en este caso de 1 y 3 horas) y el sucesivo tratamiento de las células con una mezcla de XTT/PMS. Tras 3 horas de incubación se midió la absorbancia a 450 y a 660 nm con un espectrofotómetro.

Medición de la actividad antioxidante intracelular

La medición de la eficacia antioxidante intracelular de las nanopartículas se evaluó con la misma metodología que la realizada para los complejos de inclusión de ciclodextrina en el capítulo 6.

De manera muy resumida, se hizo el ensayo con H₂-DCFDA, un fluoróforo sensible a los ROS y capaz de penetrar las células pasivamente. Las células fueron tratadas con las formulaciones e irradiadas con una lámpara de luz UV-B. Posteriormente a las células se añadió el H₂-DCFDA y se midió la fluorescencia a 488/522 nm (excitación/emisión).

Captación celular de ELR-NPs marcadas con fluorescencia

Se marcaron las ELR-NPs con una doble etiqueta fluorescente (rojo Nilo como carga útil de las ELR-NPs y el biopolímero ELR marcado con la fluoresceína) para evaluar su internalización por parte de las células de epitelio corneal (HCE). Las células HCE se sembraron en un portaobjetos Permanox[®] multicámara de 8 pocillos a una densidad de 15x10³ células/pocillo. Las células HCE se lavaron dos veces con PBS y luego se incubaron con las ELR-NPs durante intervalos de tiempo predeterminados (5, 15, 30, 60 y 90 minutos). La captación celular de las ELR-NPs marcadas se monitorizó mediante un microscopio confocal Leica TCS SP5X equipado con un objetivo de aceite 63x (Wetzlar, Alemania). Las imágenes obtenidas se analizaron con el programa Image J (LOCI, Universidad de Wisconsin).

Distribución de las ELR-NPs en los tejidos de la córnea porcina *ex vivo*

Para evaluar la penetración *ex vivo* de las ELR-NPs en estructuras oculares se obtuvieron globos oculares de cerdo blanco doméstico (*Sus scrofa domestica*) del matadero local Justino Gutiérrez SL. (Laguna de Duero, Valladolid). Los globos oculares enucleados se desinfectaron, limpiaron del tejido muscular y conjuntivo anexo, se lavaron con PBS y se colocaron en placas de 12 pocillos. Para evitar el derrame de las soluciones de ELR-NPs durante la instilación, se colocó un anillo de silicona de 12 mm sobre la córnea de los globos oculares porcinos. Los ojos se incubaron con 300 μ L de una solución de 2 mg/mL de ELR-NPs marcadas con fluorescencia. Tras tiempos predefinidos de incubación (5,15,30 y 60 minutos) se lavaron los globos con PBS, se cortaron las córneas y se incluyeron en medio OCT (Tissue-Tek O.C.T. Compound, Sakura, EE.UU.). Finalmente, las córneas porcinas se observaron con un microscopio de fluorescencia invertido (Leica DMI 6000B, Wetzlar, Alemania).

Análisis estadístico

Para los ensayos celulares, todos los datos se expresan como media \pm error estándar de la media (SEM). El análisis estadístico de los datos se realizó mediante un análisis unidireccional de varianzas (ANOVA) seguido de las pruebas post-hoc de Tukey o Games-Howell. Para ello se utilizó el programa informático SPSS (SPSS 20.0; SPPS, Inc., Chicago, IL, EE.UU.).

11.7.3. Resultados

Biocompatibilidad *in vitro* de las ELR-NPs

Se evaluó la viabilidad de las células HCE tras la exposición a corto plazo a los tres tipos de formulaciones. Como se observa en la **figura 11.3**, ninguno de los tipos de ELR-NPs disminuyó significativamente la viabilidad celular, por lo que todas las formulaciones pueden considerarse seguras. Las ELR-NPs vacías (sin ningún fármaco encapsulado) no comprometieron la viabilidad de las células HCE, destacando la elevada biocompatibilidad del material utilizado para la preparación de las ELR-NPs.

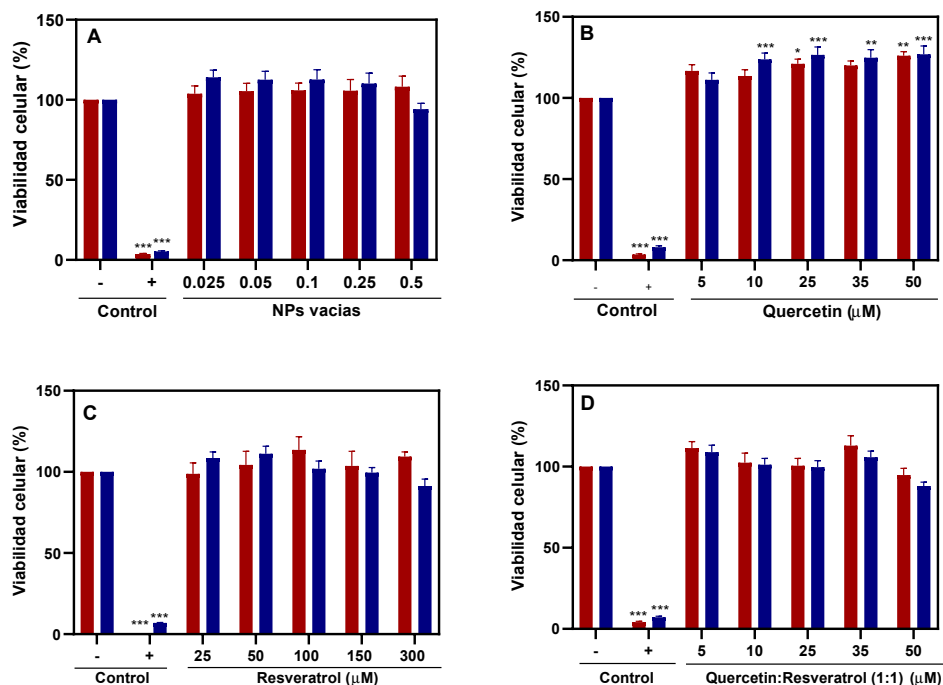


Figure 11.3 - Viabilidad de las células HCE tras el tratamiento con (A) vacías y cargadas ELR-NPs con (B) QUE; (C) RSV; and (D) QUE/RSV después 1 (baras rojas) y 3 horas (baras azules) de exposición. Los rangos de concentración informados se refieren a las concentraciones de polifenol encapsulado dentro de las ELR-NPs. El control negativo era el medio de cultivo, el positivo BAK (0,005%). Los datos representan la media de tres experimentos independientes \pm SEM. * $p < 0,05$, ** $p < 0,01$, *** $p < 0,001$ en comparación con las células de control tratadas con medio de cultivo.

Actividad antioxidante intracelular de las ELR-NPs

La capacidad de las ELR-NPs cargadas con polifenoles para neutralizar las especies de radicales libres desarrolladas intracelularmente se evaluó empleando $H_2DCF-DA$, un compuesto que en presencia de ROS se convierte en un metabolito fluorescente. En la **figura 11.4** se representa el desarrollo de ROS intracelulares tras el tratamiento con las distintas formulaciones de ELR-NPs.

Entre las formulaciones cargadas con los compuestos polifenólicos, la que contenía QUE demostró ser la más eficiente en la eliminación de especies radicales. Las QUE-ELR-NPs disminuyeron significativamente las ROS a $5 \mu M$ de QUE encapsulada ($p < 0,05$). Este efecto mantuvo una respuesta significativa constante a concentraciones iguales o superiores a $25 \mu M$ de QUE en el interior de las ELR-NPs ($p < 0,01$). Respecto a las RSV-ELR-NPs, fueron capaces de disminuir las ROS de forma dosis dependiente, obteniendo una reducción importante a $150 \mu M$ de RSV ($p < 0,05$). Aunque portaban tanto QUE como RSV, las QUE/RSV-ELR-NPs no

aparecieron como la formulación más eficaz para contrarrestar el desarrollo de ROS. Las NPs vacías no mostraron ninguna actividad barredora, lo que indica que todo el efecto obtenido con las NPs cargadas con compuestos polifenólicos se obtiene gracias a la actividad de esos compuestos. El mayor efecto antioxidante de las ELR-NPs portadoras de QUE es dado por el mayor número de grupos hidroxilo presentes en su estructura con respecto a los grupos hidroxilo de RSV. Además los grupos hidroxilo que se encuentran adyacentes en un anillo, como en la estructura química de QUE, pueden formar una estructura de quinona estabilizada por resonancia capaz de interactuar con los radicales libres de una forma más pronunciada (Tu *et al.*, 2015).

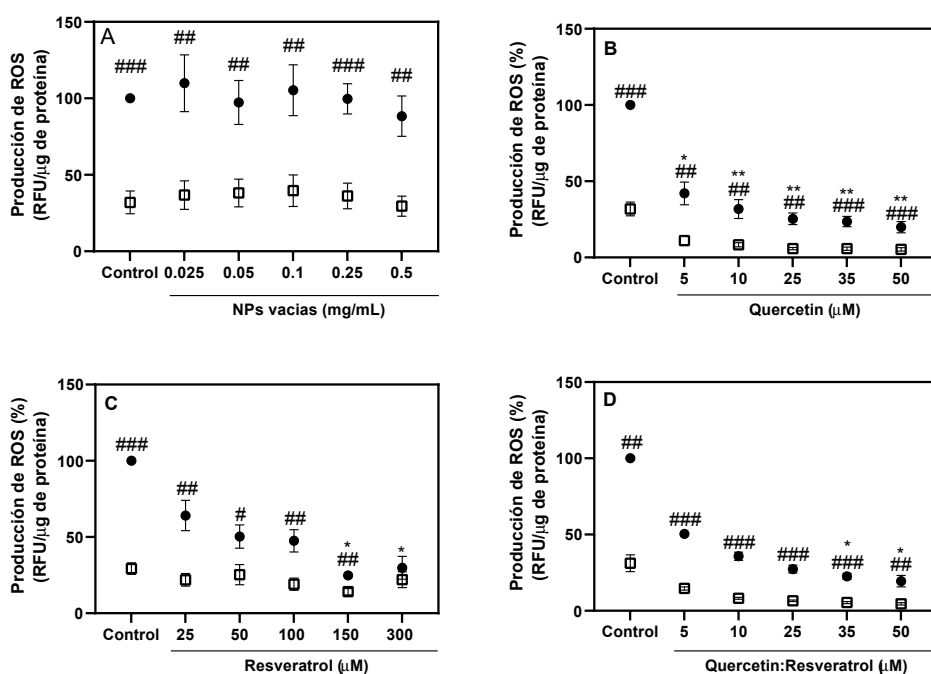


Figure 11.4 - Producción intracelular de ROS en células HCE expuestas a luz UV-B durante 15 segundos. La capacidad de depuración de (A) vacías ELR-NPs y cargadas con: (B) QUE; (C) RSV; and (D) QUE/RSV esta representado en células expuestas y controles (expuestas solo a medio de cultivo). (●) Expuestos a UV-B; (□) No expuestos a UV-B. Los datos representan la media de tres experimentos independientes \pm SEM. * $p < 0.05$, ** $p < 0.01$, *** $p < 0.001$, en comparación con células expuestas a UV-B; # $p < 0.05$, ## $p < 0.01$, ### $p < 0.001$ comparación intergrupos.

Captación celular de las ELR-NPs

La captación celular de las ELR-NPs fabricadas con polímero (EI)₂ marcado con fluoresceína y cargadas con rojo Nilo mediante el proceso SAS se estudió utilizando microscopía confocal. Como se puede observar en la figura 5, las ELR-NPs accedieron eficientemente al interior de las células tras 5 minutos de incubación. La carga útil (rojo), junto con las ELR-NPs (verde)

se localizan principalmente en el citoplasma, más concretamente en las proximidades de la membrana celular. El aumento de la fluorescencia roja con el tiempo confirmó una captación dependiente del tiempo de las ELR-NPs cargadas con rojo Nilo. Por el contrario, la fluorescencia verde correspondiente a las ELR-NPs disminuyó, sugiriendo que tras la liberación del rojo Nilo el biopolímero fue probablemente degradado debido a la presencia de proteasas celulares. El rojo Nilo no encapsulado, disuelto en PBS, mostró una captación celular muy pobre, como se esperaba (**figura 11.5**).

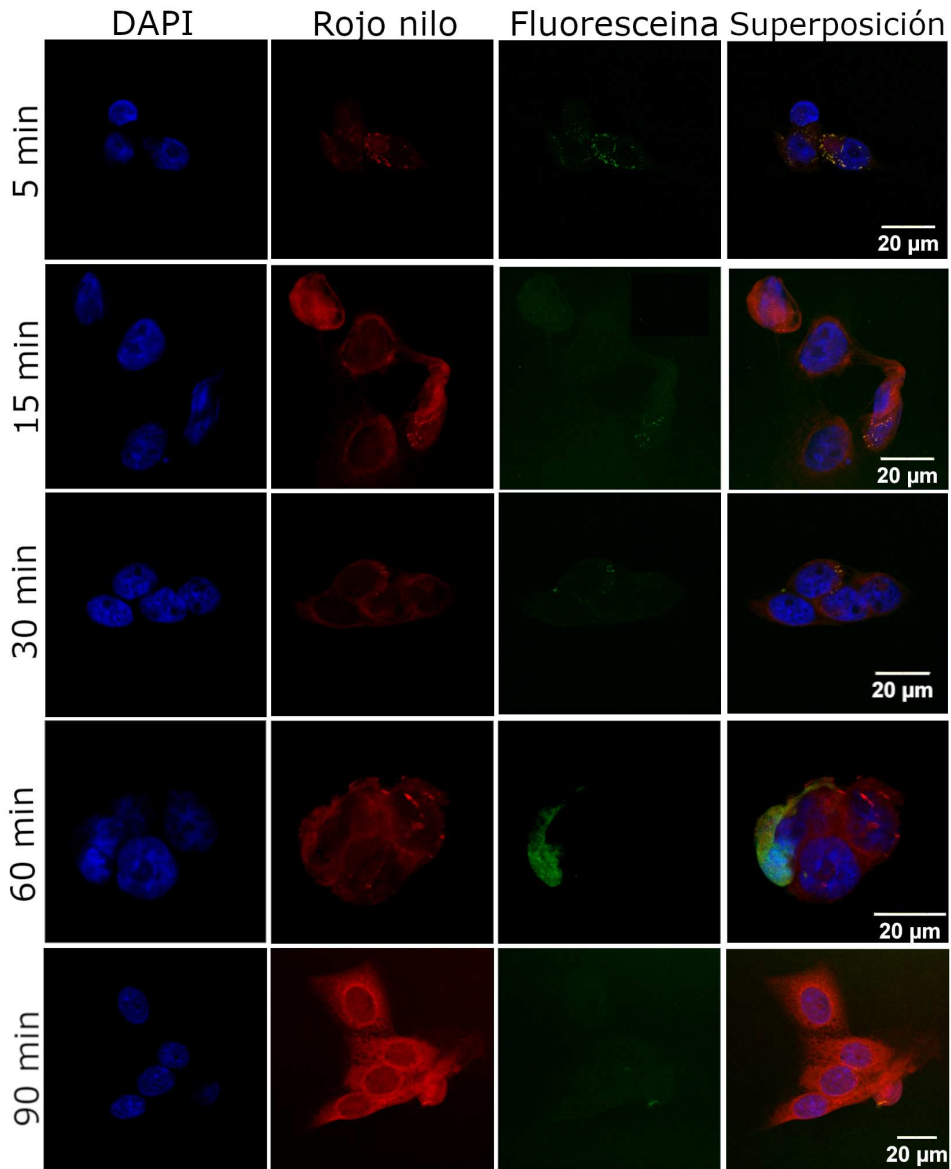


Figure 11.5 - Microfotografías confocales de ELR-NP marcadas con fluoresceína cargadas con rojo del Nilo y absorbido por las células HCE después de la exposición durante 5, 15, 30, 60, y 90 minutos. El rojo nilo se observa en rojo; los núcleos celulares en azul, contrateñido con DAPI; ELR-NPs en verde. Barra de escala 20 μm .

Penetración de las ELR-NPs en córneas porcinas *ex vivo*

Se utilizaron las intensidades de fluorescencia en secciones transversales de la córnea porcina para estimar la distribución de las ELR-NPs marcadas con fluoresceína y cargadas con rojo Nilo

a través de las diferentes capas de la córnea. El rojo Nilo se utilizó como modelo de fármaco hidrófobo debido a su importante hidrofobicidad y su baja solubilidad en agua.

Tras el tiempo de contacto de las ELR-NPs con las córneas porcinas más bajo estudiado (5 minutos), ya pudo observarse una ligera intensidad de fluorescencia roja sobre el epitelio corneal debido a la penetración del rojo Nilo (**figura 11.6**). Al cabo de 15 minutos, la intensidad de la fluorescencia roja se extiende por igual por todo el epitelio. Esta señal se solapa con menor intensidad con la fluorescencia verde procedente del marcaje del polímero en las ELR-NPs. Aunque, la señal verde tiene su mayor intensidad en las capas epiteliales superficiales, se puede observar una tímida señal a través del epitelio. Esto indica que la mayoría de las ELR-NPs se retienen en la superficie corneal, pero también que algunas de ellas se distribuyen en el epitelio liberando su carga útil, en este caso el rojo Nilo. Además, la intensidad de la fluorescencia aumentó con el incremento del tiempo de contacto de las ELR-NPs, lo que sugiere un patrón de penetración dependiente del tiempo. En cuanto al rojo Nilo no formulado, disuelto en aceite de oliva, hasta los 30 minutos de incubación no se pudo detectar ninguna señal fluorescente. A los 30 minutos, esta señal se vuelve de intensidad muy débil, aumentando a los 60 minutos de incubación. Aunque se observó señal de fluorescencia roja ésta fue de menor intensidad respecto a la registrada con las ELR-NPs cargadas con el fluorocromo.

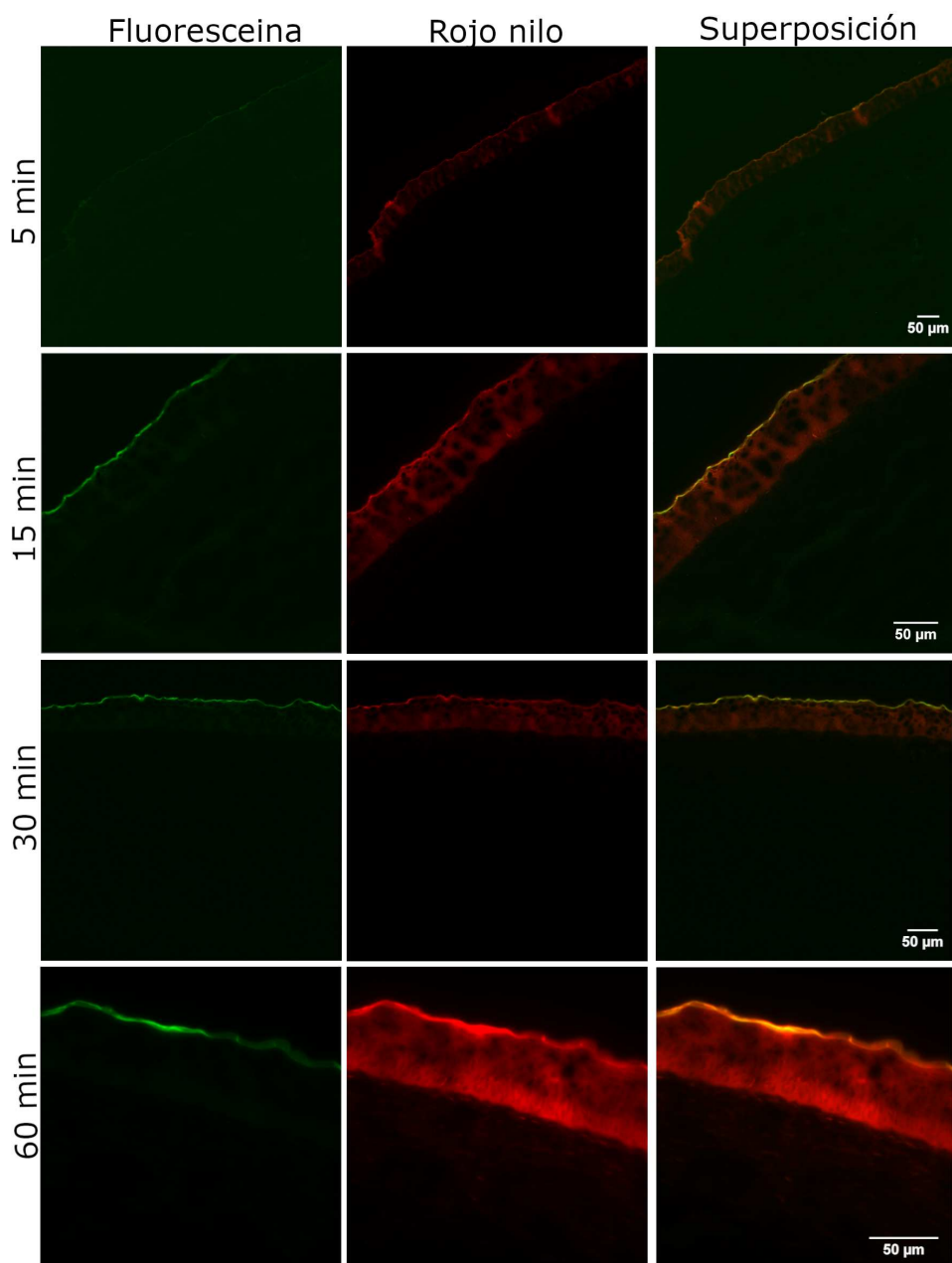


Figure 11.6 - Microfotografías de fluorescencia de la penetración *ex vivo* de tejidos corneales de ELR-NPs marcadas con fluoresceína y cargadas con rojo Nilo. Rojo-rojo Nilo, verde-fluoresceína; barra de escala 50 µm. E-epitelio corneal; S-estroma.

11.7.4. Conclusiones

Este estudio demuestra que el uso de una combinación de fluidos supercríticos y un re-combinámero basado en la secuencia de elastina es apropiado para la formulación de moléculas hidrófobas como QUE y RSV y la obtención de micropartículas. Estas micropartículas son capaces de reorganizarse en nanopartículas una vez dispersadas en solución a temperatura fisiológica. Todos los tipos de ELR-NPs preparadas fueron biocompatibles con las células de epitelio corneal humano (HCE). Además, se registró una excelente actividad antioxidante de las formulaciones eliminando especies ROS intracelulares producidas por exposición a UV-B. Finalmente, la penetración de las ELR-NPs cargadas con rojo Nilo en corneas porcinas *ex vivo* demostró ser más ventajoso con respecto al control, (compuesto libre) porque se consiguió aumentar la captación epitelial de las dos moléculas de interés. En definitiva, las formulaciones de ELR-NPs cargadas con polifenoles son una estrategia prometedora para una eficaz administración tópica oftálmica de pequeñas moléculas hidrófobas.

11.8. Lentes de contacto embebidas en micelas: Un enfoque innovador para la administración oftálmica

11.8.1. Objetivo

Las lentes de contacto (LC) son productos sanitarios que se colocan en la superficie ocular, sobre la córnea y la esclera, con el fin de corregir defectos refractivos. El concepto de la posible utilización de las LC para administrar agentes terapéuticos se propuso por primera vez en 1965 (Sedláček *et al.*, 1965). Se basa en que las LC terapéuticas pueden superar los principales inconvenientes de las formulaciones oftálmicas tópicos relacionados con la baja biodisponibilidad del medicamento y la necesidad de una administración frecuente. El prolongado tiempo de contacto de las LC con las estructuras oculares (unas 8 horas al día en LC diarias) mejora la biodisponibilidad del agente terapéutico hasta en un 50 %, mientras que la modulación de las tasas de liberación reduce notablemente las frecuencias de dosificación (Choi *et al.*, 2018; Grassiri *et al.*, 2021). La combinación de las LC y de portadores coloidales, como las micelas, es parte de muchos estudios relacionados con el tema de las LC medicadas. Este tipo de combinación permite el control de la cinética de liberación de fármacos (González-Chomón *et al.*, 2013; Maulvi *et al.*, 2021).

En consecuencia, el objetivo de este capítulo era mejorar la solubilidad de QUE y RSV mediante la encapsulación en micelas Pluronic® F127 y la posterior carga de las micelas en hidrogeles basados en HEMA o HEMA/MAA. Se llevó a cabo la caracterización fisicoquímica de las micelas y la determinación de los parámetros más relevantes de los hidrogeles, como el atrapamiento de los disolventes y la transmisividad. El trabajo realizado en este capítulo se llevó a cabo como parte de una estancia de un mes en el grupo I+D Farma, Departamento de Farmacología, Farmacia y Tecnología Farmacéutica de la Universidad de Santiago de Compostela (España).

11.8.2. Metodología

Preparación de los hidrogeles

La mayoría de las lentes de contacto (LC) blandas contienen HEMA como monómero estructural del hidrogel. Éste puede copolimerizarse con diferentes monómeros, como el ácido metacrílico MAA. El MAA sirve como monómero funcional que puede mejorar las interacciones entre el fármaco o la nanoestructura y el hidrogel, a través de interacciones electrostáticas, ya que, a pH fisiológico, el MAA está ionizado y tiene carga negativa.

Para el presente estudio se prepararon dos tipos de hidrogeles mediante polimerización térmica (tabla 11.4). Como moldes para la preparación de los geles se utilizaron placas de vidrio presilanizado con dimensiones de 10 cm x 14 cm. La anchura de los hidrogeles se controló con el uso de marcas de teflón, que se colocaron entre las placas de vidrio, cada una de ellas de 0,2 mm de espesor.

Las soluciones de monómero, junto con el reticulante (EGDMA) y el iniciador (AIBN) se mezclaron agitando a 150 rpm y a temperatura ambiente antes del llenado de los moldes. El proceso de polimerización se llevó a cabo durante las primeras 12 h a 50°C y durante otras 24 h a 70°C. Tras el proceso de polimerización, los hidrogeles se quitaron de los moldes cuidadosamente y se lavaron en agua hirviendo durante 15 minutos. En base a las necesidades de cada ensayo, los hidrogeles se cortaron en discos de diferentes diámetros (10 mm y 14 mm) y se colocaron en 500 mL de agua milliQ para completar el procedimiento de lavado.

Después de la polimerización, los monómeros no reaccionados se eliminaron en un proceso de purificación colocando los hidrogeles alternativamente en agua milliQ y solución de NaCl (0,9 %) al menos 4 veces al día. La eliminación completa de los monómeros libres se controló mediante espectrofotómetro UV-Vis.

A parte se prepararon las micelas de Pluronic® F127 cargadas con QUE o con RSV, que después de una caracterización fisicoquímica de base se insertaron en los hidrogeles. La tabla 8.2 (ver pág. 122 en este documento) resume la codificación y la carga de cada combinación de hidrogel y micelas preparadas.

Table 11.4: Composición de los hidrogeles.

Tipo hidrogel	HEMA (mL)	MAA (μ L)	AIBN (mg)	EGDMA (μ L)
HEMA	3	-	14,48	12,10
HEMA/MAA	3	25,83	14,78	12,10

Absorción de disolventes

Para asegurar la completa deshidratación de los discos de hidrogel antes de realizar el ensayo, se calentaron en una estufa a 37 °C durante toda la noche. Los discos secos se pesaron y se colocaron en viales, a los que se añadieron 4 mL de solución micelar que contenía QUE o RSV, o de soluciones de fármaco libre (0,100 mg/mL) en EtOH:H₂O (50:50 v/v). Los discos se dejaron a temperatura ambiente y protegidos de la luz. En los momentos programados (0, 5, 1, 2, 4, 6 y 24 h), los discos se secaron con papel absorbente y se pesaron. La absorción de agua de los hidrogeles se calculó a través del aumento de peso mediante la siguiente ecuación:

$$\text{Captación de disolventes (\%)} = \frac{W_t - W_0}{W_0} \times 100 \quad (11.7)$$

En la ecuación, W_0 y W_t representan el peso del hidrogel seco e hinchado, respectivamente, en un momento determinado (t).

Medida de la transmitancia

La transmitancia de la luz (%) de los hidrogeles hidratados cargados con micelas o con fármacos libres se midió con un espectrofotómetro UV-Vis (Agilent Cary 60 UV-Vis, Waldbronn, Alemania). La transmitancia se recogió de 200 a 700 nm con intervalos de 1 nm.

11.8.3. Resultados

Adsorción de disolventes y transmitancia

Todas las formulaciones examinadas se caracterizaron en términos de absorción de disolvente y transmitancia luminosa. Como se puede ver en la **tabla 11.5** ambos tipos de hidrogeles absorbieron rápidamente cuando se sumergieron en micelas o en soluciones de fármaco libre, alcanzando el equilibrio al cabo de una hora. Los hidrogeles basados en HEMA o HEMA/MAA cargados con micelas fueron capaces de absorber hasta el 80 % del disolvente. Estos resultados concuerdan con los comunicados anteriormente para LC blandas de la misma composición. Por el contrario, los hidrogeles que se sumergieron en soluciones de fármaco libre (50:50 EtOH:H₂O v/v) mostraron un mayor porcentaje de absorción de disolvente, debido a la presencia de EtOH.

Para cumplir los criterios de aprobación (ISO estándares), las LC deben tener una transmisión de la luz superior al 90% en el rango visible del espectro (400-700 nm). La **figura 11.7** muestra de que todas las formulaciones estudiadas cumplían el criterio mencionado y que la inclusión de nanotransportadores como micelas en la red de hidrogeles no influía significativamente en esta propiedad.

Después de caracterizar los hidrogeles en términos de adsorción de disolventes y de transmitancia, los hidrogeles basados en HEMA y HEMA/MAA se intentaron cargar con las micelas portadoras de QUE o RSV. Aunque se observó una carga parecida en ambos tipos de hidrogeles, el estudio de liberación no registró ningún perfil. Lo cual indica una posible dificultad en

Table 11.5: Absorción de disolventes a las 24 horas de hidrogeles HEMA y HEMA/MAA cargados con formulaciones micelares o con fármacos libres (media \pm SEM; n=2).

Código de Formulación ^a	Captación de disolvente (%)	Código de Formulación	Captación de disolvente (%)
HMR	62,55 \pm 0,82	MMR	70,22 \pm 3,12
HR	160,47 \pm 8,06	MR	236,69 \pm 7,94
HMQ	75,74 \pm 2,01	MMQ	87,91 \pm 8,42
HQ	195,094 \pm 2,37	MQ	188,88 \pm 7,69

^aLos códigos de las formulaciones se listan en la Tabla 8.2 en la pág. 122

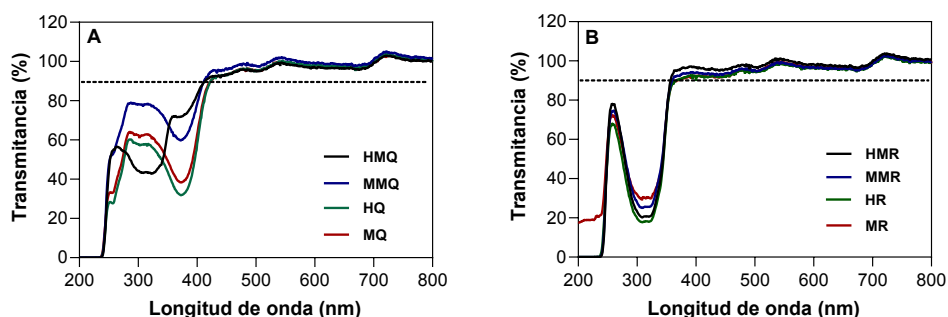


Figure 11.7 - Espectro de transmitancia de discos de hidrogel cargados con: **A)** QUE and QUE/Pluronic[®] F127 micelas, and **B)** RSV and RSV/ Pluronic[®] F127 micelas. El 90% de transmitancia solicitada se indica con una línea discontinua. La codificación de las formulaciones está en la tabla 8.2.

la carga de los sistemas coloidales en los hidrogeles.

11.8.4. Conclusiones

La combinación de LC basadas en hidrogeles y sistemas coloidales ha sido propuesta por la comunidad científica como una posible solución para la formulación de fármacos hidrófobos y su administración a las estructuras de la parte anterior del ojo. Las micelas Pluronic[®] F127 demuestran ser capaces de mejorar la solubilidad acuosa de QUE y RSV, exhibiendo además una excelente eficacia de encapsulación. Los dos hidrogeles probados presentan una buena absorción de disolventes y mantienen la transparencia necesaria en la región visible del espectro. Aunque se trata de un enfoque muy prometedor, es necesario realizar ciertos ajustes en la selección de los materiales y los métodos de preparación para poder resolver los problemas encontrados con la carga del transportador coloidal.

11.9. Limitaciones y trabajo futuro

Este trabajo de tesis tiene varias limitaciones. Éstas se enumeran a continuación junto con las propuestas para su resolución.

1. Los liposomas son un tipo de portador versátil para la administración de diversos agentes terapéuticos. A pesar de ello, durante el desarrollo de nuestra formulación nos hemos encontrado con varios retos. La escasa eficacia de carga de los principios activos hace que la formulación sea ineficiente en términos de efecto terapéutico y costes de producción. Debido a estas limitaciones, no fue posible realizar una caracterización fisicoquímica completa.

Para futuros estudios, se proponen una revisión de la composición liposomal y del método de carga del (los) API(s).

2. Los complejos de inclusión con ciclodextrinas representan un método muy versátil de formulación de compuestos hidrofóbicos. Además, el proceso de fabricación es sencillo. No obstante, para disponer de una formulación candidata deberán realizarse estudios de estabilidad ampliados siguiendo las directrices de la ICH. Esto podría abarcar la adición de otro tipo de excipientes que podrían mejorar aún más la estabilidad de las formulaciones. Todos los productos para aplicaciones tópicas oculares deben ser estériles; para lograrlo se pueden utilizar varios métodos de esterilización (método térmico, por radiación, etc.). Estos métodos tienen el riesgo de inducir la degradación del API. Aunque se ha demostrado la biocompatibilidad y la actividad antioxidante intracelular, no se ha confirmado el efecto sobre otras funciones biológicas, como por ejemplo el bloqueo de la cascada de inflamación. Todos los experimentos *in vitro* se realizaron en monocapas de cultivo celular que; a pesar de ser modelos muy fiables, no representan el comportamiento realista y la arquitectura de un tejido u órgano vivo.

Por lo tanto, para futuros trabajos se propone estudiar en las formulaciones: i) la estabilidad a largo plazo siguiendo las directrices de la ICH; ii) el efecto del proceso de esterilización; iii) la interacción *in vitro* en modelos 3D de los tejidos de la superficie ocular; y iv) si son capaces de desarrollar también una actividad anti-inflamatoria.

3. Las nanopartículas elaboradas a partir de elastina recombinante surgieron como una estrategia de formulación muy interesante y versátil. Aunque el proceso de producción da lugar a la formación de un polvo, la estabilidad puede representar un problema. Los estudios de liberación deberán ser rediseñados para poder determinar toda la queratina liberada, ya que una posible degradación imposibilita la determinación real de la cinética de liberación. Aunque se ha observado una eficiente captación celular de las ELR-NPs, sería conveniente profundizar en el estudio del mecanismo por el que se produce dicha captación.

Por lo tanto, para futuros estudios se sugiere profundizar en el desempeño de este tipo de formulaciones analizando i) la estabilidad de las ELR-NPs en forma sólida y en solución;

ii) redefinición de los estudios de liberación; iii) realización de estudios *in vitro* en modelos 3D de los tejidos de la superficie ocular; iv) si son capaces de desarrollar también una actividad antiinflamatoria y v) el mecanismo de captación celular de las ELR-NPs.

4. Las lentes de contacto embebidas con micelas presentan un enfoque prometedor de la administración oftálmica, especialmente por la posibilidad de ampliar el tiempo de contacto y el control de la liberación del API. Sin embargo, tuvimos problemas durante el proceso de carga de la base de hidrogel de las lentes de contacto. Esto limitó en parte los estudios de caracterización y la realización de posibles ensayos *in vitro*. Además, el tiempo limitado para la realización y mejora de los experimentos condicionó los resultados de este estudio.

Futuros trabajos deberán de considerar las siguientes propuestas i) reformulación de la idea original basada en la carga de micelas en los hidrogeles; ii) reconsiderar otros métodos de carga de hidrogeles; iii) realizar la caracterización fisicoquímica del sistema mejorado y iv) estudios *in vitro*.

11.10. Conclusiones de la tesis

Este trabajo de tesis se centró en el desarrollo de estrategias de formulación para los compuestos naturales quercetina y resveratrol, con el propósito de su aplicación terapéutica como tratamiento oftálmico tópico para la Enfermedad del Ojo Seco y otros trastornos que afectan a la superficie ocular. El enfoque en el desarrollo de la formulación era necesario, ya que los efectos beneficiosos de los compuestos de interés han sido probados previamente tanto *in vitro* como *in vivo*, pero su uso estaba limitado debido a sus pobres características intrínsecas, como son la susceptibilidad a la degradación o la pobre solubilidad acuosa. Este estudio demuestra que es posible, mediante la aplicación de distintos enfoques de formulación, alcanzar un nivel relevante de mejora de las características de un candidato a principio activo farmacéutico (API). A continuación, se presentan las principales conclusiones de este trabajo de tesis, que se corresponden con los objetivos planteados al inicio del trabajo.

1. Las cuatro estrategias de formulación propuestas en este trabajo de tesis han alcanzado distintos niveles de desarrollo. Con respecto a la formulación liposomal, el principal reto fue la extremadamente baja eficacia de encapsulación de los dos polifenoles, que los hacía ineficaces para administrar dosis terapéuticas. En el caso de los complejos de inclusión con ciclodextrinas, la solubilidad de QUE y RSV mejoró linealmente con el aumento de la concentración de ciclodextrina en la solución. Asimismo, se logró una mejora considerable de la estabilidad de ambos compuestos. Se observó una mejora adicional tanto de la solubilidad como de la estabilidad de QUE y RSV con la adición de ácido hialurónico a los complejos binarios CD:fármaco preformados. Dado que las formulaciones de ELR-NPs se produjeron como sólidos, su estabilidad se consideró suficiente para la duración del presente estudio. Además, las ELR-NPs ofrecieron una liberación sostenida tanto para QUE como para RSV. La incorporación de micelas en las lentes de contacto que parecían

hidrogeles no alteró parámetros cruciales de los hidrogeles, como la transmitancia de luz y la absorción de agua. Sin embargo, surgieron complicaciones con los estudios de liberación, que se revisarán.

2. Las formulaciones de QUE y RSV en complejos de inclusión binarios con ciclodextrinas y ternarios con la adición de ácido hialurónico se han considerado biocompatibles con las células epiteliales corneales y conjuntivales humanas. Las ELR-NP, portadoras de QUE, RSV o ambos polifenoles no alteraron la viabilidad celular de las células epiteliales corneales humanas, por lo que se consideran biocompatibles con esta línea celular.
3. Las formulaciones de ciclodextrina y ELR-NPs mostraron una excelente capacidad para eliminar las especies ROS intracelulares en dos líneas celulares de la superficie ocular. Se estudió la actividad antiinflamatoria de los complejos de inclusión. Sin embargo, no se obtuvieron resultados consistentes. Deben considerarse nuevos ajustes en el modelo inflamatorio *in vitro*.
4. Se ha demostrado que las ELR-NP marcadas con fluoresceína y portadoras de rojo nilo son capaces de penetrar y liberar su carga útil en las células epiteliales de la córnea humana. Además, el mismo sistema mostró una excelente penetración en un modelo corneal *ex vivo*. Los estudios de captación celular y *ex vivo* de las demás formulaciones presentadas en este trabajo no se estudiaron debido a limitaciones de tiempo y de producción de un sistema eficaz marcado con fluorescencia.

Como conclusión general, puede afirmarse que los complejos de inclusión con ciclodextrinas (binarios y ternarios) y ELR-NPs han dado los resultados más prometedores para un posible desarrollo futuro de una formulación oftálmica tópica. Ambas formulaciones influyeron positivamente en propiedades cruciales de los dos compuestos en examen. Sin embargo, en ambos casos se requieren estudios más profundos.

References of Chapter 11

- Abengózar-Vela, A., Calonge, M., Stern, M.E., González-García, M.J. and Enríquez-De-Salamanca, A.,
Quercetin and resveratrol decrease the inflammatory and oxidative responses in human ocular surface epithelial cells,
Investig. Ophthalmol. Vis. Sci. **56**, 2709 (2015)
<https://doi.org/10.1167/iovs.15-16595>
- Al-Amin, M.D., Mastrotto, F., Subrizi, S, Sen, M. ,Turunen, T. , Arango-Gonzalez, B., Ueffing, M., Urtti, A.,
Salmaso, S., and Caliceti, P.,
Tailoring surface properties of liposomes for dexamethasone intraocular administration,
J. Control. Release **354**, 2023 (323–336)
<https://doi.org/10.1016/j.jconrel.2023.01.027>
- Bally, B., and Cullis, R.,
Dopamine accumulation in large unilamellar vesicle systems induced by transmembrane ion gradients,
Chem. Phys. Lipids **47**, 97–107 (1988).
- Bangham, A.D., Standish, M.M., and Watkins, J.C.,
Diffusion of univalent ions across the lamellae of swollen phospholipids,
J. Mol. Biol. **13**, 1965 (238–252)
[https://doi.org/10.1016/S0022-2836\(65\)80093-6](https://doi.org/10.1016/S0022-2836(65)80093-6)
- Bozzuto, G., and Molinari, A.,
Liposomes as nanomedical devices,
Int. J. Nanomedicine **10**, 2018 (975–999)
<https://doi.org/10.1016/j.bpj.2018.04.022>
- Campardelli, R., Baldino, L., and Reverchon, E.,
Supercritical fluids applications in nanomedicine,
J. Supercrit. Fluids **101**, 2015 (193–214)
<https://doi.org/10.1016/j.supflu.2015.01.030>
- Challa, R., Ahuja, A., Ali, J. and Khar, R.K.,
Cyclodextrins in drug delivery: An updated review,
AAPS PharmSciTech **6**, 329–357 (2005)
<https://doi.org/10.1208/pt060243>
- Choi, S.W., and Kim, J.,
Therapeutic contact lenses with polymeric vehicles for ocular drug delivery: A review,

- Materials **11**, 1125–1145 (2018)
<https://doi.org/10.3390/ma11071125>
- Cocero, M.J., Martín, Á., Mattea, F., and Varona, S.,
Encapsulation and co-precipitation processes with supercritical fluids: Fundamentals and applications,
J. Supercrit. Fluids. **47**, 2009 (546–555)
<https://doi.org/10.1016/j.supflu.2008.08.015>
- Del Valle, E.M.M.,
Cyclodextrins and their uses: A review,
Process Biochem. **39**, 1033–1046 (2004)
[https://doi.org/10.1016/S0032-9592\(03\)00258-9](https://doi.org/10.1016/S0032-9592(03)00258-9)
- Gao, X., Noda, Y., Rubinstein, I., and Paul, S.,
Vasoactive intestinal peptide encapsulated in liposomes: effects on systemic arterial blood pressure,
Pharmacol. Lett. **54**, 247–252 (1994).
- Girotti, A., Fernández-Colino, A., López, I.M., Rodríguez-Cabello, J.C., and Arias, F.J.,
Elastin-like recombinamers: Biosynthetic strategies and biotechnological applications,
Biotechnol. J. **6**, 2011 (1174–1186)
<https://doi.org/10.1002/biot.201100116>
- Girotti, A., Gonzalez-Valdivieso, J., Santos, M., Martin, L., and Arias, F.J.,
Functional characterization of an enzymatically degradable multi-bioactive elastin-like recombinamer,
Int. J. Biol. Macromol. **164**, 2020 (1640–1648)
<https://doi.org/10.1016/j.ijbiomac.2020.08.004>
- González-Chomón, C., Concheiro, A., and Alvarez-Lorenzo, C.,
Soft contact lenses for controlled ocular delivery: 50 years in the making,
Ther. Deliv. **4**, 1141–1161 (2013)
<https://doi.org/10.4155/tde.13.81>
- Grassiri, B., Zambito, Y., and Bernkop-Schnürch, A.,
Strategies to prolong the residence time of drug delivery systems on ocular surface,
Adv. Colloid Interface Sci. **288**, 1–15 (2021)
<https://doi.org/10.1016/j.cis.2020.102342>
- Hu, J., Xie, L., Zhao, W., Sun, M., Liu, X., and Gao, W.,
Design of tumor-homing and pH-responsive polypeptide-doxorubicin nanoparticles with enhanced anticancer efficacy and reduced side effects,
Chem. Commun. **51**, 2015 (11405–11408)
<https://doi.org/10.1039/c5cc04035c>
- Immordino, M.L., and Cattel, L.,
Stealth liposomes: review of the basic science , rationale , and clinical applications , existing and potential,
Int. J. Nanomedicine **3**, 297–315 (2006).
- Lachowicz, M., Stańczak, A. and Kołodziejczyk, M.,
Characteristic of cyclodextrins: their role and use in the pharmaceutical technology,
Curr. Drug Targets **21**, 1495–1510 (2020)
<https://doi.org/10.2174/1389450121666200615150039>

- Liu, L. and Guo, Q.X.,
The driving forces in the inclusion complexation of cyclodextrins,
J. Incl. Phenom. **42**, 1–14 (2002)
<https://doi.org/10.1023/A:1014520830813>
- Loftsson, T. and Duchêne, D.,
Cyclodextrins and their pharmaceutical applications,
Int. J. Pharm. **329**, 1–11 (2007)
<https://doi.org/10.1016/j.ijpharm.2006.10.044>
- Loftsson, T. and Stefánsson, E.,
Effect of cyclodextrins on topical drug delivery to the eye,
Drug Dev. Ind. Pharm. **23**, 473–481 (1997)
<https://doi.org/10.3109/03639049709148496>
- Martín, A., and Cocero, M.J.,
Micronization processes with supercritical fluids: Fundamentals and mechanisms,
Adv. Drug Deliv. Rev. **60**, 2008 (339–350)
<https://doi.org/10.1016/j.addr.2007.06.019>
- Maulvi, F.A., Desai, D.T., Shetty, K.H., Shah, D.O., and Willcox, M.D.P.,
Advances and challenges in the nanoparticles-laden contact lenses for ocular drug delivery,
Int. J. Pharm. **608**, 1–9 (2021)
<https://doi.org/10.1016/j.ijpharm.2021.121090>
- Price, R., Poursaid, A., and Ghandehari, H.,
Controlled release from recombinant polymers,
J. Control. Release. **190**, 2014 (304–313)
<https://doi.org/10.1016/j.jconrel.2014.06.016>
- Reverchon, E.,
Supercritical-assisted atomization to produce micro- and/or nanoparticles of controlled size and distribution,
Ind. Eng. Chem. Res. **41**, 2002 (2405–2411)
<https://doi.org/10.1021/ie010943k>
- Rodrigues, S., Banerjee, A., Kanekiyo, T., and Singh, J.,
Functionalized liposomal nanoparticles for efficient gene delivery system to neuronal cell transfection,
Int. J. Pharm. **7**, 2019 (1–56)
<https://doi.org/10.1016/j.ijpharm.2019.06.026>
- Rodríguez-Cabello, J.C., González de Torre, I., Ibañez-Fonseca, A., and Alonso, M.,
Bioactive scaffolds based on elastin-like materials for wound healing,
Adv. Drug Deliv. Rev. **129**, 2018 (118–133)
<https://doi.org/10.1016/j.addr.2018.03.003>
- Ryu, J.S., and Raucher, D.,
Anti-tumor efficacy of a therapeutic peptide based on thermo-responsive elastin-like polypeptide in combination with gemcitabine,
Cancer Lett. **348**, 2014 (177–184)
<https://doi.org/10.1016/j.canlet.2014.03.021>

- Santos, D.T., and Meireles, M.A.A.,
Micronization and encapsulation of functional pigments using supercritical carbon dioxide,
J. Food Process Eng. **36**, 2013 (36–49)
<https://doi.org/10.1111/j.1745-4530.2011.00651.x>
- Saokham, P., Muankaew, C., Jansook, P. and Loftsson, T.,
Solubility of cyclodextrins and drug/cyclodextrin complexes,
Molecules **23**, 1–15 (2018)
<https://doi.org/10.3390/molecules23051161>
- Sedláček, J.,
Possibility of the application of ophthalmic drugs with the use of gel contact lenses,
Cesk. Oftalmol. **21**, 509–512 (1965).
- Shi, P., Gustafson, J.A., and Andrew MacKay, J.,
Genetically engineered nanocarriers for drug delivery,
Int. J. Nanomedicine **9**, 2014 (1617–1626)
<https://doi.org/10.2147/IJN.S53886>
- Silva, R., Ferreira, H., Little, C., and Cavaco-Paulo, A.,
Ultrasonics sonochemistry effect of ultrasound parameters for unilamellar liposome preparation,
Ultrason. - Sonochemistry. **17**, 2010 (628–632)
<https://doi.org/10.1016/j.ultsonch.2009.10.010>
- Tu, B., Liu, Z.J., Chen, Z.F., Ouyang, Y., and Hu, Y.J.,
Understanding the structure-activity relationship between quercetin and naringenin: in vitro,
RSC Adv. **5**, 2015 (106171–106181)
<https://doi.org/10.1039/c5ra22551e>
- Vallejo, R., Gonzalez-Valdivieso, J., Santos, M., Rodriguez-Rojo, S., and Arias, F.J.,
Production of elastin-like recombinamer-based nanoparticles for docetaxel encapsulation and use as smart drug-delivery systems using a supercritical anti-solvent process,
J.Ind.Eng.Chem. **93**, 2015 (361–374)
<https://doi.org/10.1016/j.jiec.2020.10.013>
- Varan, G., Varan, C., Erdoğar, N., Hincal, A.A. and Bilensoy, E.,
Amphiphilic cyclodextrin nanoparticles,
Int. J. Pharm. **531**, 457–469 (2017)
<https://doi.org/10.1016/j.ijpharm.2017.06.010>
- Wang, W., Despanie, J., Shi, P., Edman, M.C., Lin, Y.A., Cui, H., Heur, M., Fini, M.E., Hamm-Alvarez, S.F., and Mackay, J.A.,
Lacritin-mediated regeneration of the corneal epithelia by protein polymer nanoparticles,
J. Mater. Chem. B **2**, 2014 (8131–8141)
<https://doi.org/10.1039/c4tb00979g>
- Wenche, M., Acharya, G., and Basnet, P.,
Resveratrol-loaded liposomes for topical treatment of the vaginal inflammation and infections,
Eur.J. Pharm. Sci. **79**, 2015 (112–121)
<https://doi.org/10.1016/j.ejps.2015.09.007>

VI

Appendices



A

Review Article



Review

Ocular Delivery of Polyphenols: Meeting the Unmet Needs

Luna Krstić ¹ , María J. González-García ^{1,2} and Yolanda Diebold ^{1,2,*} 

Abstract: Nature has become one of the main sources of exploration for researchers that search for new potential molecules to be used in therapy. Polyphenols are emerging as a class of compounds that have attracted the attention of pharmaceutical and biomedical scientists. Thanks to their structural peculiarities, polyphenolic compounds are characterized as good scavengers of free radical species. This, among other medicinal effects, permits them to interfere with different molecular pathways that are involved in the inflammatory process. Unfortunately, many compounds of this class possess low solubility in aqueous solvents and low stability. Ocular pathologies are spread worldwide. It is estimated that every individual at least once in their lifetime experiences some kind of eye disorder. Oxidative stress or inflammatory processes are the basic etiological mechanisms of many ocular pathologies. A variety of polyphenolic compounds have been proved to be efficient in suppressing some of the indicators of these pathologies in *in vitro* and *in vivo* models. Further application of polyphenolic compounds in ocular therapy lacks an adequate formulation approach. Therefore, more emphasis should be put in advanced delivery strategies that will overcome the limits of the delivery site as well as the ones related to the polyphenols in use. This review analyzes different drug delivery strategies that are employed for the formulation of polyphenolic compounds when used to treat ocular pathologies related to oxidative stress and inflammation.

B

Original Research Paper I



Article

Potential Ophthalmological Application of Extracts Obtained from Tuna Vitreous Humor Using Lactic Acid-Based Deep Eutectic Systems

Maha M. Abdallah ^{1,2}, Inês C. Leonardo ^{1,2}, Luna Krstić ³, Amalia Enríquez-de-Salamanca ^{3,4}, Yolanda Diebold ^{3,4}, María J. González-García ^{3,4}, Frédéric B. Gaspar ^{1,2}, Ana A. Matias ², Maria Rosário Bronze ^{1,2,5} and Naiara Fernández ^{2,*}

Abstract: A green technique was developed to extract hyaluronic acid (HA) from tuna vitreous humor (TVH) for its potential application in managing dry eye disease. Deep eutectic solvents (DES) were used to extract HA and were synthesized using natural compounds (lactic acid, fructose, and urea). The DES, the soluble fraction of TVH in DES (SF), and the precipitated extracts (PE) were evaluated for their potential use in dry eye disease treatment. *In vitro* experiments on human corneal epithelial cell lines and the effect on dry eye-associated microorganisms were performed. The influence of the samples on the HCE viability, their intracellular reactive oxygen species (ROS) scavenging capacity, inflammatory response, and antimicrobial properties were studied. According to the results, all samples displayed an antioxidant effect, which was significantly higher for PE in comparison to SF. Most of the tested samples did not induce an inflammatory response in cells, which confirmed the safety in ophthalmic formulations. In addition, the DES and SF proved to be efficient against the studied bacterial strains, while PE did not show an antimicrobial effect. Hence, both DES and SF at defined concentrations could be used as potential compounds in dry eye disease management.

C

Original Research Paper II

International Journal of Pharmaceutics 624 (2022) 122028



ELSEVIER

Contents lists available at ScienceDirect

International Journal of Pharmaceutics

journal homepage: www.elsevier.com/locate/ijpharm



Improved ocular delivery of quercetin and resveratrol: A comparative study between binary and ternary cyclodextrin complexes

Luna Krstić^a, Pekka Jarho^b, Marika Ruponen^b, Arto Urtti^{b,c}, María J. González-García^{a,d,*}, Yolanda Diebold^{a,d}

Abstract: The number of patients affected by Dry Eye Disease (DED) had notably increased worldwide, addressing the need of novel therapeutic approaches. Polyphenols, quercetin (QUE) and resveratrol (RSV) show necessary antioxidant and anti-inflammatory properties to manage DED, but their application as topical eyedrops is restricted by low aqueous solubility and low chemical stability. Cyclodextrins (CD) are widely used to improve physico-chemical characteristics of drugs. Consequently, the aim of this study was to make a comparison between binary complexes with quercetin, resveratrol and cyclodextrins and tertiary complexes adding hyaluronic acid (HA). Both complexes were able to enhance solubility and stability of QUE and RSV. AFM imaging and DLS measurements disclose the formation of spherical nanoaggregates within tertiary complexes of both QUE and RSV with mean diameters of 103 and 82 nm. Neither complex demonstrated cytotoxic effect in *in vitro* studies in corneal (HCE) and conjunctival (IM-ConjEpi) cell lines. In HCE cells, complexes containing QUE or RSV at their highest concentrations were able to scavenge more than 95 % of the ROS that were produced intracellularly ($p < 0.005$). Similar response was observed with IM-ConjEpi cells. The antioxidant effect was maintained in the complexes with HA. This confirmed their potential as viable topical treatment for DED.



Original Research Paper III

Experimental Eye Research 223 (2022) 109220



Contents lists available at [ScienceDirect](https://www.sciencedirect.com)

Experimental Eye Research

journal homepage: www.elsevier.com/locate/yexer



Research article

Characterization and functional performance of a commercial human conjunctival epithelial cell line



Laura García-Posadas^{a,*}, Ismael Romero-Castillo^a, Nikolaos Katsinas^a, Luna Krstić^a, Antonio López-García^a, Yolanda Diebold^{a,b}

Abstract: The conjunctiva is a complex tissue that covers the eye beginning at the corneal limbus and extending over the inner surfaces of the eyelids. Due to its important functions in maintaining the health of the ocular surface, adequate *in vitro* models of conjunctival structure and function are essential to understand its roll in different pathologies. Because there is scarcity of human conjunctival tissue that can be used in research, cell lines are often the only option for initial studies. An immortalized human conjunctival epithelial cell (IM-HConEpiC) line is now commercially available; however, it is not very well characterized. In this study, we have developed a new protocol to culture these cells without the use of collagen-coated culture surfaces, but with a defined cell culture medium. We characterized IM-HConEpiCs cultured under these conditions and corroborated that the cells maintained a conjunctival epithelial phenotype, including acidic and neutral mucins, junctional proteins E-cadherin and zonula occludens 1, and expression of CK8 and CK19, among others. In addition, we analyzed the response to oxidative stress and inflammatory stimuli and found that IM-HConEpiCs respond as expected for conjunctival epithelial tissue. For instance, cells exposed to oxidative stress increased the production of reactive oxygen species, and that increase was blocked in the presence of an antioxidant agent. In addition, after stimulation with TNF- α , IM-HConEpiCs significantly increased the production of IL-1 β , IL-6, IL-8, and IP-10. Therefore, with this study we conclude that IM-HConEpiCs can be a useful tool in functional studies to determine the response of the conjunctiva to pathological conditions and/or to test new therapeutic strategies.

E

Original Research Paper IV

In Preparation

ELR-based Nanoparticles as a Platform for Ophthalmic Delivery of Quercetin and Resveratrol

Luna Krstić, Reinaldo Vallejo, Soraya Rodriguez-Rojo, Alessandra Girotti, F. Javier Arias, María J. González-García, Yolanda Diebold

Abstract: Thanks to their modulable properties, elastin-like recombinamers (ELR) have gained attention as a stimuli-responsive material for the preparation of advanced drug delivery systems. Supercritical CO₂ represents a sustainable alternative to the use of organic solvents. For that reason, we have prepared an ELR-based particulate system bearing two promising polyphenolic compounds, quercetin (QUE) and resveratrol (RSV). The system aimed for topical ophthalmic applications is made through a one-step supercritical-antisolvent (SAS) process. After the SAS process, solid micro-particles loaded with QUE, RSV, or both were obtained. Given the stimuli-responsive properties of the recombinamer used, these micro-particles, once placed in solution at physiological temperature, rearrange into nano-particles with an average size of 56.7 ± 1.0 - 61.5 ± 2.6 nm. The ELR-based system was capable of sustaining the polyphenol release. All formulations were biocompatible with Human Corneal Epithelial cells (HCE). Additionally, all formulations exhibited excellent intracellular scavenging activity of reactive oxygen species (ROS). To monitor the cellular uptake of the system, particles bearing a double fluorescent-tag were prepared. This consisted of encapsulating Nile red, a fluorescent dye, in a fluorescein-modified ELR polymer. The system successfully delivered the fluorescent payload to the cells. Furthermore, the same system showed to be able to efficiently deliver the payload to the corneal epithelium in a time-dependent manner using *ex vivo* porcine globes.

